British and Fennoscandian Ice-Sheet interactions during the quaternary

Bethan Joan Davies

6.2.4 LFA 3: The Middle Diamicton

LFA 3: Sedimentology and Stratigraphy

LFA 3 is a complex, dark brown, clast-rich diamicton that directly overlies either bedrock, as in exposures A, I and J, LFA 2 as in exposures B and C, and LFA 1 as in exposures F, G and H (see Figure 6.3). Several lithofacies are exhibited. Firstly, there is a massive dark brown diamicton (LF 3a). Secondly, this facies is interbedded with LFA 2 in Exposure D2 (forming facies LF 3b). Thirdly, there is a bedded, deformed, sand and gravel facies, interbedded within the diamicton (LF 3c). There is also a bed of well-sorted, planar bedded sand, upturned into a large sub-vertical fold, present only in Exposure E1 (LF 3d). LFA 3 also contains two laminated diamicton facies: brown and grey clay laminations, a seen in Exposure C at 14 m O.D. (LF 3e), and a red and brown laminated diamictic facies (LF 3f), as visible in Exposure C at 44 m O.D. (refer to Figure 6.3).

LF 3a: Diamicton Facies

The diamicton facies (LF 3a) is dominated by northern British erratics such as Carboniferous and Magnesian limestones, sandstones and coal, with rare igneous erratics. Clast macro-fabrics are moderate, with an S_1 value typically around 0.5 to 0.6. Clasts are generally faceted, with well-developed stoss and lee ends, and multiple striae. They range in size from very fine gravel to large cobbles and boulders.

At Warren House Gill, LF 3a is first exposed cropping-out directly on the limestone bedrock in Exposure A (Figure 6.24). The Magnesian Limestone bedrock here crops out at 16 m O.D. LF 3a is a dark brown diamicton, interbedded with bedded, poorly sorted sands. The contact with the limestone bedrock is unconformable and erosive, with stringers emanating from the limestone bedrock into the diamicton. The clasts within the diamicton are faceted and striated, with well-orientated striations (Figure 6.24). Within the diamicton, a whole bivalve shell (unpaired) was found, but was so soft it was impossible to extract from the diamicton. The diamicton is clast-rich, with clasts ranging from fine gravel to cobbles.

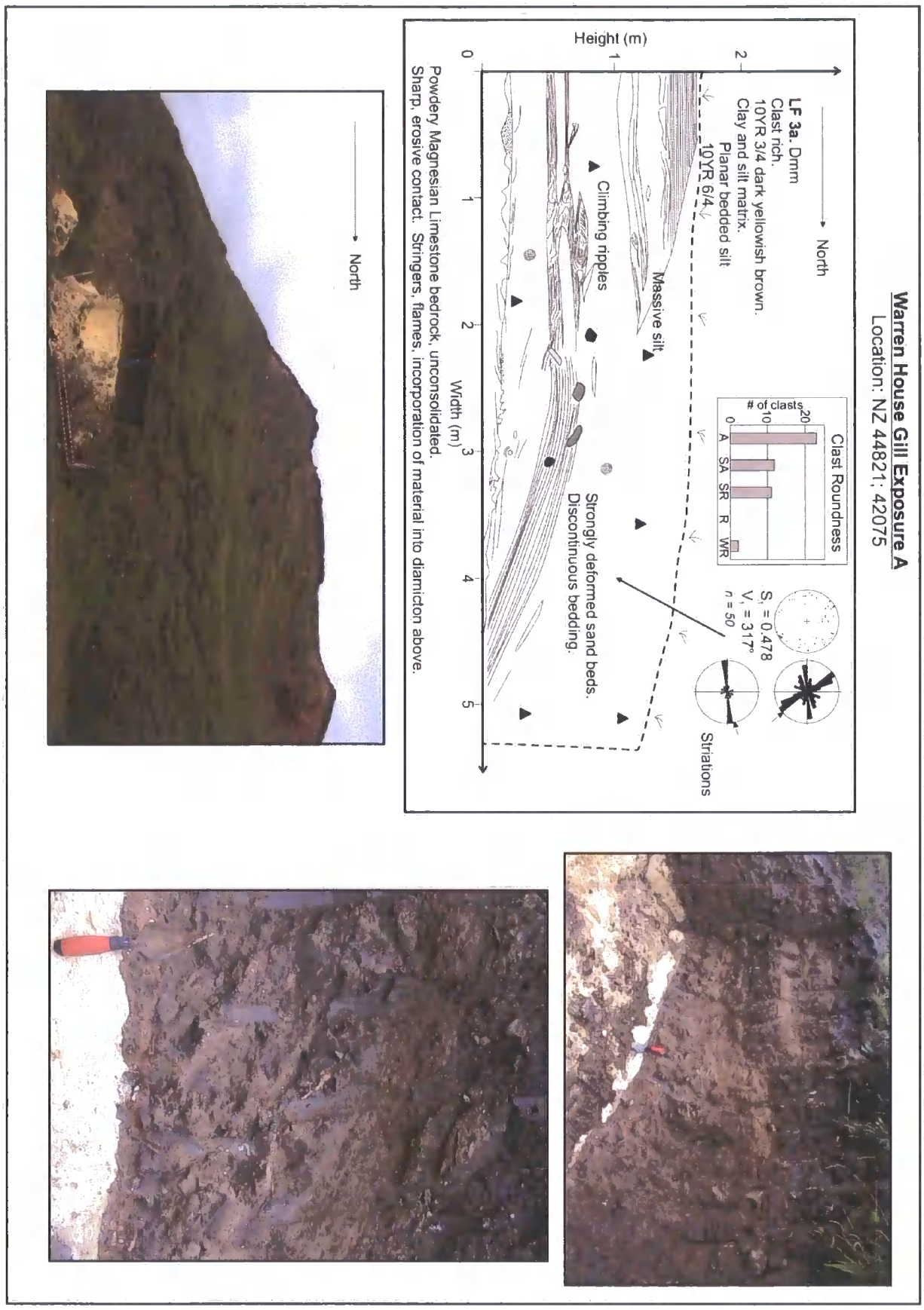

Figure 6.24: Sketch and photographs of LF 3a, Exposure A, Warren House Gill. Clast Fabric: S_1 = 0.478; S_2 = 0.402; S_3 = 0.120.

LF 3a is well exposed in Exposure B (Figure 6.15 and Figure 6.16), where it contains predominantly sub-angular to angular clasts, and has a weak clast macro-fabric, with an S_1 value of 0.57. The clasts indicate an orientation from northeast to southwest. This is supported by the stringers emanating from point sources within the diamicton; the smearing out of sandstone and limestone follows a north-south orientation. Within the diamicton are numerous sand lenses with convex bases and flat tops, containing bedded sands (Figure 6.16). Although part of the exposure is covered with colliery waste, the vertical profile (Figure 6.3) shows that this diamicton is over 35 m thick. At 53 m O.D., the diamicton is overlain by LF 4a, the red-bedded sands.

In Exposure C, there are vast thicknesses of LF 3a, interbedded with LF 3e and LF 3f (laminated diamictons; Figure 6.25). A large recumbent sand fold (LF 3c) of coarse, bedded, poorly sorted sand and gravel, is situated within LF 3a at the base of its outcrop (Figure 6.18). At this location, LF 3a is characterised by a dark brown, clast-rich diamicton, with faceted, striated and bullet-shaped clasts. Stringers emanating from point sources are clearly apparent, and are orientated north-south.

In Exposure E1, a narrow, massive diamicton overlies LFA 2 (Figure 6.26). Bedrock was not reached in this trial pit. This diamicton (LF 3a) is overlain by a large, well-bedded sand, upturned sub-vertically. Above this bedded sand, LF 3a again crops out. It is a massive, clast-rich diamicton, with abundant sandstone and limestone clasts. It is characterised by smeared soft clasts such as red marl.

On the northern side of the Warren House Gill stream, as the bedrock rises, LFA 3 is more massive. There are few pods of sand, but there are still stringers from point sources. In Exposure G, the clast macro-fabric remains weak with an S_1 value of 0.57. The a-axes are clustered from a north-westerly to a south-easterly direction. LF 3a here is a dark brown colour, with abundant gravel, including Carboniferous Limestone, sandstone, coal, orthoquartzite, and Magnesian Limestone. Stringers from point sources (such as deformable soft clasts) extend from north to south. It is overlain by LF 4a, the red-bedded sands.

A number of clast macro-fabrics taken from LF 3a, mostly at the base of the lithofacies (around 10-20 m O.D.) showed that although the S_1 values are generally not that strong (~0.5), the S_1/S_3 comparison indicates clustering around the principal eigenvector (V_1). Figure 6.27 illustrates the variation in eigenvectors. The axis of V_1 remains fairly

consistent throughout all of the fabrics in this facies, indicating primarily a northwest-southeast orientation.

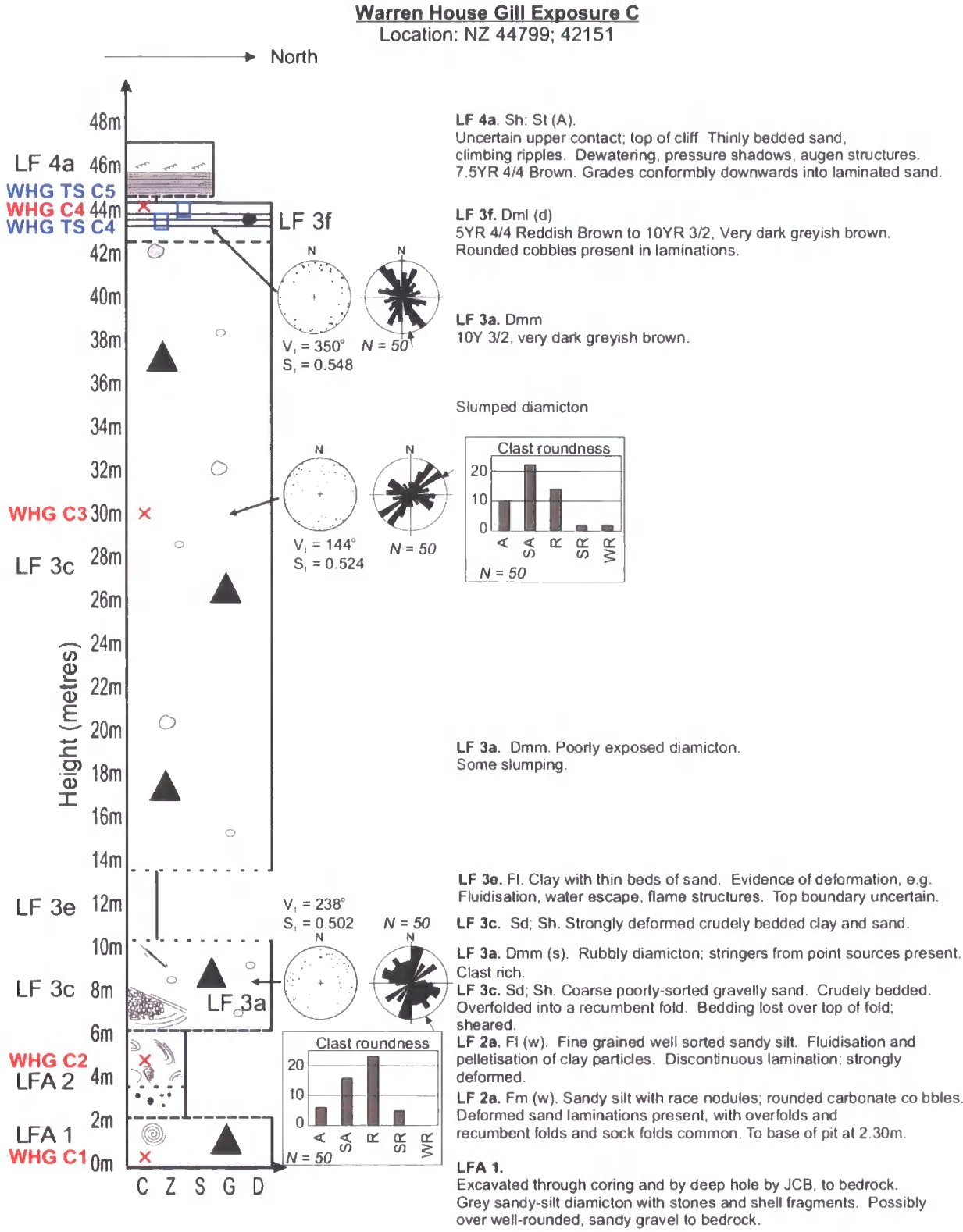

Figure 6.25: Vertical profile of Exposure C, Warren House Gill, showing sample locations.

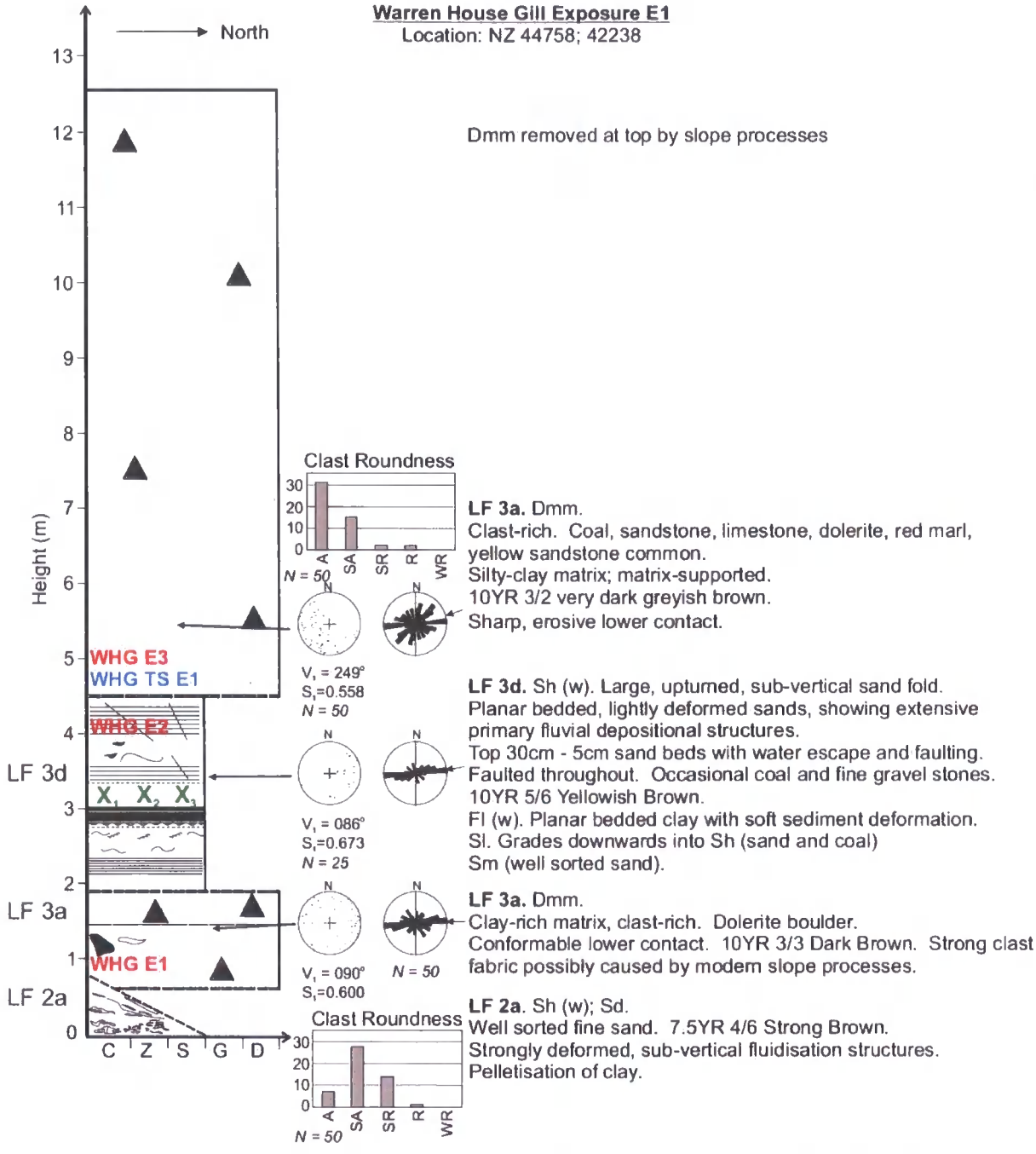

Figure 6.26: Vertical profile of Exposure E1. Clast macro-fabric values: Lower clast fabric (LF 3a); S_1 = 0.600, S_2 = 0.312, S_3 = 0.154. Upper clast macro-fabric (LF 3a): S_1 = 0.558; S_2 = 0.327; S_3 = 0.114.

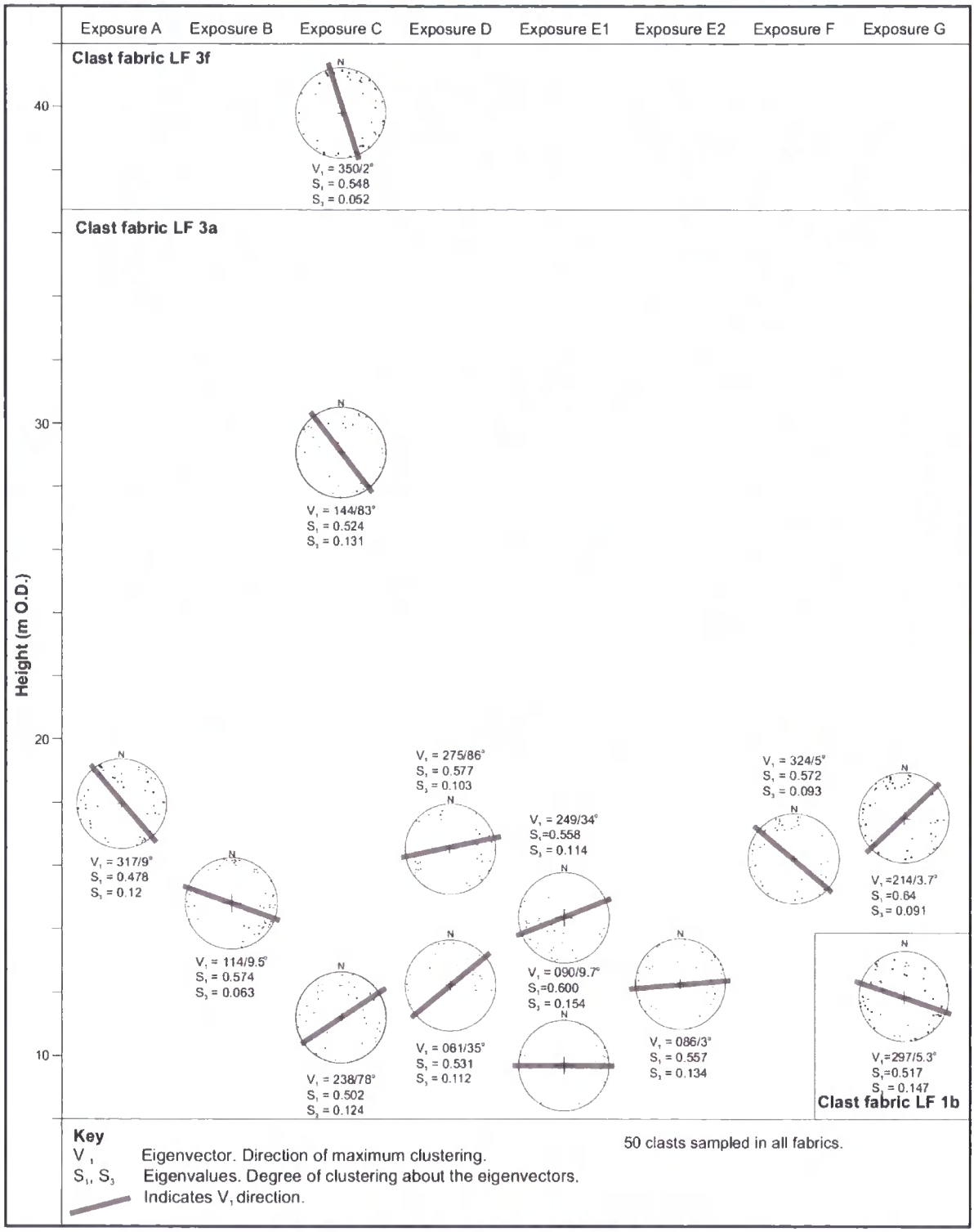

Figure 6.27: Clast macro-fabric data from Warren House Gill

Thin Section Analysis: LF 3a

WHG TS D*iv* was taken from LF 3a, the diamicton immediately above LF 2b in Exposure D (Figure 6.28 and Table 6.3). Macroscopically it is a massive, homogenous diamicton, with one large sub-rounded skeleton grain. There are several rounded and

augen-shaped intraclasts (Figure 6.29). There are a couple of large vugh voids (processing artefacts). The contact with LFA 2 is unfortunately not visible in this thin section.

Most of the skeleton grains are sub-rounded, though the finer skeleton grains are more angular. They consist of a variety of lithologies, from Type II and III Pebbles to coal grains, limestone, siltstone, red marl, several schist, basalt, and other igneous lithic fragments, plagioclase feldspar, and quartz. There are rare small shell fragments. Smaller grains are arranged around larger skeleton grains in turbates, which are often associated with pressure shadows and lineations. The soft intraclasts show evidence of rotation and incorporation into the matrix. These pebbles often have their own internal plasmic fabric. The diamicton matrix material has a strong masepic/skelsepic plasmic fabric (Figure 6.29).

WHG TS C5 (Figure 6.30, Figure 6.31 and Table 6.3) was taken from LF 3a, Exposure C, above the laminations (Figure 6.25). On macroscopic inspection, it is a massive, dark-brown, matrix-supported diamicton, with several large angular skeleton grains and many fine sand grains. Matrix material is evenly distributed across the slide. WHG TS C5 has angular to sub-angular skeleton grains under the microscope. It is poorly sorted with a wide range of skeleton grains, which include coal, quartz, intraclasts and sandstone. Type II and III Pebbles are present and there are rotational structures with associated skelsepic plasmic fabrics. There are rare marine foraminifera fossils.

Table 6.3: Micromorphological Summary of LFA 3.

Sample	Location	Facies	Skeleton			Matrix		Void type	Sedimentary Structures				Deformation Structures													Plasmic Fabric				
			Sorting	Grain shape <500µm	Grain shape >500µm	Texture	Microfabric		Laminations	Dropstones	Microfossils	Dump Structures	Section Elements	Faulting	Folding	Rotations	Grain lineations	Pressure Shadow	Crushed Grains	Grain stacks	Pebble Type I	Pebble Type II	Pebble Type III	Water escape	Fluidised Bedding	Skelsepic	Lattisepic	Masepic	Bi-Masepic	Unistrial
WHG Ex D2	Ex D2	LF 3b	D	SA	SA - SR	F		P L					Be; Bo; Ba; F St			●●●	●●●	●		●		●●	●●●			●●●		●●●		
WHG E1	Ex E above sands	Massive diamicton LF 3a	D	SR	SA-SR	F		L			●					●●	●					●●	●●			●●		●		
WHG C5	Ex C	Massive diamicton LF 3a	D	A - R	A	F		P L			●					●●●	●	●		●		●●	●●●			●	●			
WHG D4	Ex D 2.4m	LF 3a	D	SA	SA - SR	F		L								●●●	●●●	●		●		●●	●●●			●●●		●●●		
WHG C4	Ex C	Laminated diamicton LF 3f	D	SA - R	SA	F		P L					Be; St			●●●	●●	●	●	●●			●●●			●●●		●		

Key

Sorting

WS	Well sorted
MS	Moderately sorted
PS	Poorly sorted
D	Diamicton

Grain shape

WR	Well rounded
R	Rounded
SA	Subangular
A	Angular

Microfabric

H	Horizontal Microfabric
V	Vertical microfabric

Voids

P	Packing induced
L	Laboratory induced

Texture

F	Fine grained
C	Coarse (no fine silt/clay)
M	Medium (some fine silt/clay)

Section Elements

Ba	Banding
Bo	Boudinage
Be	Bedding
Sh	Shear
F	Flow
St	Stringer

●●● Indicates feature is strongly present / numerous

●● Indicates feature is present

● Indicates feature is rarely / occasionally present

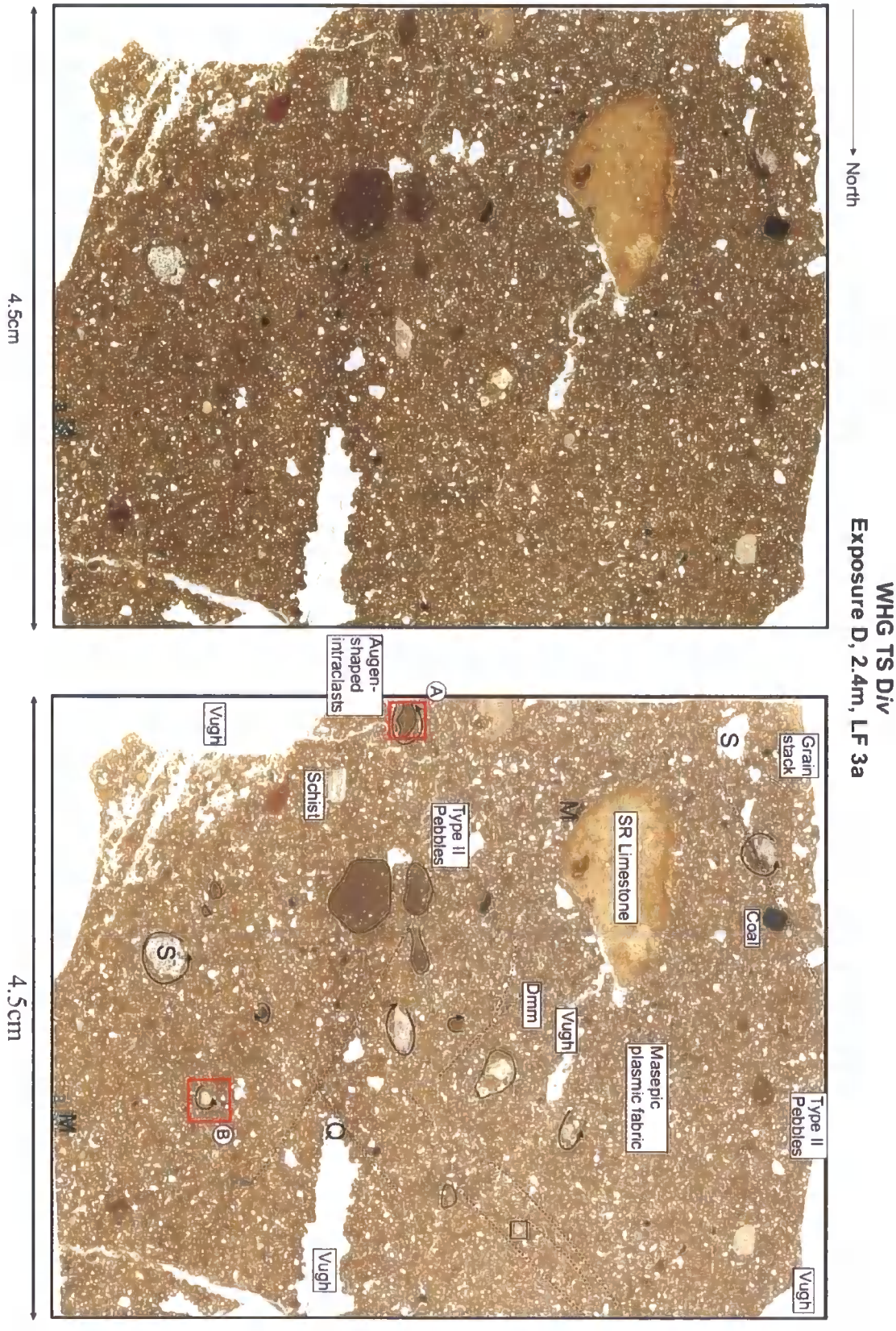

Figure 6.28: Thin section slide from WHG TS D*iv*, taken from LF 3a, Exposure D, 2.4 m. Locations of features which are sub-resolution of the scan are highlighted, such as grain stacks, strong plasmic fabric development and grain lineations. S - Sandstone. Q – Quartz grain.

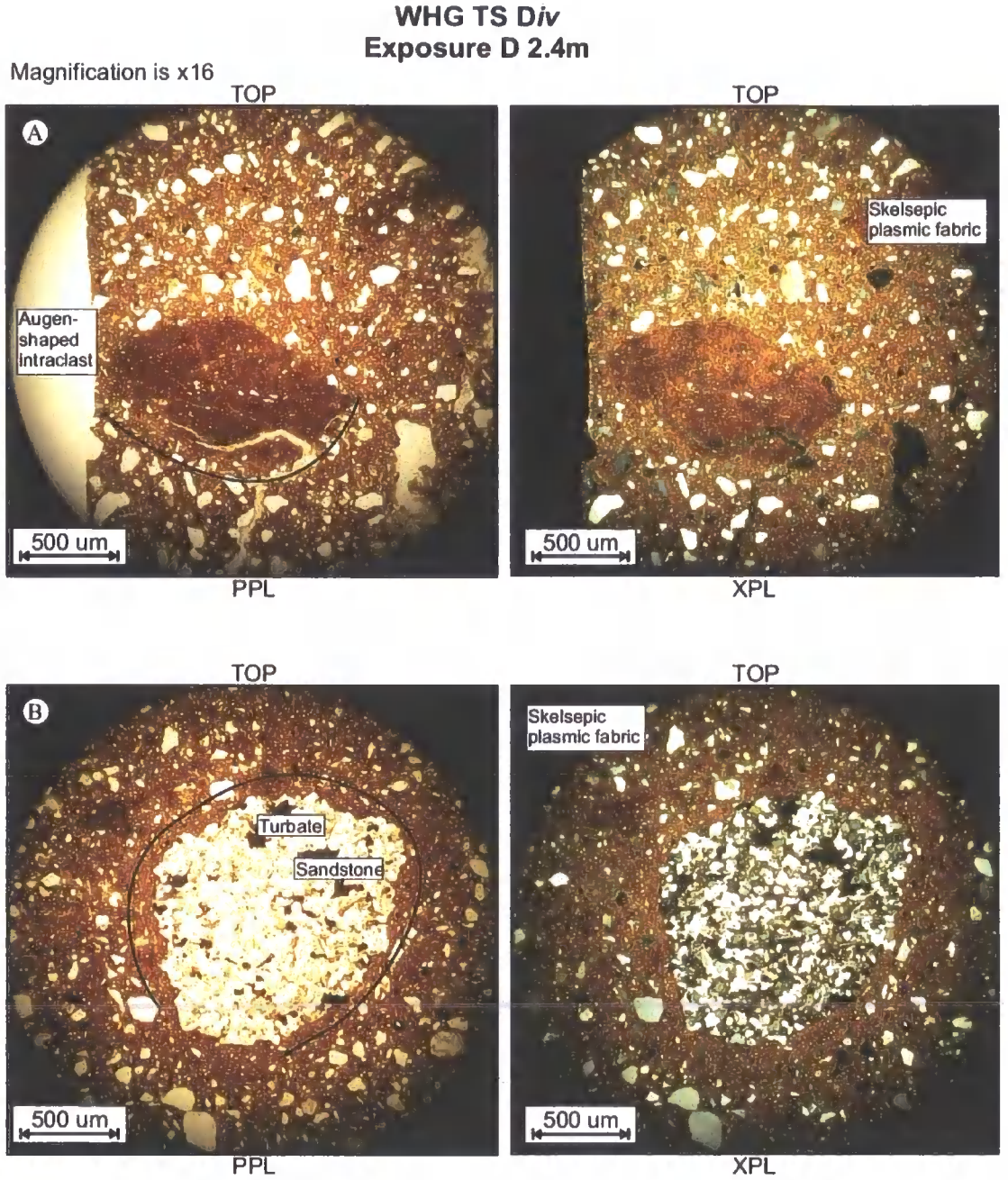

Figure 6.29: Photomicrographs of WHG TS D*iv*, showing rotational structures and augen-shaped, rotated intraclasts.

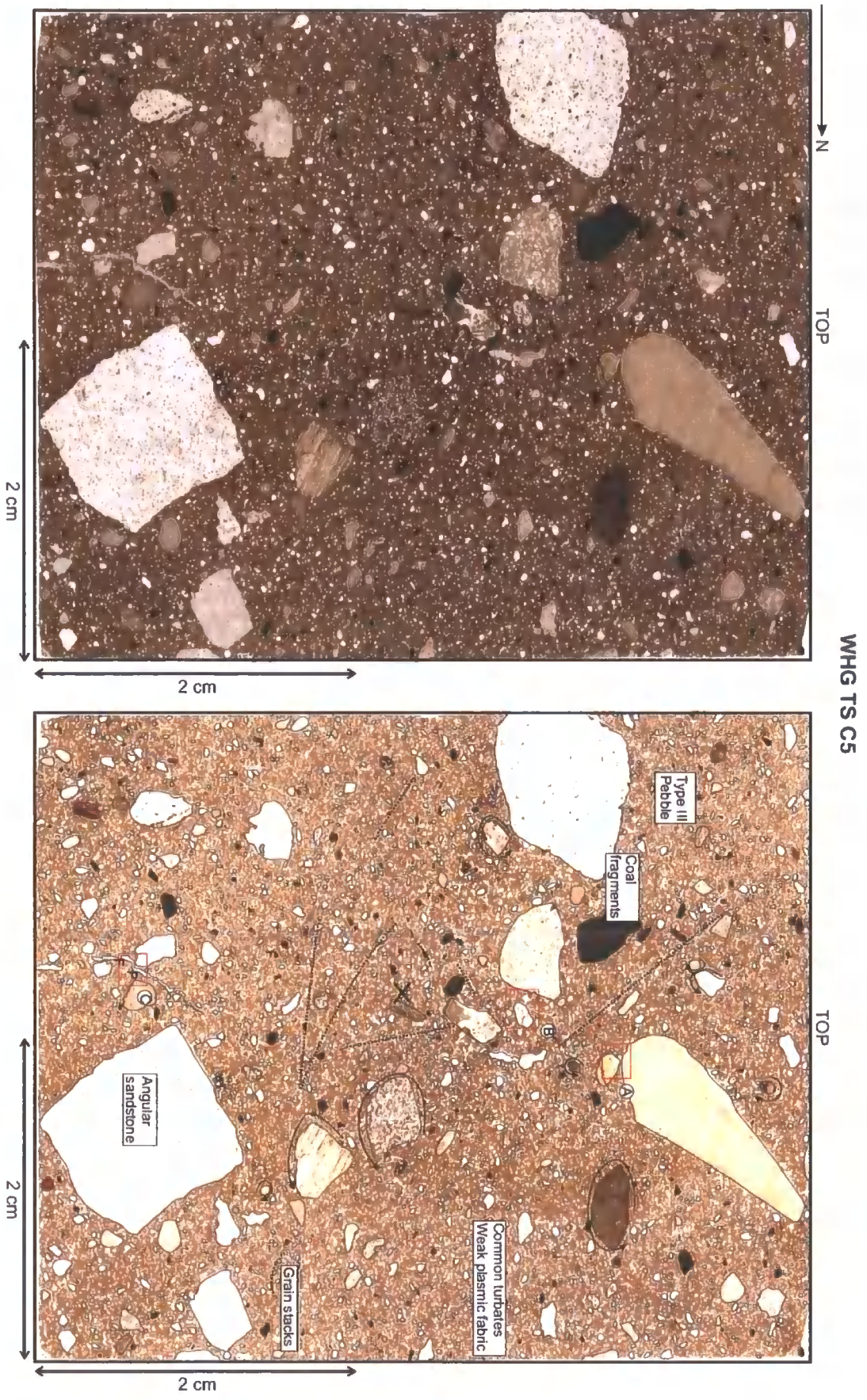

Figure 6.30: Thin Section sample WHG TS C5, LF 3a, taken directly above laminations in Exposure C, Warren House Gill. Location of sub-resolution features is annotated on diagram.

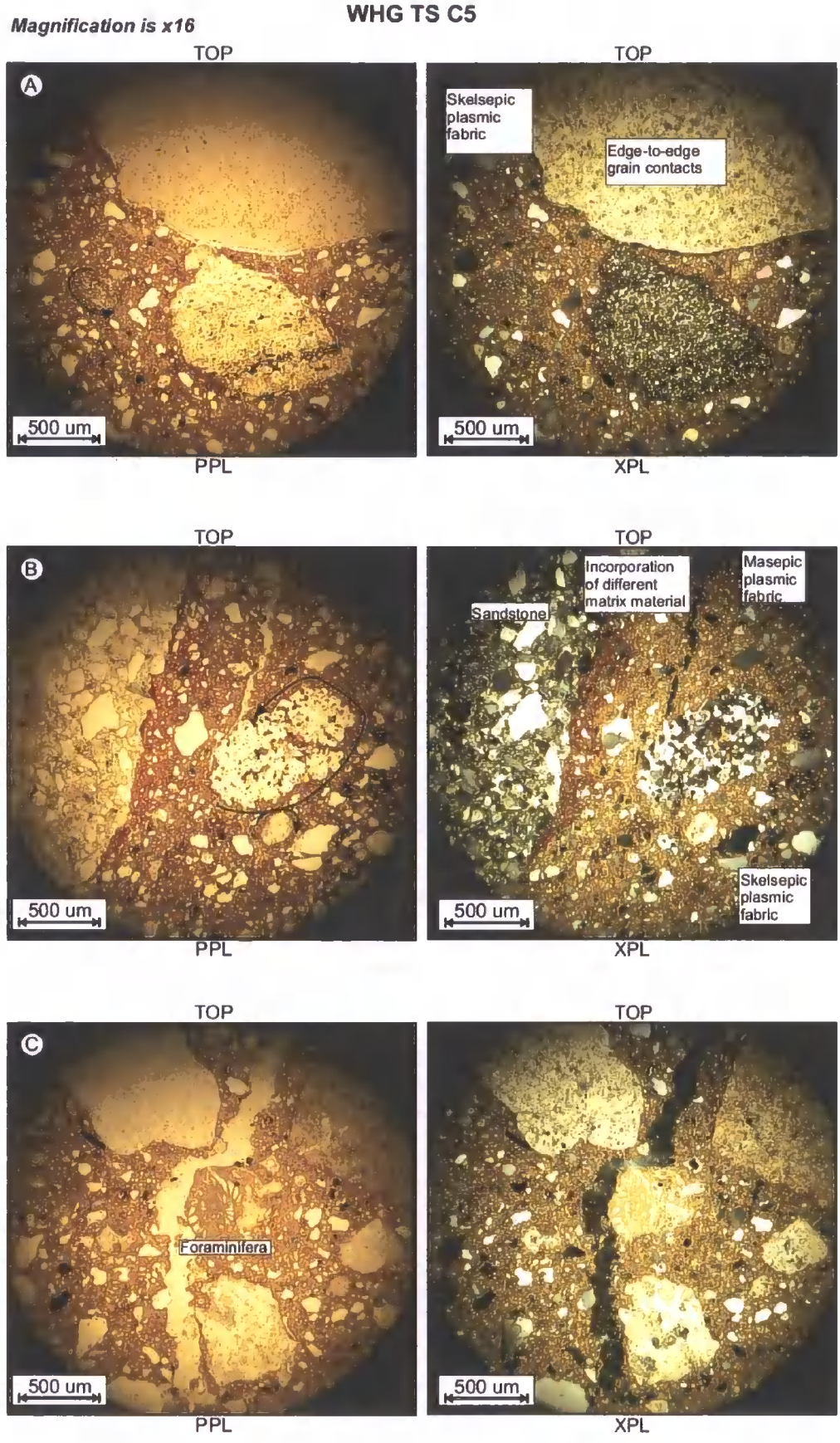

Figure 6.31: Photomicrographs of WHG TS C5, showing edge-to-edge grain contacts, plasmic fabrics, and marine microfossils.

WHG TS E1 was sampled from the diamicton above the sand fold in Exposure E1 (Figure 6.26). It is characterised macroscopically by the unusual, branching, dendritic voids (Figure 6.32). It is a diamicton with large, irregularly shaped lithic fragments. Dark coal grains are abundant. Other lithic grains include quartzite, oolitic limestone, basalt, granite, sandstone, pyrite, micro-granite, and siltstone. The sediment is well consolidated, but has an uneven matrix density.

The dendritic, irregular voids have diffuse boundaries, and the edges of the voids are paler, indicating leaching (Figure 6.33 C). They are discontinuous, and wind through the sediment. Associated with the voids are woody organic fragments and framboid pyrite nodules (Figure 6.33 A and B). These could be modern or ancient root fragments. Some of the voids are stained with manganese. The lithologies of the skeleton grains are variable, and include quartz, oolitic limestone, coal, granite and microgranite, siltstone, and soft intraclasts. They are irregular and sub-angular in shape. Structural analysis indicates the presence of turbates and lineations of grains. Some of the coal grains are fractured. The fines are orientated around fine skeleton grain to form a skelsepic plasmic fabric (Figure 6.33).

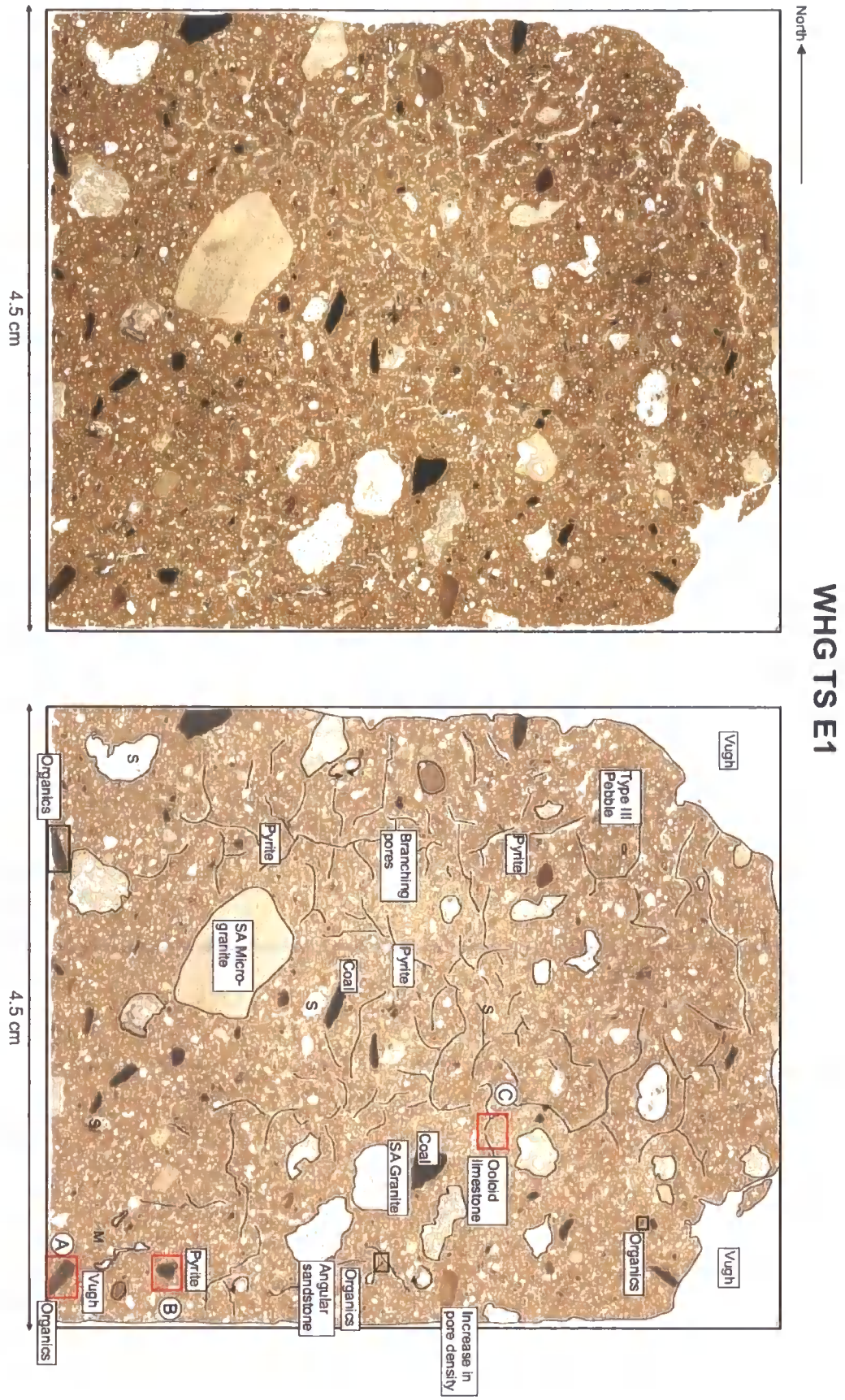

Figure 6.32: Thin section slide WHG TS E1, from LF 3a, Exposure E1, above sand fold. Location of sub-resolution features is annotated on slide.

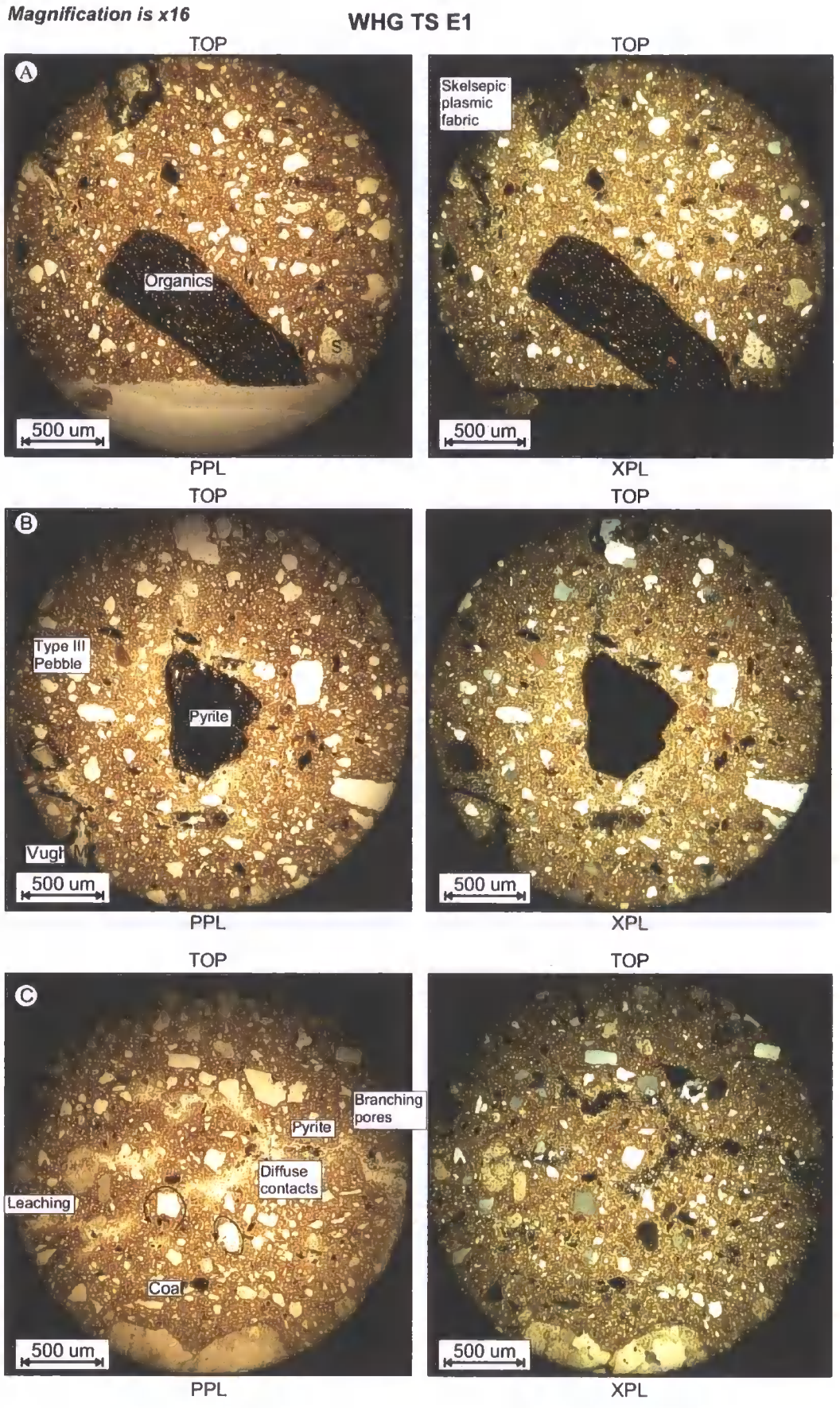

Figure 6.33: Photomicrographs, WHG TS E1

LF 3b: Tectonite facies

The contact between LFA 2 and LFA 3 is poorly exposed but is visible in Exposure D2 (LF 3b), where they are complexly interbedded. LF 2a is well exposed in the base of the trial pit, and is overlain sharply and unconformably by a dark brown diamicton (LF 3a). The silts show evidence of shear, loading and soft sediment deformation (Figure 6.34). Above this, the diamicton is interbedded and mixed with coarse, poorly-sorted sands (LF 3b; Figures 6.25 and 6.26).

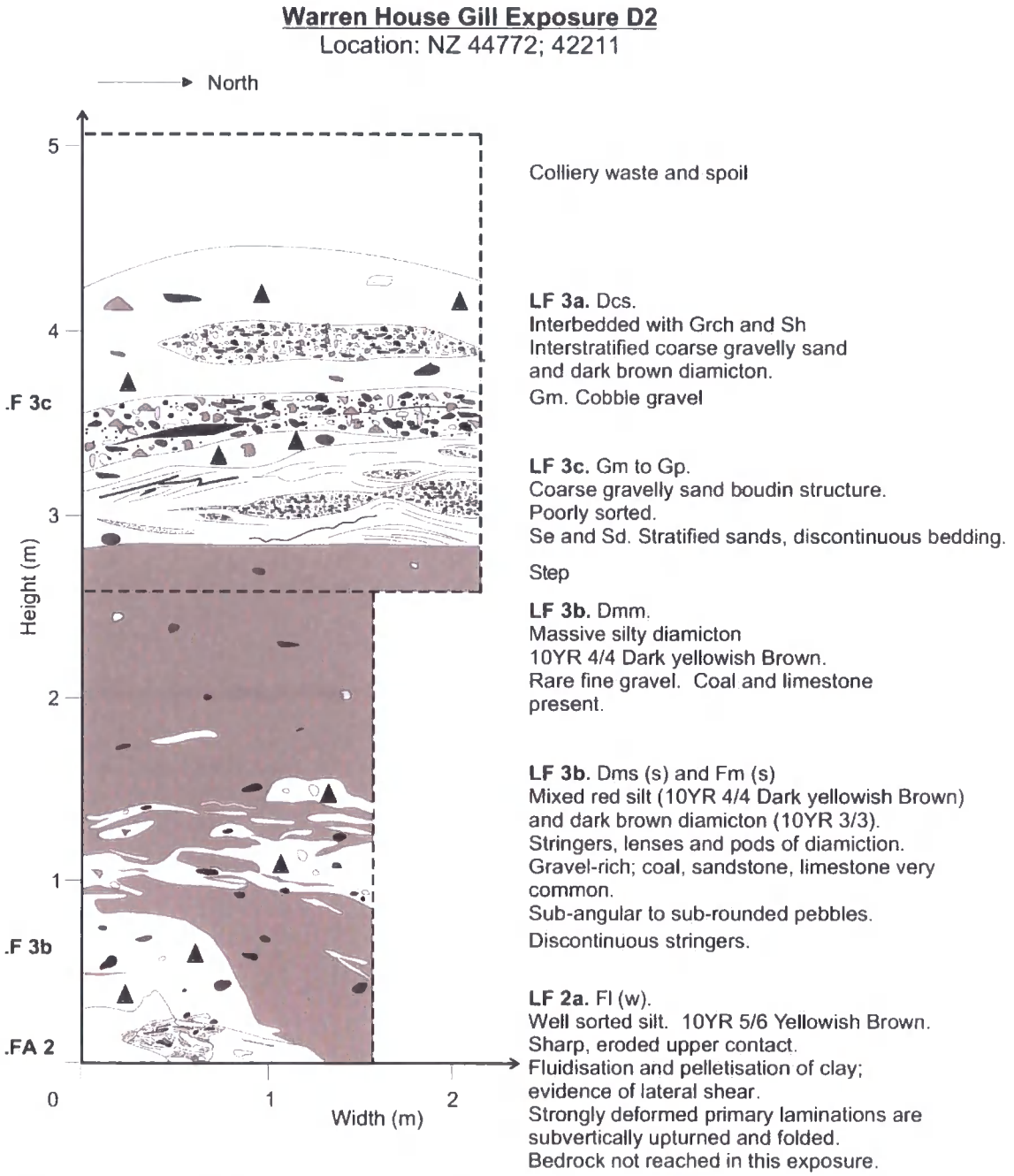

Figure 6.34: Sketch of Exposure D2, LF 3b, Warren House Gill, showing contact between LFA 2 and LF 3b.

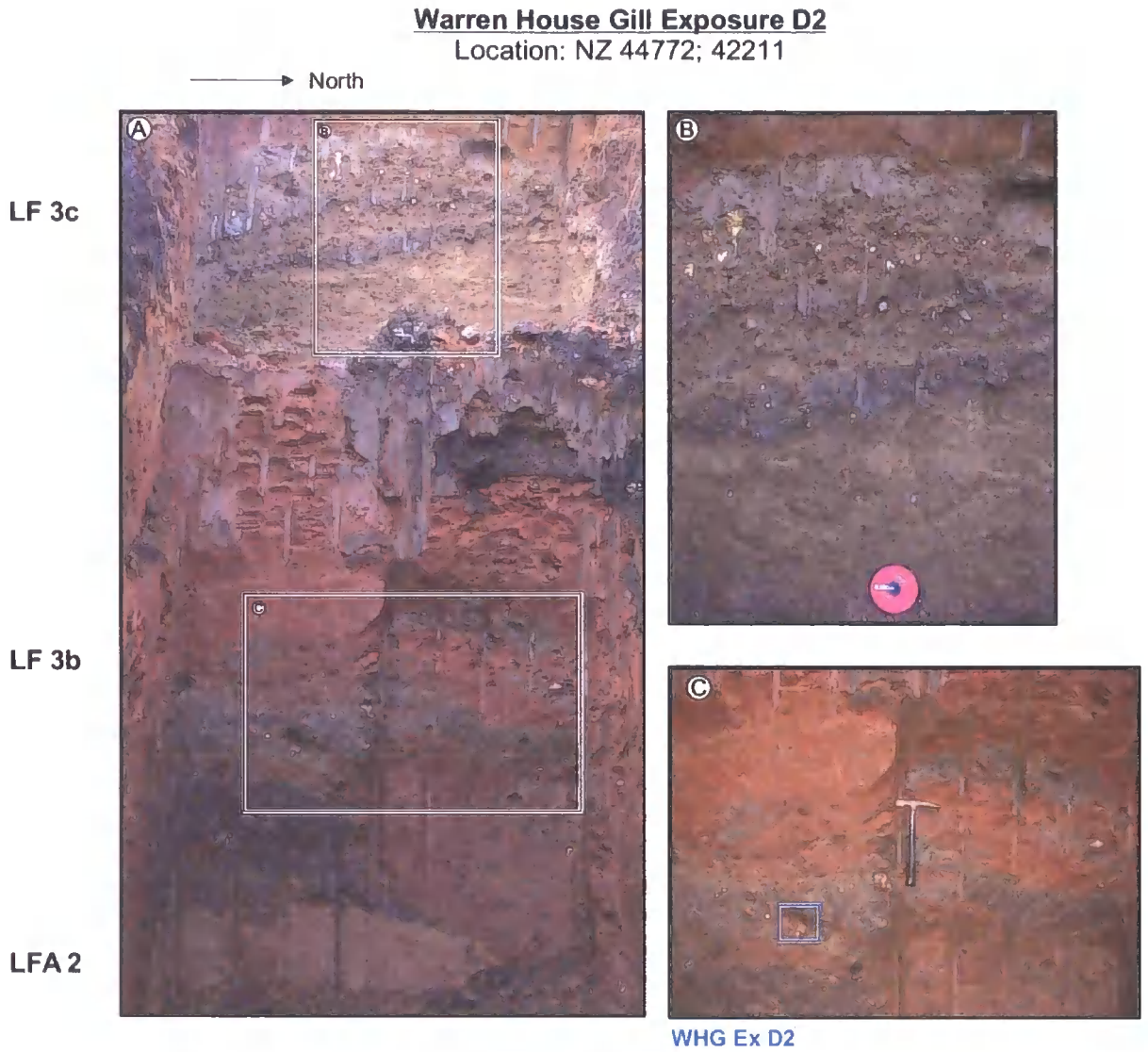

Figure 6.35: Photographs of Exposure D2, showing location of thin section sample WHG Ex D2 within the interbedded diamicton and red sands/silts (Photograph C). LF 3a shows pinching and swelling interbedded sand, gravel and diamicton (Photograph B). LF 3b exhibits interbedded diamicton and sand, with stringer formation into LF 3a above. Geological hammer for scale is 32 cm long.

Thin Section Analysis: LF 3b

WHG ex D2 was taken from LF 3b, the interbedded, tectonised contact between LFA 3 and LFA 2 in Exposure D2 (Figure 6.35). The slide is characterised and divided by the bright red sands, which dissect the brown, poorly-sorted diamicton (Figure 6.36). The larger fine gravel skeleton grains are sub-rounded and irregularly dispersed. The matrix is consolidated and is unevenly distributed across the slide.

The skeleton grains include limestone, sandstone, quartz, feldspar, basalt and other igneous lithic fragments, shell fragments, and soft sediment pebbles (Figure 6.37 A; Table 6.3). The contact between the sands and diamicton varies between sharp and diffuse

(Figure 6.33 C), while the diamicton is characterised by subtle banding. Individual bands are boudinaged and deformed. Within the diamicton, there are grain lineations and turbate structures, including rotated, augen-shaped intraclasts (Figure 6.37 B). Plasma has been squeezed between skeleton grains as a 'necking' structure. Rotations are also associated with pressure shadows (Figure 6.37). There is a limited amount of skelsepic plasmic fabric development in both the sands and diamicton.

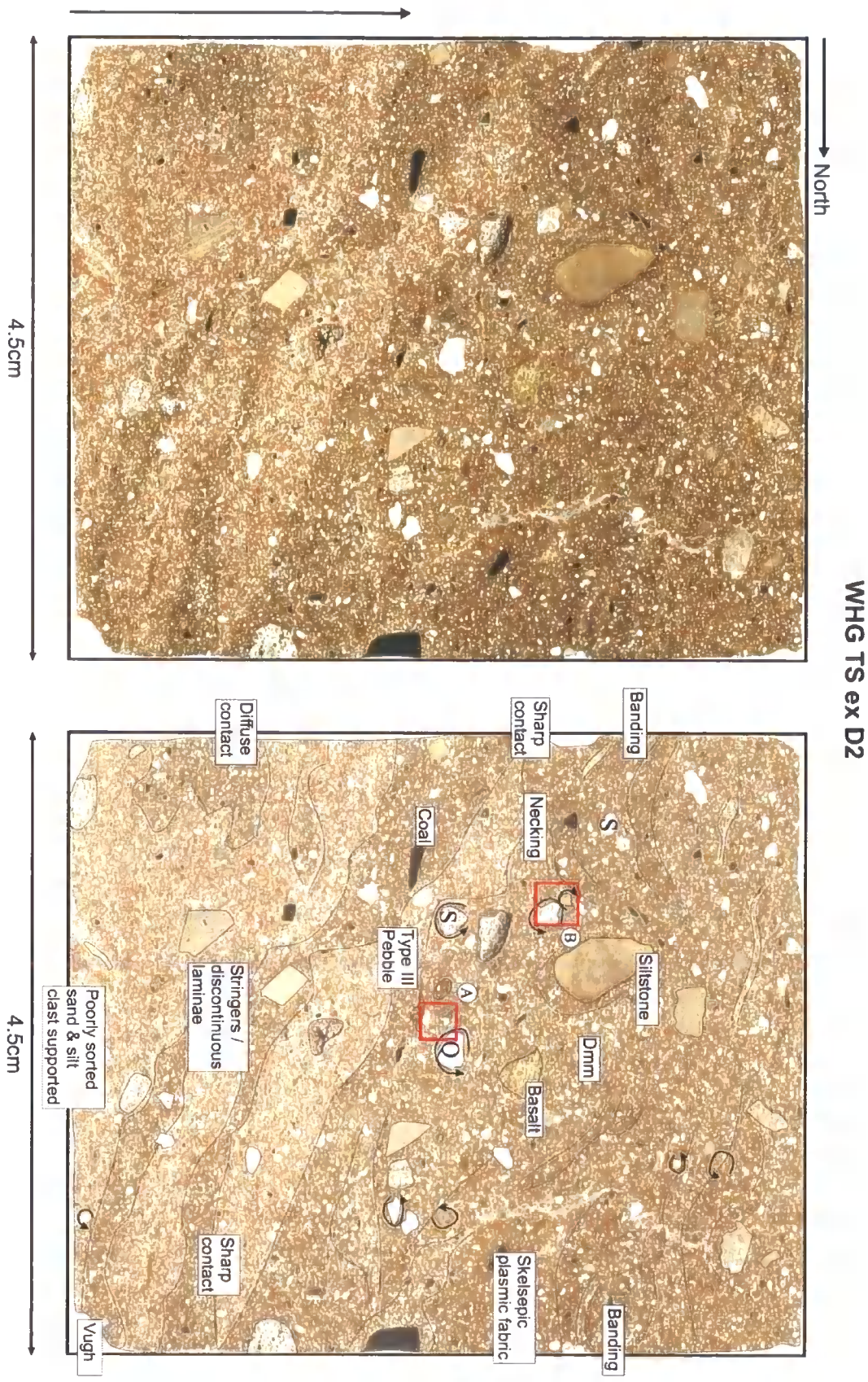

Figure 6.36: Thin section sampled from interfingering LFA 3 and 2 at Exposure D2, Warren House Gill. Location of strong plasmic fabric development is shown. S – Sandstone. Q – Quartz grain.

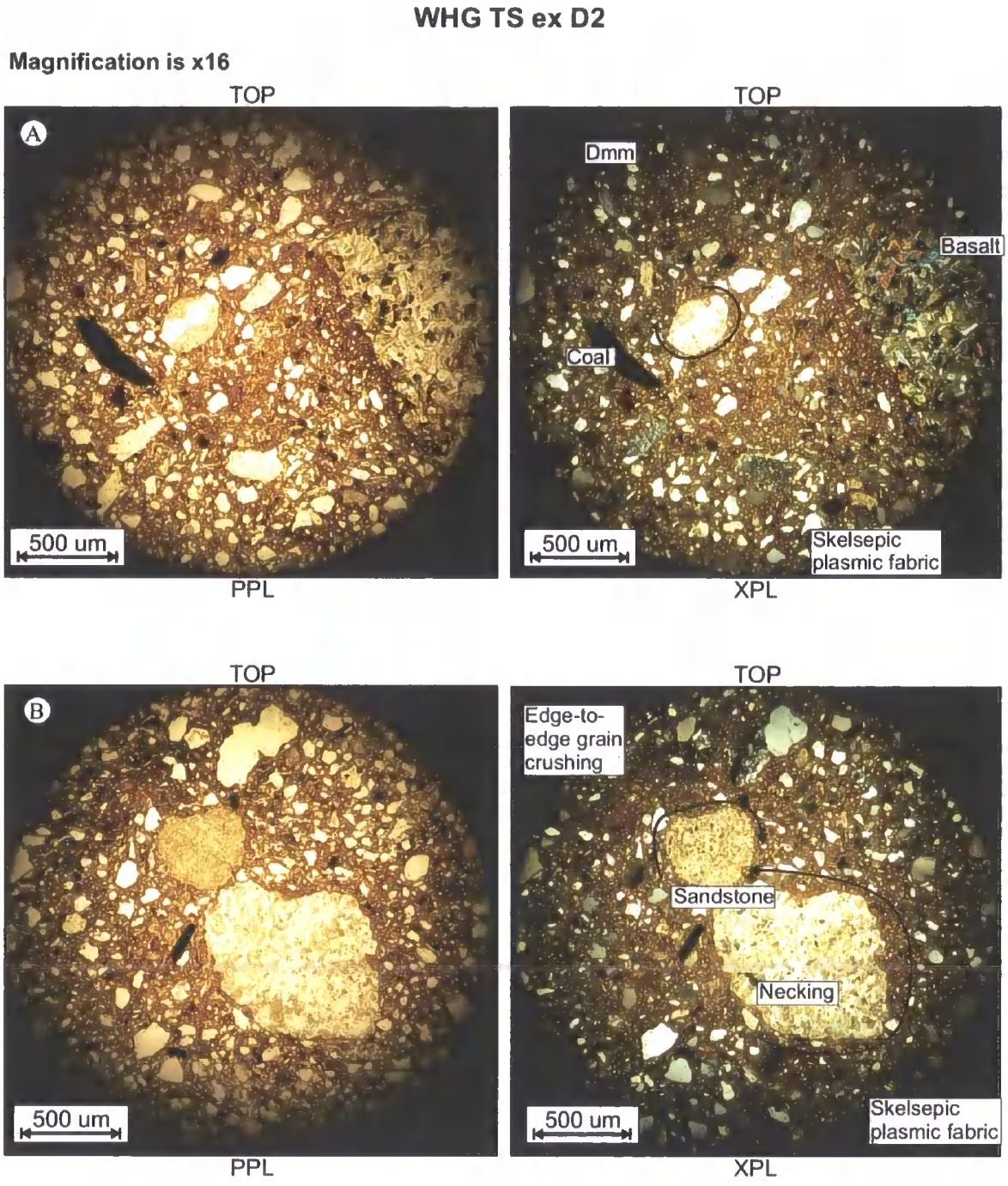

Figure 6.37: Photomicrographs of thin section WHG Ex D2, showing plasmic fabric, rotational structures, and bedding.

LF 3c: Interbedded sand and gravel facies

LF 3c is highly variable and encompasses strongly deformed, faulted, folded, discontinuous, bedded sands and gravels, which pinch and swell (e.g., Figure 6.38; LF 3c). It is interbedded into LF 3a at low heights (approximately 10 m O.D.) in the buried

palaeovalley. Examples of this can be seen in exposures B, C, D, D2 and E2 (Figures 6.8 and 6.24).

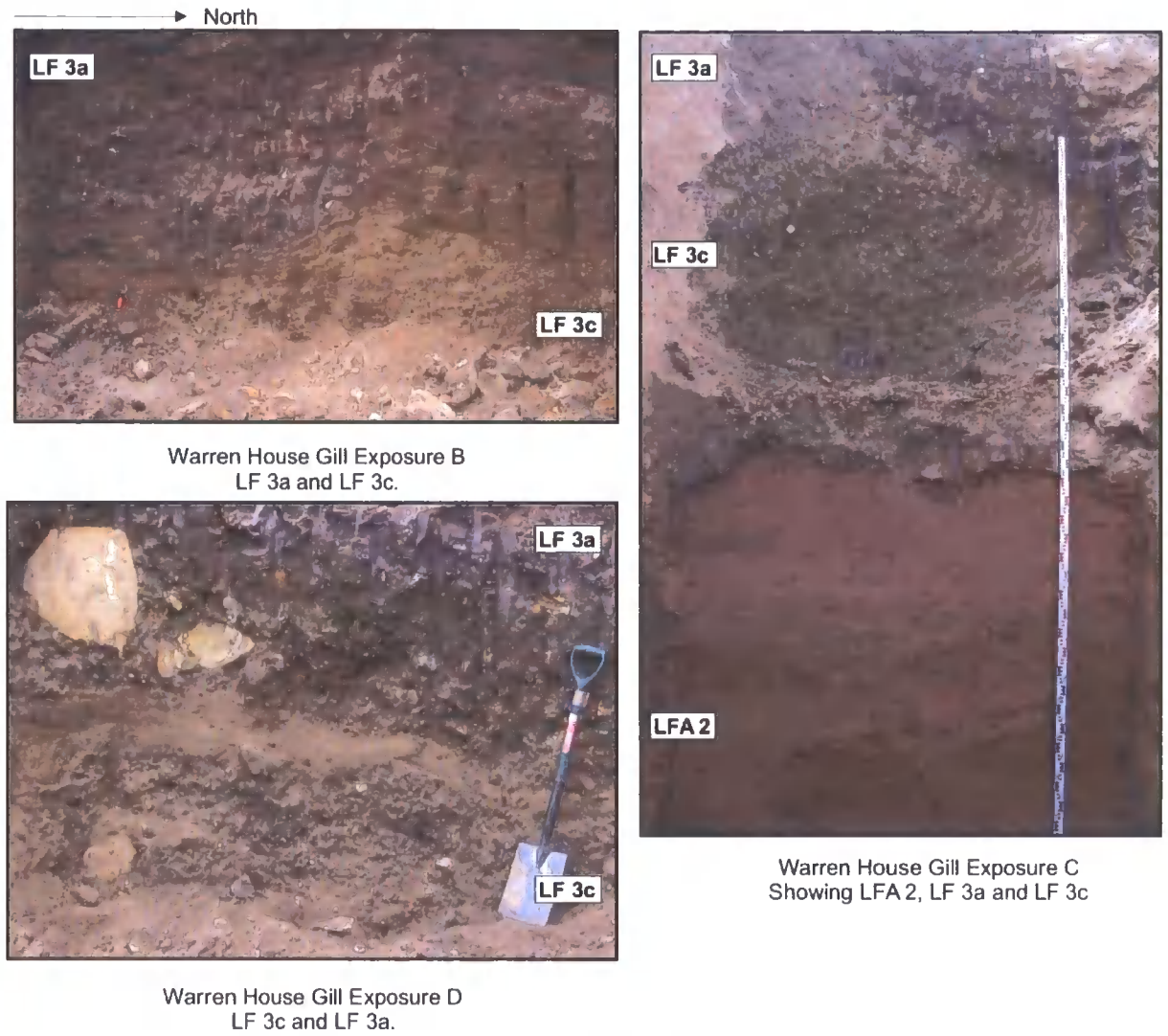

Figure 6.38: Photographs of tectonised sand lenses of LF 3c interbedded with LF 3a (the Middle Diamicton). LF 3c of Exposure B contains recumbently folded beds of coarse sand and well-sorted fine gravel. Exposure D contains poorly-sorted, coarse gravelly sand which pinches and swells. LF 3c of Exposure C contains a large recumbently folded bed of coarse, poorly-sorted sand and gravel. Spade is 1 m long.

The strongly deformed bedded sands in Exposure B (LF 3c; Figure 6.15) comprise interbedded coarse, poorly sorted sands and moderately sorted medium sand. The sands are folded into a large recumbent fold. They continue to the south as stratified sands. They fine upwards from a poorly-sorted, clast-supported, coarse sand and gravel to a moderately-sorted sand. The coarse sand and gravels are incised into the diamicton below. In Exposure D2 (Figure 6.25), the bedded sands (LF 3c) pinch and swell, and are interbedded with the dark brown diamicton (LF 3a).

LF 3c in Exposure C (Figure 6.38) comprises a large bed of crudely bedded, coarse, poorly-sorted sand and gravel, recumbently folded but still exhibiting numerous primary bedding structures (Figure 6.18). The diamicton within which it is exposed (LF 3a) is gravel-rich, containing abundant limestones and sandstones, with a weak clast macro-fabric (S_1 value of only 0.5), showing a weak clustering of the a-axes from northeast to south-west (Figure 6.25).

LF 3d: Planar bedded sand facies

In Exposure E1, LF 3a overlies a well-sorted fine sand (LF 2a; Figure 6.26) with abundant sub-vertical fluidisation and soft-sediment deformation structures. It is overlain by a diamicton (LF 3a) with a strong clast macro-fabric (Figure 6.39). LF 3a is dissected by a large sub-vertical fold of sand (LF 3d; Figure 6.40). The sand retains many original primary depositional features such as sand and clay couplets, draped ripples, dunes, planar-bedded sand, and pebble lags. It is crosscut by normal faults that have a consistently strong orientation from northeast to southwest. There is strong evidence of water escape, soft sediment deformation and faulting as the angle of the bedding increases from horizontal to vertical (Figure 6.40).

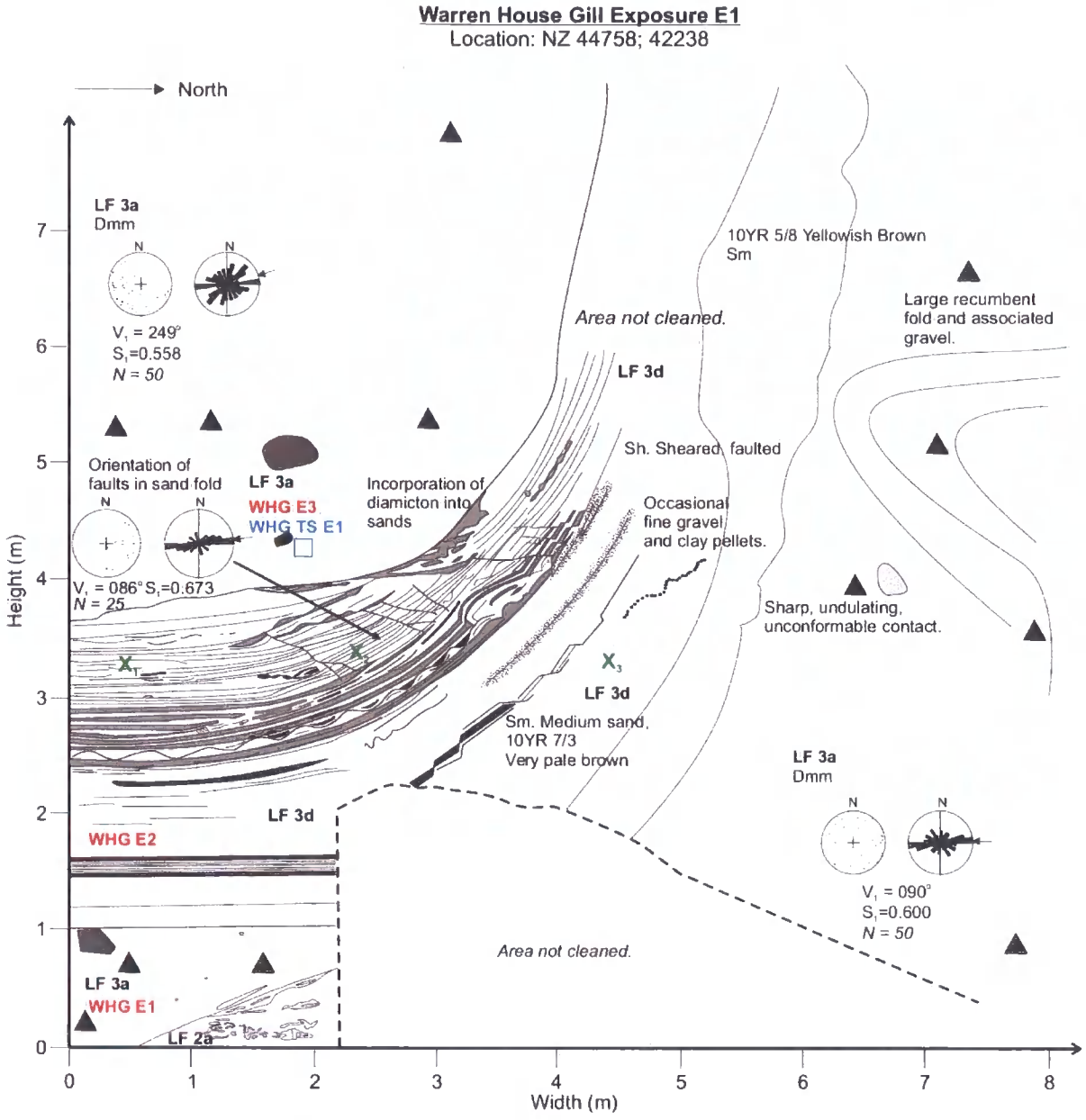

Figure 6.39: Detailed sketch of sand fold in Exposure E1, Warren House Gill. Green crosses represent OSL samples.

LF 2a: Well-sorted fine sand, 7.5YR 4/6 Strong Brown. Strongly deformed, fluidised, rounded clay intraclasts.

LF 3a (below sand fold): Diamicton, silty-clay matrix, unconformably overlies LF 2a. 10YR 3/2 Very Dark Greyish Brown. Gravel-rich with faceted, striated, far-travelled clasts, ranging from fine gravel to boulders. Magnesian Limestone, dolomite, dolerite, coal and sandstone common.

LF 3f: Large sand bed, upturned sub-vertically. Planar bedded, lightly deformed. 10YR 5/6 Yellowish brown.

LF 3a (above sand fold): Massive diamicton, gravel-rich, 10YR 3/2 Very dark greyish brown. Silty-clay matrix, matrix-supported. Sharp, erosive lower contact.

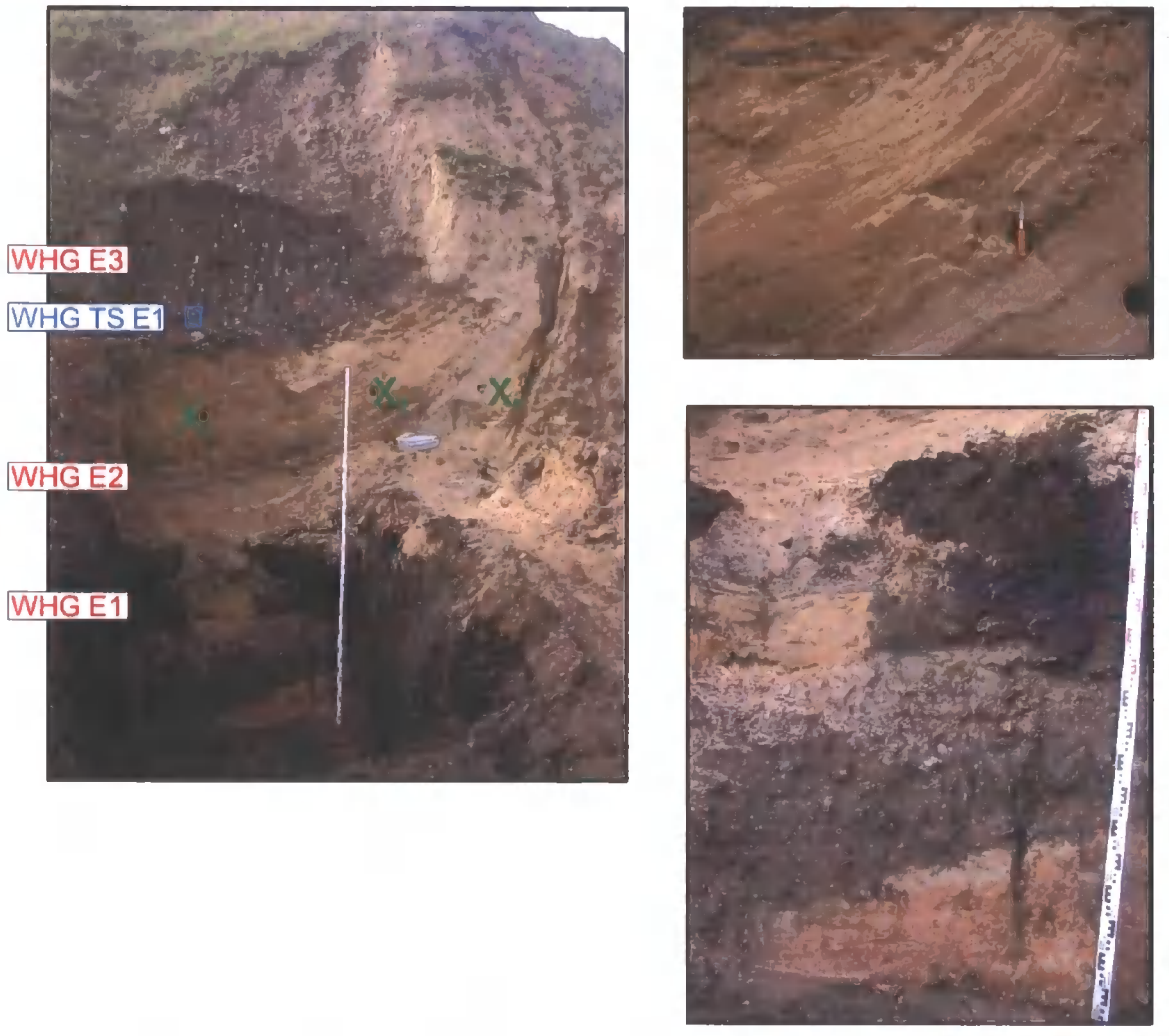

Figure 6.40: Photographs of Exposure E1, Warren House Gill, showing location of thin section sample WHG TS E1. Detail of faulted beds in sand fold are shown (Penknife for scale is 19 cm long when extended). Contact between LFA 2 and 3 is shown. LF 2a can be seen as the pink-beige silts in the bottom-right picture.

LF 3e and LF 3f: Laminated Diamicton Facies

In Exposure C at 10 m height in the section there are a number of 10 cm thick beds of well-sorted clay (LF 3e). This is overlain by LF 3a, unfortunately poorly exposed (Figure 6.25). Towards the top of Exposure C, sets of alternating very dark greyish brown, very dark grey, and reddish brown diamict laminations occur (LF 3f). Clasts and cobbles have deformed laminations below, and laminations are draped over them (Figure 6.41). Contacts are conformable and the laminations are normally graded. Thin-section samples of this investigate the laminations in more detail.

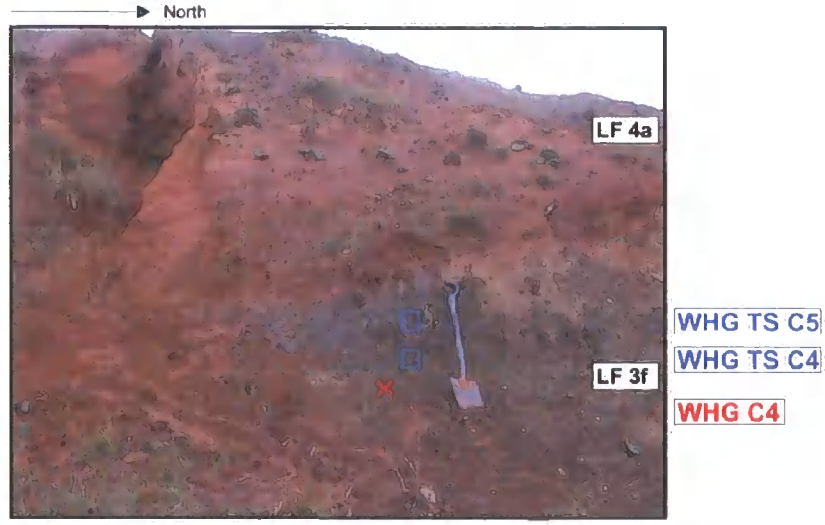

Exposure C LF 3d and LF 4a,
Warren House Gill.

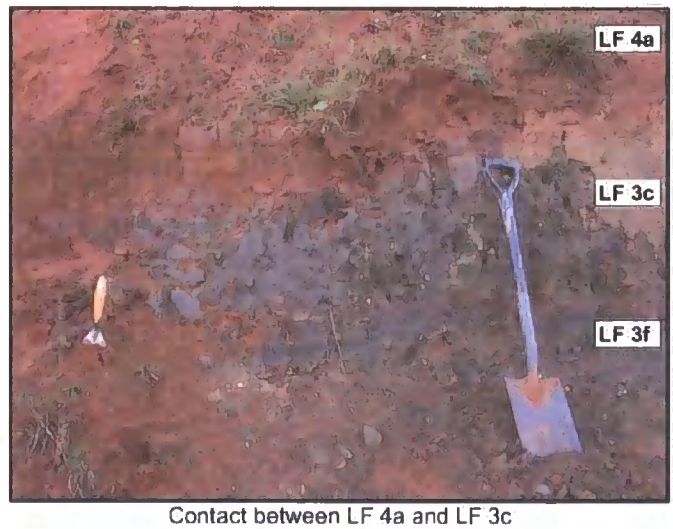

Contact between LF 4a and LF 3c
with laminated diamicton (LF 3f).

Dropstone in laminations (LF 3f)

Figure 6.41: Photographs and detail of LF 3f and LF 4a, Exposure C. Spade is 1 m long. Knife is 19 cm long when extended.

Thin Section Analysis: LF 3f

WHG TS C4 (Figure 6.42; Table 6.3) was taken from LF 3f, the laminations exposed in Exposure C, at Warren House Gill (Figure 6.25). Macroscopic inspection reveals five well-defined beds. Bed 1 at the base is a light brown diamicton. It is conformably overlain by another light brown diamicton with large angular skeleton grains. Bed 3 is a dark brown diamicton. Bed 4 is a red, fine sand with sparse clay material. Bed 5 conformably overlies Bed 4, and has a dense brown matrix with rare coal grains.

Microscopic inspection of WHG TS C4 reveals large differences between the beds. Bed 1 has very common Type III Pebbles (van der Meer, 1993) and rotational structures. It is a diamicton with common fine sand grains and occasional coarse sand grains. It has a moderate birefringence with a strong skelsepic-lattisepic plasmic fabric. Bed 2 is a diamicton with several large skeleton grains of fine gravel size. It has large rounded arenaceous coal grains. Planar voids are present, probably laboratory induced. Type III Pebbles are rare. There are occasional rotational structures with an associated skelsepic plasmic fabric. A lattisepic fabric is also present. The upper boundary is conformable and gradational (Figure 6.43).

Bed 3 is a diamicton with evenly distributed, edge-rounded skeleton grains. There are suggestions of aligned grains and associated masepic plasmic fabrics. Rotational structures and Type III Pebbles are common and are associated with very strong skelsepic plasmic fabrics. Attenuated, boudinaged beds of red silt are present. The upper contact is conformable. Bed 4 includes sub-angular to sub-rounded edge-rounded skeleton grains. They are variable in size and the bed is poorly sorted. There is a strong presence of rotational structures, boudinaged structures, stretched Type III Pebbles, crushed grains, a strong skelsepic plasmic fabric and a weak or moderate lattisepic fabric. The contact with Bed 5 is sharp, unconformable and undulating. Bed 5 is fine grained with small, sub-angular to sub-rounded skeleton grains. Structural analysis also reveals crushed grains, rare planar voids, Type III Pebbles, and rotational structures.

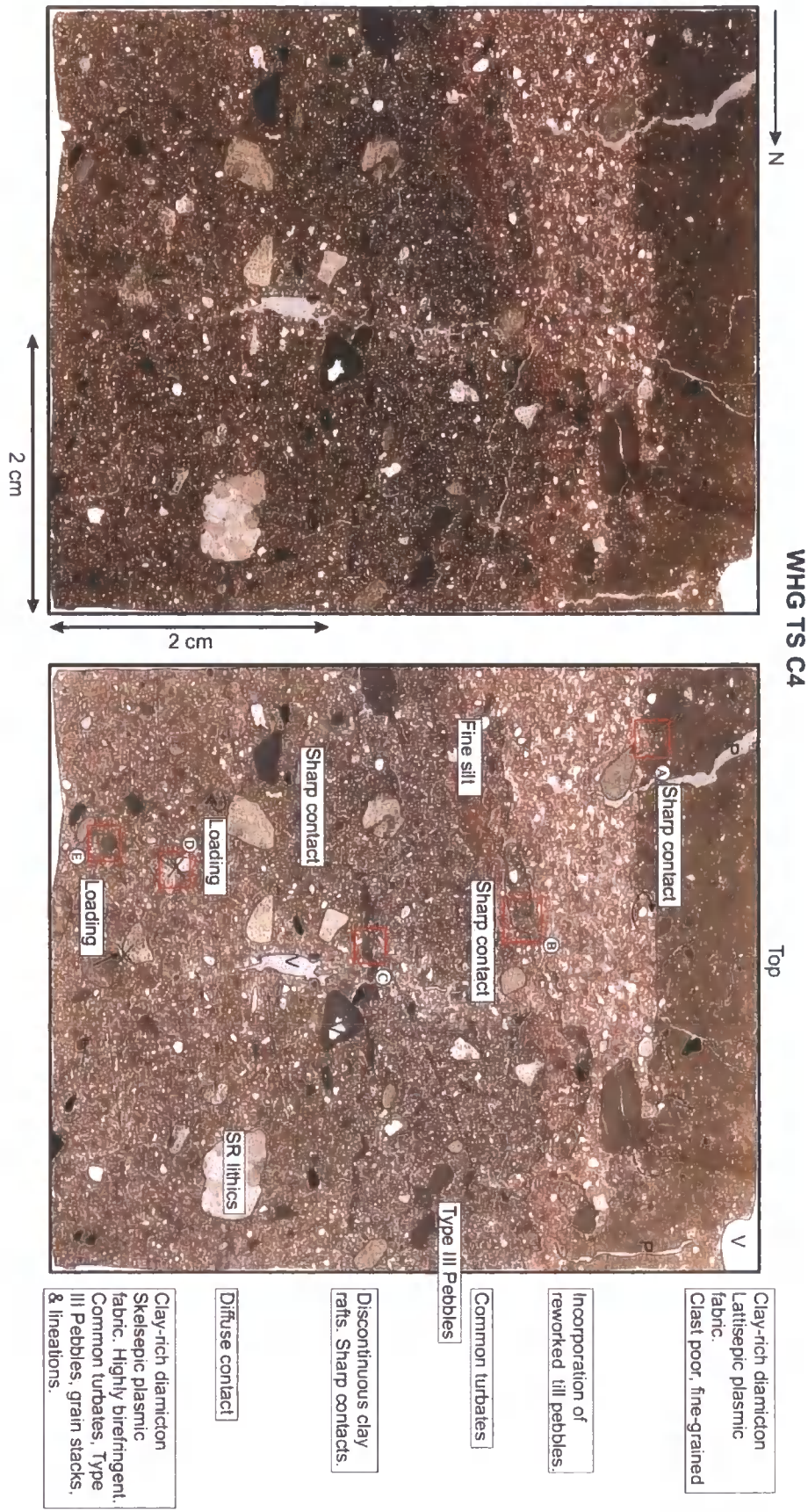

Figure 6.42: Photograph of thin section WHG TS C4, Warren House Gill. Taken from LF 3f, the Laminated Diamicton. Location of plasmic fabric development and other sub-resolution features is annotated on the scan.

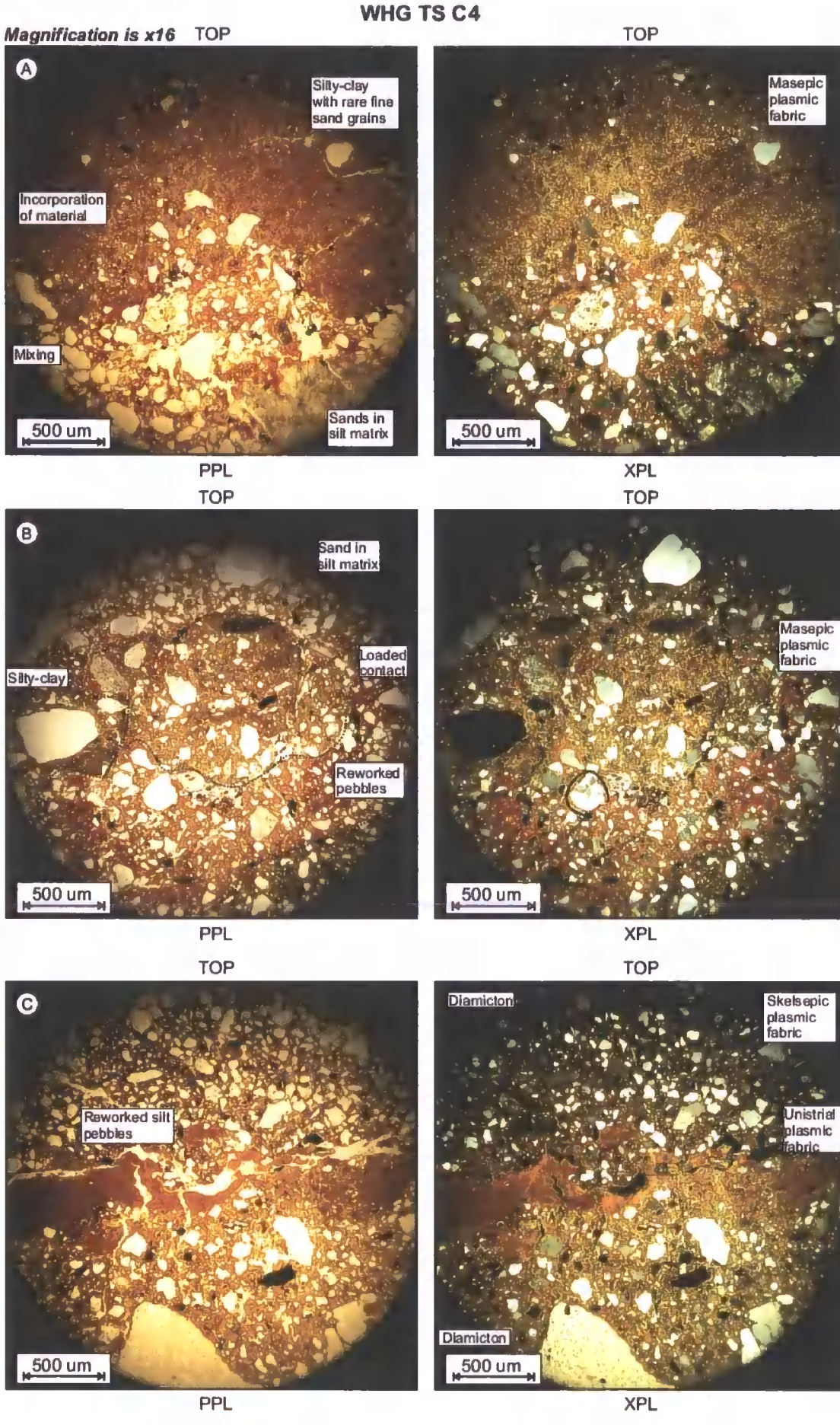
WHG TS C4
Magnification is x16
TOP
A
Silty-clay with rare fine sand grains
Incorporation of material
Mixing
Sands in silt matrix
500 um
PPL
TOP
Masepic plasmic fabric
500 um
XPL
TOP
B
Sand in silt matrix
Loaded contact
Silty-clay
Reworked pebbles
500 um
PPL
TOP
Masepic plasmic fabric
500 um
XPL
TOP
C
Reworked silt pebbles
500 um
PPL
TOP
Diamicton
Skelsepic plasmic fabric
Unistrial plasmic fabric
Diamicton
500 um
XPL

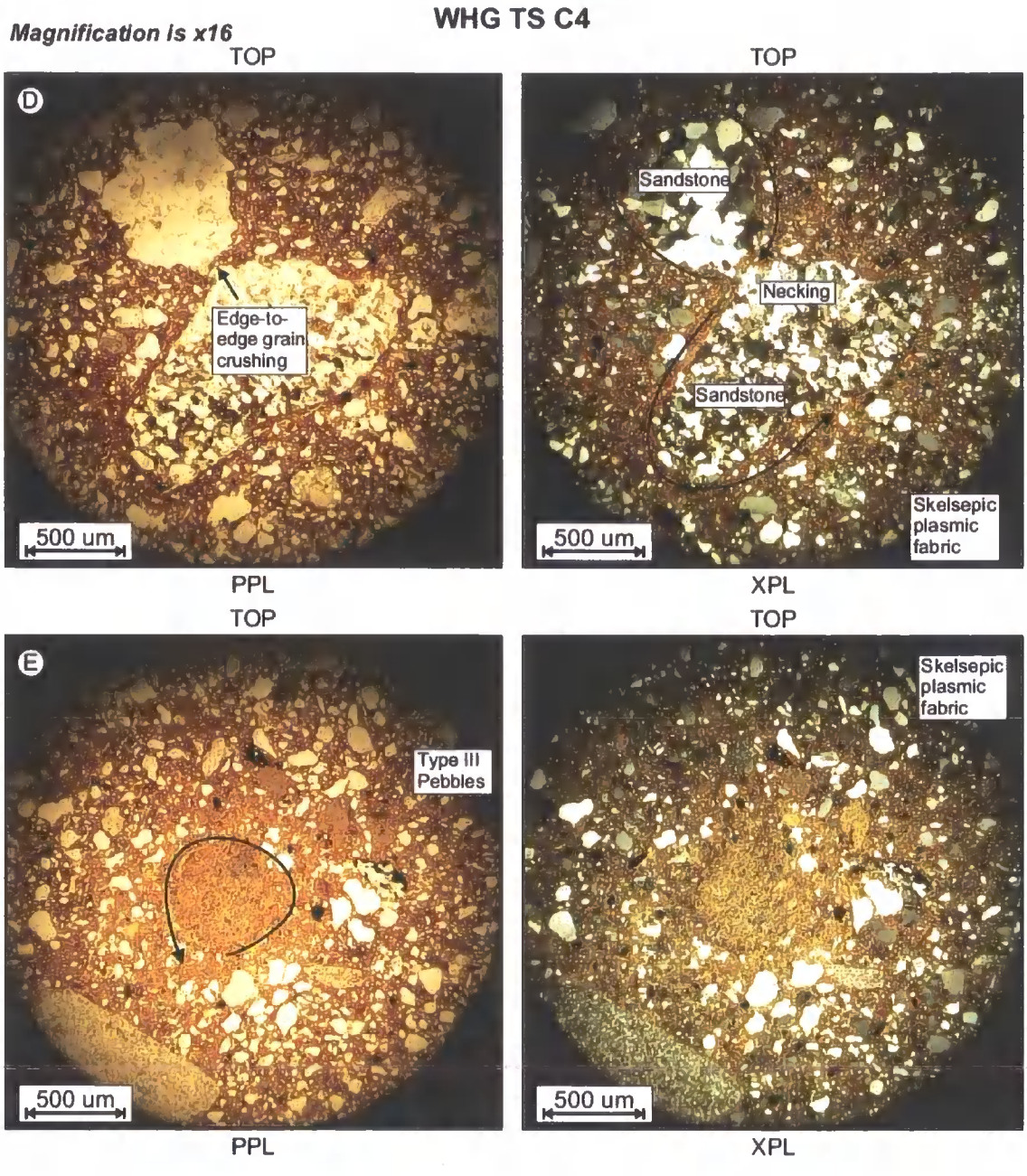

Figure 6.43: Photomicrographs of WHG TS C4. Refer to Figure 6.36 for location of images.

6.2.5 LFA 4: The Red Clays, Silts, Sands and Gravels

LF 4a: Sedimentology of the Red Sands

LF 4a is exposed above LFA 3 at Warren House Gill, and comprises red coloured, bedded sands, silts and clays. It crops out only between Exposure K and Bluehouse Gill (Figure 6.3 and Figure 4.2), and is texturally very variable. In Exposure H, LFA 3 is conformably overlain by a stratified sandy clay (Figure 6.44), which coarsens upwards and becomes increasingly well-sorted, massive reddish-brown sand grading into stratified and

then laminated sand (LF 4a; Figures 6.42, 6.43 and 6.44). It is overlain by a 5 cm thick, horizontal, well-sorted, clay bed with conformable contacts, and then by a well-sorted sand with Type A climbing ripples (Allen, 1963), disturbed by minor faulting and shears. The sand then grades into a massive sand with occasional pods of coarser, yellow sand. This is dissected by a bedded diamicton, which dips across the sands at 20°. It is slickensided, and constitutes deformed, folded, clay laminations (Figures 6.42 and 6.43). This diamicton is overlain conformably by onlapping planar-bedded fine sand and then by Type A climbing ripples. The sand above this is increasingly disturbed, with discontinuous planar bedding, increasing faulting and shearing, water-escape and soft-sediment deformation structures (Mills, 1983), boudinaged sand and loading structures. The sandy silt immediately below the top diamicton is massive and homogenous. It has a conformable upper contact and fines into a well-sorted clay. This is overlain by the gravel-rich diamicton (LFA 5), which has a sharp, erosive contact with the clay bed below (Figure 6.47).

Whilst the red sands (LF 4a) occur at 18 m O.D. in Exposure H, they occur at 52 m O.D. in Exposure B and 50 m in Exposure C. This variation in height is a key feature of this lithofacies association. Unfortunately, the slumped hill slopes make it difficult to observe lateral continuity between the exposures.

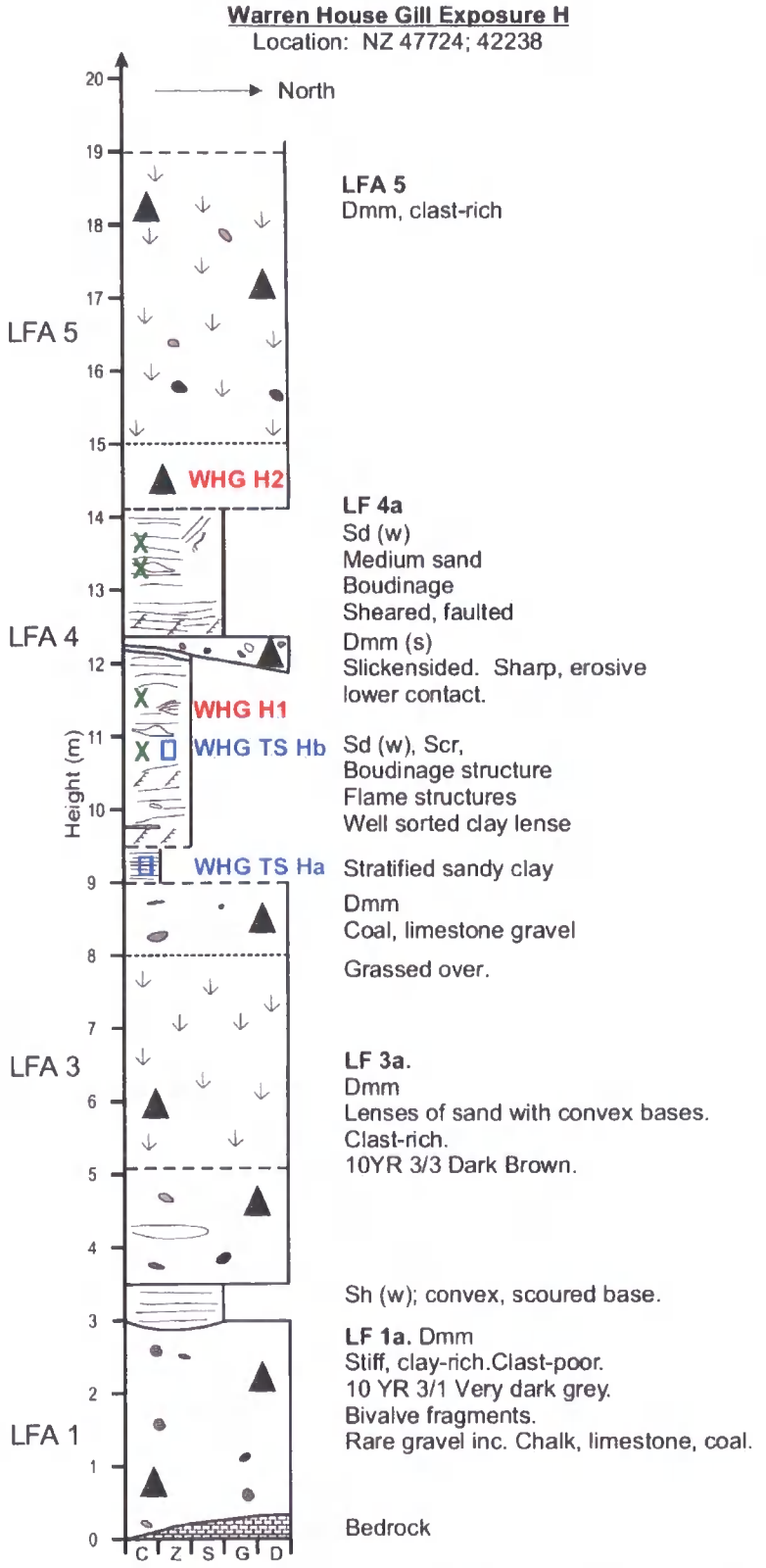

Figure 6.44: Warren House Gill Exposure H. LFAs 1, 3, 4a and 5 are exposed in this vertical profile.

Figure 6.45: Photographs of Exposure H, LF 1a, LF 3a, LF 4a and LFA 5. Spade for scale is 1 m long.

Figure 6.46: Photo-mosaic of LF 4a: LF 4a, Exposure H. The clay is clearly visible at the base of the exposure, grading into well-sorted sands.

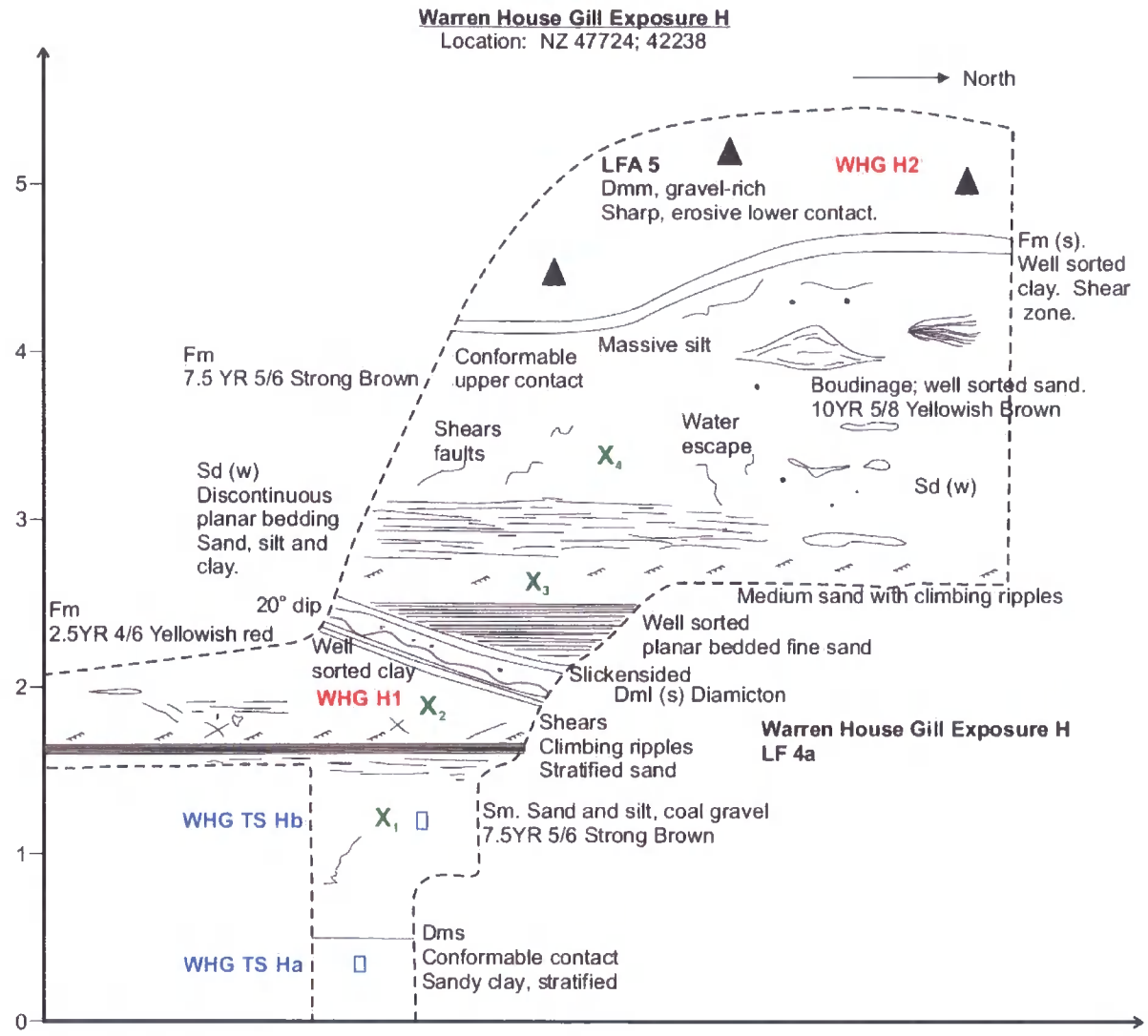

Figure 6.47: Detailed sketch of LF 4a; Exposure H, Warren House Gill.

LF 4a: Thin-section analysis

WHG TS Ha (Figure 6.48 and Table 6.4) was sampled from the base of LF 4a of Exposure H, where a stratified sandy clay diamicton is exposed (Figure 6.44). It is macroscopically complex, and has three distinct beds. Bed 1 is a massive, dark brown, matrix-supported diamicton with numerous fine sand skeleton grains. It has a very sharp unconformable upper contact. Bed 2 is a red coloured silt with a well-sorted matrix. Bedded and folded laminations are visible. Again, it has a sharp upper contact (Figure 6.49 B). Bed 3 is a dark brown, massive, matrix supported diamicton (Figure 6.49 A).

A microscopic investigation reveals further differences between the beds. Bed 1 is matrix-supported with common coal, quartz, feldspar and limestone skeleton grains. It demonstrates weak rotation structures. The upper boundary is unconformable and there are

some stringers (Figure 6.49 E). It is an uneven, undulating contact. The plasmic fabric of Bed 1 is weak with low birefringence. There is occasional weak skelsepic plasmic fabric. The plasma is of an even density and distribution, and the diamicton constitutes beds of matrix-poor diamicton, with conformable, convolute and loaded contacts (Figure 6.49 F).

Bed 2 is a well-sorted, fine-grained silt with little plasma material. Its lower contact ranges from diffuse and conformable to sharp and erosive (Figure 6.49 E). There is little clay material. Structural analysis reveals aligned grains, weak rotation structures and Type II Pebbles. Deformed and faulted laminations are visible with common water-escape structures (Figure 6.49 D) and rip-up clasts, indicating fluidisation and soft sediment deformation. The disjointed rafts of laminated clay have subsequently been crosscut by clay-lined normal faults. There is a weak skelsepic fabric in the clay laminations. The rare voids are planar and are laboratory induced.

A matrix-poor, fluidised sand overlies the silt bed. It has an erosive, complex, lobate boundary and shows some evidence of rotation (Figure 6.47 D). The matrix-poor sand is overlain by second bed of silt, again including rafts of clay. There is disharmonic folding and convolute lamination, and some water escape into the silt. It has sharp contacts with the overlying diamicton (Bed 3). Bed 3 has numerous fine edge-rounded sand grains (Figures 5.71 and 5.72). There is some weakly developed, folded lamination, depicted by a less dense matrix. Soft sediment rip-up pebbles (Figure 6.49 C) and rare weak rotational structures are present. There is a rare weak skelsepic plasmic fabric associated with the rotational structures.

Table 6.4: Micromorphological Summary of LF 4a.

Sample	Location	Lithofacies	Skeleton			Matrix		Void type	Sedimentary Structures				Deformation Structures												Plasmic Fabric				
			Sorting	Grain shape <500µm	Grain shape >500µm	Texture	Microfabric		Laminations	Dropstones	Microfossils	Dump Structures	Section Elements	Faulting	Folding	Rotations	Grain lineations	Pressure Shadow	Crushed Grains	Grain stacks	Pebble Type I	Pebble Type II	Pebble Type III	Water escape	Fluidised Bedding	Skelsepic	Lattisepic	Masepic	Bi-Masepic	Unistrial
WHG Ha	Ex H 9m	Clay below red sands	WS	A	SR	F		L					Be St Sh	••	•••	•	•					•		•••		•				
WHG Hb	Ex H 11m	Red silts	WS	A	SR - R	F/M		P					Be	•		•	•					••		•••	••	•		•		

Key

Sorting		*Grain shape*		*Microfabric*		*Texture*		*Section Elements*	
WS	Well sorted	WR	Well rounded	H	Horizontal Microfabric	F	Fine grained	Ba	Banding
MS	Moderately sorted	R	Rounded	V	Vertical microfabric	C	Coarse (no fine silt/clay)	Bo	Boudinage
PS	Poorly sorted	SA	Subangular			M	Medium (some fine silt/clay)	Be	Bedding
D	Diamicton	A	Angular	*Voids*				Sh	Shear
				P	Packing induced			F	Flow
•••	Indicates feature is strongly present / numerous			L	Laboratory induced			St	Stringer
••	Indicates feature is present								
•	Indicates feature is rarely / occasionally present								

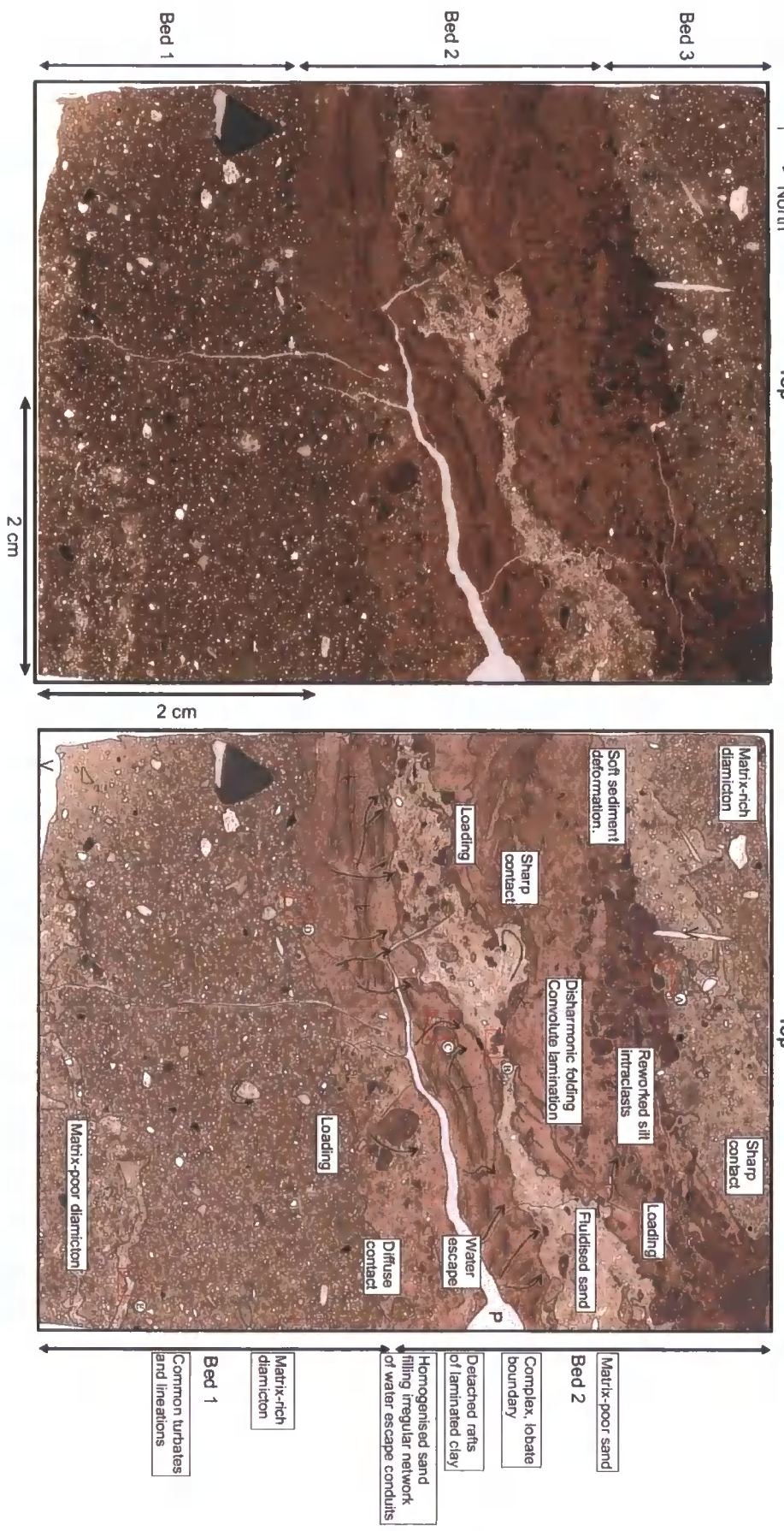

Figure 6.48: Thin section sample WHG TS Ha. Locations of sub-resolution features are noted.

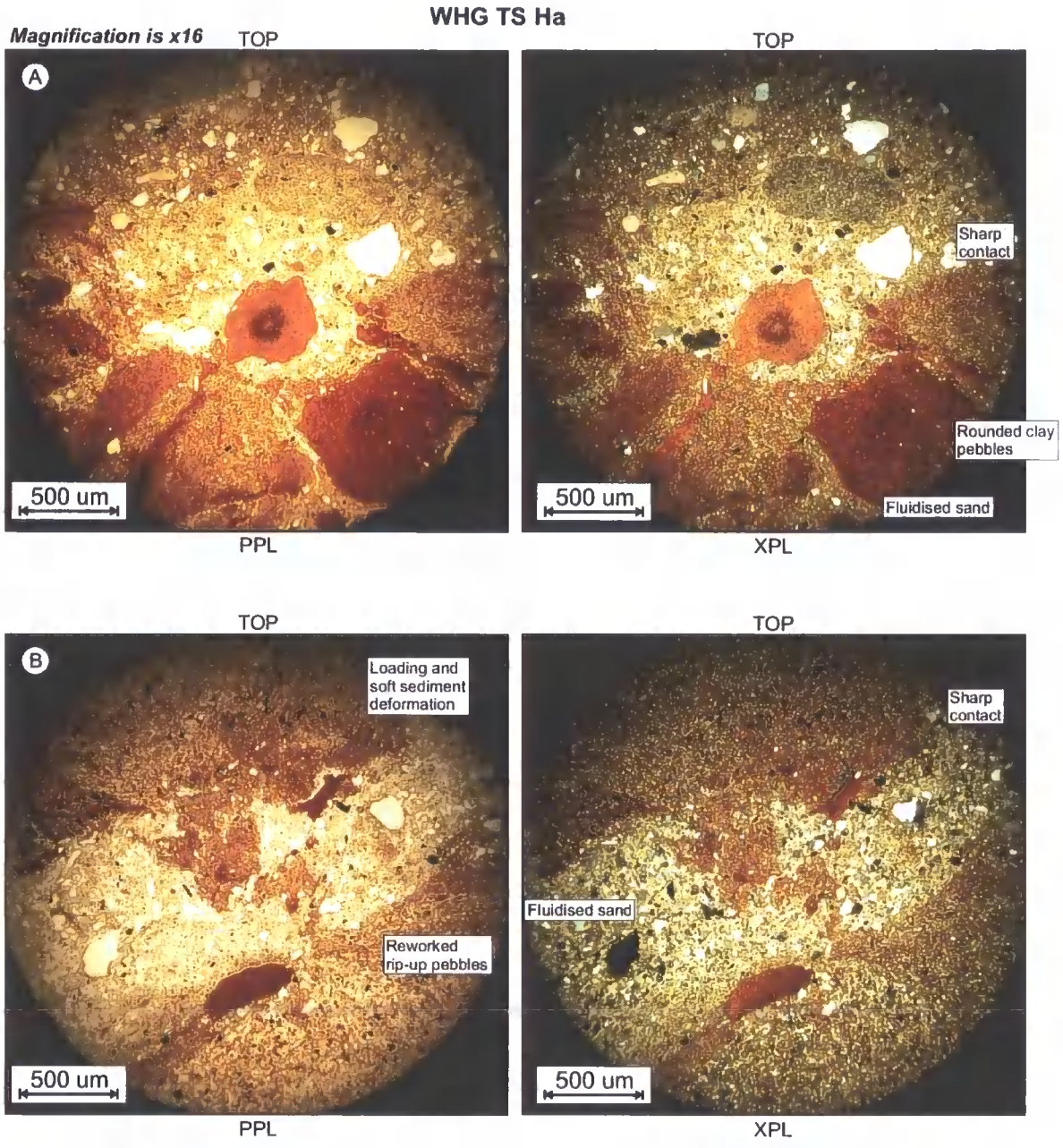
WHG TS Ha
Magnification is x16
TOP
A
500 um
PPL
TOP
Sharp contact
Rounded clay pebbles
Fluidised sand
500 um
XPL
TOP
B
Loading and soft sediment deformation
Reworked rip-up pebbles
500 um
PPL
TOP
Sharp contact
Fluidised sand
500 um
XPL

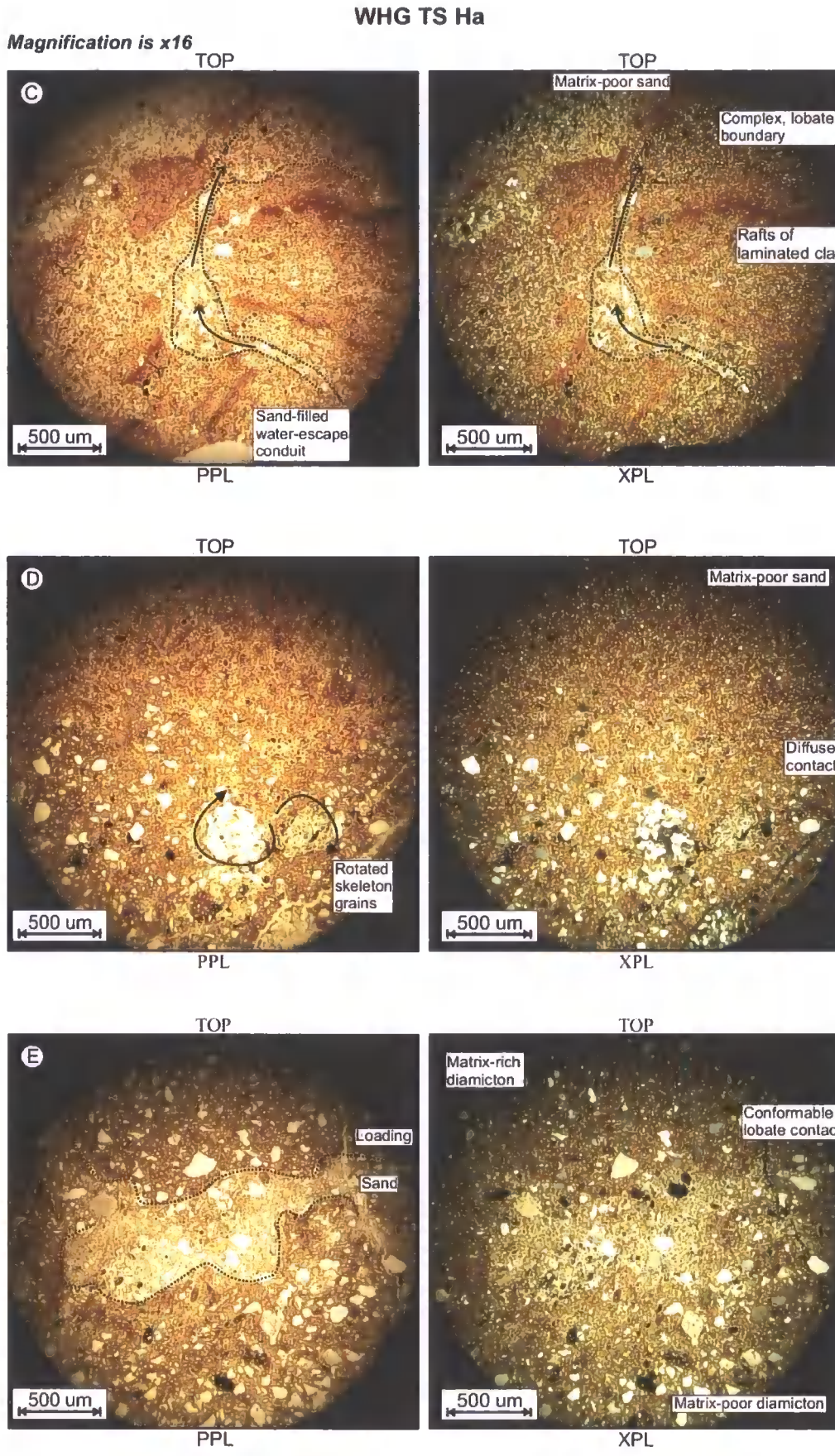

Figure 6.49: Photomicrographs of WHG TS Ha (LF 4a), showing detail of contacts, soft sediment deformation, and fluidised diamicton.

WHG TS Hb (Figure 6.50) was sampled from the middle of LF 4a, Exposure H, where well-sorted fine sands are crosscut by a bedded diamicton (Figure 6.44). Macroscopic inspection of the slide showed four complex beds. Bed 1 is a light, reddish brown, massive, well-sorted, matrix-supported fine silt. It is of an even density and distribution, and has a sharp, unconformable upper boundary. Bed 2 is divided into two; 2a is a diamicton with fine sand and silt grains. Bed 2b is a denser, finer, well-sorted silt with a sharp upper boundary. Bed 3 is a light brown, moderately-sorted, sandy silt. It is evenly distributed and is massive. Bed 4 is a well-sorted, massive, dark reddish brown silty clay with a convoluted, loaded lower contact. Planar voids are present throughout.

Microscopic inspection reveals more detail. Bed 1 is massive and contains angular well-sorted fine silt grains (> 100 μm). No voids are present. There are numerous sub-parallel lineations of grains. There is a weak skelsepic plasmic fabric. The upper contact is sharp, convolute and deformed. There has been some rotation of the larger skeleton grains, dragging sand and silt grains down into Bed 1.

Bed 2a mostly consists of fine sand grains with some large rounded grains greater than 500 μm and numerous silty Type III intraclasts. The sand grains show evidence of rotation. There is a weak skelsepic plasmic fabric occasionally present. Bed 2a is overlain by a massive, fine, well-sorted silt (Bed 2b). There is extensively deformed bedding, with faulting, rip-up-clasts and water-escape structures through to Bed 3 above (Figure 6.51 B and C). The fluidised clay contains numerous rotated intraclasts. Cutting through this are rare faults. There is a weak masepic plasmic fabric.

Bed 3 is very similar to Bed 1. It has a deformed, sharp, unconformable upper contact. It has massive, clast-supported silt grains with very little clay present. There is some weakly developed lamination. It has sharp contacts with Beds 2 and 4, though there has been mixing in places. Bed 4 is also a massive, fine, well-sorted silt, coloured a dark reddish brown. Crosscutting clay lined micro-faults are much in evidence. Rip-up-clasts and water-escape structures are present. There is some disharmonic folding, and incorporation and remobilisation of the material in Bed 3 below (Figure 6.51 A). A moderate masepic plasmic fabric is present. There is evidence of loading, and of mixing with the bed below.

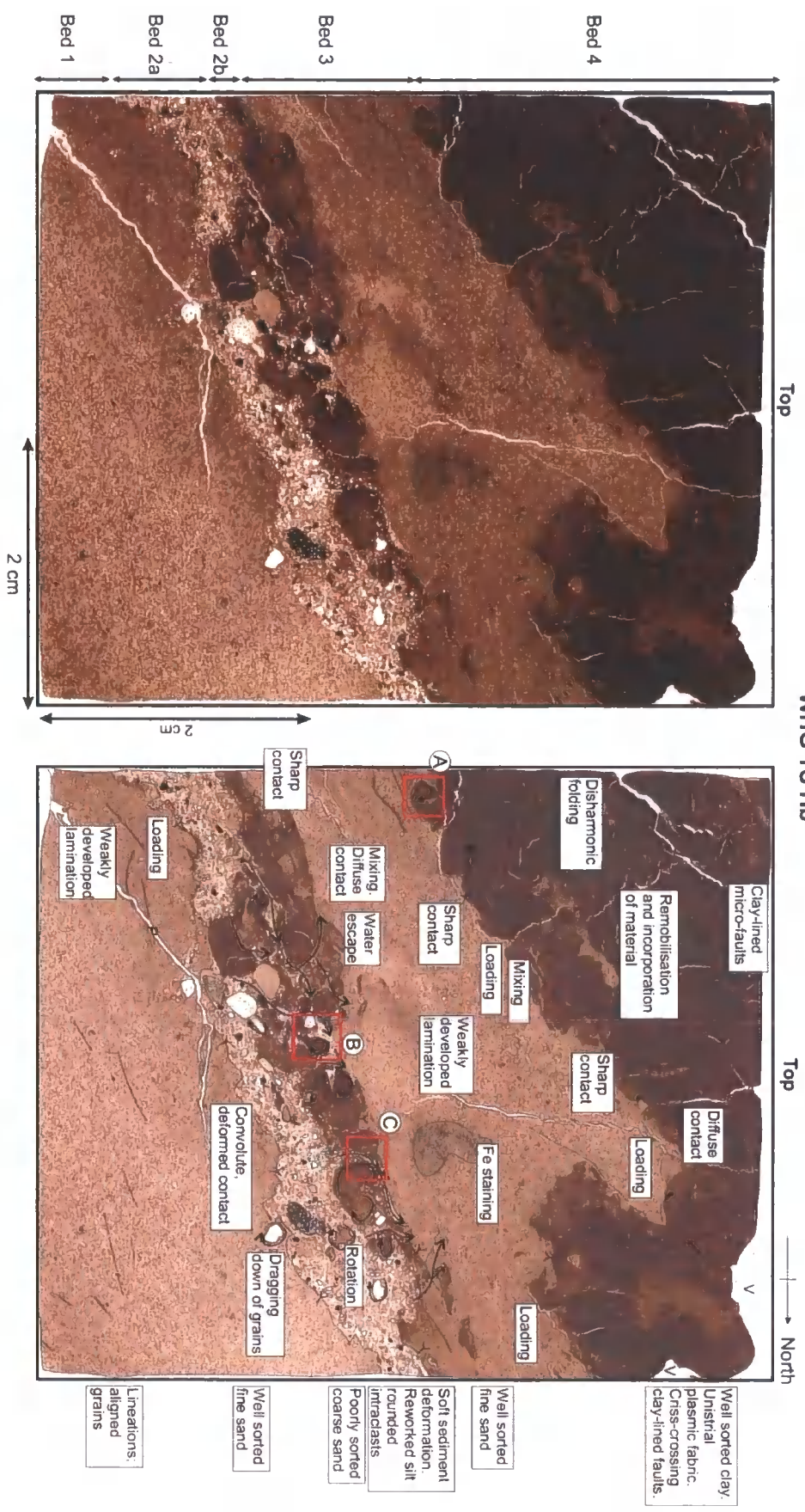

Figure 6.50: Thin Section sample WHG TS Hb (LF 4a). Locations of sub-resolution features are highlighted.

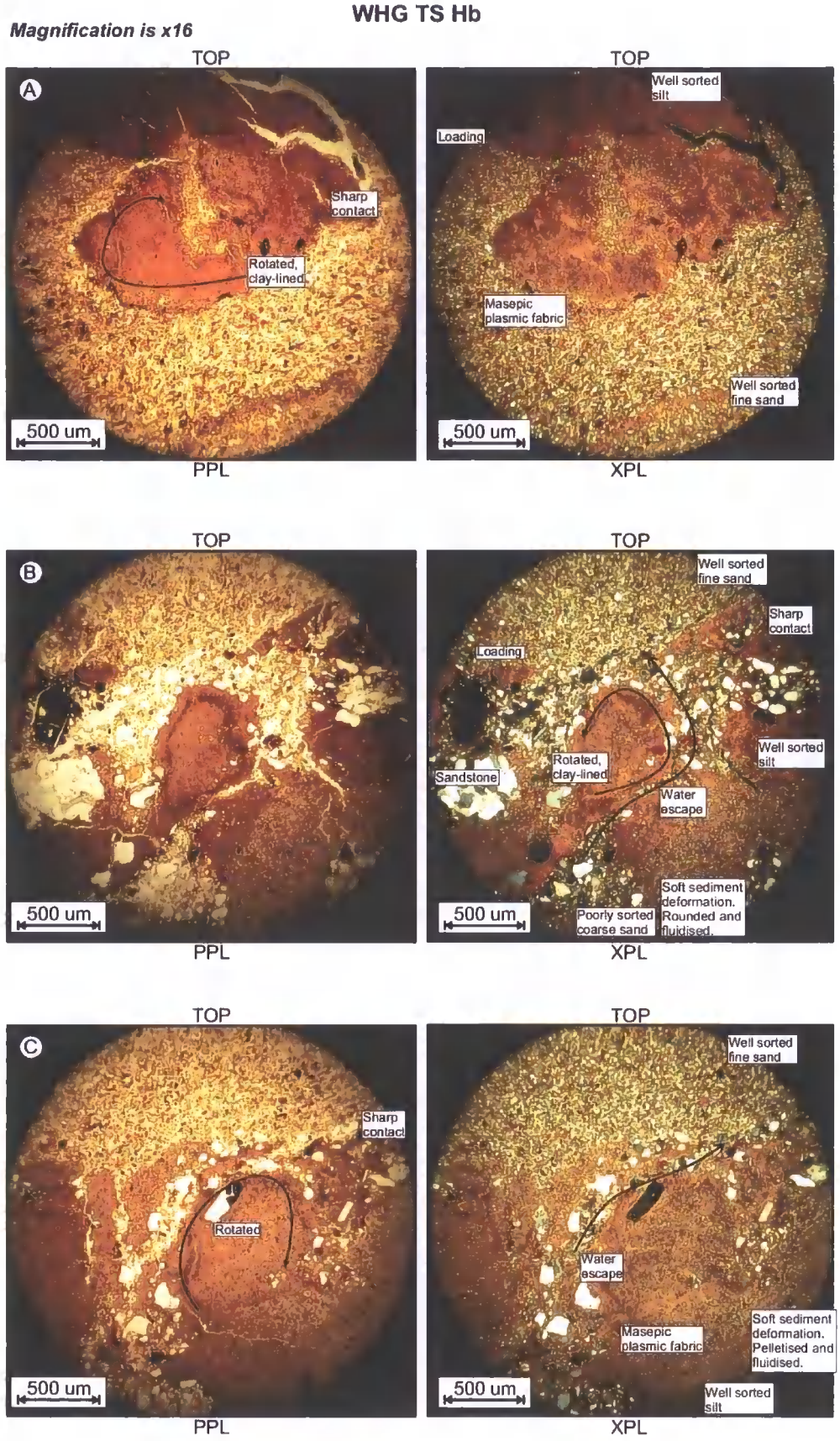

Figure 6.51: Photomicrographs of WHG T Hb, showing soft sediment deformation, water escape, and rotation and pelletisation of silt bed.

Sedimentology: LF 4b. Red cobble gravel

Exposure K presents the different facies of LFA 4 (Figure 6.52). Here, the bedrock rises to 14 m O.D. Sand and cobbles lie directly on the bedrock, and stratigraphically younger diamictons are absent. Coarse, poorly-sorted, sub-rounded cobble-pebble gravel grades conformably into ripple-cross laminated red sands. These beds alternate between laminated red sands and fine, and coarse, cobble and pebble gravels. The sands show planar lamination, ripple-cross lamination (Type A; Allen, 1963), sometimes containing clast lags. The sands vary between well-sorted fine sand to poorly-sorted, coarse, gravelly sand (Figure 6.52). The sand beds vary between conformable lower contacts to erosive, convex bases. The whole 15 m exposure of sands and gravels is overlain unconformably by a clast-rich diamicton (LFA 5).

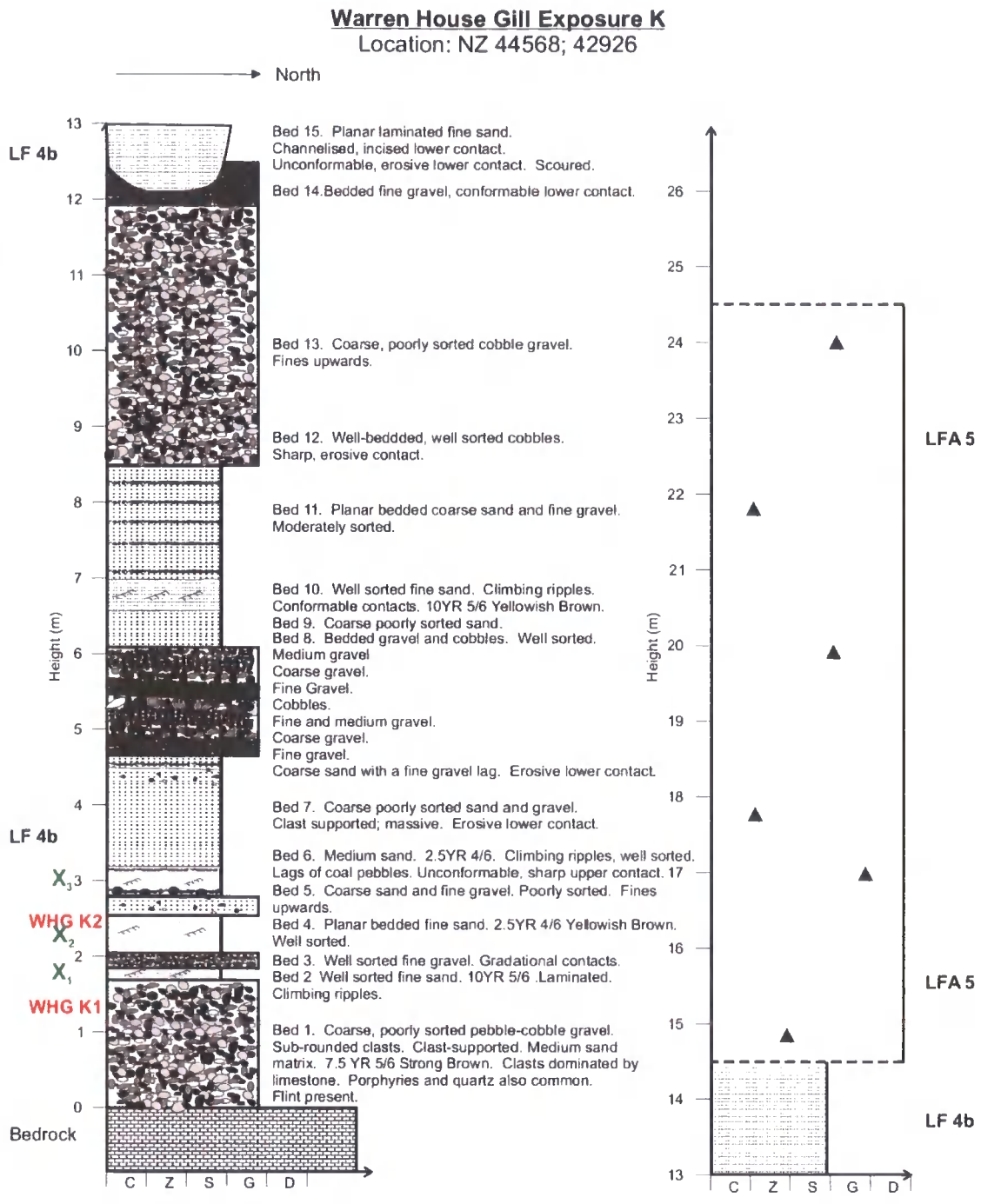

Figure 6.52: Detailed vertical profile of LF 4b, Exposure K, Warren House Gill, showing bulk samples (red) and OSL samples (green).

6.2.6 LFA 5: The Upper Diamicton

LFA 5 is best exposed in exposures B, H and K (Figure 6.3). It is a massive, clast rich, dark-brown diamicton unconformably overlying the red-bedded sands. Erratics such as Carboniferous Limestone, coal, sandstone, greywacke, and orthoquartzite are common. It

is absent in some exposures (e.g. Exposure C). LFA 5 is inaccessible at Warren House Gill, and so was difficult to sample and analyse.

6.3 Geochemical, Lithological and Biological Analyses

6.3.1 Lithological Analyses

Lithological Characteristics

LFA 1 grades from a dark grey (10 YR 4/1) well-sorted clay to a dark olive brown (2.5 YR 3/3) diamicton with increasing clast content, tectonised sand laminations and a vigorous reaction to HCl. Sample WHG C2 (LF 2a) was taken from the silts at 3 m height in Exposure C. They are a yellowish-brown (10YR 5/6) well-sorted silt (Table 6.12), and their reaction to HCl is vigorous.

LFA 3 is highly variable with multiple facies, including massive diamicton (LF 3a), tectonised diamicton (LF 3b), deformed beds of coarse to fine, well-sorted to poorly-sorted sand (LF 3c and LF 3d), and laminated diamicton (LF 3e and LF 3f). In colour, it is mostly a very dark grey (10YR 3/1) to a dark yellowish brown (10YR 3/4). It is gravel-rich with abundant typical British lithologies such as sandstones, limestones, and rare far-travelled erratics such as granite, quartzose lithologies, andesite and rhyolite. The stones are striated and faceted, and are predominantly sub-rounded to sub-angular in shape. LF 3a has a moderate reaction to HCl. Very rare shell fragments are present.

The two facies of LFA 4 at Warren House Gill are significantly different. They vary between a well-sorted, brown sand (10YR 4/3 to 10YR 5/4), such as samples WHG K1 and WHG H1 (LF 4a), to well-sorted, rounded cobble gravels in a silty-sand matrix, such as WHG K2 (LF 4b; Figure 6.44 and Figure 6.52). LFA 5 was sampled from the upper diamicton at 14.5 m in Exposure H (WHG H2). It is a gravel-rich brown diamicton (10YR 4/3), which has only a moderate reaction to HCl, possibly due to weathering. The gravels are generally faceted and sub-angular in shape.

Particle Size Distribution

The particle-size distribution of LFA 1 (Table 6.5) shows it to be a fine-grained diamicton with very little coarse sand and rare gravel when compared to the two other diamictons at Warren House Gill (Figure 6.53). Table 6.6 shows the well-developed particle size envelopes separating the individual lithofacies associations at Warren House Gill. Detailed PSA shows that LFA 1 coarsens upwards (Table 6.6 and Figure 6.54). Samples WHG G1, G2 and G3 have very similar, fine-grained particle size distributions.

The sample WHG F1, located higher in the lithofacies, is coarser. While still having a large amount of clay, the amount of silt is less and the percentage sand considerably increased. The diamicton samples WHG G4 and F3 are presented for comparison and have obviously far more gravel and substantially less sand.

Table 6.5: Average percentage particle size for the different lithofacies associations at Warren House Gill. LFA 4 is separated into the fine-grained sand (LF 4a) and coarse-grained gravel facies (LF 4b).

Particle diameter	LFA 1	LFA 2	LFA 3	LF 4a (WHG H1)	LF 4b (WHG K2)	LFA 5
% Clay	27.06	11.58	17.51	4.30	1.90	9.55
% Silt	40.22	77.97	33.50	27.63	4.22	8.91
% Fine sand	26.46	9.33	26.41	68.08	7.04	26.45
% Coarse sand	6.42	1.12	9.05	0.00	8.27	12.65
% Fine gravel	0.72	0.00	8.32	0.00	28.49	17.50
% Coarse gravel	1.11	0.00	6.21	0.00	50.08	24.94

Table 6.6: Particle size distribution for LFA 1 samples. Samples from LF 3a are included for comparison.

Particle Diameter	G1 LF 1a	G2 LF 1a	G3 LF 1b	F1 LF 1b	F3 LF 3a	G4 LF 3a
% Clay	26.74	26.96	28.45	27.09	17.77	14.65
% Silt	49.25	42.61	43.37	26.67	29.21	29.91
% Fine sand	18.60	21.56	21.02	40.68	31.04	32.84
% Coarse Sand	4.35	8.24	6.89	1.57	1.63	6.88
% Fine Gravel	0.61	0.73	0.89	0.98	6.61	7.55
% Coarse gravel	0.44	0.91	0.38	4.01	14.75	9.17

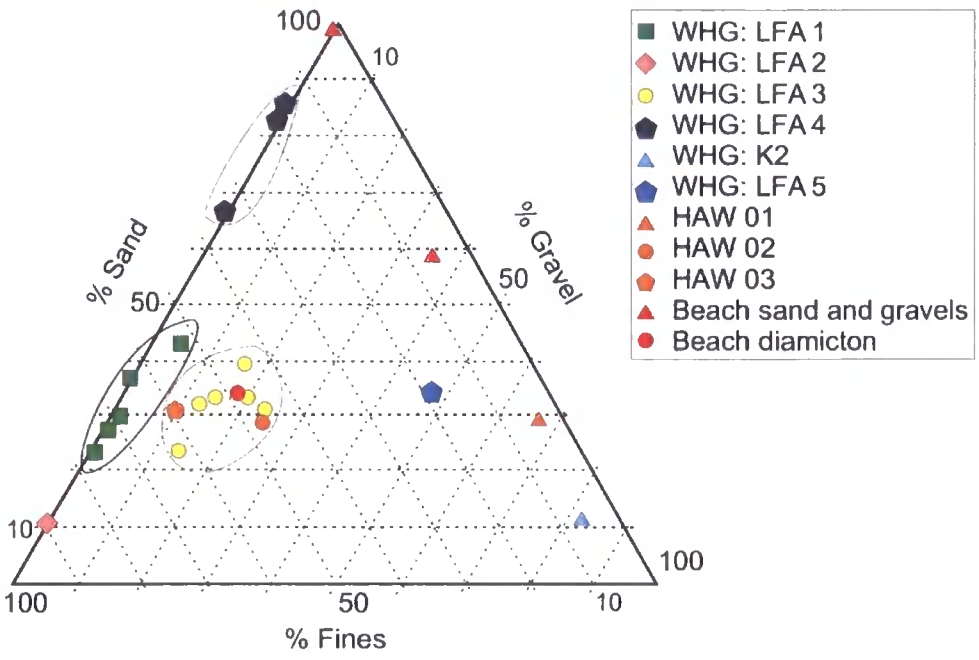

Figure 6.53: Particle-size distribution ternary diagram.

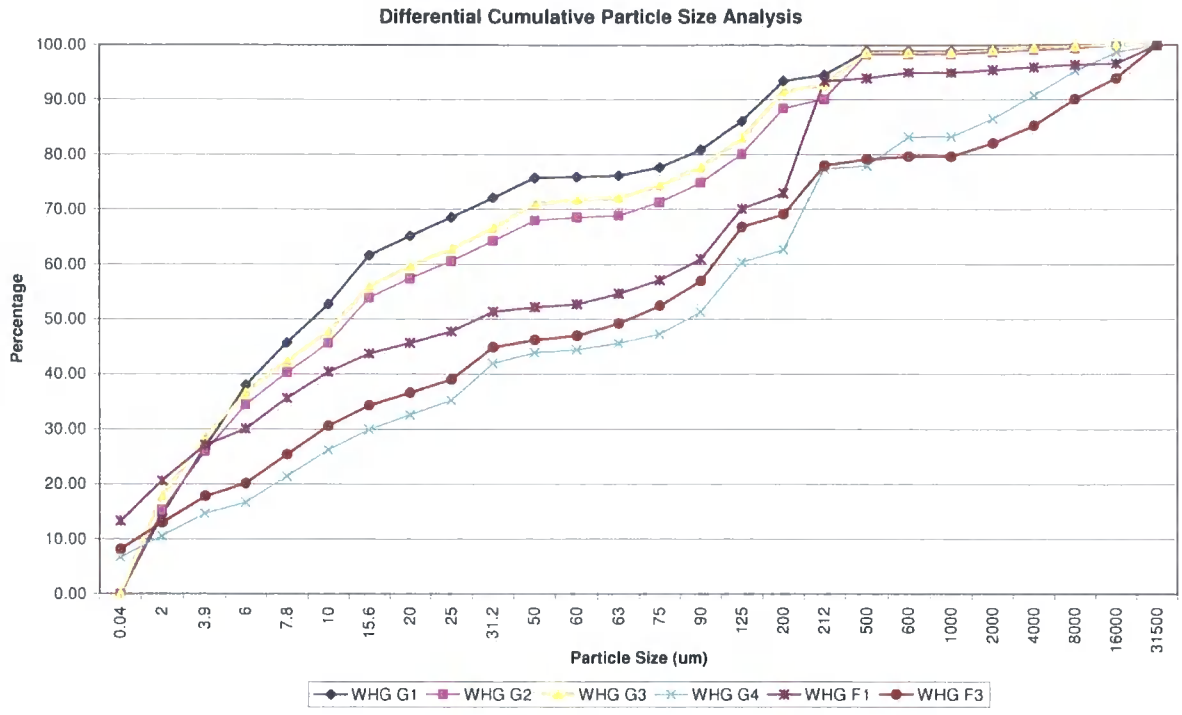

Figure 6.54: Differential Cumulative chart of particle-size analysis for LFA 1.

Samples WHG G4 and WHG F3 from LFA 3 are inserted for comparison. Sample WHG G1 can be seen to be much finer than samples WHG G2 and G3, taken from the facies above. Sample WHG F1 is coarser still, with a lower silt and clay content.

The particle-size distribution of LFs 3a and 5 is consistent throughout the lithofacies associations and on this basis the diamictons plot closely together, distinct from LFA 1 (Figure 6.53). LFA 5 is a relatively sandy (12.7 % coarse sand) diamicton with a comparatively low proportion of fines and a high proportion of gravel (24.9 % coarse gravel). The particle size distribution for LFA 5 is very similar to LF 3a (Figure 6.53).

Samples WHG E1 and E3, both LFA 3, show some local variations, and although sample E1 has a considerable percentage of coarse gravel, this is probably accounted for by the presence of a few large clasts. Sample E3 is generally coarser with high percentages of fine material. Sample WHG E2 was taken from the large sand fold, and shows that the sand is well-sorted, mostly fine, and with very little silt or gravel (Table 6.7). The particle-size distribution of LFA 3 consistently plots closely together with the lowest diamicton at Hawthorn Hive (Figure 5.25).

Table 6.7: Particle size distribution for diamictons (E1 and E3) and sands (E2) at Exposure E, Warren House Gill.

Particle Diameter	WHG E1 Lower diamicton	WHG E2 Sand fold	WHG E3 Diamicton above sand
% Clay	16.36	2.87	14.77
% Silt	29.91	12.82	40.05
% Fine sand	26.79	56.34	17.73
% Coarse Sand	6.08	28.97	14.17
% Fine Gravel	6.05	0.00	6.98
% Coarse gravel	18.81	0.00	7.30

Clast Lithological Analysis

The clast lithologies of LFA 1 (Table 6.8 and Figure 6.55) differ profoundly from that of the other diamictons. LFA 1 is significantly lower in Magnesian Limestone (52.6 %) and Carboniferous Limestone (3.0 %), but is comparatively enriched in crystalline and quartzose erratics including granite (3.7 %), lavas, flint (3.9 %), chalk (2.5 %), and in the Triassic red marl (3.3 %) erratics. Figure 6.55 illustrates the dominance of igneous and Cretaceous clasts, and the low proportions of Carboniferous erratics. LFA 3 is vastly higher in Magnesian Limestone (68.2 %), sandstone (10.4 %) and greywackes (6.8 %) than LFA 1. Carboniferous Limestone is only a minor component with 3.4 % of the clasts. There are comparatively minor percentages of orthoquartzite and very little vein quartz.

Clast-lithological analysis of LF 4b (WHG K2) reveals similarities with LFA 5 (Figure 6.55). The clast counts are dominated by Magnesian Limestone (70.1 %); however, Carboniferous Limestone clasts are significantly more numerous than in LFA 3 at 10.7 %. Sandstone clasts are significantly lower in number than in LFA 3 with only 4.7 %.

Lithologically and mineralogically, LFA 5 is similar in character to LFA 3. The lithological content is dominated by Magnesian Limestone, with a very high 76.8 %. Carboniferous Limestone is comparatively high compared to LFA 3 with 9.9 % abundance. Greywacke is present in similar amounts (4.2 %), while there is very little sandstone (1.9 %) and a very low abundance of igneous erratics. The lithologies are dominated by locally derived durable and non-durable varieties, and there are very few far-travelled erratics (Table 6.8).

Table 6.8: Average percentage clast lithologies at Warren House Gill, 8-16 and 16-32 mm. For detailed raw counts, refer to Appendix IV.

	Lithofacies Association	LFA 1	LF 3a	LF 4b (WHG K2)	LFA 5
	n	*710*	*3212*	*677*	*263*
Igneous	*Diorite*	0.54	0.00	0.00	0.00
	Granite	3.74	0.49	0.59	0.00
	Gabbro	0.00	0.03	0.00	0.00
	Rhyolite	1.35	0.53	0.29	0.00
	Andesite	2.13	0.18	0.15	0.38
	Basalt	0.17	0.03	0.00	0.00
	Porphyry	1.19	0.24	1.33	0.38
	Felsite	0.34	0.10	0.00	0.00
Metamorphic	*Gneiss*	0.34	0.00	0.00	0.00
	Slate	0.27	0.00	0.00	0.00
	Schist	0.20	0.00	0.00	0.00
Sandstone and sedimentary	*Sandstone*	1.86	10.38	4.72	1.90
	Arenite Sandstone	0.00	0.31	0.00	0.00
	Quartzitic Sandstone	1.52	1.74	2.21	3.04
	Siltstone	0.17	0.68	0.00	0.00
	Breccia	0.10	0.00	0.00	0.00
Cretaceous	*Flint*	3.85	0.00	0.00	0.00
	Chalk	2.49	0.00	0.00	0.00
Jurassic	*Ironstone*	0.00	0.33	0.00	0.76
	Mudstone	0.10	1.17	0.59	0.00
Triassic	*Brown orthoquartzite*	2.03	1.27	0.15	0.76
	Red orthoquartzite	0.54	0.18	0.00	0.00
	White orthoquartzite	7.45	0.30	1.18	0.00
	Brown Vein Quartz	0.94	0.10	0.00	0.00
	Red Vein Quartz	0.47	0.00	0.00	0.00
	White Vein Quartz	6.96	0.54	0.88	0.00
	Red Marl	3.26	0.19	0.00	0.00
Permian	*Magnesian Limestone*	52.64	68.29	70.31	76.81
	Yellow Sands	0.10	1.07	0.00	0.00
	Whin Sill Dolerite	1.07	0.73	1.92	1.14
	New Red Sandstone	0.00	0.00	0.00	0.00
Carboniferous	*Carboniferous Limestone*	2.98	3.43	10.62	9.89
	Chert	0.10	0.00	0.00	0.00
	Coal	0.20	1.18	0.00	0.76
Devonian	*Shale*	0.00	0.09	0.00	0.00
	Old Red Sandstone	0.00	0.31	0.29	0.00
Ordovician and Silurian	*Arkose Sandstone*	0.10	0.29	0.00	0.00
	Greywacke	0.80	6.82	4.87	4.18

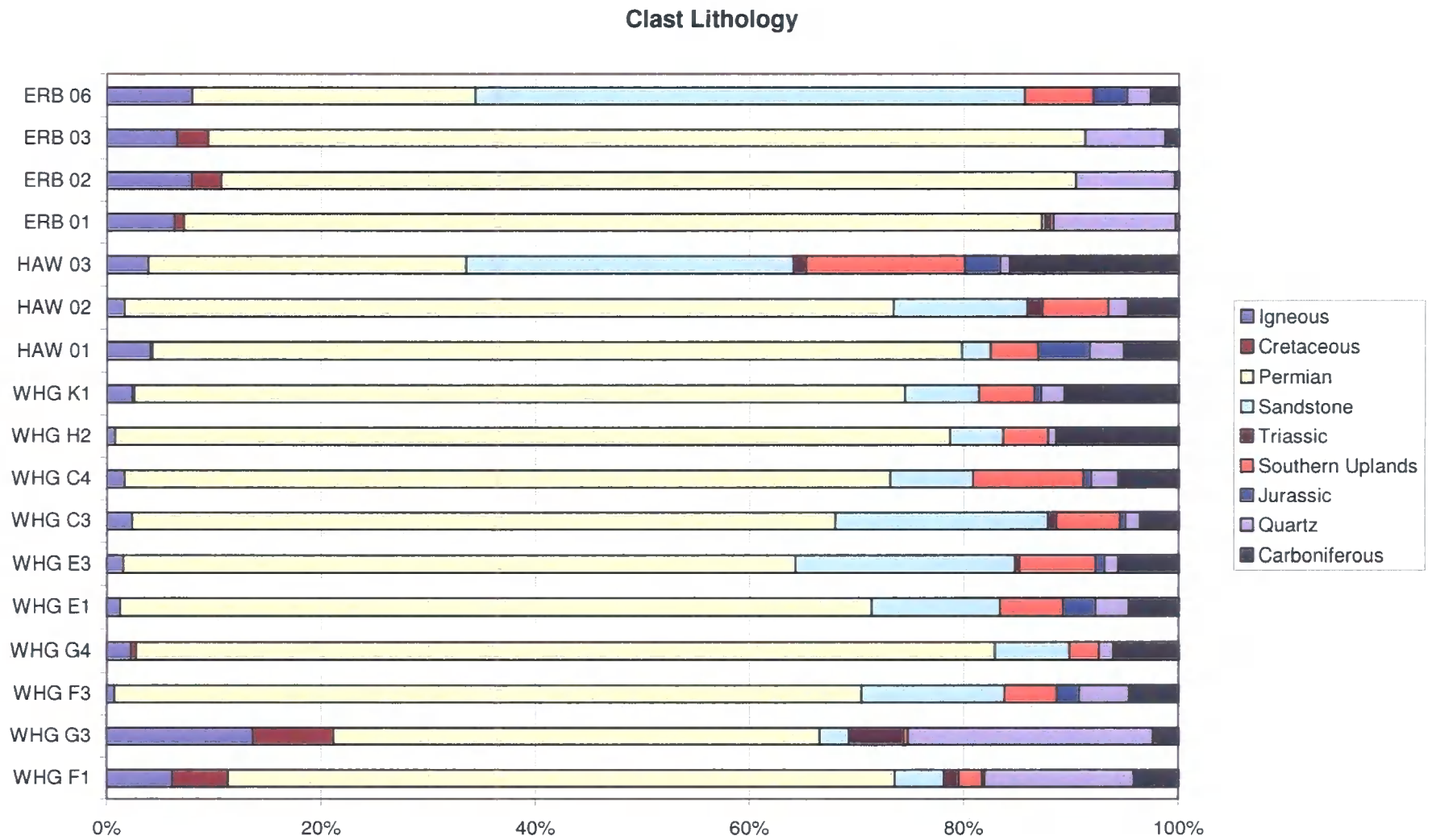

Figure 6.55: Composition of gravel lithologies (percentage) in samples from Hawthorn Hive to Blackhall Rocks.

The triplot of 'Carboniferous Limestone and sandstones,' 'Permian', and 'Crystalline and Other' illustrates the similarities and differences between the glacigenic sediments at Warren House Gill (Figure 6.56). The Warren House Gill lithofacies are here compared to those at Hawthorn Hive and Shippersea Bay. The low proportions of Magnesian Limestone compared to the relatively high proportions of crystalline and Eocene erratics (Table 6.8) accounts for the significant correlation within LFA 1 and the difference to the other glacigenic lithofacies associations. The beach gravels are also clearly differentiated by their high percentage of crystalline erratics and low proportions of Carboniferous and sandstone lithologies.

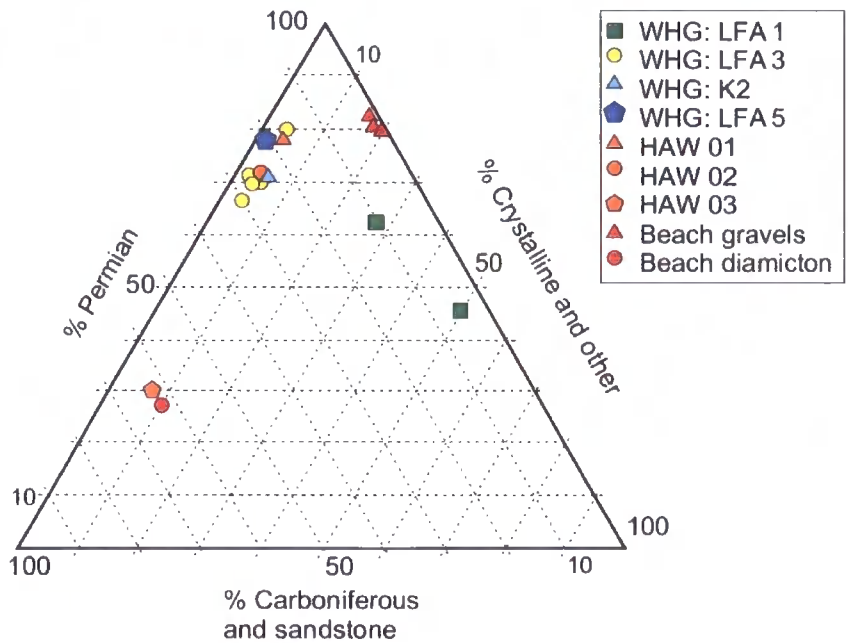

Figure 6.56: Triplot showing variations in clast lithologies from Hawthorn Hive to Blackhall Rocks. LFA 1 at Hawthorn Hive (HAW 02) contains far higher percentages of limestone, while LFA 3 at Hawthorn Hive (HAW 03) contains less Permian material.

The proportion of near, far, durable and non-durable lithologies can be useful in the discrimination between lithofacies and can impart valuable information. Figure 6.57 demonstrates that LFA 1 has far fewer locally derived lithologies than the other diamictons and gravel deposits at Warren House Gill, and a strong component of far-travelled erratics, including non-durable igneous erratics.

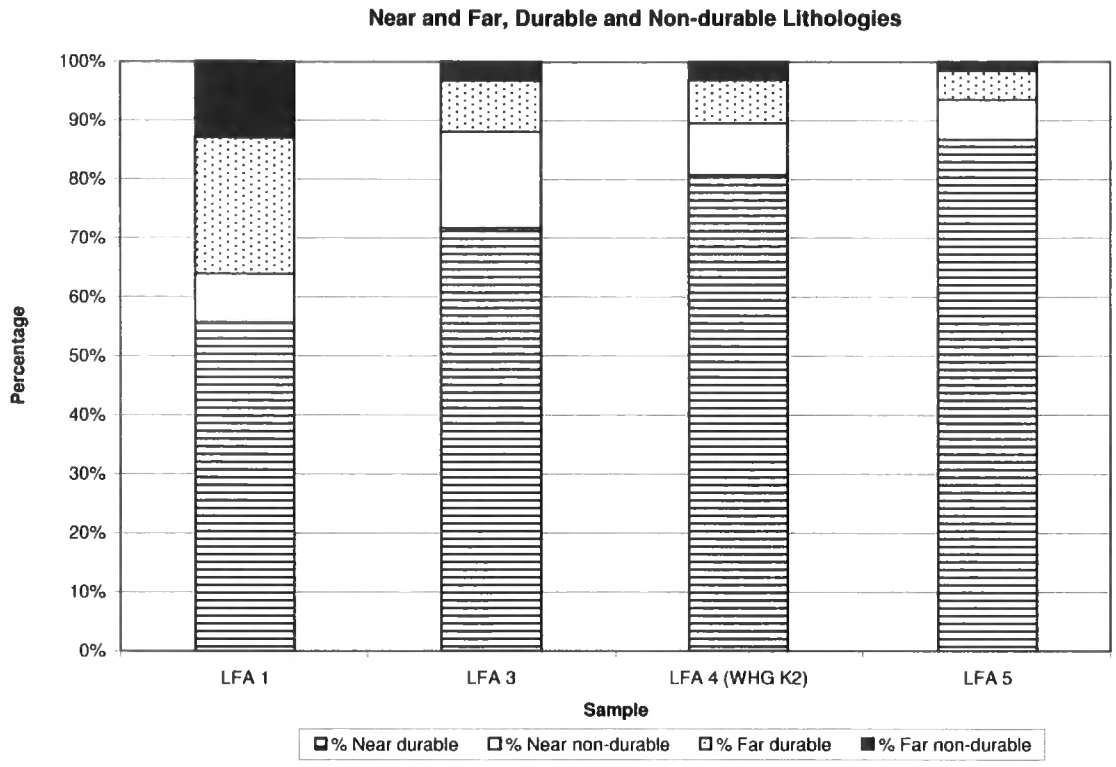

Figure 6.57: Near, Far, Durable and Non-Durable lithologies at Warren House Gill.

The variations in clast lithologies were explored further using cluster analysis techniques (Figure 6.58). As the data is not normally distributed, non-parametric techniques are necessary. Cluster analysis allowed differentiation of LFA 1 and the beach gravel, but failed to distinguish between LFAs 3, 4 and 6. WHG F1 and WHG G3 both clustered tightly together, and were clearly distinguished from both the beach gravels and the other lithofacies at Warren House Gill. The presence of Cretaceous and quartzose lithologies such as flint clearly differentiates the beach and LFA 1 from any other sediments.

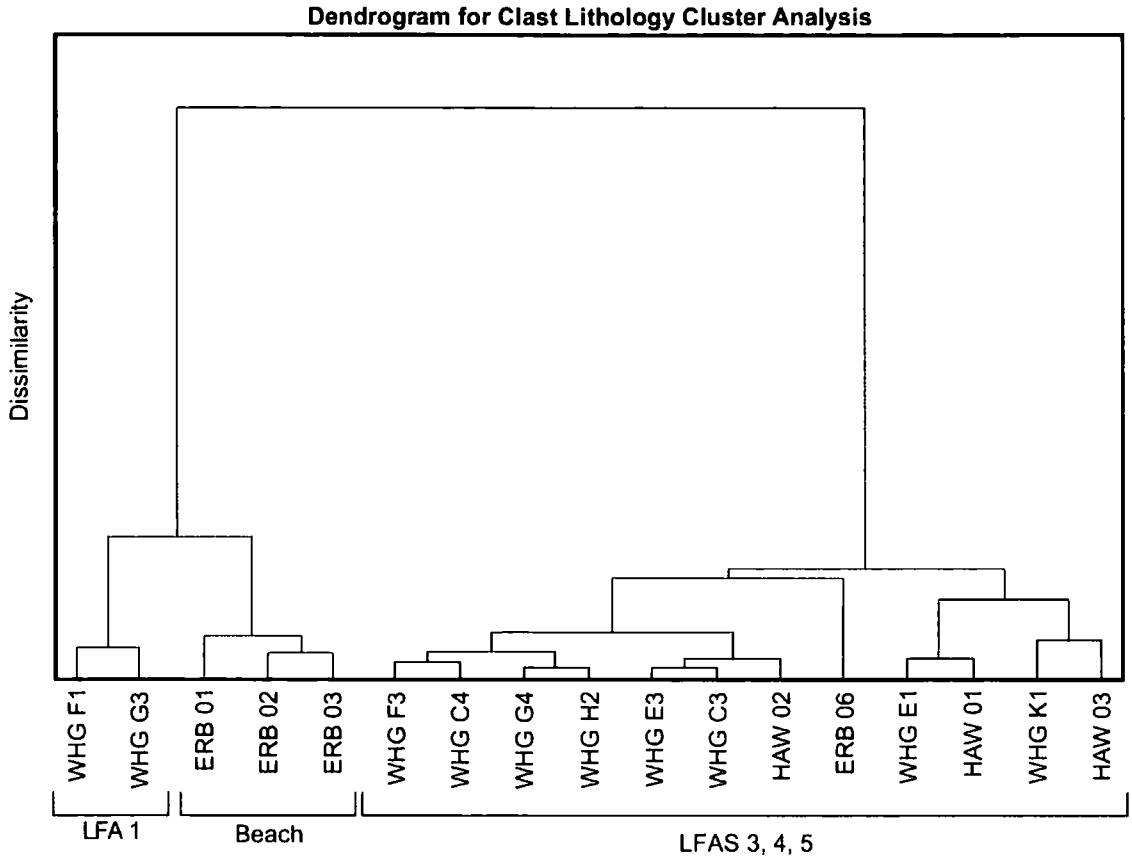

Figure 6.58: Cluster Dendrogram for Clast Lithological Analysis. Three principal groups are clearly distinguished; LFA 1, the Easington Raised Beach, and LFAs 3, 4 and 5.

A PCA on the correlation matrix and covariance matrix was performed in parallel with the cluster analysis. The Cretaceous, Permian, Quartzose and Southern Uplands lithologies were identified as the most important lithologies in the differentiation between the assemblages at Warren House Gill. The first two components accounted for 68 % of the variation in the dataset, meaning that they are acceptably representative of most of the variation present. Component 1 (52 % of the variation) is composed principally of Cretaceous and Quartzose lithologies on the positive axis, and Southern Uplands material plots negatively on the axis, as shown in Figure 6.59. Component 2 is mostly composed of Permian and Jurassic lithologies, and accounts for 16 % of the variation. The third component accounts for 11 % of the dataset, and is mostly related to the amount of sandstone present. The PCA on the correlation matrix clearly distinguishes between the beach deposits, LFA 1 and the other lithofacies. LFA 1 plots to the bottom right due to the presence of igneous and Cretaceous erratics, and low amounts of Permian erratics (Figure 6.59). The PCA fails to discriminate between all other lithofacies at Warren House Gill.

These graphs show that LFA 3 is comparatively enriched in Southern Uplands, Carboniferous, Sandstone, and Permian lithologies.

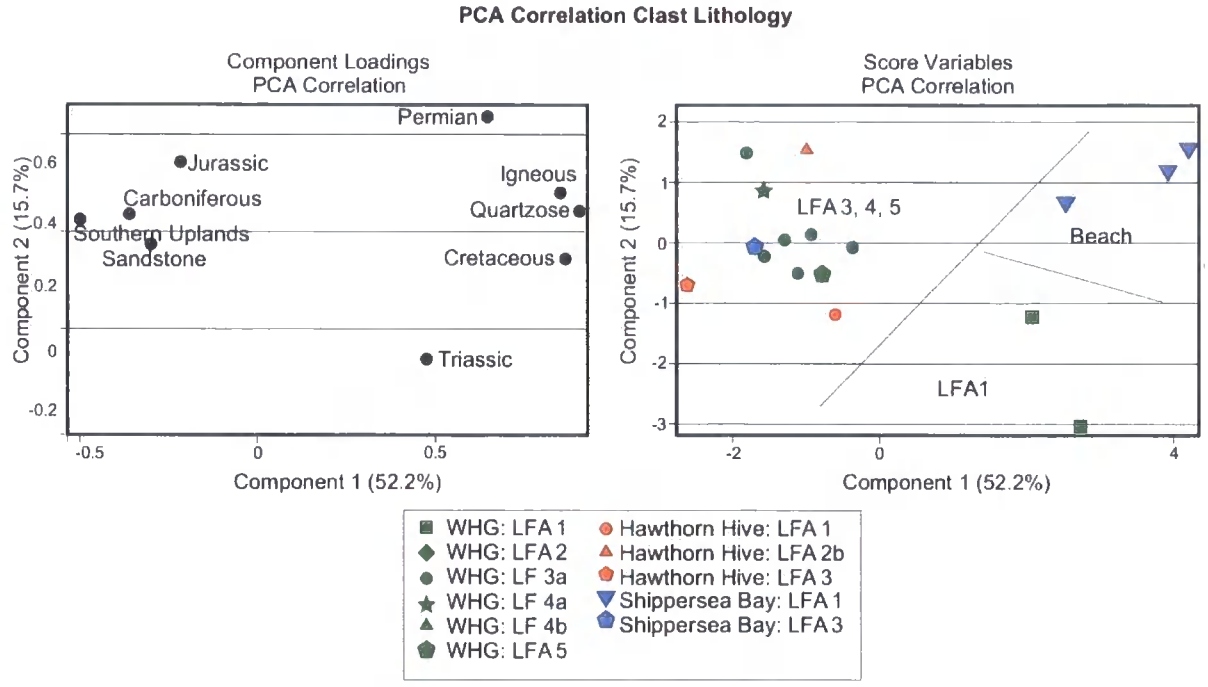

Figure 6.59: Annotated PCA Correlation on Clast Lithological Data. Divisions are drawn on by eye to emphasise distinction.

Heavy Mineral Analysis

HMA also shows that LFA 1 is distinct from the other lithofacies associations at Warren House Gill; for example, there are very few opaque minerals (38.7 %; Table 6.9 and Figure 6.60). LFA 1 is typified by relatively high proportions of ferriactinolite (8.8 %), monazite (6 %), hypersthene (4.4 %), hornblende (3.6 %), and apatite (2.3 %), and by relatively low percentages of zircon (2.5 %) and kyanite (2.2 %) when compared to other lithofacies. Additionally, the presence of minor amounts of rare minerals such as pumpellyite and piemontite is unusual in British glacigenic deposits.

The heavy-mineral suite within LFA 2 (Table 6.9) is made up of abundant garnet (17.1 %), epidote (14.4 %), clinopyroxenes (9.9 %), and biotite (16.1 %). There are lower percentages of sphene (6.6 %), zoisite (6.1 %), carbonate minerals (3 %), and hornblende (3 %). LFA 2 thus shows similarity to LFA 1. LFA 3 is enriched in garnet (12.6 %) and dolomite (16.4 %), followed by biotite (9.0 %), muscovite (7.5 %), andalusite (6.3 %) kyanite (6.0 %), zoisite (6.3 %), epidote (4.4 %), chloritoid (4.1 %) and minor amounts of staurolite.

The heavy-mineral suite of LFs 4a and 4b is similar to LFA 3 and LFA 5 in many ways (Table 6.9). There is a significant amount of locally sourced dolomite (19.3 %); garnet (14.2 %), biotite (11.2 %) and zoisite (8.7 %) are the next most common minerals. Kyanite (7.3 %), muscovite (6.8 %), andalusite (4.9 %), chlorite (4.2 %) and tourmaline (3.6 %) are also present. The heavy-mineral suite of LFA 5 is distinct from the other lithofacies at Warren House Gill. There is abundant garnet (28.7 %) and zircon (16.0 %). The lithofacies is also comparatively enriched in apatite (4.5 %). LFA 5 is poor in dolomite (4.1 %) and has limited amounts of mica minerals. There are no amphiboles, which is sharply contrasted with LFA 3.

Indices of ratios of ultra-stable heavy minerals (refer to Chapter 2.5.4) can be used to identify provenance-specific characteristics independent of hydraulic sorting, diagenesis, and chemical and mechanical stability (e.g., Morton & Hallsworth, 1994; Morton *et al.*, 2005; Morton & Hallsworth, 2007). Figure 6.61 shows the results of these indices. Chrome spinel-zircon, apatite-rutile, and apatite-garnet fail to discriminate between the lithofacies. LFA 1 does generally cluster closely together, but there is considerable overlap. However, the apatite-monazite index does produce a dichotomy between the lithofacies. LFA 2 plots very close to LFA 1, as does the one outlier from LFA 3 (sample WHG F3). LFA 5 is dominated by ultra-stable species, such as apatite, zircon, garnet, tourmaline, rutile and brookite. The lack of unstable mineralogies suggests that this deposit has been weathered, and possibly reworked. However, the mature suite of heavy minerals presents ratios very similar to those of LFA 3 (Figure 6.61).

Table 6.9: Average percentage (non-opaques) heavy mineralogy at Warren House Gill, 63-125 and 125-250 μm fraction. For detailed raw counts, refer to Appendix IV.

	Heavy-mineral Phase	LFA 1	LFA 2	LFA 3	LFA 4	LFA 5
	n	***4646***	***1204***	***21276***	***6346***	***2058***
	% Opaques	38.67	44.25	77.98	73.83	76.18
	% Non Opaques	61.33	56.75	22.02	26.17	24.82
	% Heavy Minerals	0.76	0.43	1.25	0.70	1.74
Silicate Group	*Olivine GP*	2.68	0.97	1.72	1.59	2.52
	Zircon	2.46	0.52	4.25	3.99	16.04
	Sphene	7.62	6.59	2.07	0.48	3.39
	Garnet GP	16.85	17.07	12.56	14.20	28.71
	Sillimanite	1.96	1.05	1.57	0.07	1.37
	Andalusite	1.98	1.46	6.29	4.85	0.69
	Kyanite	2.18	1.10	6.97	7.33	4.12
	Staurolite	1.07	0.18	0.46	0.57	0.00
	Chloritoid	2.77	0.13	0.61	0.19	0.00
Epidote Group	*Zoisite / Clinozoisite*	4.45	6.13	6.33	8.65	7.35
	Piemontite	0.11	0.00	0.00	0.00	0.00
	Epidote	8.22	14.42	4.37	1.23	2.29
	Lawsonite	0.04	0.00	0.17	0.14	0.46
	Axinite	1.47	2.02	0.13	0.08	0.00
	Pumpellyite	0.03	0.00	0.46	0.00	0.00
	Tourmaline GP	1.95	1.57	1.80	3.61	4.33
Pyroxene Group	*Enstatite*	1.25	1.05	1.09	0.46	0.22
	Hypersthene	4.37	1.50	1.22	0.15	0.46
	Diopsidic Clinopyroxene	0.80	0.00	2.19	1.11	1.14
	Augitic Clinopyroxene	3.82	9.90	2.59	0.35	0.23
Amphibole Group	*Tremolite*	0.00	0.00	0.00	0.06	0.00
	Ferriactinolite	8.79	0.00	1.39	0.00	0.00
	Hornblende	3.55	2.96	0.70	0.55	0.00
	Diallage	0.18	0.44	0.08	0.00	0.00
	Glaucophane	0.00	0.00	0.03	0.00	0.00
Mica Group	*Muscovite*	4.06	3.17	7.50	6.76	4.53
	Glauconite	0.91	0.00	0.16	0.13	0.00
	Biotite	3.95	16.08	8.95	11.22	2.25
	Chlorite GP	1.43	6.11	4.05	4.20	0.45
Oxides	*Rutile*	0.79	0.26	1.97	1.80	4.56
	Brookite	0.80	0.84	1.58	3.96	6.84
	Spinel GP	0.12	0.00	0.19	0.15	0.22
	Anatase	0.31	0.00	0.18	0.54	0.00
Carbonates	*Dolomite / Calcite*	1.73	3.04	16.35	19.27	4.08
Sulphates	*Baryte*	0.00	0.00	0.00	0.34	0.00
Sulphides	*Sphalerite*	0.00	0.00	0.05	0.00	0.00
Phosphates	*Apatite*	2.29	2.62	1.92	2.70	4.53
	Monazite	6.99	0.79	1.07	0.25	0.23

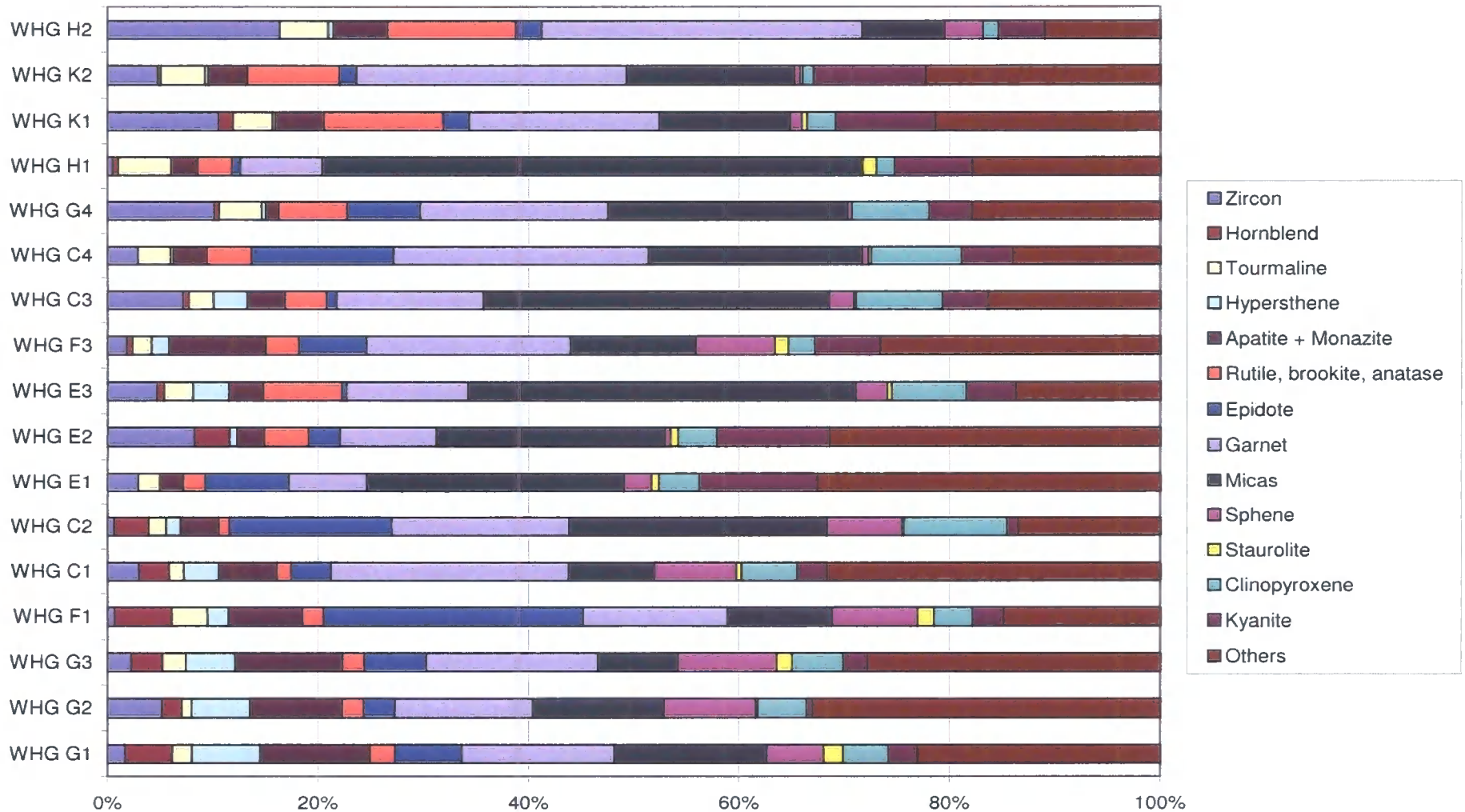

Figure 6.60: Compound bar chart showing proportions of heavy mineral species. LFA 1 contains higher percentages of hypersthene and hornblende. LFA 3 (WHG E1 to WHG G4) contains more kyanite, micas, and less sphene.

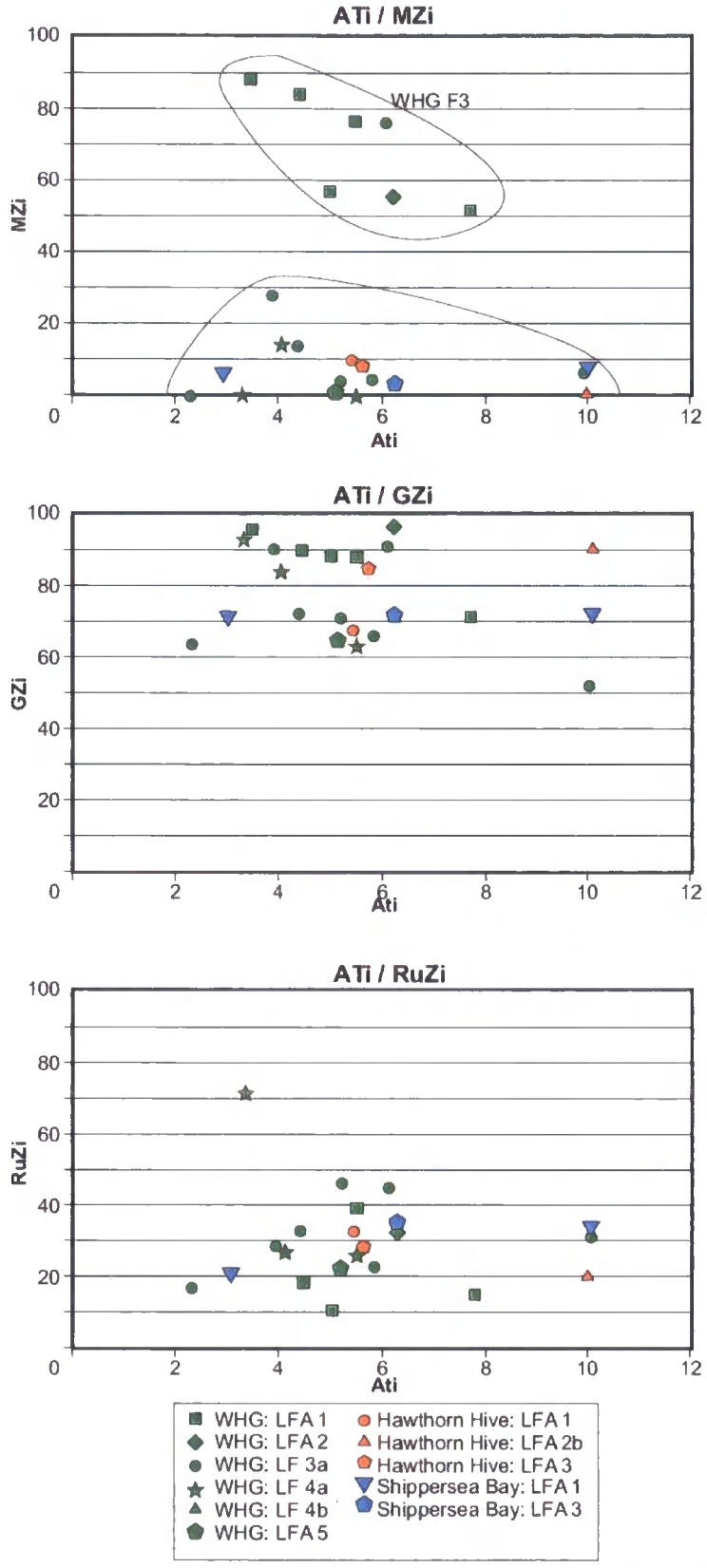

Figure 6.61: Graphical representation of ratios of ultra-stable heavy minerals. Annotations are drawn on by hand to emphasise distinction. ATi: Apatite-Tourmaline index. MZi: Monazite-Zircon index. GZi: Garnet-Zircon index. RuZi: Rutile-Zircon Index. See Chapter 2, Section 2.5.4.

To explore and to simplify the heavy-mineral data set further, the mineral species were divided into groups: silicates, epidote group, pyroxene group, amphiboles, carbonates and phosphates. Use of descriptive statistics such as a correlation matrix shows that carbonates, amphiboles, pyroxenes and phosphates are inter-related and explain much of the variance in the dataset. A ternary diagram of the relative proportions of these groups of minerals clearly differentiates between LFA 1 and the other lithofacies associations (Figure 6.62). LFA 1 forms a tightly clustered group, caused by the high proportions of amphiboles and pyroxenes, but with low proportions of phosphates.

Principle Components Analysis (PCA) was performed on all samples, using both covariance and correlation matrices. The covariance matrix best differentiated the lithofacies. Pyroxenes, carbonates, phosphates, epidotes, amphiboles and pyroxenes are the most important mineral groups for this (Figure 6.62). The first two principle components explain 66 % of the total variance, and their plots are therefore an accurate representation of the whole dataset. The LFA 1 samples again plot in a well-defined envelope, due to the comparatively high proportion of amphiboles. This PCA shows a clear dichotomy between LFA 1 and other sediments, but does not discriminate between the other lithofacies. LFA 2 always plots nearby, perhaps demonstrating that the sediments of LFA 2 are derived from LFA 1. One outlier of LFA 3 (WHG F3) always plots close to LFA 1.

In the PCA analysis (Figure 6.62), LFA 3 plots in a wide scatter, reflecting inter-sample heterogeneity. It is similar in composition to LFAs 4 and 5, and to the beach sands and diamicton in Shippersea Bay. Variation in LFA 3 is mostly explained by Component 2, reflecting the variation in Carbonate and Epidote groups of minerals. This result is also reflected in the scores of ultra-stable heavy minerals (Figure 6.61).

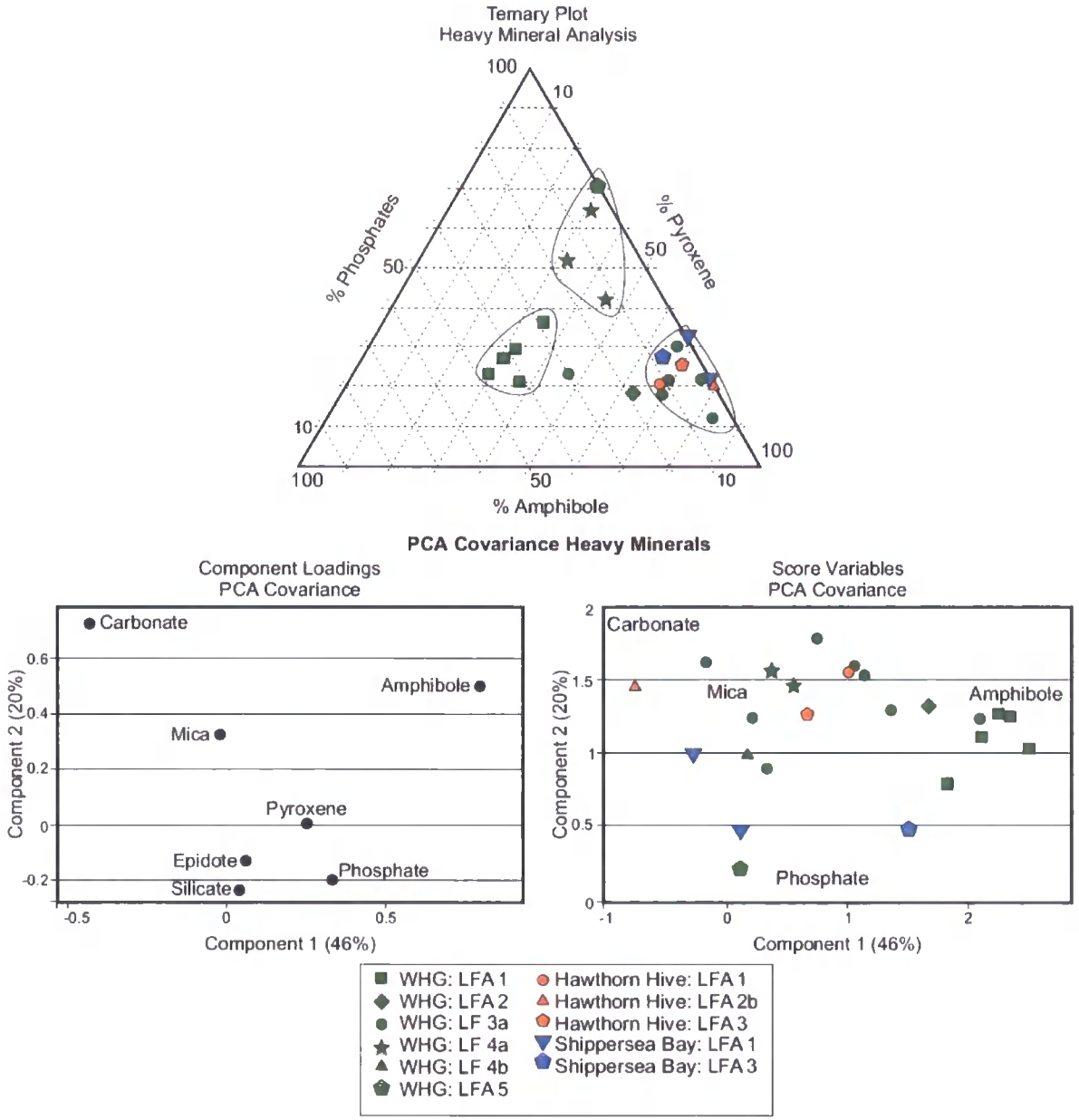

Figure 6.62: Ternary diagram and PCA plots of heavy mineral suites of lithofacies of Warren House Gill.

A cluster analysis was performed along side the PCA (Figure 6.63). The resulting dendrogram showed that the samples form three principle clusters. LFA 1 forms a tight, well-defined cluster, illustrating its uniqueness at Warren House Gill. The cluster dendrogram was not efficient enough to discriminate between the other lithofacies, which are mainly grouped together. The most weathered and most leached samples also clustered together.

WHG H2 plots closely to LFA 3 and 4 in the various statistical analyses of the dataset, but interestingly, does not show an affinity with either HAW 03 or ERB 06, the other

topmost lithofacies outcropping from Hawthorn Hive to Blackhall Rocks. The ratios of ultra-stable heavy minerals, cluster analysis and principle components analysis is not efficient enough to distinguish between LFAs 3, 4 and 5 at Warren House Gill.

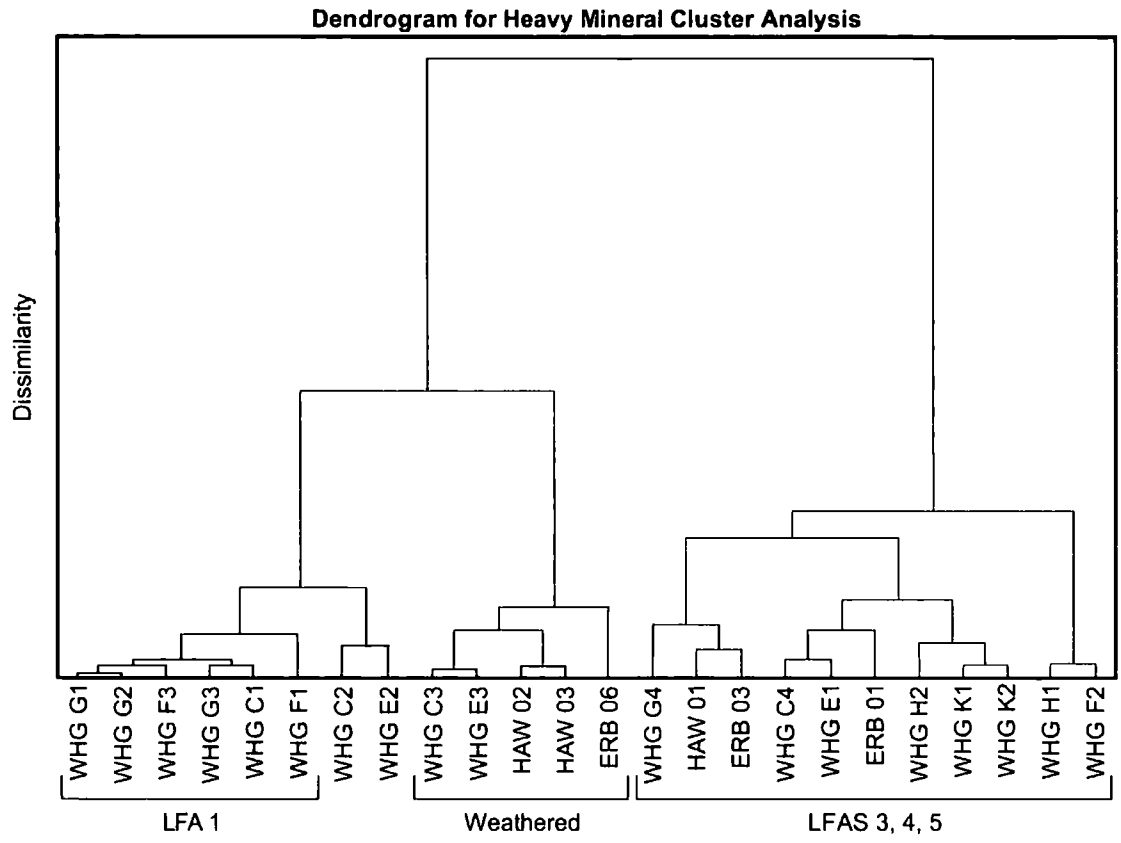

Figure 6.63: Dendrogram showing clustering of samples.

Geochemical Analysis

The geochemical analysis showed that, compared to the other samples at Warren House Gill, LFA 1 samples WHG G1, G2 and G3 all have significantly lower lead, rubidium, aluminium, and calcium contents (Table 6.10). Titanium, iron, magnesium, and aluminium explain a substantial proportion of the variation between lithofacies within the dataset. A cluster analysis of the abundant metals revealed that there are four principle groups of sediments (Figure 6.64). Firstly, LFA 1 sediments from exposures G and F group closely together. WHG C2, the beige silts, and WHG E2, the sand fold, plot very closely to LFA 1. WHG C2 is probably partly derived from LFA 1. WHG F2 and WHG E2 are sand folds and sandy inclusions within the diamict matrix, and this may account for their positions. WHG F3 may be at least partly mixed with LFA 1, accounting for its similarity to WHG F1.

Table 6.10: Geochemistry results, high abundance metals, for all samples at Warren House Gill. For detailed raw counts, refer to Appendix IV.

SAMPLE		High Abundance Metals (Average concentration, mg / kg)						
		Na_{23}	Mg_{24}	Al_{27}	K_{39}	Ca_{44}	Ti_{48}	Fe_{57}
LFA 1	WHG C1	7850	1811	16303	16022	13931	3140	21023
	WHG G1	7163	2004	26463	17602	15237	3933	30560
	WHG G2	8167	1703	24342	17930	14840	3949	30930
	WHG G3	9913	1710	22528	18363	14962	4038	32240
	WHG F3	5290	13000	203000	20600	61600	3250	29200
	WHG F1	4600	14600	209000	24300	55900	3730	31000
LFA 2	*WHG C2**	*8970*	*2629*	*13761*	*17447*	*16174*	*3723*	*25110*
LFA 3	WHG C3	3522	5403	11428	14437	23814	3051	24895
	WHG C4	6550	5790	185000	22200	130000	2530	24400
	WHG E1	4440	7400	161000	15600	57500	2540	21900
	WHG E2	4237	2969	3972	6849	25202	1606	14432
	WHG E3	3631	4460	8494	13798	26515	2992	24831
	WHG G4	6030	3880	174000	18000	87800	2550	62400
	WHG F2	5390	18400	245000	25400	85400	3540	33400
LFA 4	WHG H1	2950	10600	291000	15400	40000	2180	17800
	WHG K1	6790	4300	245000	23300	75200	2290	25500
	WHG K2	5230	11100	277000	13300	60400	1750	14500
LFA 5	WHG H2	6270	7380	204000	16900	59000	2410	27800

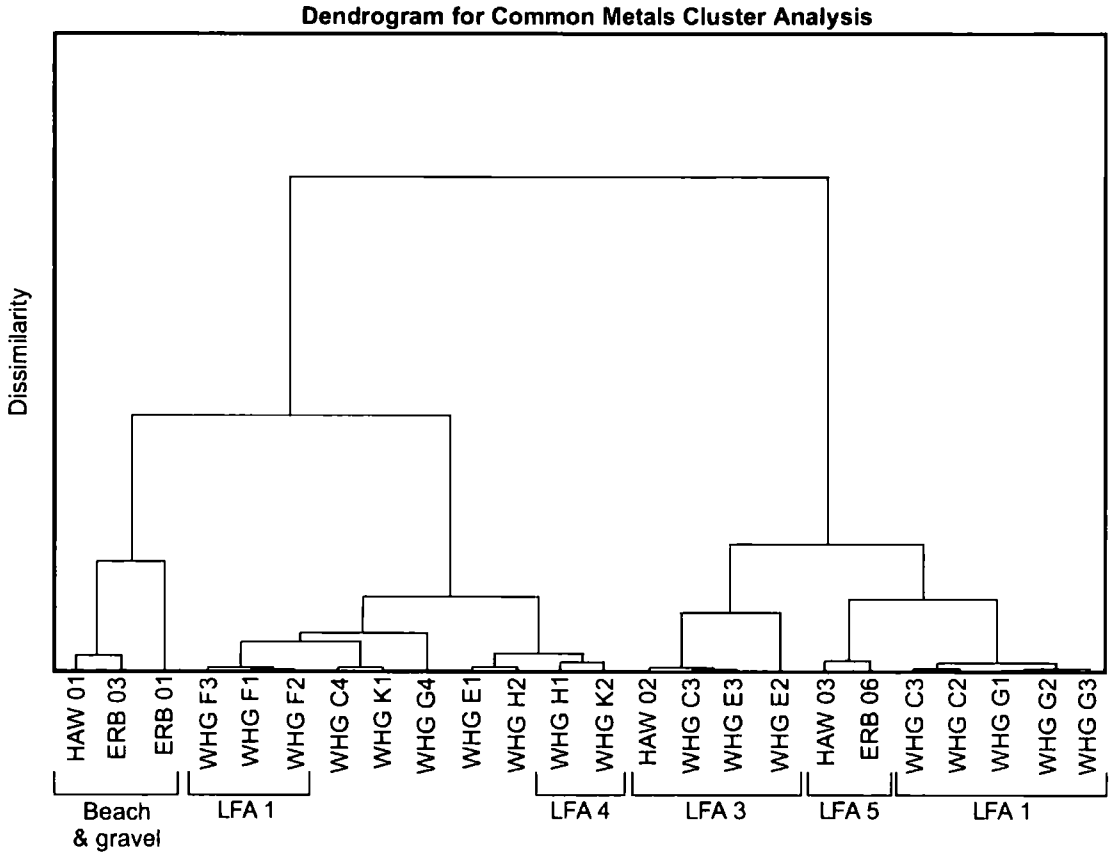

Figure 6.64: Cluster dendrogram, common metals analysis.

A PCA Covariance on the abundant metals further emphasises the uniqueness of LFA 1 at Warren House Gill (Figure 6.65). Components 1 and 2 together make up 80 % of the covariance, so this is an acceptable simplification of the dataset. Component 1 is dominated by aluminium and secondarily by calcium, whilst Component 2 is strongly controlled by magnesium. LFA 1 forms two distinct groups, as indicated by the cluster analysis, with the samples from Exposure F plotting closely to samples from LFAs 3 and 4. The limited influence of the bedrock on Exposure G can be inferred by its distance from the locally derived calcium and magnesium metals. The analysis of the trace metals shows a similar pattern; again, LFA 1 clusters closely together and near LFA 2 while remaining distinct from LFAs 3, 4 and 6. Geochemically, LFs 4a and 4b resembles LFA 3 and LFA 5 (Figure 6.65), which are all similar to the lower diamicton at Hawthorn Hive. Sample WHG E2 is poor in many metals, possibly due to leaching through the bedded sands.

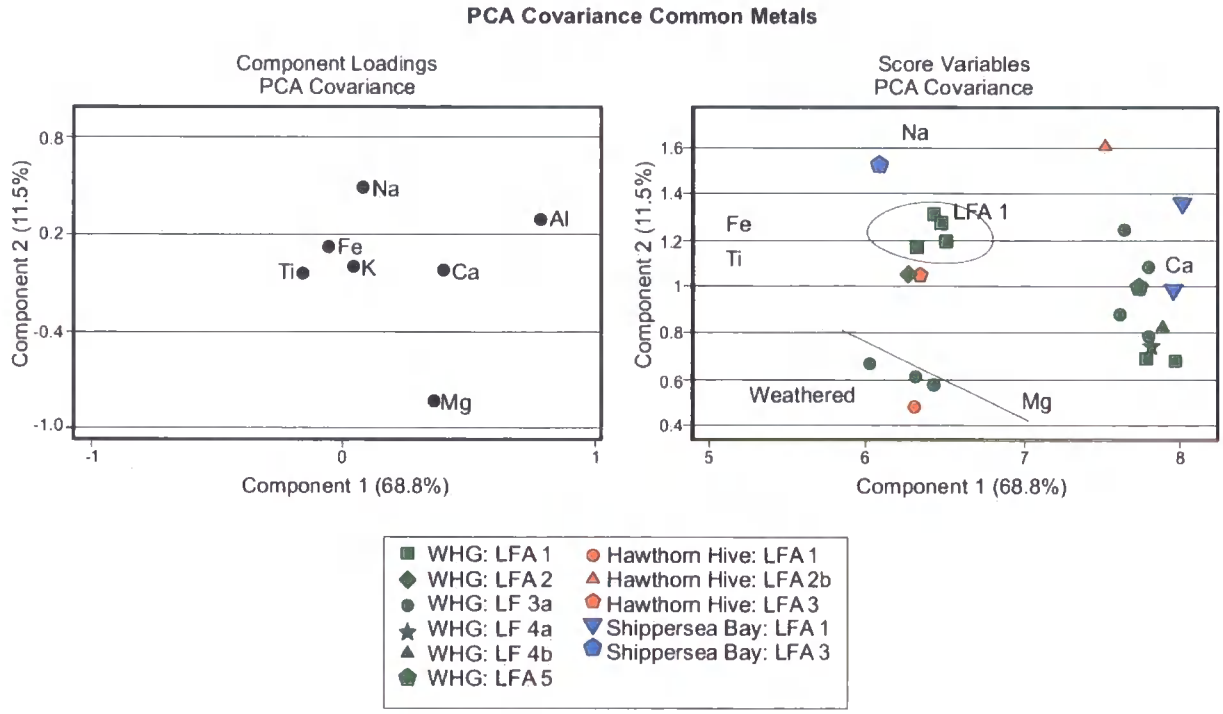

Figure 6.65: Annotated Principle Components Analysis (Covariance) of Common Metals

6.3.2 Biological Analyses

Foraminifera

LFA 1 incorporates fragments of bivalves, and sample WHG F1 yielded *Chlamys* sp., *Hiatella* sp., and *Balanus* sp. fragments. These were too broken and poorly preserved to

identify to genus level. Samples WHG F1 (89 specimens counted) and WHG G2 (221 specimens counted) contained well-preserved calcareous benthic arctic foraminifera species (Figure 6.66), with high percentages of *Elphidium excavatum* forma *clavata.* Subsidiary species include *Cassidulina reniforme*, *Cibicides lobatulus*, *Haynesina germanica,* and planktonic forms.

Samples from both the pink silts and the black mud beds yielded no pollen, but sample WHG C2 yielded rare (82 specimens counted) and very small foraminifera (Figure 6.66). The fauna are in good condition and show little signs of reworking. They consisted primarily of unidentified planktonics. Benthic calcareous species include *Elphidium* sp., *Haynesina germanica* and *Brizalina variabilis.* There are very rare examples of *Cibicides lobatulus* and *Cassidulina* sp. Some of these species are very similar to those in LFA 1, while others (*Haynesina germanica* and *Brizalina variabilis*) are new, and are characteristic of temperate intertidal environments.

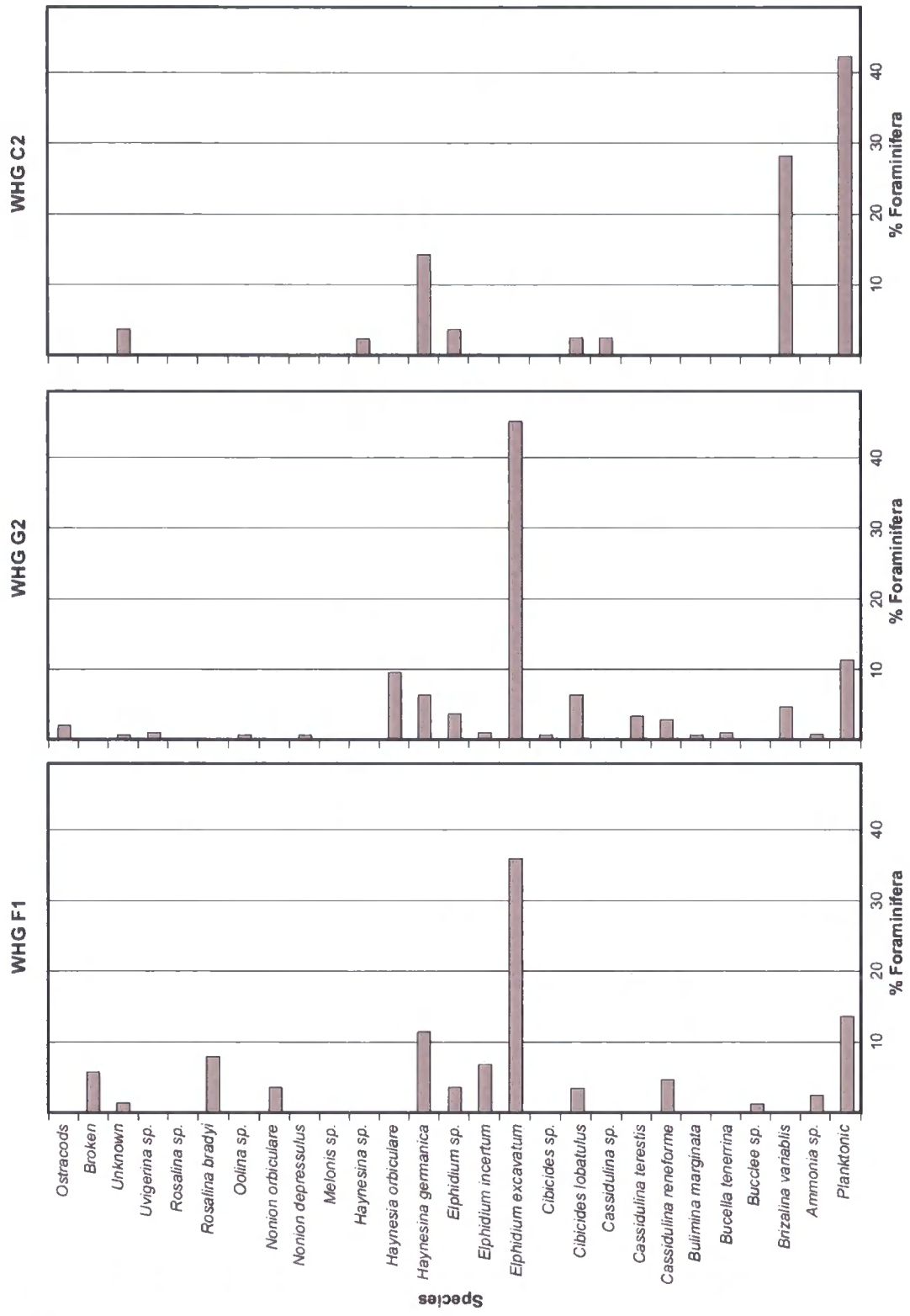

Figure 6.66: Percentages of foraminifera in LFA 1 and LFA 3

Palynological Analysis

Sample WHG F1 was analysed by Dr. Riding of the British Geological Survey for palynomorphs and dinoflagellate cysts (Table 6.11). Wood fragments are common, but the

residue is dominated by other plant tissue, and a mixture of Carboniferous to Quaternary age palynomorphs (Riding, 2007). Refer to Appendix IV for the palynomorph report.

Carboniferous spores in WHG F1 are relatively rare, and are largely *Densosporites* and *Lycospora pusilla*. Jurassic grains and the characteristic Early Cretaceous forms *Cicatricosisporites* spp. (spores) and *Cribroperidinium* (dinoflagellate cysts) were observed in low numbers (0.3 %). Significant numbers of Eocene dinoflagellate cysts were identified, including *Areosphaeridium diktyoplokum, Deflandrea oebisfeldensis, Eatonicysta ursulae,* undifferentiated chorate (i.e. process-bearing) forms, and *Homotryblium* spp. *Areosphaeridium diktyoplokum* and *Eatonicysta ursulae* range from the Ypresian to Priabonian and the Ypresian to Lutetian respectively (Powell, 1992). The range of *Deflandrea oebisfeldensis* is Late Palaeocene to Early Eocene (Powell, 1992). Large amounts of Quaternary pollen are present. These include *Alnus, Corylus, Filicales, Pinus, Sphagnum*-type, and *Tilia* (Riding, 2007).

LFA 3 contains abundant kerogen and palynomorphs. The most prominent elements were wood fragments, with lower proportions of some plant tissue and well-preserved palynomorphs, virtually all of Carboniferous age (Riding, 2007). These Carboniferous palynomorphs are dominated by *Densosporites* and *Lycospora pusilla*. There are lower numbers of *Calamospora* sp., *Cirratriradites saturni, Endosporites globiformis, Florinites* sp., *Radiizonates* sp., and *Tripartites vestustus. Endosporites globiformis* is indicative of the Namurian and Westphalian (Smith & Butterworth, 1967). There are extremely low numbers of Quaternary spores, such as *Pinus*.

Table 6.11: Palynomorphs and dinoflagellate cysts at Warren House Gill (Riding, 2007).

Sample	WHG F1 (LFA 1)	WHG F3 (LFA 3)
Carboniferous spores	33 (2.3 %)	Ca. 99 %
Jurassic dinoflagellate cysts	1 (0.1 %)	-
Late Cretaceous palynomorphs	4 (0.3 %)	-
Eocene dinoflagellate cysts	168 (11.8 %)	-
Quaternary miospores	1045 (73.4 %)	Ca. 1 %
Non age-diagnostic	172 (12.1 %)	-

6.4 Chronostratigraphy

6.4.1 Amino Acid Racemisation

LFA 1: The Basal Shelly Diamicton

Amino acid racemisation of marine bivalve fragments by Dr. Penkman and Miss Demarchi of York University used the new technique developed by Dr. Penkman to date intra-crystalline amino acids (see Chapter 2). Unfortunately a well-developed database for different shell species is still to be developed, and no absolute chronostratigraphy could be established for *Hiatella* shells within WHG F1 (LFA 1).

The *Hiatella* shells were compared to similar terrestrial shells (*Valvata* sp. and *Bithynia* sp.). Unfortunately, diagenesis appears to be different between the two species, so the dates remain inconclusive at this stage. The acids THAA and FAA were analysed (Figure 6.67). Amino acid diagenesis between THAA/FAA Asx and THAA/FAA Gla showed diagenesis consistent with an age of MIS 9 – MIS 11. However, the diagenesis of THAA / FAA Ala and THAA / FAA Val gave much older ages, rendering the age inconclusive. There is a different degradation pattern between *Hiatella* and terrestrial reference genera (*Valvata* and *Bithniya).* A direct comparison for age estimation is not possible now, and more independently dated samples of *Hiatella* are needed, to make a detailed study of the diagenesis patterns.

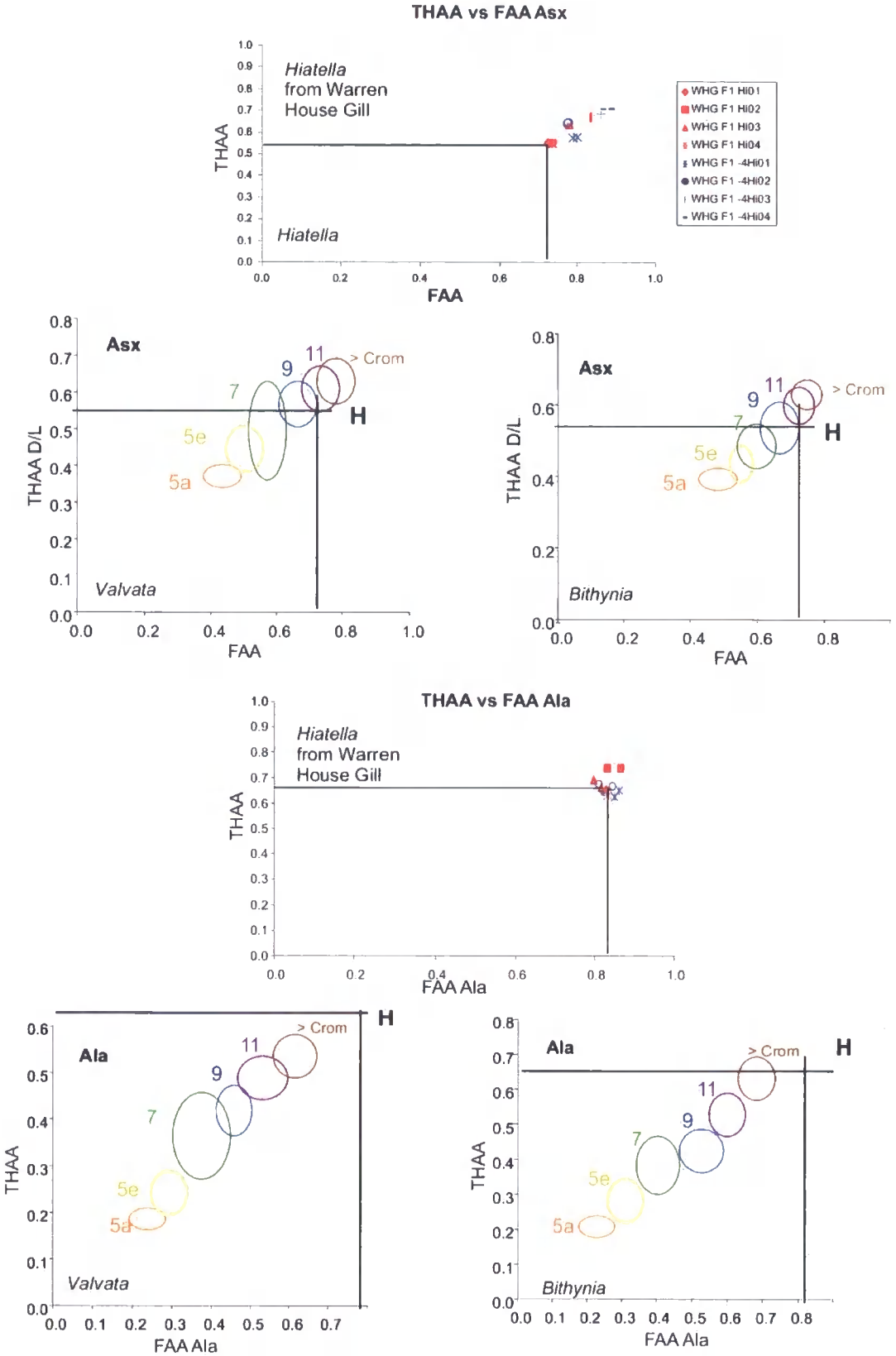

Figure 6.67: AAR from Hiatella shells from LFA 1, Warren House Gill, compared to Bithynia and Valvata. The Species Effect creates a different diagenesis of different acids in different shells, making the AAR ages inconclusive, but suggestive of the Middle Pleistocene. > Crom is before the Cromerian.

6.4.2 Optically Stimulated Luminescence Dating

LFA 2: The Beige Silts

The beige silts were sampled for OSL dating, but the grain-size is too fine to yield replicable, reliable age results. Uranium-series dating on the carbonate race nodules is ongoing (Dr. Pawley and Dr. Candy, pers. comm.).

LFA 3: The sand fold

Ongoing OSL work has attempted to date the fold nose in Exposure E1. This sand is shown to be younger than the overlying LF 4a. The OSL dates on the fold nose yielded results of 80 ka BP, but were overestimating the dose rate by 10 to 20 %. Reliable age estimates only overestimate by 5 % at the most, so these dates have very large error margins. Work is ongoing to attempt to better constrain these ages, but as of time of writing, these ages can be considered reliable to within the early Devensian (80 to 40 ka BP; Dr. Pawley, pers. comm.). Further work to constrain the age of these sands is ongoing.

LF 4a: The red sands and silts

The red sands and silts were sampled for OSL dating in both Exposure K and Exposure H by Dr. Pawley, and they yielded ages of between MIS 6 to 10. However, these dates cannot be considered reliable, particularly as they overly 80 ka BP age on the sand fold in Exposure E1. The luminescence signal will not give consistent outputs during repeated measurements. It is the opinion of Dr. Pawley (pers. comm.) that prior to further tests and ongoing work to exclude feldspar, mathematical tests, and multiple aliquot procedures on grains that have been ground to silt size and re-etched in HF to exclude inclusions of feldspar, these dates cannot be considered reliable.

A persistent problem with the quartz crystal lattice is apparent here. According to Dr. Pawley (pers. comm.), the Carboniferous quartz, which was derived from the volcanic and metamorphic complex of Scotland, has a very short transportation history. This type of quartz has caused problems in many regions outside of northeast England, but also in the Swale Valley and in the Vale of York (Dr. Pawley, pers. comm.). Inclusions of feldspar within the quartz grains can also affect the age result.

It is likely that the main problem is that the crystal lattice is flawed, which has been repeatedly found in sandstones with a short transportation history (Dr. Pawley, pers.

comm.). Given that they overly the Devensian sediments, of whose age Dr. Pawley is more confident of, these dates are therefore rejected, subject to ongoing research.

6.5 Interpretation

6.5.1 LFA 1: The Basal Shelly Diamicton

Summary of LFA 1

LFA 1 is visible in exposures D2, F, G and H. In exposures F, G and H, it rests directly on Magnesian Limestone bedrock. In Exposure E2 (LF 1c), it is interbedded with LFA 2 (the beige silts). LFA 1 is a grey, clay-rich diamicton with rare clasts that include granite, chalk, limestone, flint and red marl. It has deformed sandy inclusions, which exhibit folding and faulting. The diamicton contains fragments of marine bivalve shells, an arctic foraminiferal assemblage, and numerous Eocene palynomorphs.

In thin section, LFA 1 shows microscopic normally graded sand laminae with conformable contacts. They are folded and faulted, and are deformed underneath and above dropstones. The thin section exhibits numerous rounded, silty intraclasts that show deformation, rotation and breakage. Mineralogical and geochemical analysis shows that LFA 1 is significantly different to the overlying lithofacies, with a unique provenance signature. AAR dating on shell fragments within LFA 1 indicates a probable minimum age from MIS 9 to the Cromerian.

LFA 1 Process Interpretation

LFA 1 at Warren House Gill is Trechmann's "Scandinavian Drift" and Thomas's "Warren House Formation" (Trechmann, 1915; Thomas, 1999). LFA 1 has the macroscale and macro- and micro-scale hallmarks of a waterlain deposit (see Table 2.5). The macroscale characteristics include Type 2 Laminations (Roberts & Hart, 2005) with far-travelled lithics, conformable contacts, dropstones, weak plasmic fabrics, turbid water foraminifera, fossil shell fragments, and stratification (Boulton & Deynoux, 1981; Domack, 1984; Powell, 1984; Eyles *et al.*, 1985; Hart & Roberts, 1994; Merritt *et al.*, 1995; Carr, 2001; Ó Cofaigh & Dowdeswell, 2001). The increase in clast content and coarsening upwards (Figure 6.54) indicates increasing proximity of the ice margin. The graded and glaciotectonised laminations are interpreted as sedimentary rather than tectonic in origin, and are related to remobilisation and subsequent resettling of material by subaqueous traction currents (Eyles & Eyles, 1983). Microscopically, the deformed graded

bedding, lack of plasmic fabric development, and stratification all indicate that this is a deformed proximal waterlain diamicton, deposited by mass flow and rain-out from a glacier terminus (Powell, 1984; Eyles *et al.*, 1985; Powell & Molnia, 1989; Hart & Roberts, 1994; Carr, 2001; Hiemstra, 2001). The diamicton is therefore interpreted as being deposited by the rapid rain-out of material from dense sediment-laden underflows into the palaeovalley; the coarsening upwards particle-size distribution (Figure 6.54) being related to the increasing proximity to the glacier terminus (cf. Lee & Phillips, 2008).

The foraminifera *Elphidium excavatum* is typically found in turbid arctic environments and is associated with glaciomarine conditions (Hald & Korsun, 1997). *Cassidulina reniforme* is typically associated with this species and supports a glaciomarine interpretation. *Cibicides lobatulus* is usually found more distal to the ice margin. The variety of species with the dominance of *Elphidium excavatum* suggests that the sediment is some distance from the glacier margin but still cold water. The presence of species such as *Haynesina germanica* indicate open-water conditions (Hald & Korsun, 1997; Jennings *et al.*, 2004). The well-preserved nature of the foraminifera tests indicates limited reworking. Glaciomarine rainout diamictons typically have paired *in situ* marine bivalves. However, the broken fragments of bivalve shells in LFA 1 are obviously reworked. There is no indication of flattened, crushed or sheared whole bivalves, so they were incorporated already broken.

Micromorphological analysis supports an interpretation as a glaciomarine rainout diamicton (cf. Table 2.5) subsequently subjected to post-depositional shearing, remobilisation, compaction, and soft sediment deformation, but which still retains some original sedimentary structures. There has been ductile deformation resulting in folding of primary bedding.

Increased shear and deformation is apparent higher up in the lithofacies, and the sediment is increasingly homogenised. WHG TS F1 preserves some evidence of primary depositional features such as graded bedding, which has been deformed but not completely homogenised. The lack of strong turbates, grain lineations, and a strong plasmic fabric indicates a low stress signal and precludes a genesis as a direct subglacial till (Carr, 2001; Khatawa & Tulaczyk, 2001). Deformation was potentially induced syn- or post-depositionally, due to ice push, dewatering, increase in ice overburden pressure, or post-depositional slope processes, inducing ductile deformation, fluidisation of laminations, grain rotation and shear (Phillips *et al.*, 2002). Brittle faulting occurred during the final

phase of deformation, probably induced by lowered porewater pressure (Hart *et al.*, 2004). It cuts across the fluidised soft-sediment deformation (Phillips *et al.*, 2007).

The S_1 value and the rose plot of the clast macro-fabric from LFA 1 (Exposure G, Figure 6.4) shows very little clustering along the a-axis. The angle of dip of the clast macro-fabric is quite variable but generally high. Glaciomarine diamictons are typified by random clast macro-fabrics with a high degree of dip (Powell, 1984; Domack & Lawson, 1985; Powell & Molnia, 1989; McCabe *et al.*, 1993; Hart & Roberts, 1994).

Powell (1984) distinguished four zones of glaciomarine deposition; distal, proximal, marginal, and ice-contact. The lower facies of LFA 1 constitutes sediments typical of distal glaciomarine facies, with muds and rare dropstones, as shown in Figure 6.68. LF 1a was predominantly formed by suspension settling with rare inputs of ice-rafted debris. This facies grades into a more proximal facies that is dominated by suspension settling (LF 1b), with increasing inputs of ice-rafted debris as the ice front advances. Turbidity currents and underflows resulted in the deposition of sand layers. These were subsequently deformed by syn- and post-depositional processes such as sediment remobilisation (Powell, 1984; Hart & Roberts, 1994).

In Exposure E2, LF 1c clearly shows mixing between LFA 1 and 2, with rooted structures, stringers, attenuated folds, deformed inclusions and boudinage. These structures are typical of subglacial glaciotectonic deformation (cf. Evans *et al.*, 1995; Roberts & Hart, 2005; Hart, 2007; Lee & Phillips, 2008; Phillips *et al.*, 2008). These penetrative, deformational processes typically occur at the shear zone, with grounded subglacial ice and shearing. The sandier facies of LFA 2 within the glaciotectonite would have resulted in a decrease in shear strength through a comparative increase in pore water content (Evans *et al.*, 2006). This deformation could therefore occur even at low shear strains (as discussed by van der Wateren *et al.*, 2000). The lack of lateral continuation of this glaciotectonite highlights the intensely localised ductile deformation. This penetrative deformation and mixing occurred most recently during the glaciation which deposited LFA 3 above, accompanied by erosion of LFA 2.

This investigation has therefore found that LFA 1 is a distal glaciomarine rainout diamicton, deposited in the base of a palaeovalley. It was conformably overlain by silts, but these were subsequently subjected to glaciotectonic deformation. The increase in deformation structures in LF 1b and LF 1c indicates that this sediment was later (and possibly repeatedly) subglacially deformed.

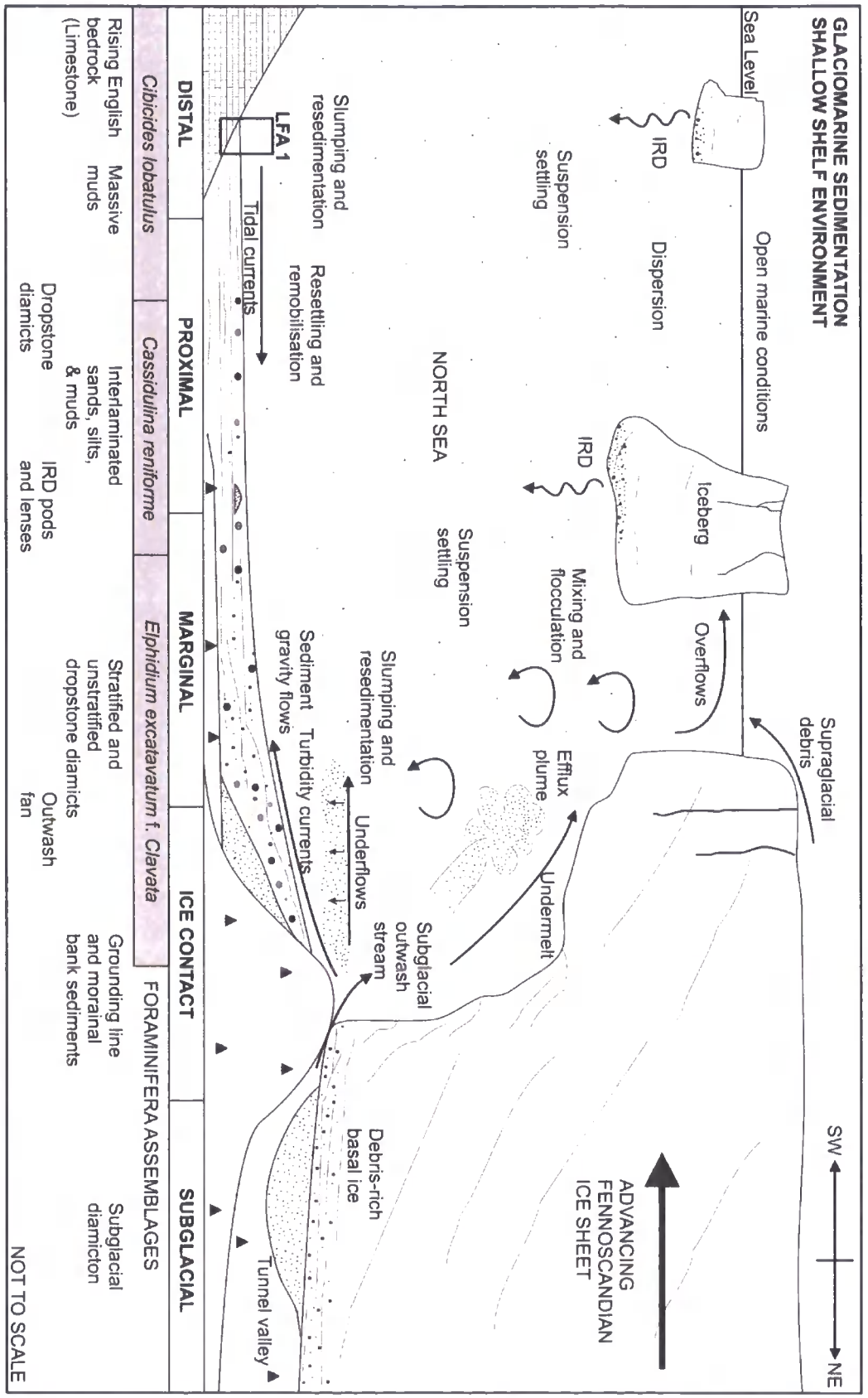

Figure 6.68: Cartoon displaying the four zones of glaciomarine sedimentation in tidewater glaciers. Modified from Hart and Roberts (1994). The principle foraminiferal assemblages are denoted by their likely dominant species.

LFA 1 Provenance Interpretation

LFA 1 at Warren House Gill incorporates palynomorphs, flint and chalk indicative of the Cretaceous (Riding, 2007). The only likely source for these fossils and erratics is the Late Cretaceous chalk in the far northeastern North Sea. There is little evidence of Carboniferous input to the palynomorph assemblage.

The heavy-mineral assemblage within the rainout diamicton is distinctly different from that of the overlying subglacial tills. Care must be taken here, as the water-lain nature of LFA 1 may result in hydrological sorting of the minerals. Less dense, platy minerals such as micas might be expected to remain in suspension longer than denser, cubic or prismatic minerals such as zircon or garnet. Processes of deposition may therefore account for some of the differences in the mineral suites. However, analysis of the ultra-stable minerals with similar hydraulogical behaviour indicates that there are provenance-specific minerals, such as the input of monazite. The settling velocities of different-shaped grains was investigated by Briggs *et al.* (1962), who argued that variations in grain shape caused drag, and concluded that both grain shape and density variations were equally important in determining heavy-mineral suites in water-lain sediments. Additionally, minerals with a high degree of sphericity may settle out before blade-shaped or platy minerals (Lee, 2003).

The statistical analysis of the heavy-mineral suite shows that the increased presence of amphiboles clearly distinguishes LFA 1 from the other lithofacies present at Warren House Gill. Diallage and ferriactinolite are associated with low-grade schists and meta-igneous pellitic rocks, such as those of the Dalradian of Scotland or the Caledonides of Norway (Bryhni & Andréasson, 1985; Strachan *et al.*, 2002). The mineral assemblage chlorite, ferriactinolite, and biotite is diagnostic of the Greenschist Facies of the Caledonide rocks of Scandinavia (Bryhni & Andréasson, 1985). They are associated with epidote, chloritoid, albite, muscovite, calcite and dolomite. Although calcite and dolomite could be locally sourced, and chloritoid is present in Scottish metamorphic rocks, epidote is not found in significant quantities in the other tills and is most likely to be derived from this particular mineral assemblage. Dolomite is not very durable and unlikely to travel significant distances (Passchier, 2007). The Greenschist Facies outcrops widely in southeastern Norway (Bryhni & Andréasson, 1985).

Hornblende occurs in LFA 1 in significantly higher percentages than in the other lithofacies at Warren House Gill. Hornblende is associated with higher temperature metamorphism (Hubert, 1971). This could potentially be sourced from the Epidote

Amphibolite facies, which underlies the Greenschist Facies in southern Norway. The diagnostic minerals of this assemblage are Al-garnet, epidote and hornblende. Accessory minerals are biotite, chlorite and muscovite (Bryhni & Andréasson, 1985). Small outcrops of epidote-amphibolite rocks also occur in the southwest Highlands (Strachan *et al.*, 2002).

The heavy minerals of LFA 1 are also distinguished from the others by the high percentages of monazite, hypersthene, and by the presence of rare minerals such as piemontite and pumpellyite. Piemontite is associated with low-grade schists and manganese ore deposits. The most likely source for this mineral is therefore the Scottish schists of the Dalradian, or Southern Uplands greywackes. Monazite is typical of acid igneous erratics (Hubert, 1971), and could be sourced from Scotland or Scandinavia. Hypersthene is found in basic igneous rocks and gneisses, such as the Carboniferous basalts of Scotland or the Permian basaltic lavas of Oslofjord (Oftedahl, 1960; Stephenson & Gould, 1995). The pyroxenes and olivine minerals could be derived from Scottish mafic igneous rocks, or the metamorphosed Norwegian basement rocks (Bryhni & Andréasson, 1985). The combination of the metamorphic minerals chloritoid, staurolite and garnet is indicative of Stonehavian metamorphism from northeast Scotland, close to the Highland Boundary Fault (Stephenson & Gould, 1995; Trewin, 2002).

The gravel clast lithology of LFA 1 includes 52.6 % Magnesian Limestone, which conflicts with original descriptions (Trechmann, 1915; Beaumont, 1967). The clast-lithological suite includes several lithologies common in northeast England, but also a significant number of far-travelled igneous erratics, some of which are distinct enough to be used for provenancing. LFA 1 has significant percentages of quartzose lithologies, potentially derived from Permian sandstones. There is relatively little local or Pennine input, reflected in the low proportions of Carboniferous Limestone (3 %), sandstone (1.9 %), coal (0.2 %), and shale (0 %).

No rhomb porphyries or larvikites from southern Norway (Smed & Ehlers, 1994) were found, though these have previously been reported (Trechmann, 1915, 1931b). These may be very rare, or may be rafted in, explaining the concentration described by Trechmann. A single large boulder recovered from the sample WHG C1 (LFA 1) is an alkali k-feldspar granite with quartz, plagioclase and minor biotite, but lacking muscovite. Alkali-feldspar granites do not occur widely in northeastern Scotland, and these are excluded by the absence of muscovite in the granite (cf. Stephenson & Gould, 1995). The most likely

source for this granite is the Permian Drammensgranit from the Oslofjord region of Norway (cf. Oftedahl, 1960; Smed & Ehlers, 1994).

Various other lithologies within LFA 1 are probably derived from Scotland. The occurrence of typical Cheviot andesite in LFA 1 shows input from the English northeastern coast. A potassium-feldspar alkali granite with muscovite and hornblende was found, which is typical of the Aberdeenshire granites (Stephenson & Gould, 1995). Several syenites were found in samples WHG G3 and WHG C1; these are variable and wide-ranging, and could be derived from either Norway, the Scottish Basement or the Grampian Highlands (Oftedahl, 1960; Smed & Ehlers, 1994; Stephenson & Gould, 1995). WHG C1 includes a single metamorphic erratic that is rich in mafic minerals, probably sourced from Aberdeenshire. It is of a lower grade than is found in Scandinavian metamorphic rocks. LFA 1 incorporates numerous archetypal Scottish Grampian Highlands acidic porphyries, from north of the Highland Boundary Fault. The schist and slate are metamorphic erratics characteristic of the Dalradian of Scotland (Figure 2.7, page 78). The remaining igneous erratics such as syenite are too indistinct to determine provenance and could originate from either the Grampian Highlands of Scotland or from Scandinavia (Smed & Ehlers, 1994). There is additionally a reasonable component of offshore material within LFA 1. Flint and chalk erratics are derived from the Cretaceous, of the northeast North Sea basin (Figure 2.11, page 90). The Triassic Red Marl outcrops in the near offshore region, and rarely in fissures in the limestone bedrock onshore.

The lithological, mineralogical, and microfossil assemblage within LFA 1 gives a very mixed signal, suggesting ice rafting from a number of different ice-sheet sources. Rhomb porphyries have been reported from the site (Trechmann, 1915). The presence of Drammensgranit, rhomb porphyry and larvikite supports a Norwegian influence. There is strong evidence of a northeasterly North Sea input with the Eocene palynomorphs, red marl, and chalk and flint erratics. There is also strong evidence of a northeasterly Scottish input, with slate, schist, Grampian granites, and more southerly Cheviot andesites. There is a substantial component of syenite and granite, which could be derived from either Norway or Scotland. The low percentages of Carboniferous lithologies and the lack of erratics typical of the Midland Valley of Scotland, such as Old Red Sandstone, imply that the ice did not extend too far to the south.

6.5.2 LFA 2: The Beige Silts

Summary of LFA 2

LFA 2 is a complex, yellowish brown, well-sorted silt, showing stratification and lamination. It is well exposed in the sections on the southern side of the palaeovalley in Warren House Gill, and crops out from 6 m to 11 m O.D. It generally rests on bedrock, but in the deepest part of the palaeovalley, in Exposure C, it overlies LFA 1. In Exposure B, rounded cobbles are present at the base. The silts are strongly deformed, showing compressional deformation and extensional deformation structures such as augens, stringer initiation, water-escape, and pinching and swelling laminations. It is complexly interbedded and intercalated with LFA 1 in Exposure E2 (LF 1c) and with LFA 3 in Exposure D2 (LF 3b). LFA 2 incorporates an intertidal foraminiferal assemblage. LFA 2 resembles LFA 1 mineralogically and geochemically.

LFA 2 Process Interpretation

LFA 2 is banked up against the southern end of the palaeovalley. It overlies bedrock in the southern end of the valley; here it has been squeezed downwards under pressure into joints in the bedrock. Rounded cobbles are present at the bedrock / silt interface. The contact between LFA 1 and LFA 2 is difficult to observe but it is glimpsed in Exposure E2. Here, a glaciotectonite (LF 1c; see above) has been formed by the mixing of the two lithofacies associations (Banham, 1977; Pedersen, 1988; as defined by van der Wateren, 1995; Benn & Evans, 1996). This probably occurred post-depositionally during emplacement of LFA 3 above; LFA 2 at this location has been extensively eroded and only a narrow bed remains.

LFA 2 was originally interpreted as an interglacial loess (Trechmann, 1920). However, the presence of microscopic graded bedding and fluviatile Type A climbing ripples in samples WHG TS D*i* and D*ii* indicate that this sediment was deposited in a shallow subaqueous environment. The heterogeneity of grain size indicates that it is unlikely to be an aeolian loess. Additionally, the presence of foraminifera indicative of tidal estuarine environments indicates that this is a marine deposit. The foraminifera are distinct species from the underlying LFA 1; they suggest a shallow inter-tidal to open-marine zone (cf. Horton & Edwards, 2006). The presence of some cold-water species indicates that the palaeovalley may have been infilled very soon after the deposition of LFA 1. The

palaeovalley was occupied by a river or stream at this time, which may have delivered sediment to an estuarine or deltaic environment.

In Exposure D, clay augen structures are visible. These are 'clast and tail' features, with the narrow clay beds extending out from the augens' 'tails'. The key features are the non-graded clay laminations, the rotated, augen-shaped clay clasts, and the lack of lateral continuity of the clay laminations. Similar structures have been observed in Norfolk and elsewhere (McCarroll & Harris, 1992; Roberts & Hart, 2005; Hart, 2007; Lee & Phillips, 2008; Ó Cofaigh *et al.*, 2008), and they are indicative of rotational, extensional shear. Simple shear such as this is indicative of subglacial deformation (Hart, 2007), where deformable clasts are subjected to longitudinal extension, compression and rotation (Hart & Boulton, 1991). Unfortunately, it was not possible to prepare a thin section from these augens, and thus their primary mode of deposition remains unclear.

LF 2b provides evidence that, after deposition, the sediments were loaded and suffered extensive shear, soft-sediment deformation, fluidisation and dewatering, as defined by Mills (1983). Thin-section samples WHG TS D1 and D2 from LF 2b show abundant evidence of soft-sediment deformation. Liquefaction and fluidisation are related to vertical displacement forces, in this case either the weight of ongoing sedimentation, or loading by ice-overburden pressure (Mills, 1983; Phillips *et al.*, 2002; Phillips *et al.*, 2007). As porewater pressure decreased the sediments faulted and fractured through brittle deformation (Hart *et al.*, 2004).

Micromorphological analysis of the shear zone between LF 2b and LF 3a in Exposure D (WHG TS D*iii*) shows that the homogenised silt with clay and silt intraclasts has been subjected to shear stress, resulting in the minor plasmic fabric development, which is hindered by a lack of fines. The massive, homogenised silt could indicate the decoupling of the ice and the bed, and the injection of water at the ice-bed interface, resulting in 'lift-off' of the bed, and the survival of the weaker soft sediment below. The repeated occurrence of glaciotectonic deformation and soft sediment deformation of LFA 2 indicates that this sediment has been overridden by glaciers, possibly more than once.

The occurrence of LFA 2 some metres above present sea level indicates a marine transgression at Warren House Gill. This may have occurred after deglaciation and before immediate isostatic rebound. Long-term uplift of the whole sequence has also been proposed by other workers (Westaway, in press), and the proposed Middle Pleistocene age suggests that there has been significant uplift since the palaeovalley was formed. The lack

of biogenic material and abundance of clastic silts indicates that this may have occurred in a cold environment. Subsequent leaching by groundwater may also have impacted the preservation of organic material within the deposit. During statistical analysis, LFA 2 consistently plots close to LFA 1, demonstrating that the sediment is primarily derived from erosion of the underlying diamicton.

The beige silts (LFA 2) that overlie LFA 1 in the buried palaeovalley therefore contain a biostratigraphy that suggests open-marine conditions. These were probably deposited after the recession of the ice sheets from the area. Even after isostatic uplift, the base of the valley would have been considerably below sea level. Long-term tectonic uplift subsequently lifted the base of the silts to above sea level.

6.5.3 LFA 3: The Middle Diamicton

Summary of LFA 3

LFA 3 is a very variable deposit with a wide variety of facies, including massive, well-consolidated diamictons, well-bedded sands, and laminated clays. It overlies bedrock, LFA 1 or LFA 2, and is up to 30 m thick. The first facies is a brown to dark-brown diamicton, with numerous sandstone, limestone, and igneous erratics (LF 3a). At outcrop, smearing of soft clasts, stringer initiation, attenuation of fold noses, boudinage and sand beds are all visible. Thin-section analysis of this facies shows diamictons with associations of planar and rotational features, soft sediment intraclasts, and well-developed skelsepic and masepic plasmic fabrics. The lithologies of clasts within LF 3a show a clear British origin, and contain significant percentages of lithologies derived from the Coal Measures and the Permian. LFA 3 was possibly deposited from around 80 ka BP (~MIS 4), and probably up to MIS 2. In some places LF 3a has been complexly folded with the underlying sediments (LF 3b).

The third facies comprises coarse, poorly-sorted, gravelly sands, which outcrop towards the base of the diamicton (LF 3c). The fourth facies comprises well-sorted, bedded sands, visible in Exposure E (LF 3d). They are folded sub-vertically, but retain many primary depositional structures, such as planar bedding and right-way-up climbing ripples. These are crosscut by normal faults. These sands contain primary bedding structures, but have been recumbently and strongly folded. The fifth facies the laminated diamictons exposed in Exposure C (LF 3e and LF 3f). The comprise 10 cm thick, well-sorted clay

beds (LF 3e), and a red and brown laminated diamicton (LF 3f). The red and brown planar silty laminations have conformable contacts. They are draped over and under dropstones and show evidence on a microscale of subtle shear, rotation and deformation.

LF 3a: Massive diamicton facies

The diamicton facies (LF 3a) is indicative of subglacial deposition by a grounded ice sheet (Sharp, 1984; Alley *et al.*, 1986; Boulton & Hindmarsh, 1987). The evidence for this includes stringers emanating from point sources, formed through the shearing of soft lithologies (Hart *et al.*, 1990; Hart & Roberts, 1994; Roberts & Hart, 2005); the faceted, striated and far-travelled lithologies, and the well-consolidated nature of the sediment. On a microscale, the diamicton is characterised by deformation structures typical of subglacial tills formed through shearing processes (Boulton & Hindmarsh, 1987; Khatawa & Tulaczyk, 2001; Ó Cofaigh *et al.*, 2005; Menzies *et al.*, 2006). These include associations of rotational and planar features, skelsepic and masepic plasmic fabrics, pressure shadows, and far-travelled lithic fragments. The evidence for LF 3a being a subglacial till is repeated in several other thin sections, such as WHG TS D*iv*, taken from the diamicton just above LF 2b in Exposure D. This includes well-developed skelsepic plasmic fabrics and rotational structures in association with grain lineations (cf. Hiemstra & Rijsdijk, 2003).

Evans *et al.* (2006) have argued that it is difficult to assign specific genesis to the spectrum of sediments formed in a deforming glacier bed. Macroscopically massive tills are common, and are formed through a continuum of deformation, flow, sliding, lodgement and ploughing, coexisting at the base of the ice. They act in concert to transport sediment and deposit it as different end members, from tectonically folded and faulted stratified material (e.g., Roberts and Hart, 2005), to texturally homogenous diamicton. A till or a till complex contains a superimposed signature of transportation and depositional processes at the ice-bed interface (Evans *et al.*, 2006). Evans *et al.* (2006) argued that the genetic fingerprinting of tills should be less process-specific as tills are polygenetic. They propose the term 'traction till' to encompass sediments that were,

> *Deposited by a glacier sole either sliding over and/or deforming its bed, the sediment having been released directly from the ice by pressure melting and/or liberated from the substrate and then disaggregated and completely or largely homogenised by shearing.*

There is a wealth of evidence for subglacial tills that show evidence of both deformation and lodgement (e.g., Boulton & Hindmarsh, 1987; Evans & Twigg, 2002; Nelson *et al.*, 2005). These two processes are end members of a continuum, and most tills are a hybrid of the two. The structures indicative of lodgement in LF 3a (such as the planar microscopic features (Menzies *et al.*, 2006), and the massive, homogenised diamictons) are juxtaposed to structures indicative of subglacial deformation, such as stringer initiation (Roberts & Hart, 2005), attenuation of folds (Lee & Phillips, 2008), deformed inclusions (Berthelsen, 1979; Evans *et al.*, 1995), deformed intraclasts (Hicock & Fuller, 1995), weak clast macro-fabrics (Hart, 1997; Bennett *et al.*, 1999), and mixing in the lower parts of the till with rooted structures, shear lenses, till wedges and attenuated folds (van der Wateren, 1995; Hart, 2007). This mixing is seen in particular in Exposure D2, where LFA 2 and 3 are interbedded, with LFA 2 forming rooted, folded stringers and deformed inclusions within LF 3a. This glaciotectonite (LF 3b) indicates grounded subglacial ice and shearing (van der Wateren, 1995; Phillips *et al.*, 2002; Hiemstra *et al.*, 2007). The thin section of the contact (WHG TS ex D2) shows stringer initiation into LF 3a, indicative of ductile deformation under water-saturated conditions. The sharp contacts of the ungraded red sand beds confirm that these are the initiation point of Type 1 laminations formed during subglacial shearing (Roberts & Hart, 2005). Most of these structures indicate that LF 3a was deposited under low-strain conditions (van der Wateren, 1995; Lee & Phillips, 2008), but strain rates can vary both laterally and through time as porewater pressure fluctuates, creating a mosaic of deformation (Piotrowski & Kraus, 1997; Fischer & Hubbard, 1999; Piotrowski *et al.*, 2004). This explains why some of the tills are more massive and show more complete homogenisation (such as exposures G and H), while delicate deformation structures remain in place elsewhere (such as exposures B, C, D, and D2).

Clast macro-fabrics from LFA 3 (see Figure 6.27 and Figure 6.69) show little degree of clustering and S_1 values are approximately 0.5, but the S_1/S_3 difference indicates clear clustering about the principle eigenvector. The fabrics generally indicate an ice flow direction from north-west to south-east, though there is considerable variation. This generally follows the orientation of the palaeo-valley, which may have locally focussed ice flow. Recent studies have highlighted the importance of recognising that till fabrics are not related to specific till facies, and must be critically interpreted (Bennett *et al.*, 1999; Carr & Rose, 2003; Larsen & Piotrowski, 2003). There is currently controversy regarding the

development of strong and weak till fabrics. Weak till fabrics have been used to infer deforming bed conditions (Hart & Rose, 2001). Laboratory experiments have shown, however, that as soft till deforms, clasts attain a flow-parallel position to present a minimum obstacle size, resulting in a strong till fabric (Hooyer & Iverson, 2000). Frequent clast collisions may result in a weaker till fabric (Ildefonse *et al.*, 1992).

When the S_1 and S_3 values are plotted on the classic May diagram as below (Figure 6.69 A), the till fabrics fall into the category 'deformation tills' (May *et al.*, 1980; Larsen & Piotrowski, 2003). This also occurs on the Benn diagram (Benn (1994); Figure 6.69 B). The values are tightly clustered, and there is little variation in S1 strength. However, the generally low fabric strengths, as shown in Figure 6.69, and variable fabric directions, are predicted by the plastic deformation model to form under low cumulative strain. Varying stress directions can result in diffuse fabrics, as seen at in LFA 3 at Warren House Gill (cf. Larsen & Piotrowski, 2003). Frequent clast collisions and transient pore-water fluctuations can result in varied till fabric patterns, responding differently to stresses (Piotrowski & Kraus, 1997). The buried valley at Warren House Gill is likely to have been infilled with LFA 3 under a low stress regime, resulting in the weaker till fabrics, as illustrated below. The diagrams below support an interpretation as a traction till, showing strong deformation.

Sample WHG TS C5 was taken directly above the laminations at Exposure C. The thin section exhibits a diamict texture and a wide variety of grain sizes. There is also an isolated foraminifera test. The lack of strong turbates, and weak plasmic fabric development suggests that this was not deposited subglacially but instead is a water-lain diamicton deposited ice-marginally (possibly ice-contact), through the deposition of turbid meltwater plumes. The absence of tiled structures precludes a genesis as a remobilised till (as defined by Menzies & Zaniewski, 2003). The millimetre-scale grain stacks and grain lineations suggest later shearing of the sediment. The necking and rotational structures are indicative of ductile deformation (as noted by Hiemstra & Rijsdijk, 2003 in ceramic clay).

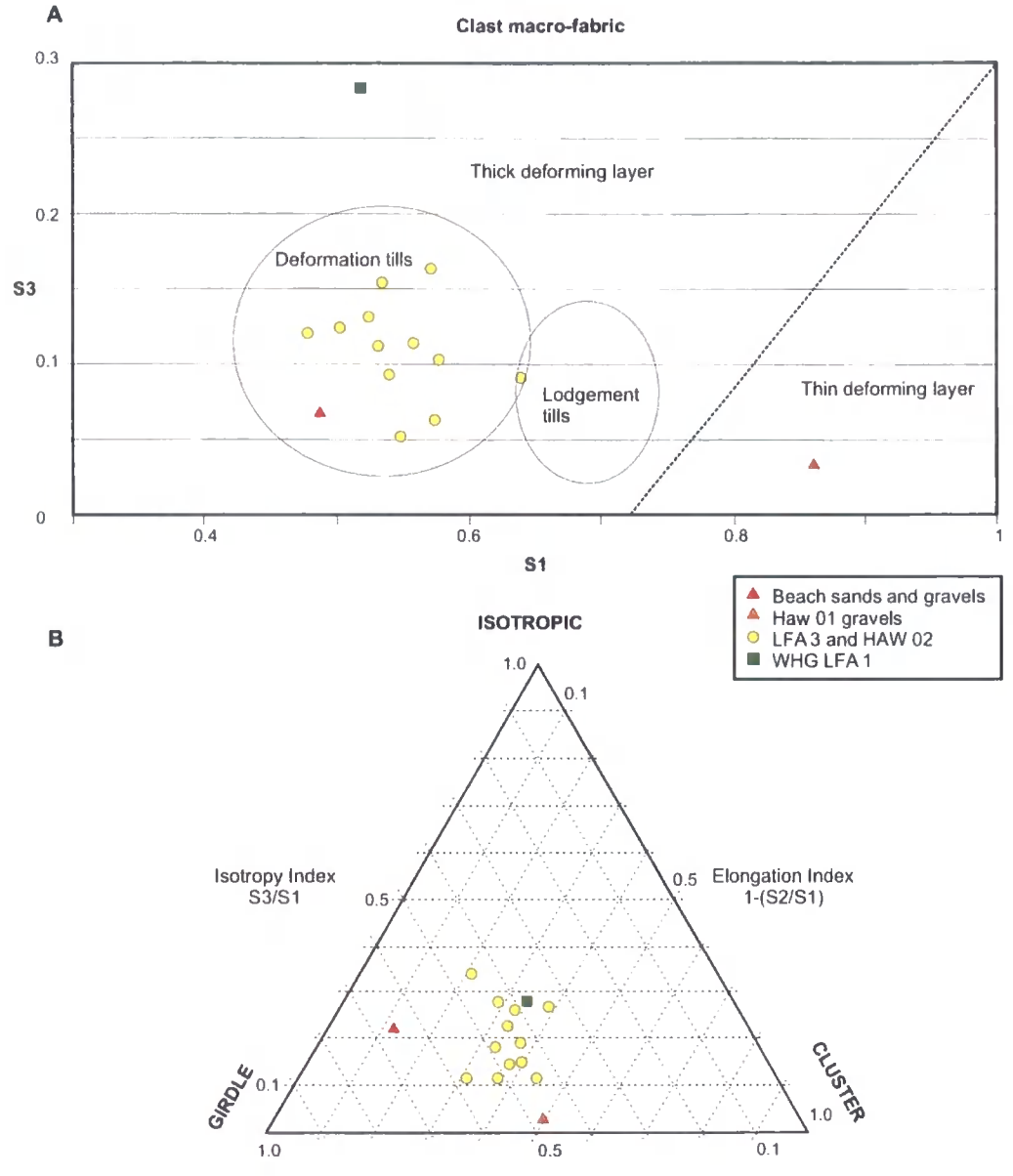

Figure 6.69: Clast macro-fabric May (A) and Benn (B) Diagrams.

Thin-section sample WHG TS E1 is a weathered diamicton with numerous structures indicative of subglacial deposition. Texturally, it is unsorted and it appears to be very well consolidated. The skeleton grains are principally composed of quartz, but there are some far-travelled grains suggesting long-distance transport. Structural analysis reveals features typical of subglacial tills such as turbates, lineations and skelsepic plasmic fabrics (Carr, 2001; Hart *et al.*, 2004; Roberts & Hart, 2005; Menzies *et al.*, 2006). The sample also has some indications of possible pedogenesis. The branching pores with diffuse boundaries and dendritic patters are interpreted here as the fossil remnants of root passages (Fitzpatrick, 1984). They lack the sharp, clearly defined boundaries of planar voids associated with

packing and laboratory practices. Additionally, the paler colour of the diamicton that traces the pores suggests that leaching has occurred. Framboid pyrite crystals are associated with marine sediments, and form *in situ* through the interaction of iron in the soil and sulphate in sea water (Fitzpatrick, 1984; Bullock *et al.*, 1985). The grains are associated with woody organic matter in the thin section.

The weathered nature of the diamicton, with the presence of root traces and organic matter, indicates that this is a subglacial till that has probably undergone some soil-forming processes. However, the till shows no sign of this at the macroscale. The till was buried and only excavated by the JCB, so this is unlikely to have been during the Holocene. Roots can penetrate several metres, but the thickness to the current land surface suggests that even plants with deep roots could not have reached the foot of the cliffs prior to coal waste dumping. These roots must therefore be older than mid-Twentieth century. However, the lack of macroscale evidence of pedogenesis and subtle nature of the evidence within the thin section makes it difficult to firmly interpret this as a palaeo-land surface, and it may just be related to twentieth century plants growing on the side of the cliff after colliery waste dumping.

LF 3c: Sand and gravel facies

The sands within LFA 3 are crudely bedded and poorly sorted. They principally crop out towards the base of LFA 3 at similar heights above sea level, but have variable morphologies and sedimentary structures. Some of the occasional small beds of sand have convex bases and flat tops. These were probably deposited by undermelt at the ice-bed interface in subglacial canals (as described by Walden & Fowler, 1994) or Nye channels, which were subsequently glaciotectonically deformed. They have suffered boudinage, folding, and shear.

The presence of channels of sorted sediments suggests that at the ice-bed interface, water-pressures were at or close to the ice-overburden pressure, indicating that even with silty sediments below, the hydraulic transmissivity of the sediments was insufficient to drain them adequately (cf. Larsen *et al.*, 2004). Channels evacuate surplus meltwater, and probably operated sporadically in response to changing water pressures.

LF 3d: Planar laminated sand facies

Another facies of LFA 3 is the large, well-sorted, sub-vertical sand fold (LF 3d). This facies retains many of its original sedimentary structures. The large sand fold in Exposure E is a significant feature and is marked clearly on Trechmann's original diagrams (Trechmann, 1920); it was protected for several decades under colliery waste. The sands have numerous hallmarks of subaerial fluvial deposition. Well-sorted parallel lamination, such as that seen in the sand fold in Exposure E2, is commonly formed by turbulent flow at high flow velocities (Allen, 1982). Clast lags point to traction current activity, while draped lamination indicates variable flow velocities. The Type B climbing ripples indicate slowly migrating ripples with high vertical aggradation rates (Allen, 1963). The parallel lamination is crosscut by normal faults, increasing in number towards the axis of the fold.

There is a limited amount of soft sediment deformation. The northerly orientation of the faults indicates that the direction of push came from the north. It is likely that these sands were part of a subaerial fluvial system, which was subsequently overrun and folded upwards into a large recumbent fold, probably related to proglacial ice-push. The top of the fold and down-ice limb were later removed by glacial erosion. Ice-marginal streams and lakes were therefore an integral part of the landsystem in which LFA 3 was deposited.

LF 3e and LF 3f: Laminated Diamicton facies

The final lithofacies are the two laminated facies in Exposure C. The lower laminations (LF 3e) crop-out from 16 m to 18 m O.D., and consist of well-sorted, stiff clays. The laminations are 10 cm thick, massive, planar-bedded, and are normally graded with conformable contacts, suggesting suspension settling in a quiet-water environment. The sediment was probably introduced through inter-flow or over-flow deposition, and possibly reflects localised subglacial or proglacial ponding (Powell, 1984; Ashley, 1995).

The upper red and brown laminated facies of LF 3f (Exposure C, 48 m O.D.) is also interpreted as a waterlain diamicton. The graded and conformable beds within the laminated facies are indicative of sedimentary origin (Eyles *et al.*, 1985). The macroscale dropstones that deform the beds underneath, and which are draped by laminations, support the ice-contact subaqueous diamicton interpretation (Ashley, 1975; Powell, 1984; Bennett *et al.*, 2000; Ó Cofaigh & Dowdeswell, 2001; Bennett *et al.*, 2002). The geometry of the boundaries as observed in thin section and in macroscale with alternating, conformable and intercalated beds of red and brown diamicton and poorly-sorted silts reflects pulsatory meltwater discharge into a standing body of water (Lee & Phillips, 2008). Macroscopic

dropstones exhibiting draped upper beds and down-warped lower beds are present, supporting an interpretation as deposition in an ice-contact, subaqueous environment (cf. Carr, 2001).

Laminae of silty sand are interpreted as having been deposited from the rapid rain out of poorly-sorted material from dense sediment-laden underflows (Ashley, 1975; Eyles *et al.*, 1989). The lack of *in situ* or derived marine micro- and macro-fossils indicates that this is probably a localised, ice-contact, glaciolacustrine deposit. The different, alternating colours of the laminations indicate injections of material from different sources, perhaps from different efflux streams containing varying concentrations of red marl excavated from off-shore.

After deposition, the sediments were loaded and dewatered, resulting in water-escape structures (Hiemstra *et al.*, 2006). The ice overrode and sheared the sediments, giving rise to microscopic grain-to-grain lineations, grain stacks, and stringers (cf. Menzies, 2000; Menzies *et al.*, 2006). Type III Pebbles, derived from the cannibalisation of material below, are common in the thin section WHG TS C4 (cf. van der Meer, 1993). The sediments were also subjected to brittle deformation, as indicated by edge-to-edge contacts and crushed grains (Menzies *et al.*, 2006).

LFA 3 Process Summary

LFA 3 is unusually thick for a subglacial till; the infilling of the palaeovalley may account for the thick diamicton sequences with weak clast macro-fabrics and the preservation of numerous delicate tectonic features, indicating a low-strain environment. There is evidence of extensive thrusting and glaciotectonism, such as in the overturned sand fold in Exposure E. Subglacial thrusting and stacking may account for the difference in altitude of the similar facies of LF 4a on either side of the palaeovalley. LFA 3 was probably deposited sub-marginally to ice-marginally, with subglacial to proglacial deposition of till, fluvial and lake sediments, all being subsequently proglacially tectonised. Submarginal to marginal glacier settings are associated with net sediment thickening, thrusting and till stacking, and are an ideal environment in which to pond sediments (Ashley *et al.*, 1985; Ashley & Warren, 1997; Phillips *et al.*, 2008).

6.5.4 LFA 4: The Red Sands and Gravels

Summary of LFs 4a and 4b

LF 4a is well exposed at Warren House Gill but does not outcrop significantly elsewhere between Blackhall Rocks and Castle Eden Dene. It is composed of several facies, and it occurs at various altitudes. The first facies, overlying LFA 3 in Exposure H, is a red sand with Type A cross-stratified ripples and planar lamination. It is overlain by a thin bed of clay, and then by another metre of red-bedded sands. A diamicton is incised into the facies. Above this, there is increasing evidence for soft-sediment deformation with boudinage and faulting. It is unconformably overlain by LFA 5, a gravel-rich, massive diamicton. A second facies (LF 4b) is exposed in Exposure K, where it lies directly on bedrock. Well-sorted sands are interbedded with coarse to fine, well-sorted, rounded fine gravels to coarse cobbles. The beds are scoured and convex. Again, this facies is overlain by LFA 5. The gravels contain mostly durable northern British clasts with some granite and porphyritic erratics.

LF 4a: Process Interpretation

A subaerial fluvial system deposited the variable red sands of LF 4a. The confined nature of the sediments within the Warren House Gill locality suggests that these are riverine, and only a small cross-section of the channel is visible. The diamicton that incises into the sediments in Exposure H could be a collapse of the channel side, and suggests that the river undercut the older diamicton. This interpretation is supported by the presence of slope-conformable slickensides, indicating slumping. The variable height of LF 4a between the two sides of the palaeovalley suggests that the fluvial system was switching on and off, and operating in the gill only sporadically, as the height of the ice-marginal sediments built up through till accretion. Ultimately, the incision of the modern stream during the Holocene led to the separation of the different facies of LF 4a on either side of the gill.

The distinctive red colour of the sands probably derives from the high amount of fine red Triassic marl, quarried from the immediate offshore region, suggesting an east-west flow direction. This indicates that the red sands are glaciofluvial in origin, flowing landwards from an ice sheet situated in the North Sea, damming normal drainage patterns. The localised outcrop is situated only immediately in and surrounding Warren House Gill. The abundant presence of soft red marl lithologies within the tills of the same colour as the red sands supports this interpretation. These red-bedded sands are therefore interpreted as a

locally red-stained facies of the Peterlee Member, perhaps related to the quarrying of red Triassic marl immediately offshore.

LF 4b: Process Interpretation

The sands and gravels in Exposure K, consisting of alternations between planar-laminated sands and well-sorted gravels, often incised into each other with convex bases, are suggestive of proglacial proximal outwash sediments. These more energetic sediments are possibly indicative of the increasing proximity of the ice margin.

LFA 3 and LF 4b Provenance

The clast macro-fabrics of LF 3a generally have low S_1 values, and exhibit some variability (Figure 6.69). However, they suggest an ice-flow direction from northwest to southeast. LFA 3 and 4 are lithologically and petrologically very similar and are likely to be genetically related.

The similarity between LFAs 3, 4 and 5 and the tills at Hawthorn Hive and Shippersea Bay means that much of the provenance indicators at those sites are also applicable here. Both LFA 3 and 4 contain significant numbers of locally derived Permian rocks, such as Magnesian Limestone (68.2 %), the yellow sands, and the Whin Sill Dolerite from the north or west. Carboniferous Limestone (3.4 %), coal, shale and most of the sandstones were sourced either from northern England and the Pennines, or possibly from the Midland Valley of Scotland (Figure 2.7). County Durham is isolated from these areas drainage-wise, so these lithologies can only have been brought in by glacial activity. Old Red Sandstone (0.3 %) is an archetypal lithology of the Midland Valley. The fragile lithologies such as sandstones and coal are unlikely to have survived long in the energetic fluvial environment, accounting for their absence from LF 4b, and the emphasis on durable limestones and quartzose lithologies in these gravels.

LFs 3a and 4b contain few far-travelled erratics. The acid porphyries could have been sourced from multiple regions of Scotland. Greywacke is likely to have been sourced from the Silurian turbidites of the Southern Uplands. The granites of LF 3a and 4b are rare and are too indistinct for provenancing. There is no indication of Cheviot porphyries or andesites.

The Triassic red marls in LF 3a occur offshore and in karstic fissures, and may have been reworked from the glaciomarine deposits below. The rare fragments of marine

bivalves are likely to have been reworked from older offshore sediments (possibly temperate marine or reworked glacigenic). There is no Eocene or Cretaceous impression. The palynomorph assemblage is dominated by Carboniferous spores, with virtually no Permian or Eocene species (Riding, 2007). There is therefore no offshore signal in this till.

Diagnostic heavy-mineral assemblages such as the garnet-andalusite-kyanite assemblage are indicative of Buchan-type metamorphism, indicating that some minerals were derived from as far north as Aberdeen (Johnson, 1991; Stephenson & Gould, 1995). The high proportion of dolomite and calcite minerals is likely to have been derived from the immediate Magnesian Limestone bedrock. The ferromagnesian minerals (olivine and pyroxenes) are probably from an ultramafic to mafic igneous source such as the Carboniferous volcanic rocks and related high-level intrusive basalts, basaltic andesites and andesites (including the Whin Sill Dolerite), such as those exposed in the Midland Valley of Scotland and southwards (Cameron & Stephenson, 1985; Trewin, 2002). There are a relatively large proportion of micaceous minerals, which could have been derived from a metamorphic or an igneous source, and which are common in many types of schistose metasedimentary rocks, diorites, granodiorites, and granites. These detrital micas could therefore originate from a number of provenance regions. LFA 3 and LF 4b contain a lithological assemblage characteristic of northern Britain, with detritus sourced from Aberdeenshire, the Southern Uplands, the Midland Valley of Scotland, and northern England.

6.5.5 LFA 5: The Upper Diamicton

Summary of LFA 5

LFA 5 outcrops at the top of the succession at Warren House Gill. It overlies the red sands and gravels in Exposure K, and is well exposed in Exposure H. LFA 5 is a massive, clast rich, well-consolidated diamicton with abundant striated, faceted clasts of widely varying lithologies. They are dominated by Permian and Carboniferous lithologies. The material is weathered, as emphasised by the presence of only ultra-stable heavy minerals. It was not possible to collect thin-section samples from this lithofacies.

Process Interpretation

The gravel-rich LFA 5 is interpreted here as a subglacial till. At outcrop, it is a massive, homogenous, consolidated diamicton, with faceted, striated clasts of wide-ranging provenance. It was probably deposited at the sole of a grounded terrestrial ice sheet (Evans *et al.*, 2006). The height of the sediment makes it very difficult to access, so it was not possible to obtain a clast macro-fabric or a thin section of this diamicton. It is correlated with the Horden Member at Hawthorn Hive, based on its stratigraphical position, and the unbroken, tabular nature of the outcrop.

Provenance Interpretation

LFA 5 at Warren House Gill contains abundant lithologies derived locally and from northern England. These include Magnesian Limestone (76.8 %), Carboniferous Limestone (9.9 %), Carboniferous and Permian sandstones (1.9 %), and Whin Sill Dolerite (1.1 %). There are very few igneous, far-travelled erratics, and there is no quartzite or quartz present. The majority of the clast lithologies are local or from the west or north. The small proportions of andesite and rhyolite originate from the Cheviots. It is possible that non-durable lithologies will have weathered out, resulting in the dominance of limestone and sandstone.

Mineralogically, this lithofacies is impoverished, with large numbers of stable and ultra-stable minerals. The non-stable minerals such as olivine were derived from the Carboniferous volcanic rocks from the Midland Valley of Scotland. Dolomite and calcite are rapidly mechanically broken down, but are derived from the immediate bedrock. Zircon (15.0 %), garnet (28.7 %), tourmaline (4.3 %), rutile (4.6 %), brookite (6.8 %), and apatite (4.5 %) comprise the majority of the remaining data set. The large proportions of near, durable lithologies and ultra-stable heavy minerals suggests that this is a reworked, weathered sediment, and that many of the minerals have been affected by dissolution or diagenesis. This is a weathered version of the uppermost till that crops out from Hawthorn Hive to Blackhall Rocks.

6.6 Discussion

6.6.1 The Warren House Formation

Lithostratigraphy

The Warren House Formation of Thomas (1999) requires redefinition. The name 'Ash Gill Member' is proposed here for the basal deposit of the 'Warren House Formation' (Thomas, 1999). The Ash Gill is a tributary to Warren House Gill (Figure 6.1), so this is an appropriate name for the Basal Shelly Diamicton (LFA 1). The Ash Gill Member is overlain by the beige silts (LFA 2), interpreted as being of estuarine origin, possibly including reworked loess. They are part of the Warren House Formation, and are here formally named the 'Whitesides Member' after the nearest gill (see Figure 6.1).

Previous researchers have interpreted the Ash Gill Member as a subglacial till (Trechmann, 1931b), or as a sediment deposited from a floating ice shelf (Beaumont, 1967). Smith and Francis (1967) argued that the 'Warren House Till' was overlain by two Devensian tills, which Francis (1972) named the Blackhall and Horden tills, with type sites at Blackhall Rocks and Horden. This study has shown that the Quaternary sediments in this region are considerably more complex and span a much longer time.

The Ash Gill Member has previously been correlated to the Bridlington Member of Yorkshire (formerly the Basement Till; Lewis, 1999; Table 1.4), based on the presence of Scandinavian lithologies, the similar marine ostracods within the Bridlington Crag of the Bridlington Member and the Ash Gill Member, and an inferred older age (Trechmann, 1915; Catt & Penny, 1966; Francis, 1972; Catt, 2007). On this basis it was assigned to MIS 6 (Catt, 1991b). However, a comparison between the lithological properties of the two sediments suggests that they were deposited independently and are not correlative (Table 6.12). The Bridlington Member is overlain by the Sewerby Raised Beach, dated to MIS 5e (Bateman & Catt, 1996; Clark *et al.*, 2004b), whereas this study suggests that the Ash Gill Member may be as old as MIS 8 - 12. Therefore, there is evidence of at least two independent incursions of Scandinavian ice towards the northeastern British coastline during the Middle Pleistocene.

Recent mapping and lithostratigraphic work in Norfolk has reinterpreted the Middle Pleistocene stratigraphy and proposed at least four lowland glaciations during the

Quaternary. Scandinavian ice was thought to have only influenced the British coastline once, during MIS 6, when the glaciofluvial Briton's Lane Fm was deposited (Hamblin *et al.*, 2005). The Briton's Lane Fm contained 4.7 % Scottish and northern English igneous erratics and 0.1 % rhomb porphyries (Table 5.17). The majority of the lithologies are locally derived Cretaceous flints. The heavy-mineral assemblage is dominated by high percentages of amphibole and epidote. Although previous workers have suggested an MIS 6 age for the outwash and correlated it to the Bridlington Member (Hamblin *et al.*, 2005), recent work by OSL dating suggests that the outwash is in fact of MIS 12 age (Pawley *et al.*, 2008).

The Ash Gill Member has more similarities to the Briton's Lane Formation, including the mixed Scandinavian and Scottish provenance signature, with a high percentage of amphibole (Table 6.12). The differences, such as increased Jurassic and Cretaceous lithologies, are due to the changing bedrock lithologies between Norfolk and County Durham. It is possible in both cases that the rare Scandinavian lithologies could have been reworked, but the strong North Sea palynomorph and lithological signature supports the northeastern provenance. An MIS 12 age for the Briton's Lane Fm and an MIS 10 or 12 age for the Ash Gill Member suggests that extensive ice sheets were present in the North Sea and in Scotland. The ice sheet that deposited the Bridlington Member may not have extended as far south as Norfolk, thus leaving no lowland depositional record in the area. However, it is dangerous to assume that tills of similar affinity would not have been deposited in most even-numbered marine isotope stages, meaning that the Ash Gill Member cannot be dated based on lithostratigraphic correlation alone.

Table 6.12: Comparison between the Briton's Lane Formation, the Bridlington Member and the Ash Gill Member.

	Briton's Lane Formation (Hamblin *et al.*, 2005; Pawley *et al.*, 2008)	Bridlington Member (Basement Till) (Catt and Penny 1966)	Ash Gill Member (This Study)
Particle Size	N/A	36-56 % clay, 28-35 % silt, 21-39 % sand	27 % clay, 40 % silt, 25 % fine sand, 5 % coarse sand, 1-2 % gravel
Colour	N/A	5 Y 3/1 to 4/2, very dark grey	10YR 4/1 dark grey
Clast macro-fabric	N/A	Two directions, primarily WNW-ESE, secondarily NNE to SSW	Random, little clustering
Structures	Cromer Ridge, 100 m high, with 30 m of bedded sand and gravel.	Inclusions of marine sediment. Isoclinal overfolds, axial trends plane in WNW-ENE direction	Laminations, dropstones, rare clasts, marine microfossils.
Process interpretation	Glaciofluvial outwash. Forms the Cromer Ridge, a push-moraine complex.	Subglacial till	Glaciomarine rain out diamicton in base of tunnel valley
Erratics	62.6 % Cretaceous (chalk and black flint), 1.3 % Jurassic, 10.3 % Permo-Trias, 0.7 % Carboniferous, 19.9 % Pleistocene (includes quartz, flint, chert, shell, wood, quartzose lithologies), 4.7 % Scottish and N England Igneous, and 0.1 % Scandinavia Igneous.	Jurassic sandstones and shales, chalk and flint, Magnesian Limestone, Carboniferous limestone and shale, Whin Sill dolerite, Scottish granites, basalts and gneisses, larvikite and rhomb porphyry.	Quartz and quartzite, limestone, Scottish porphyries and granites, flint, chalk, red marl, Whin Sill dolerite, and rare Norwegian Drammensgranit.
Heavy Minerals	55 % opaques. 1.4 % apatite, 21.9 % amphibole group, 26.6 % epidote, 22.3 % garnet.	Rich in garnet, hornblende, epidote and dolomite.	Rich in hypersthene, amphiboles, monazite, actinolite, sphene, chloritoid, staurolite.
Microfossils	N/A	N/A	Eocene palynomorphs. Marine, open water, cold-water foraminifera.
Shell species	N/A	Arctic marine; *Arctica islandica* and *Macoma balthica*	Open water marine; *Chlamys, Hiatella,* and *Balanus.*
Chrono-stratigraphy	MIS 12 (OSL direct dating on sands)	Indirectly dated. Underlies Sewerby Raised Beach dated to MIS 5e. MIS 6?	AAR dating on shells – fauna MIS 9 to Cromerian age, but inconclusive. Relationship to raised beach at MIS 7 suggests MIS 8 or older.

Chronostratigraphy

Previous workers have assigned the Ash Gill Member of the Warren House Formation to MIS 6, based on correlation with the Bridlington Member (Basement Till) in Yorkshire (Francis, 1972; Lewis, 1999). Other workers, assuming that the Easington Raised Beach was of MIS 7 age (after Bowen *et al.*, 1991), and that the Easington Raised Beach was stratigraphically younger than the Ash Gill Member, have argued that the Ash Gill Member was deposited between MIS 8 and 12 (Lunn, 1995). Controversy over the age of this important sediment therefore still reigns.

Unfortunately, it was not possible, despite repeated attempts, to date the Ash Gill Member directly. Stratigraphic work regarding the AAR on shells is ongoing (Dr. Penkman, pers. comm.), and Uranium Series is currently being attempted on race nodules within the overlying silts (Dr. Candy, pers. comm.). The Easington Raised Beach incorporates flint gravel, which may have been derived from the Warren House Formation. The OSL ages on LF 4a remain inconclusive at this stage, and the only overlying direct chronostratigraphic control rests with the Early Devensian age on the fold nose within the sand. If it is assumed that the raised beach, at MIS 7, is stratigraphically younger than the Ash Gill Member, and that the Ash Gill Member contains a shell fauna of MIS 9 - Cromerian, then the most likely, and simplest, age for the Ash Gill Member is between MIS 12 to 8.

An MIS 12 age for the Ash Gill Member is more probable than MIS 8 - 10, as the oxygen-isotope curve suggests an exceptionally large peak in global ice volume during MIS 12 (Shackleton & Opdyke, 1973). Scandinavian ice is therefore most likely to have crossed the North Sea during MIS 12. Additionally, there is widespread evidence for a large-scale glaciation in Britain, the North Sea and in Scandinavia during MIS 12 (e.g., Hamblin *et al.*, 2005; Sejrup *et al.*, 2005; Pawley *et al.*, 2008).

The presence of a glaciomarine deposit at Warren House Gill during MIS 12 implies that there was no large ice-sheet in Britain at the time of deposition. Recent work in Norfolk has suggested the presence of a large, active, and dynamic BIIS during MIS 12 (Hamblin *et al.*, 2005). The most likely explanation is that the buried palaeovalley of Warren House Gill was filled with pressurised water under subglacial conditions during the MIS 12 glaciation. After the recession of the ice sheet, the Briton's Lane Fm was deposited in Norfolk. On further recession, the palaeovalley was flooded with marine water and the Ash Gill Member was deposited. Scandinavian and Scottish ice sources were present in the

vicinity, infilling the palaeovalley with detrital material from both Norway, the Cheviots, northeastern England, and Scotland. Grain size changes indicating ice sheet proximity could be related to oscillations of the ice margin(s).

Long term tectonic uplift and landscape position of the Warren House Formation

In this project, the Easington Raised Beach has been independently dated to MIS 7 (190,000 BP). Westaway (in press) argued that an MIS 7 age means an uplift rate of 0.19 mm per annum. This would normally mean that the older Ash Gill Member would be considerably higher in the landscape than the Easington Raised Beach. However, the landscape position of the Ash Gill Member can be reconciled as it was deposited in the base of a deep palaeovalley. Uplift of 81.7 m at a constant rate of 0.19 mm per annum since MIS 12 would mean that the Ash Gill Member would now rest at sea level, and that the Easington Raised Beach would be at 33 m O.D., as shown in Figure 6.70.

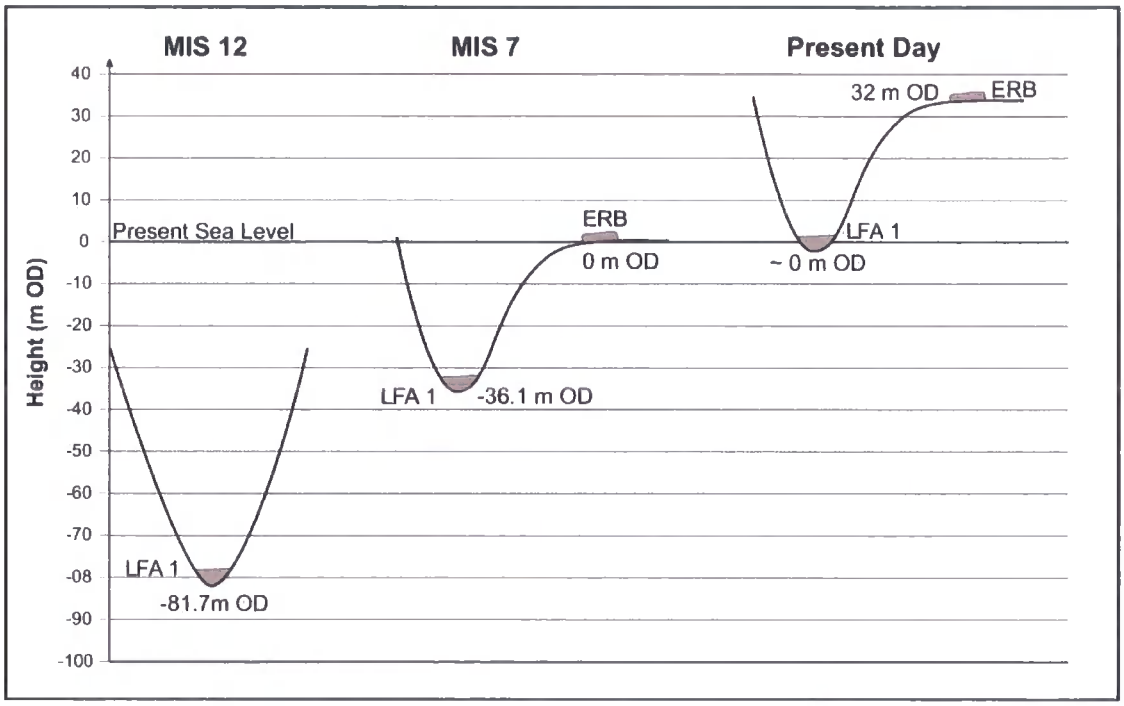

Figure 6.70: Uplift diagram for LFA 1 and the Easington Raised Beach.

The inferred depth of -81.7 m O.D. for the base of the palaeovalley indicates that this palaeovalley may be a tunnel valley. Tunnel valleys are incised subglacially by a variety of processes, including erosion by pressurised subglacial meltwater (Huuse & Lykke-Andersen, 2000; Hooke & Jennings, 2006; Jørgensen & Sandersen, 2006; Kristensen *et al.*,

2008), but may be post-glacially modified by fluvial processes. There are many examples in the North Sea (Wingfield, 1990; Ehlers & Wingfield, 1991; Praeg, 2003), which provide good analogues for the palaeovalleys which characterise the east coast of County Durham (refer to Figure 1.4). Tunnel valleys can be infilled with glaciomarine, glaciofluvial, glaciolacustrine, or subglacial sediments, and this has been observed in the North Sea Basin (Wingfield, 1990; Huuse & Lykke-Andersen, 2000; Praeg, 2003). The North Sea Basin contains tunnel valleys at seabed, interpreted to have formed beneath the margin of the last ice sheet. These tunnel valleys are underlain by larger buried tunnel valleys, which formed beneath the southern margin of the Anglian ice sheet (Balson & Cameron, 1985; Long *et al.*, 1988). These tunnel valleys can be infilled with glaciofluvial, glaciomarine, or subglacial sediments (Huuse & Lykke-Andersen, 2000; Praeg, 2003; Hooke & Jennings, 2006).

6.6.2 The Easington Raised Beach

The Easington Raised Beach (see Chapter 5) has a varied heavy-mineral suite and varied clast lithologies, clearly demonstrating the input of far-travelled material. This suggests that marine erosion acted upon a glacigenic deposit, and deposited this material into the raised beach. For the lithologies to have reached such high percentages, the glacigenic deposit would have been particularly widespread. Previous authors (Trechmann, 1952; Francis, 1972; Lunn, 1995; Thomas, 1999) have suggested that the Warren House Formation, near Horden, was the glacigenic deposit responsible for the far-travelled lithologies within the raised beach.

Statistical comparison of the Easington Raised Beach to the Ash Gill Member and other east-coast Quaternary sediments raises some interesting points. Clast-lithological analysis of the Ash Gill Member showed that it includes significant amounts of quartzose lithologies, which are very rare in the other tills in County Durham (Figure 6.56 and Figure 6.59). Other lithologies unique to the Easington Raised Beach and the Ash Gill Member include flint and Scandinavian erratics, as reported by Trechmann (1931a; 1952). Drammensgranit was found in the Ash Gill Member, supporting a Scandinavian derivation, but no other typical Scandinavian lithologies were found either in this study or at Warren House Gill. Cheviot andesites were found in both the Easington Raised Beach and in the Ash Gill Member. Both the Easington Raised Beach and the Ash Gill Member contain far

higher percentages of igneous lithologies than the other lithofacies in the region (Figure 6.55). These are typically not very durable, and large numbers of igneous material would need to be continuously input into the beach to maintain these numbers. Analysis of the heavy-mineral fraction of the Easington Raised Beach and the Ash Gill Member also shows some similarities. Both contain significant percentages of epidote (Figure 6.60). Epidote is not a durable mineral, and would need frequent inputs to maintain these percentages. Epidote is also rare in tills deposited by Scottish-sourced ice sheets in County Durham.

Although detailed statistical analysis does not group the Easington Raised Beach with either the Ash Gill Member or the local Devensian tills, it is clear that the Easington Raised Beach incorporates derived lithologies and materials from a glacigenic deposit sourced in Scandinavia, which crossed the North Sea Basin (Figure 2.11). The problem arises that although the Ash Gill Member is the only local Scandinavian deposit, and may have once been far more widespread, other Scandinavian tills may once have existed along the eastern England coastline. The Bridlington Member, for example, is dated to MIS 6 as it is overlain by the Ipswichian Sewerby Raised Beach (Catt & Penny, 1966; Bateman & Catt, 1996; Catt, 2001b). Other Scandinavian deposits may well once have existed along the coastline, and the Ash Gill Member may post-date the deposition of the Easington Raised Beach, and be correlative with the Bridlington Member (MIS 6 age). As the Easington Raised Beach does not directly overlie the Warren House Formation, the stratigraphic relationship therefore remains somewhat vague.

Previous workers have dated the raised beach to MIS 7 based on amino acid stratigraphy (Bowen *et al.*, 1991), and others have argued that Scandinavian erratics in the beach are directly derived and reworked from the Ash Gill Member (Trechmann, 1931a). However, although there are strong similarities between the lithologies of the beach and Ash Gill Member with several lithologies unique to these two sediments, this study found no statistical relationship between the two.

The vast majority of the clasts within the beach are locally derived Permian lithologies. The large number of quartzose lithologies and rare flint lithologies bears resemblance to the lithologies within the Ash Gill Member. However, these lithologies are very durable and could survive several cycles of reworking. Therefore there is no direct, clear lithostratigraphical evidence that the beach contains derived clasts from the Ash Gill Member.

Recent OSL work in Norfolk has shown that Scandinavian ice reached the north Norfolk coastline during 12 (Pawley *et al.*, 2008). Evidence from Yorkshire suggests that ice also reached here during MIS 6 (Catt & Penny, 1966; Catt & Digby, 1988; Bateman & Catt, 1996; Catt, 2001b). However, in the absence of any other evidence, the simplest answer is that the Easington Raised Beach includes minerals and clasts derived from the Ash Gill Member, and that Scandinavian ice reached the British coastline during MIS 6 and 12. This suggests that the Warren House Formation is MIS 12 in age, and is potentially correlated to the Briton's Lane Sand and Gravels (as described by Pawley *et al.*, 2004; Hamblin *et al.*, 2005).

6.6.3 The Blackhall Member

Lithostratigraphy

LFA 3, the Blackhall Member, is the lowest subglacial traction till that outcrops between Hawthorn Hive to Blackhall Rocks. LFA 3 at Warren House Gill is lithologically and statistically very similar to the lower till at Hawthorn Hive (LFA 1), and is correlated to it. The particle-size distribution, geochemistry, and petrology of the Blackhall Member are generally tightly clustered and distinct from the Warren House Formation (LFA 1). It consistently plots close to LFAs 4 and 5 (e.g., Figure 6.56). The statistical analysis of heavy mineral and clast-lithological data is generally not efficient enough to distinguish LFA 3 from LFA 5 (WHG H2), although the upper tills from Hawthorn Hive (LFA 3) and Shippersea Bay (LFA 3), plot separately. This suggests that both these traction tills, although they may be different in age, may have had similar ice-accumulation areas.

Along the cliff tops, the Blackhall Member (LFA 3) is overlain by the Peterlee Member (LFA 2 at Hawthorn Hive and Shippersea Bay), interpreted as ice marginal outwash sediments. The sequence is overlain by the Late Devensian Horden Member (LFA 5), which stretches unbroken from Sunderland southwards, with local variations in abundances of different lithologies and a changing matrix geochemistry. This member is part of the East Durham Formation (see Table 1.5), as defined by Thomas (1999).

The sand and gravel facies of LFA 4, the Peterlee Member, at Warren House Gill mirrors the provenance signature of the underlying Blackhall Member (e.g., Figure 6.59, Figure 6.62 and Figure 6.63), although the heavy mineral assemblage does show some affinity for the Horden Member at Warren House Gill (Figure 5.34). It is most likely that

these glaciofluvial sediments are related to the deposition of the Blackhall Member and that LF 4a represents a restricted, riverine deposit at Warren House Gill, though they do outcrop rarely south of Hawthorn Hive. LFs 4a and 4b are similar mineralogically and geochemically. They are also distinct from LFA 2 at Hawthorn Hive, which instead is a widespread tabular deposit, associated with the Horden Member, outcropping periodically from Hawthorn Hive southwards (see Chapter 4.4). This is likely to be a Devensian outwash deposit and separate from the older red sands and gravels at Warren House Gill.

Blackhall Rocks is the type-site of the Blackhall Member (Lower Boulder Clay) of Francis (1972) and Thomas (1999); this is the lower till from Hawthorn Hive southwards. This till is said to cover the bedrock from here to north of Tynemouth (Eyles *et al.*, 1982), and encompasses the tills at Whitburn Bay. Francis (1972) correlated the Blackhall Member with the Drab Till (Skipsea Member) of Holderness, where it overlies the Dimlington Silts (Catt & Penny, 1966). However, work by this author at Whitburn Bay suggests that this is incorrect (see Chapter 3). As the ice that deposited the till melted, vast quantities of meltwater were produced, which are evident in the sands and gravels exposed in the cliff sections from Hawthorn Hive southwards.

Geomorphological and striae evidence (Beaumont, 1971; Livingstone *et al.*, in prep, in press) indicates that ice flowing through the Tyne Gap, an influential artery of the BIIS, would have reached eastern Britain. The geology of the Tyne Gap, comprising Carboniferous limestones, sandstones and shales, with outcrops of Whin Sill Dolerite, reflects that of the Blackhall Member (Livingstone *et al.*, in prep), supporting the indication that Pennine and Scottish ice sources were key to the formation of this ice lobe. However, no indication of Lake District erratics such as the Shap granite was found in County Durham. Lake District erratics decrease in an easterly direction in the Tyne Gap, due to the increasingly dominant influence of southeasterly flowing ice from the North Tyne valley (Dwerryhouse, 1902; Trotter, 1929).

The Blackhall Member therefore came from the northeast and flowed towards County Durham through the Tyne Gap. It here competed with ice providing a different striation set showing a southwards flowing trajectory, i.e., by the ice lobe which deposited the Horden Member.

Chronostratigraphy

The Blackhall Member is an Early Devensian deposit. While the OSL ages on the fold nose in Exposure E1 have large errors, they suggest that an Early Devensian age (80 to 40 ka BP). This is also overlain by a till which shows more extensive weathering than the other facies of LF 3a. It is possible that the lower facies of this till was deposited during an earlier, more extensive phase of the BIIS, such as during the Ferder Episode, as defined by Carr *et al.* (2006). The BIIS and the FIS were joined in the North Sea at this time. As the Blackhall Member flowed eastwards, away from the British coastline, it is apparent that the North Sea Lobe was not active at this time, and that the ice junction between the BIIS and the FIIS was some distance offshore.

A great thickness of sediment overlies this MIS 4 age on the folded sands; the Blackhall Member may therefore encompass a considerable period, and include sediments derived from a later stage of Devensian glaciation. There is no direct evidence, however, that the sediments were exposed subaerially during this time.

The character of the complex sediments associated with the Blackhall Member suggests that they were deposited in an active-temperate, marginal to a submarginal environment, with active thrusting, stacking, glaciotectonism and abundant meltwater. There is evidence for overridden proglacial / ice-contact small-scale lakes or ponds and abundant localised meltwater, as indicated by the overlying red glaciofluvial outwash sands and gravels, all of which are commonly associated with active ice margins (Evans & Twigg, 2002). The preservation of underlying sediments with some glaciotectonism is common in these environments (Evans & Twigg, 2002). Complex till sequences may develop through repeated thrusting and stacking where the glacier margin is stationary for some time (e.g., Evans, 2003a; Phillips *et al.*, 2008). In addition, LF 4c (the Peterlee Member) exists as an unbroken outwash fan from Hawthorn Hive southwards, indicating subaerial glaciofluvial deposition (see Chapter 4).

The Blackhall Member pinches out against the flanks of the knoll on which the raised beach at Shippersea Bay is preserved, which is covered only with the weathered upper till. In some places, the bedrock between Hawthorn Hive and Blackhall Rocks is directly overlain by sands and gravels. The patchy distribution of the Blackhall Member is possibly partly in response to changing subglacial conditions related to the changing topography and variable permeability of the bedrock and the common incised valleys, and partly due to subsequent erosion by the upper till and the middle sands and gravels.

6.6.4 The Horden Member

Lithostratigraphy

Mineralogically and lithologically, the upper till of Hawthorn Hive and the till in Shippersea Bay share many provenance characteristics. Statistically both are similar in nature to LFA 3 and LFA 5 at Warren House Gill, and share several typical provenance indicators, apart from some weathering-induced differences. All indicate a northern British source region, with inputs from the Grampian Highlands, Aberdeenshire, the Midland Valley, the Cheviots, and northern England. The presence of red marl and rare bivalve fragments suggests that the ice sheets may have flowed down the eastern coast of Britain at one time and incorporated marine sediments.

LFA 5 is laterally extensive and overlies the tabular sands and gravels from north of Hawthorn Hive to Castle Eden Dene and beyond. The mineralogy of LFA 5 is dominated by ultra-stable minerals such as zircon, tourmaline, apatite, rutile and garnet, suggesting that it may be very weathered. It is difficult to distinguish statistically between LFAs 3, 4a and 4b and 5. The ternary diagram of clast lithologies clearly groups LFA 5 (WHG H2) with LFA 3, whilst ERB 06 and HAW 03, the uppermost till facies in Shippersea Bay and Hawthorn Hive respectively, plot independently. The PCA shows ERB 06 and HAW 03 plotting to the left of the x-axis, influenced by their high proportions of Carboniferous and sandstone erratics, whilst WHG H2 (LFA 5) again plots close to LFA 3 samples. WHG H2 (LF 4a) plots as an outlier in the ternary plot of heavy minerals (Figure 6.62), while both HAW 03 and ERB 06 plot close to LFA 3. The PCA has a wide scatter and is not efficient enough to discriminate between lithofacies other than LFA 1 and 2. The metals analysis also does not discriminate between the lithofacies associations. Altogether, LFA 5 at Warren House Gill (WHG H2) shows more of an affinity with LFA 3 than with the upper till facies at Hawthorn Hive and Shippersea Bay. This could be related to local variations, as it is some distance south of Shippersea Bay, and local erosion and incorporation of LFA 3. Due to slumping, poor exposures, and vertical height in the coastal cliffs, it is difficult to observe the upper till at Warren House Gill in detail.

LFA 5, the upper till of Warren House Gill, Hawthorn Hive and Shippersea Bay, is interpreted here as the Horden Member (previously Upper Boulder Clay) has a type site on the southern side of Warren House Gill (Francis, 1972), and extends inland only a short distance. This till is correlated with the Skipsea Member in Yorkshire (see Chapter 3). The

intervening sands and gravels have been named the Peterlee Sands and Gravels (Francis, 1972), and these gravels outcrop extensively in the region. For a summary, see Table 6.13.

This study was not able to provide chronostratigraphic control for the deposition of the Horden Member in Country Durham. However, correlation to the Skipsea Member (see Chapter 3), suggests that it was deposited by a North Sea Lobe flowing parallel to the coast of eastern Britain during a late stage of MIS 2, probably during the Dimlington Stadial, as defined by Catt and Penny (1966) and Rose (1985).

Active-Temperate Marginal Glacial Landsystem

Temperate glacier margins are wet-based, and are located in terrains with discontinuous or no permafrost (Evans, 2003b). There are three dominant depositional domains with characteristic sediment-landform associations typically recognised on recently deglaciated active temperate glacier forelands (e.g., Evans & Twigg, 2002). Firstly, areas of extensive, low-amplitude, marginal, dump, squeeze, and push moraines, derived from material on the glacier foreland. The incremental thickening of ice-marginal wedges of till has also been proposed (Benediktsson *et al.*, 2008). The typical marginal sediments include subglacially derived diamictons with large numbers of striated and faceted clasts, reworked glaciofluvial sediments, and glaciotectonised overridden lacustrine laminated sands and muds. Secondly, subglacial landform assemblages of flutings, drumlins and overridden push moraines are common (Evans, 2003b). These features are linked to the subglacial deforming layers. Thirdly, there are large areas of glaciofluvial forms such as recessional ice-contact fans, possibly associated with eskers. Sandur fans are prograded from subglacial or englacial meltwater sources. Within enclosed depressions, proglacial lakes will expand and contract in response to changing drainage networks (*ibid.*).

Table 6.13: Comparison of tills at study site

	Warren House Gill		Shippersea Bay	Hawthorn Hive	
	LFA 3	**LFA 5**	**Upper Till**	**Lower Till**	**Upper Till**
Average Particle Size	17.5 % clay, 33.5 % silt, 34.5 % sand, 14.5 % gravel	9.6 % clay, 8.9 % silt, 39.1 % sand, 42.4 % gravel	16.3 % clay, 32.8 % silt, 34.7 % sand, 17.3 % gravel	9.3 % clay, 37.9 % silt, 30.9 % sand, 21.97 % gravel	19 % clay, 40 % silt, 33.7 % sand, 7.3 % gravel
Colour	10YR 3/2 Very dark greyish brown	10YR 4/3 Brown	10YR 3/6 Dark Yellowish Brown	10YR 3/1 Very dark grey	10YR 3/3 Dark Brown
Clast macro-fabric	NE-SW	N/A	N/A	NW-SE	NW-SE
Sedimentology	Clast rich diamicton	Massive diamicton	Sandy diamicton, massive, clast-rich, sub-angular gravel	Clast-rich diamicton	Massive diamicton
Structures	Massive to laminated diamicton, some tectonised sand folds	-	-	Massive, some tectonised laminations	-
Process interpretation	Subglacial traction till	Subglacial till	Subglacial till	Subglacial till	Subglacial till
Average Clast Lithology	68 % Magnesian Limestone, 3.4 % Carboniferous Limestone, rare slate, schist, gneiss, Felsite, basalt, andesite, rhyolite, granite, diorite erratics.	76.8 % Magnesian Limestone, 9.9 % Carboniferous Limestone, rare porphyries and andesites.	20.7 % Magnesian Limestone, 1.3 % Carboniferous Limestone, rare slate, basalt, andesite, gabbro and granite erratics.	70.1 % Magnesian Limestone, 3.1 % Carboniferous Limestone, rare red marl, granite, and rhyolite erratics.	27.6 % Magnesian Limestone, 13.1 % Carboniferous Limestone, rare schist, red marl, andesite and granite erratics.
Average Heavy Minerals	Enriched in garnet, andalusite, kyanite, pyroxenes, staurolite, chloritoid, micas, and dolomite.	Enriched in garnet, kyanite, tourmaline, zircon, apatite	Enriched in garnet, andalusite, kyanite, pyroxenes, tourmaline, epidote, lawsonite, staurolite, chloritoid.	Enriched in garnet, andalusite, kyanite, pyroxenes, tourmaline, epidote, lawsonite, staurolite, chloritoid.	Enriched in garnet, andalusite, kyanite, pyroxenes, tourmaline, epidote, lawsonite, staurolite, chloritoid.
Microfossils	Rare reworked bivalves and forams	-	-	-	-
Chrono-stratigraphy	?80 ka BP (fold nose in sand)	-	Overlies MIS 7 raised beach	N/A	N/A
Stratigraphic correlation	***Blackhall Member***	***Horden Member***	***Horden Member***	***Blackhall Member***	***Horden Member***

The Horden Member exhibits many of the characteristic hallmarks of a temperate glacial marginal landsystem, such as proglacial lakes; Glacial Lake Wear was discussed extensively in Chapter 3. Additionally, in the stretch of coastline from Hawthorn Hive to Blackhall Rocks, proglacial outwash sediments are extensively exposed. Ice-contact slope and recessional moraines were mapped by the British Geological Survey, indicating the extent of the Horden Member (Figure 1.6), and they mark the limit of the onshore advance of the ice lobe. Ice-contact slopes were also recorded in the buried valley at Hawthorn Hive. The Horden Member can therefore be understood within the context of an ice-marginal, terrestrial, temperate glacier landsystem. The striation map compiled by Beaumont (1967) shows how the south-westerly flowing ice lobe interacted with the south-easterly flowing Blackhall Member, resulting in complex, multiple striae orientations.

It is likely that the North Sea Lobe, which deposited the Horden Member, was constrained in the North Sea by contact with Fennoscandian ice. The shape of the North Sea Lobe (see Chapter 1, Figures 1.2 and 1.3) is very difficult to explain without contact with a larger, more dominant Fennoscandian ice sheet. However, this is controversial and does not agree with recent work in the North Sea Basin (Carr *et al.*, 2006), which argues for ice-free, glaciomarine conditions in the central North Sea during the Dimlington Stadial.

6.6.5 Quaternary Lithostratigraphy in County Durham

The findings of this study call for a re-assessment of the accepted lithostratigraphic scheme in northeastern England. A new stratigraphical scheme is proposed below, with new names for the members of the formations, new stratotypes, with new chronostratigraphy, process and provenance interpretations (Table 6.14). The new stratigraphical scheme replaces and updates that proposed by Thomas (1999), and provides substantial new information and understanding regarding the dynamics of British lowland Middle and Upper Pleistocene glaciations during the Quaternary. The stratotype for the Horden Member is revised, and new names are provided for the older glacigenic sediments in Warren House Gill.

Table 6.14: Revised Quaternary Formations of County Durham

	Name	Stratotype	Sedimentology	Genesis	Provenance	Chrono-stratigraphy	Regional Correlatives
The East Durham Formation	*The Horden Member*	Upper diamicton at Warren House Gill	Upper clast-rich diamicton, massive	Subglacial till	Scotland and northern Britain	MIS 2 Late Devensian	Skipsea Member Bolders Bank Fm
	The Peterlee Member	Middle gravels at Blackhall Rocks	Poorly to well-sorted sands and gravels Red sands at Warren House Gill	Proglacial outwash	Scotland and northern Britain	MIS 2 Late Devensian	
	The Blackhall Member	Lower diamicton at Blackhall Rocks	Lower clast-rich diamicton, massive to laminated, containing tectonised sand beds.	Ice-marginal subglacial traction till	Scotland and northern Britain	80 to 40 ka BP	Middle till at Warren House Gill. Ferder Episode?
The Easington Formation		Calcreted gravels in Shippersea Bay	Well-sorted, bedded, rounded sands and gravels	Interglacial beach	Local and from underlying sediments	MIS 7	-
The Warren House Formation	*Whitesides Member*	Beige Silts at Warren House Gill	Beige silts, some deformed laminations, foraminifera present.	Estuarine silts	Local and from underlying sediments	-	-
	Ash Gill Member	Basal diamicton at Warren House Gill	Grey clast-poor diamicton, sand laminations, bivalve fragments	Glaciomarine rain-out diamicton	Mixed Scottish and Norwegian	?MIS 8-12	Briton's Lane Sand and Gravels

6.7 Conclusions

Previous researchers have claimed that the tripartite sequence exposed in coastal cliffs in County Durham consists of two Devensian tills with an older, Scandinavian till at the base of a buried palaeovalley (Trechmann, 1931b, 1952; Smith & Francis, 1967; Francis, 1972), which was overlain by an interglacial loess and by a raised beach (Trechmann, 1931a). Other workers argued that the 'Scandinavian Drift' was correlated to the Bridlington Member in Yorkshire (Catt & Penny, 1966; Catt, 1991b; Clark *et al.*, 2004b; Catt, 2007). Recent research in Norfolk (Lee *et al.*, 2004; Hamblin *et al.*, 2005; Pawley *et al.*, 2008) has highlighted both the importance and complexity of Middle Pleistocene glaciations in Europe, and the need for rigorous testing in areas removed from north Norfolk to see if the models can be applied elsewhere.

This study aimed to clarify and investigate British and Fennoscandian ice sheet interactions during the Quaternary. It reached several major conclusions:

- The 'Warren House Formation' is redefined here. It first comprises a glaciomarine rainout diamicton, which is named here as the 'Ash Gill Member'. It has a mixed provenance indicating ice rafting from grounded, calving ice-sheets originating both in Scandinavia and in northeast Scotland. Second, the Ash Gill Member is overlain by pink estuarine silts, the 'Whitesides Member'.
- The age of the Ash Gill Member is older than MIS 6 and is most likely to be MIS 8 to MIS 12 in age. Additionally, the Ash Gill Member is unlikely to be correlative with the Bridlington Member of Yorkshire. A correlation with the Briton's Lane Sand and Gravels of north Norfolk is more probable. This suggests that there have been at least two separate incursions of Scandinavian ice towards the eastern British coastline during the Quaternary.
- The overlying Blackhall Member is a subglacial traction till deposited during the Devensian, possibly LGM (pre-Dimlington Stadial). It shows a provenance from the Grampian Highlands, the igneous and metamorphic terrain of northeastern Scotland, the Midland Valley of Scotland and northern England. It was possibly deposited during a more expansive phase of the BIIS, with the BIIS and FIS confluent in the North Sea Basin.

- The Blackhall and Horden Members extend from Hawthorn Hive southwards to Holderness. The Horden Member correlates with the Skipsea Member and the Bolders Bank Fm offshore. Both onshore tills indicate sources of ice from the eastern coast of Scotland near Aberdeenshire, the Grampian Highlands, and the Midland Valley of Scotland.

This research has therefore provided substantial new information that supports recent work in Norfolk dating Scandinavian outwash sediments to MIS 12 (Pawley *et al.*, 2008), and old assertions regarding the genesis of the 'Warren House Formation' have been updated.

CHAPTER 7

The North Sea Basin

7.1 Introduction

7.1.1 Introduction

This chapter analyses the Quaternary sediments from boreholes (BH) offshore from eastern Britain in the North Sea Basin (NSB). The chronostratigraphy in this chapter uses the north-west European terms. The NSB is a subsiding Palaeozoic to Holocene multi-stage rift zone within the northwest European craton (Cameron *et al.*, 1992). Rapid subsidence during the Pliocene and Pleistocene resulted in a deep succession of Quaternary sediments, thickening towards the east (Figure 7.1). The principle axis of subsidence in the southern part of the basin trends north-north-westwards, parallel with the UK coastline from the Firth of Forth to the Wash. Subsidence has been up to 255 m over 730,000 years, at a rate of 0.35 m per 1000 years, resulting in the thickness of Quaternary sediments increasing eastwards. Towards the eastern British coastline, the Quaternary sediments gradually disappear to nothing, and boreholes near the coastline show bedrock at the seabed (*ibid.*).

The southern NSB (south of 56°N) is shallow, with water-depths of less than 40 m (Figure 7.2). This region was probably above global eustatic sea level during the last glacial cycle, and may have been dry land (Carr *et al.*, 2006). In the north-central NSB, between 56°N and 59°N, water depths reach 100 m to 140 m, with the current sea floor close to global eustatic sea level at the LGM. North of 59°N, the sea floor is around 140 m to 200 m deep. Carr *et al.* (2006) argued that this region would have been below global eustatic sea level even at the climax of glaciation, implying marine or glaciomarine conditions. At the northern margin of the NSB, at the continental shelf, water depths drop off from 200 m to more than 1500 m (Andrews *et al.*, 1990).

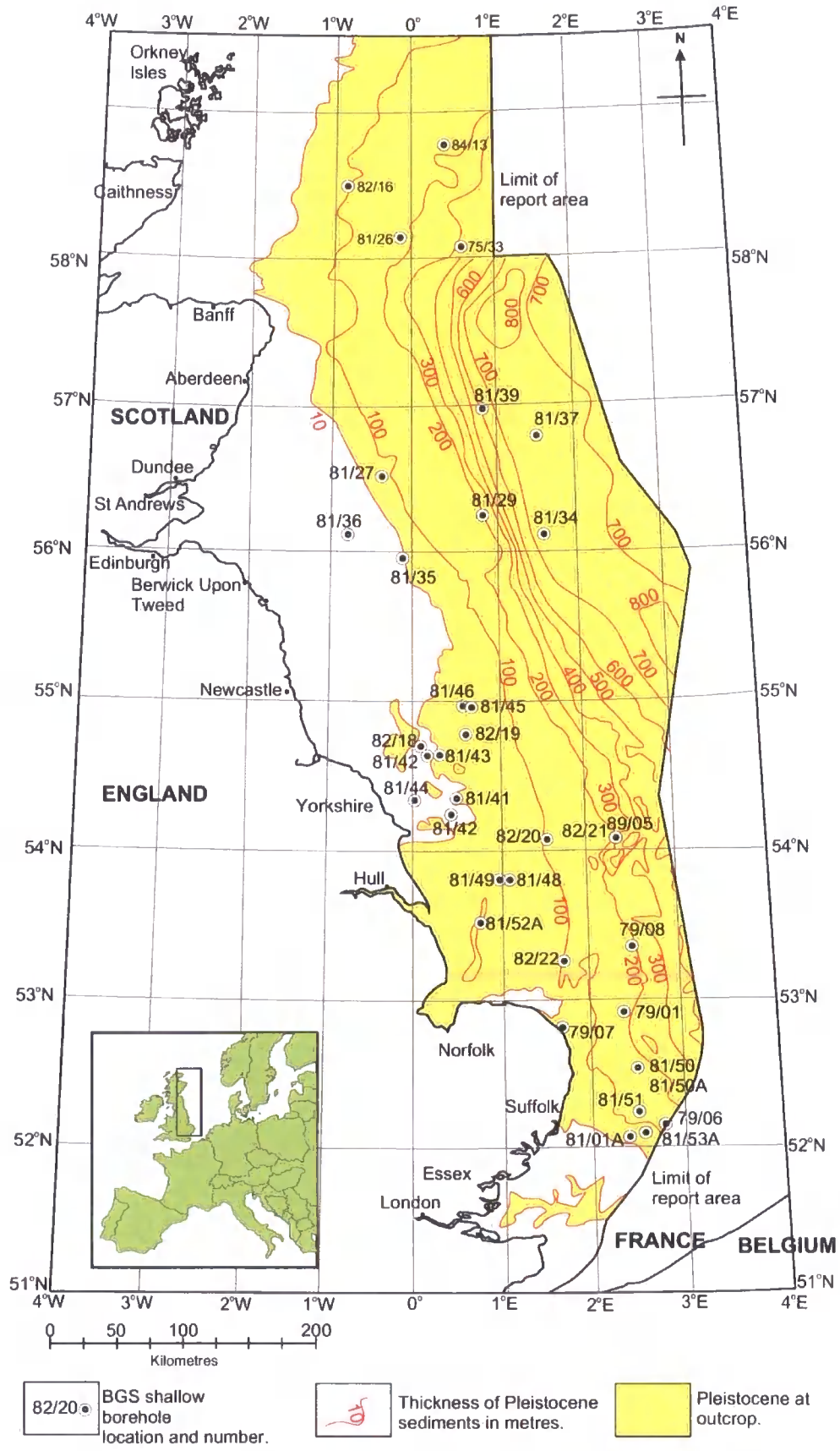

Figure 7.1: Location of significant BGS Boreholes and thickness of Quaternary sediments (Cameron *et al.*, 1992; Gatliffe *et al.*, 1994).

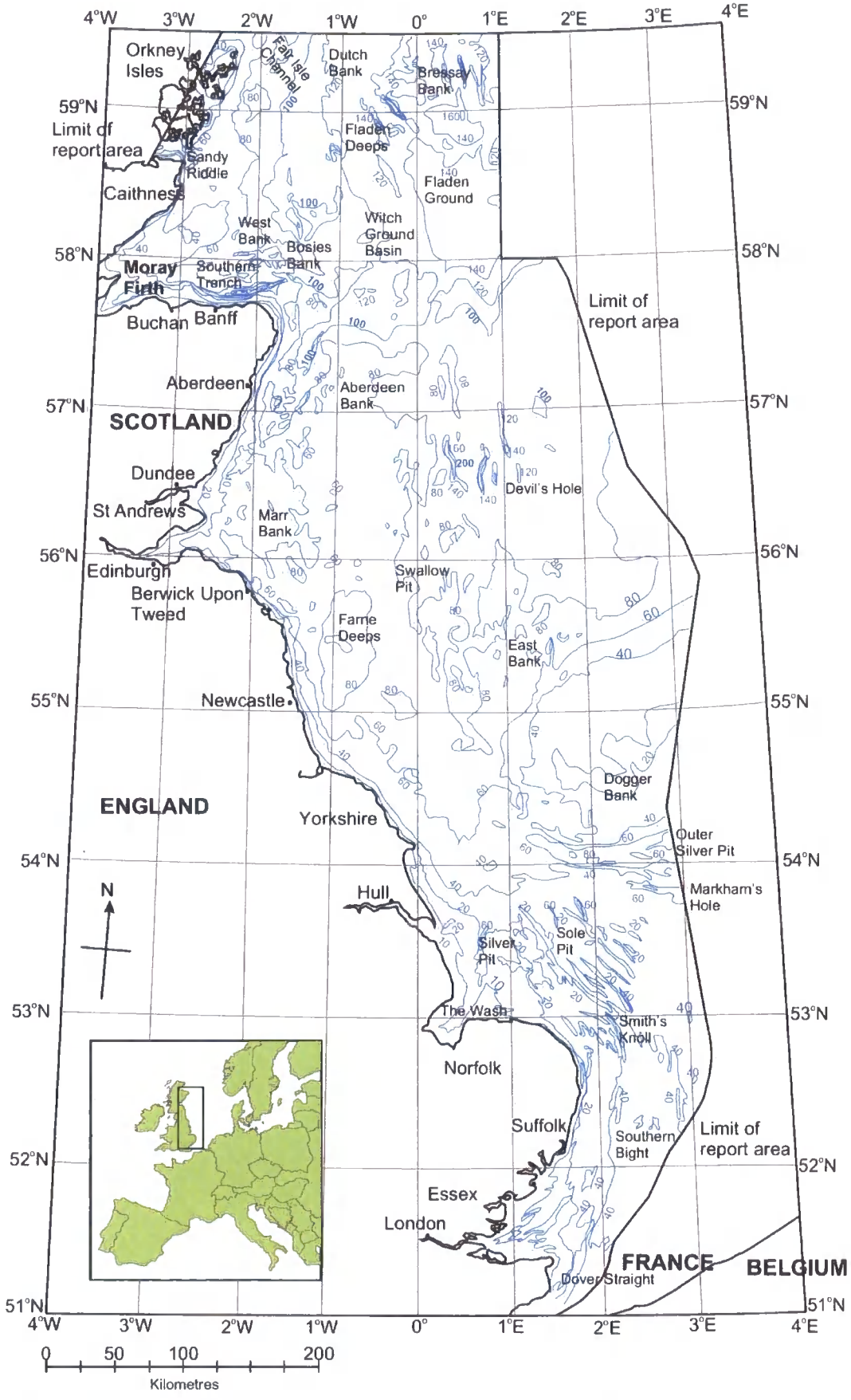

Figure 7.2: Bathymetry of the North Sea (Cameron et al., 1992; Gatliffe et al., 1994).

7.1.2 Rationale

The NSB is a sediment sink that can provide detailed information regarding Quaternary glacial-interglacial cycles. Reconstructing and constraining onshore-offshore lithostratigraphic correlations is important for creating a model for British and Fennoscandian ice-sheet interactions during the Quaternary, as the North Sea would have been a powerful and important control and barrier to the ice sheets. The eastern limits of the BIIS and western limits of the FIS during the Quaternary are poorly understood, which creates difficulties in accurately modelling their dynamic interactions through time and space. Onshore / offshore correlations between Quaternary sediments in the North Sea and in eastern England and The Netherlands are vague, as the offshore succession is essentially seismostratigraphical, whereas the mostly lithostratigraphical and biostratigraphical onshore stratigraphy lacks mappable equivalents (Cameron *et al.*, 1992). Correlations between land and sea are therefore tentative and stratigraphic control may be poor. Investigating the sediments deposited in the NSB and attempting to correlate them with sediment formations and sediment-landform associations onshore in eastern England can therefore greatly help to constrain and model dynamic interactions between British and Fennoscandian ice sheets during the Quaternary.

7.1.3 Aims and Objectives

This work aims to better understand and reconstruct the dynamics of British and Fennoscandian ice sheets in the NSB throughout the Quaternary. Furthermore, this chapter explores the offshore lateral correlatives of coastal glacigenic sediments in County Durham. In order to achieve these aims, there are several subsidiary objectives:

1. To understand the process history of a subsample of glacigenic sediments in the North Sea;
2. To reconstruct the provenance signature of these glacigenic sediments in the North Sea;
3. To critically investigate potential correlations:
    a. with onshore Devensian glacigenic sediments, such as at Whitburn Bay, Easington, and Warren House Gill,

b. with pre-Devensian onshore sediments such as the Bridlington Member and the Ash Gill Member.

7.1.4 Methodology

This thesis uses thin-section analysis together with quantified heavy mineral and geochemical analysis (see Chapter 2) to identify the process history and provenance of some key formations in the North Sea Basin. Formations which were possible offshore correlatives of the onshore sediments in County Durham were targeted; formations in the boreholes closest to County Durham were also targeted. Unfortunately, large spatial distances between samples was inevitable due to the lack of near boreholes. Multiple and replicate samples were taken from each lithofacies. Where possible, multiple samples of the same formation were taken from different boreholes. The number of samples available was limited, due to the precious and limited nature of the boreholes, and only very small samples were taken (~ 250 g).

7.2 North Sea Stratigraphy

7.2.1 Lower Pleistocene Sediments of the North Sea

Although ice-rafting from offshore northwest Britain is documented on the continental slope from the Late Pliocene, expansive glaciation of the continental shelf is not recognised until around 0.45 MA (Sejrup *et al.*, 2005). However, Cameron *et al.* (1992) argued that the majority of the Quaternary sediments in the southern North Sea are Early Pleistocene deltaic sediments, which make up approximately 80 % of the total thickness (Table 7.1). These thick, extensive sediments were deposited under stable climatic conditions. The remaining lithofacies, the 'non deltaic division', are mostly either glacigenic or interglacial marine sediments, according to Cameron *et al.* (1992). They have been extensively described and interpreted within the BGS memoirs, and their proposed stratigraphical framework is summarised below (Tables 7.1 and 7.2).

Stoker *et al.* (1985) argued that in the central North Sea (north of 56°N), the basal facies of the stratigraphy is the Aberdeen Ground Formation (Type BH 81/34; Table 7.2). This forms a wedge-shaped facies that is up to 130 m deep in the central part of the Devil's Hole area, thinning to the west (Stoker *et al.*, 1985), where it rests on pre-Quaternary strata. Stoker *et al.* (1985) described the Aberdeen Ground Formation (Fm) as comprising very dark grey to brown, stiff to hard silty muds, which are locally interbedded with thin, yellowish-brown, firm, shelly and pebbly sands and coarsely interlaminated muds and sands. They proposed that the bulk of the formation, bioturbated argillaceous sediments, was deposited in a inner to middle shelf environment, with sand horizons indicating tidal activity. In the west, the sediments are poorly-sorted muddy-gravelly sands and muds, which Stoker *et al.* (1985) interpreted as proximal to distal glaciomarine sediments and subglacial tills, but they remained uncertain of the relationship between the two facies. The Bruhnes-Matuyama boundary was identified within the Aberdeen Ground Fm, suggesting a Late Waalian to Cromerian age. The presence of the extinct foraminifera *Cassidulina teretis* and the dinoflagellate cyst *Operculodinium israelianum* supports an Early Pleistocene age (Stoker *et al.*, 1985).

Table 7.1: Pleistocene formations of the southern North Sea (Cameron et al., 1992; Gatliffe et al., 1994).

Inferred chronostratigraphy		Formation	Depositional Environment
Holocene (MIS 1)	Non-Deltaic Division	Various	Marine
Upper Weichselian (MIS 2)		Sunderland Ground (SG)	Subglacial to proglacial: glaciolacustrine to glaciomarine
		Botney Cut (BCT)	Glaciolacustrine to glaciomarine
		Kreftenheye (KR)	Periglacial: fluvial
		Twente (TN)	Periglacial: aeolian
		Well Ground (WLG)	Periglacial: fluvial
		Dogger Bank (DBK)	Proglacial: glaciomarine to glaciolacustrine
		Bolders Bank (BDK)	Subglacial: terrestrial
Lower Weichselian (MIS 4)		Brown Bank (BNB)	Marine to lacustrine
Eemian (MIS 5e)		Eem (EE)	Marine
Saalian (MIS 6)		Tea Kettle Hole (TKH)	Periglacial: aeolian
		Cleaver Bank (CLV)	Proglacial: glaciomarine
Holsteinian (MIS 11)		Egmond Ground (EG)	Marine
		Sand Hole (SH)	Marine (lagoonal)
Elsterian (MIS 12)		Swarte Bank (SBK)	Subglacial
Lower Pleistocene to Middle Pleistocene	Deltaic Division	Yarmouth Roads (YM)	Non-marine (fluvial) to intertidal
Lower Pleistocene		Aurora (AA)	Marine
		Outer Silver Pit (OSP)	Marine
		Markham's Hole (MKH)	Marine
		Winterton Shoal (WN)	Marine
		Ijumuiden Ground (IJ)	Marine
		Smith's Knoll (SK)	Marine
		Westkapelle Ground (WK)	Marine
Pliocene		Red Crag (RCG)	Marine

Incised into the Aberdeen Ground Fm in the north-central North Sea are numerous large channels, locally in excess of 100 m deep. Andrews *et al.* (1990) interpreted these as tunnel valleys that were infilled with the Ling Bank Fm, which subcrops extensively in the central North Sea. In BH 81/34, the Ling Bank Fm subcrops from 55-142 m below the sea bed (Stoker *et al.*, 1985). The lower part of the formation was deposited under marine interglacial conditions, with the upper part reflecting falling sea level associated with a cooling climate. The fill therefore represents a late glacial / interglacial / early glacial cycle (Andrews *et al.*, 1990). A Holsteinian age has been suggested (Table 7.2).

Table 7.2: Regional names and approximate correlatives of formations in the North Sea Basin (Andrews et al., 1990; Cameron et al., 1992; Gatliffe et al., 1994; Cameron & Holmes, 1999)

System	Series	MIS	UK Land Stage	NW European stages	Seismostratigraphy						
					North and West		Central North Sea		South East		
Quaternary	*Holocene*	1	Holocene	Holocene	Forth Formation (FH)	St Andrews Bay member		Witch Ground Fm	Witch Ground Fm	Hirundo Fm	Botney Cut Fm
						Largo Bay member	Forth Fm				
	Upper Pleistocene	2	Devensian	Weichselian	Cape Shore Formation		Swatchway Fm				
		3			Wee Bankie Formation (WBA)	Marr Bank Fm				Bolders Bank	Twente Fm
		4			Ferder Formation	Coal Pit Formation				Dogger Bank FM	
		5e	Ipswichian	Eemian							Eem Fm
	Middle Pleistocene	6 to 8	Wolstonian	Saalian	Mariner Fm	Fisher Formation			Alkaid member	Cleaver Bank Fm	
		11	Hoxnian	Holsteinian		Ling Bank Formation				Sand Hole and Egmond Ground formations	
		12	Anglian	Elsterian		Aberdeen Ground Formation				Swarte Bank Fm	
		13 to 15	Cromerian Complex	Cromerian Complex					Yarmouth Roads Fm		
	Lower Pleistocene	16	Beestonian	Bavelian					Aurora Fm		
				Menapian					Outer Silver Pit Fm		
				Waalian					Markham's Hole Fm		
				Eburonian	Shackleton Fm				Winterton Shoal Fm		
				Tiglian					Ijmuiden Ground Fm		

7.2.2 Middle Pleistocene Sediments of the North Sea

Sejrup *et al.* (2005) proposed that evidence of ice-rafting on the UK continental shelf indicates that a BIIS was active and ice-rafting material in each of the main glacial stages (MIS 12, 10, 8, 6, 4 and 2). During the Elsterian (MIS 12), full glacial conditions in the NSB led to the erosion and infilling of a major system of tunnel valleys in the southern North Sea (Balson & Jeffery, 1991). These are up to 12 km wide and locally up to 400 m deep (Cameron *et al.*, 1987). Balson and Jeffery (1991) described them as trending NNW-SSE in the NSB, and stated that they are most extensively developed between 53°N and 54°N, and east of 2°E. These valleys are boat-shaped (scaphiform) with an irregular thalweg, and were formed by pressurised subglacial meltwater (Balson & Jeffery, 1991).

The Swarte Bank Fm infills tunnel valleys in the NSB (Cameron *et al.*, 1992; Gatliffe *et al.*, 1994), and does not extend beyond the limits of the Dogger Bank (Figure 7.3). Cameron *et al.* (1992) described the Swarte Bank Fm as a chalky-Jurassic, stiff, grey diamicton, with some lenses of coarse-grained glaciofluvial sand. It is overlain in some places by stiff, grey, glaciolacustrine muds and passes upwards into marine clays with benthonic foraminiferal assemblages characteristic of waters periodically frozen to the bottom. Scourse *et al.* (1998) correlated the Swarte Bank Fm with the Lowestoft Till of East Anglia due to similar lithological properties, and interpreted as a subglacial till. Cameron *et al.* (1992) argued that it is Elsterian in age, based on its stratigraphical position between the Cromerian Complex Yarmouth Roads Fm and sediments with interglacial Holsteinian fossil assemblages (Ehlers *et al.*, 1984).

Gatliffe *et al.* (1994) stated that the Swarte Bank Fm is overlain by the Sand Hole and Egmond Ground formations (Table 7.2, and Figures 7.3 and 7.4), deposited in open-marine conditions during the Holsteinian (MIS 11) under ameliorating climatic conditions as the ice sheet decayed and sea levels rose. Scourse *et al.* (1998) noted that the lower facies of the Sand Hole Fm contained a dinoflagellate cyst assemblage characteristic of cool temperate to arctic environments in the North Atlantic, and that the upper facies contained a dinoflagellate cyst flora suggestive of temperate marine conditions similar to the present North Sea, and therefore of interglacial status.

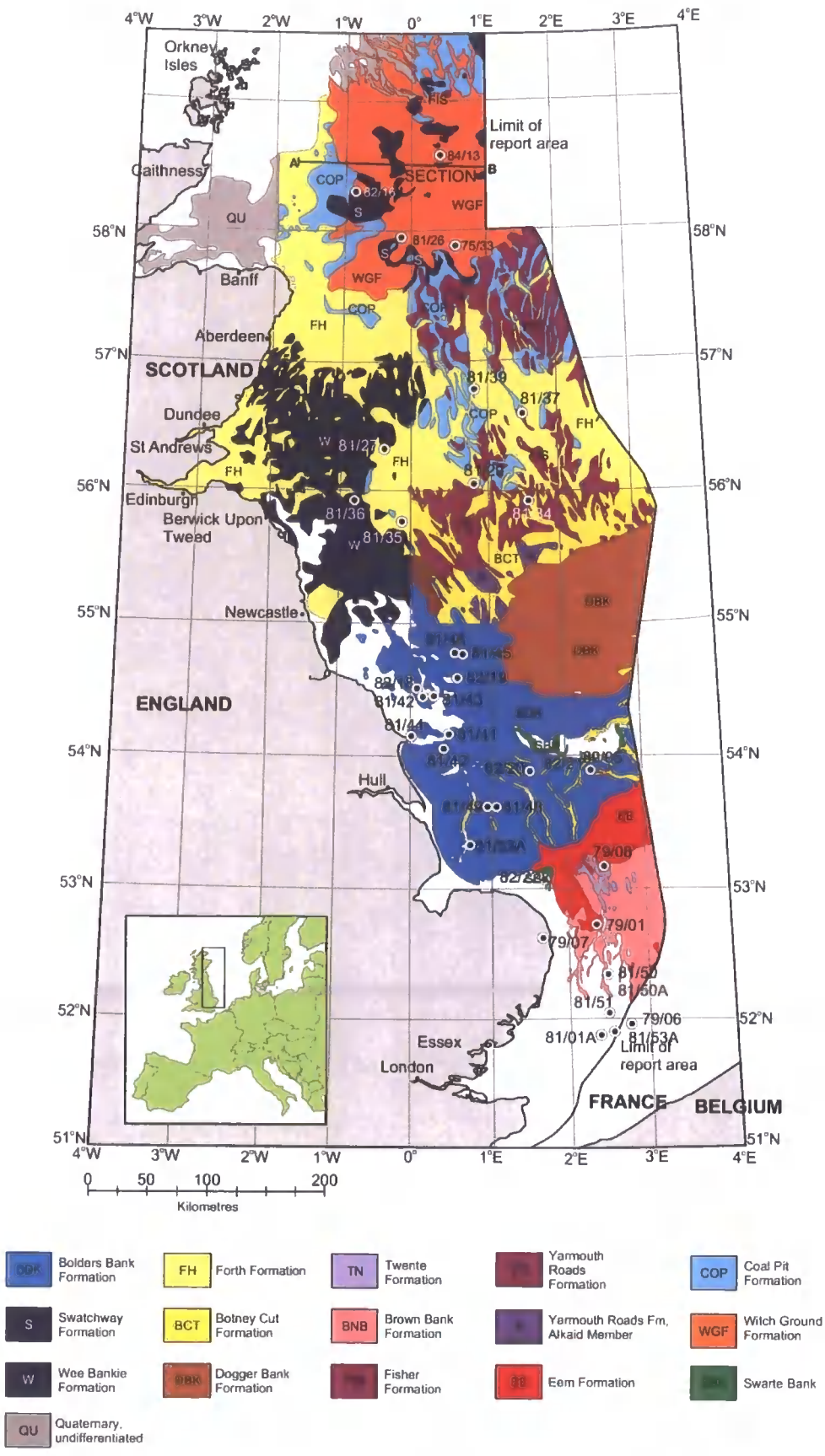

Figure 7.3: Map of Pleistocene Sediments in the North Sea (Andrews et al., 1990; Cameron et al., 1992; Gatliffe et al., 1994). The Aberdeen Ground Fm does not crop-out at sea bed. Refer to the cross-section in Figure 7.4.

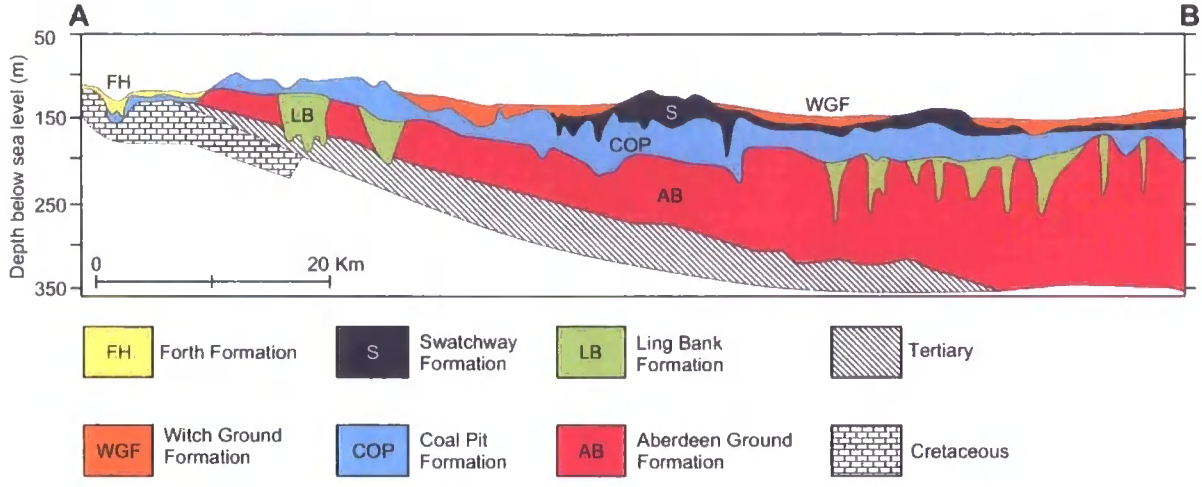

Figure 7.4: West-East cross-section to illustrate Quaternary formations in the northern North Sea. Figure 7.3 shows location of section AB. From Andrews et al., (1990).

The Cleaver Bank Fm subcrops beneath the Dogger Bank. It is a tabular body of stiff, dark-grey clays with some chert and chalk, and an arctic dinoflagellate-cyst assemblage with abundant reworked Palaeogene cysts. Gatliffe *et al.* (1994) therefore interpreted it as a proximal glaciomarine diamicton of eastern provenance, which continued east of 4°E into the subglacial, Saalian, Scandinavian, Brokumriff Fm.

The Fisher Fm is widely distributed north of 56°N, and may be partly correlative with the Alkaid member of the Yarmouth Roads Fm. It overlies the Ling Bank Fm in BH 81/34 (Figure 7.5), where a major unconformity from a marine transgression is overlain by around 6 m of interbedded fine-grained sand to stiff, dark-grey mud (Stoker *et al.*, 1985; Andrews *et al.*, 1990). It is overlain by the Coal Pit Fm in BH 81/26 (Figure 6.5). Parallel sub-horizontal reflectors are interrupted by small, intra-formational channels. It is the oldest sediment outcropping north of 56°N. An arctic, marine foraminiferal fauna supported the interpretation as a glaciomarine diamicton deposited during the Saalian (Gatliffe *et al.*, 1994).

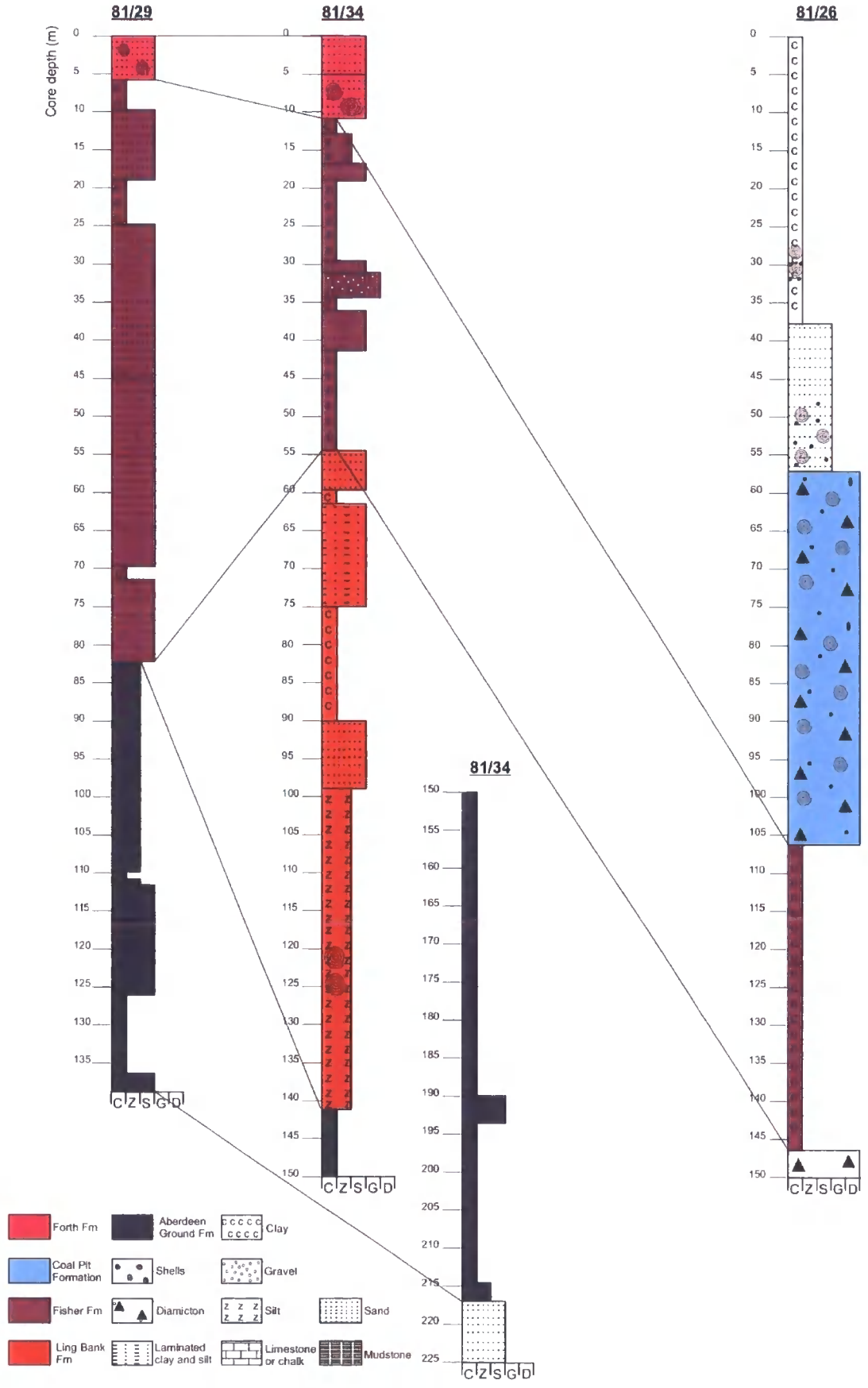

Figure 7.5: Correlation of Boreholes 81/26, 81/29 and 81/34.

7.2.3 Upper Pleistocene Sediments of the North Sea

The Early Weichselian

Stoker *et al.* (1985) stated that the Coal Pit Fm was widely distributed in the northern North Sea (Figure 7.3), where it locally exceeds 120 m in thickness. In type BH 81/37, the lower part of the Coal Pit Fm consisted of interbedded, bioturbated sand, and dark grey, stiff clay with shells, clasts and wood fragments. It resembles sediments deposited today, signalling the presence of the North Atlantic current (Stoker *et al.*, 1985). The upper part of the formation is a stiff, shell-rich, laminated clay with scattered clasts. Micropalaeontological data indicated that the Coal Pit Fm was deposited under harsh climatic conditions, possibly in a glaciomarine environment (Stoker *et al.*, 1985). The formation included an ameliorative phase in BH 81/37 and BH 75/33, representing Eemian strata. Stoker *et al.* (1985) therefore proposed that the formation probably ranged from Saalian to Weichselian in age. Thin-section analysis of the Coal Pit Formation (BH 81/26) by Carr *et al.* (2006) indicated that the sediment had undergone significant deformation under high confining stress regimes, suggesting that the upper facies of the Coal Pit Fm was a subglacial till.

Carr (2004b) distinguished an Early Weichselian glaciation, the 'Ferder glacial episode', which occurred during MIS 4 (~70 ka BP). This resulted in substantial glaciation of the North Sea Basin, and a till in the northern North Sea (the Ferder Formation). Carr *et al.* (2006) suggested that to the south, at least part of the Coal Pit Fm is laterally contiguous with the Ferder Fm. The Ferder Fm extends from the Norwegian Channel to the continental shelf margin west of Shetland as a continuous facies (up to 80 m thick), comprising fine-grained diamictons with shell fragments. Carr *et al.* (2006) argued that micromorphological analysis, the spatial extent, and the geometry of the formation suggested that it reflected extensive glaciation across the northern North Sea Basin, with confluence of the British and Fennoscandian ice sheets (Figure 7.6), and with the northern ice front terminating in a marine environment at the shelf edge. The interpretation of a subglacial origin for the Coal Pit and Ferder Fm sediments led Carr *et al.* (2006) to suggest that they were correlative and were deposited in MIS 4 during large-scale glaciation of the North Sea Basin. However, the uncertain and wide-ranging stratigraphic status of the Coal Pit Fm rendered this interpretation only provisional. The evidence for extensive glaciation in the NSB during MIS 4 has significant implications for onshore correlations. In

Chapter 6, evidence to suggest that the Blackhall Member was deposited during MIS 4 was discussed, and this is a possible correlative for the Ferder Fm.

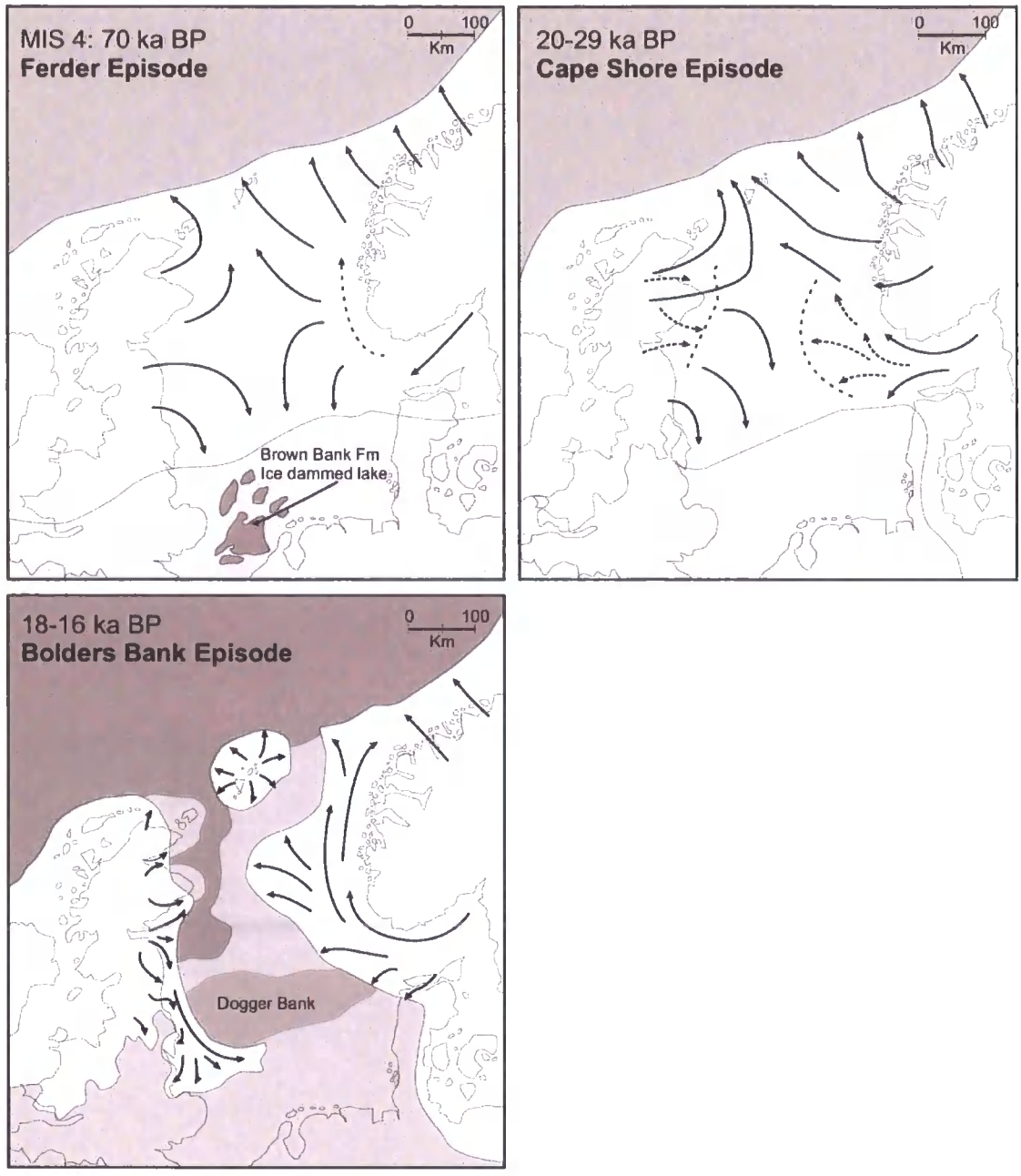

Figure 7.6: The Weichselian in the NSB (from Carr et al., 2006).

The Last Glacial Maximum

Ehlers and Wingfield (1991) argued that incised valleys present both in the North Sea Basin and inland in northern Germany provided further evidence of extensive glaciation of the North Sea. The tunnels were interpreted as subglacial meltwater channels formed in the marginal zone of ice sheets, which occur only within ice sheet limits. Most occur within till

limits, but erosion and reworking can mean that the infilled incisions remain where till sheets have been removed (Ehlers & Wingfield, 1991). These tunnel valleys in the NSB extend beyond the till sheet limits, thus indicating that the extent of Late Devensian ice in the North Sea was greater than the sedimentary records suggested. Ehlers and Wingfield (1991) argued that the FIS and BIIS may have met in the North Sea, and that parts of the central and southern North Sea could have been extensively glaciated. Sejrup *et al.* (2000; 2005) agreed that the British and Scandinavian ice sheets were confluent from 29 to 25 cal. kyr BP, and separated after this time. The maximum limit of the ice sheet was probably reached around 29 cal. ka BP, coinciding with a peak in clastic sedimentation on the Barra Fan (Knutz *et al.*, 2001; Sejrup *et al.*, 2009).

The complexity of the Late Weichselian is increasingly recognised in the North Sea Basin, and a two-stage model is generally favoured (see Chapter 3, this thesis). Carr *et al.* (2006) suggested that mid- to Late-Weichselian glaciation of the North Sea Basin occurred during the 'Cape Shore glacial episode' (Figure 7.6). The Cape Shore Fm extends across the northern NSB from the Norwegian Channel to the Continental Shelf, and overlies the Ferder Fm. It may be correlative with the Swatchway Fm in the central NSB. The lower part of the Cape Shore Fm is distinguished by sub-horizontal reflectors indicating sedimentary bedding, and the upper part is characterised by fine-grained massive diamictons (*ibid.*). This upper facies of the Cape Shore Fm contained evidence for subglacial glaciotectonic origin, with a microfabric indicating a unidirectional stress field and not sediment settling out from suspension. Carr *et al.* (2006) therefore argued that the majority of the Cape Shore Fm was deposited under marine conditions, and that the upper part was subsequently reworked and deformed subglacially. They proposed that the Swatchway Fm, which overlies the Coal Pit Fm in the central NSB, was partly contiguous with the Cape Shore Fm. Thin-section analysis supported an interpretation as a subglacial till. Within the Norwegian sector of the North Sea, the Tampen Fm is laterally equivalent to the Swatchway Fm, and indicates the extension of ice beyond the Norwegian Channel during the LGM (*ibid.*).

Carr *et al.* (2006) have coalescent British and Fennoscandian ice sheets until 20 ka BP. This provides a window and a mechanism to turn the east coast North Sea Lobe southwards; calibrated radiocarbon dates on the Dimlington Silts at Skipsea show that the Skipsea Till was deposited by the North Sea Lobe at 21,475 ± 140 cal. yr BP (Bateman *et*

al., 2008). After the LGM, ice flow would continue to follow this pattern, though relaxation might allow expansion eastwards.

Fast-flowing ice-streams in the NSB have been revealed through detailed bathymetric and seismic reflection surveys along the north-west European continental shelf. Graham *et al.* (2007) argued that the upper part of the Coal Pit, Swatchway and Witch Ground formations exhibited variable thicknesses across the Witch Ground Basin, and exhibited both iceberg plough marks and streamlined bedforms. The streamlined bedforms of the Witch Ground Basin trended from NW-SE with a second, lower set trending NE-SW (Figure 7.7), and were interpreted as Mega Scale Lineations (MSGL), formed at the base of a fast-flowing ice stream (*ibid.*). The lower NE-SW lineations occurred on a strong seismic reflector at 80 m below seabed, at the top of the Ling Bank / Fisher formations (MIS 9-6) that infill a pre-Eemian tunnel valley. Graham *et al.* (2007) proposed that the MSGL bedforms within the younger NW-trending flowset defined an ice stream that extended 100 km along the axis of the Witch Ground Basin, with a maximum width of 30-50 km. Late Weichselian sediments dated to 27.3 cal. kyr BP overlie the uppermost MSGL, providing a minimum age for their formation (Sejrup *et al.*, 1994). This implies that during the Late Weichselian, the ice-sheet in the central North Sea was characterised by zones of fast-flow as well as regions of slow-moving, stagnant ice (Graham *et al.*, 2007).

This theory agrees with the Cape Shore Episode model proposed by Carr *et al.* (2006), with complete ice cover in the central and northern NSB at the late Weichselian maximum (Figure 7.6). The source of the ice-stream is contentious, but Graham *et al.* (2007) suggested that it was a branch of the Norwegian Channel Ice Stream. This could mean that the confluence caused the deflection of the Moray Firth ice stream towards the north-west, and the BIIS and FIS converged on the western margin of the Witch Ground Basin, east of Orkney and Shetland.

The Olex bathymetric database compiled by the Norwegian company Olex is based on echo-sounder data acquired by commercial fishing vessels and research vessels. It creates a detailed seabed DEM that provides excellent views of the morphology and distribution of seabed landforms. Analysis by Bradwell *et al.* (2008) around the northern margin of the UK showed channels and ridges around St Kilda, west of Orkney and Shetland, in the Moray Firth, offshore Strathmore, and flanking the western margin of the Norwegian Channel (Figure 7.8). The channels fell into two groups. Group A trended north to

northwest, and were widely distributed across the NSB. The Group A Channels range from 3 km to 50 km in length, and have a strongly consistent orientation. The majority occurred around the northern margin of the Witch Ground Basin, and some were located on the southern edge of the basin (Bradwell *et al.*, 2008).

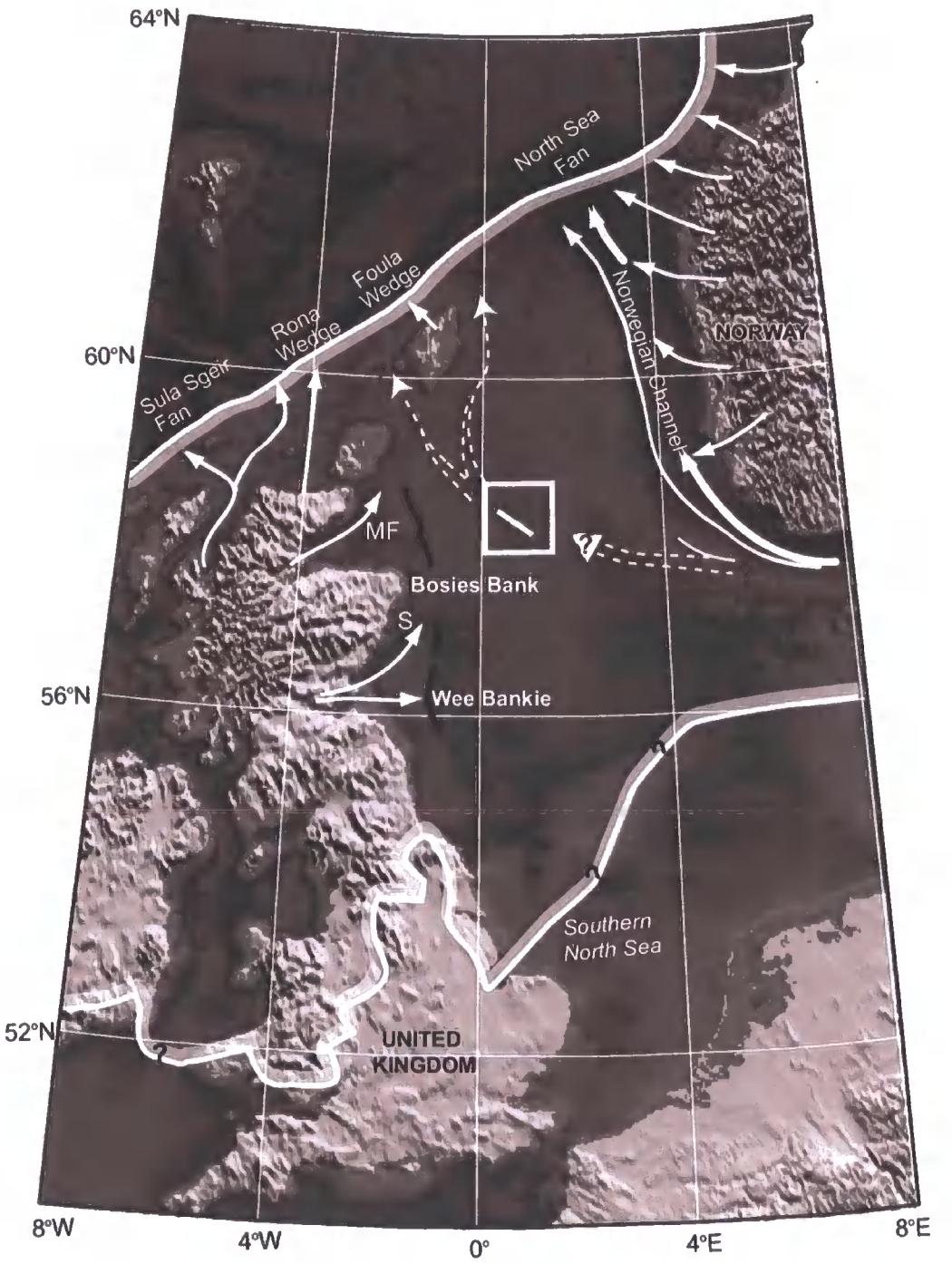

Figure 7.7: From Graham *et al.* (2007). Reconstruction of ice sheet limits for MIS 2 with location of fast flowing ice streams (solid arrows) for other independent evidence. The youngest Witch Ground Fm MSGLs are identified in the boxed area. One reconstruction for the Witch Ground Ice Stream as a divergent flow from the Norwegian Channel Ice Stream is shown. UK offshore moraines indicated by

black lines. MF is Moray Firth ice stream (Merritt *et al.*, 2003). S is the Strathmore Ice Stream (Golledge & Stoker, 2006). Norwegian Channel Ice Stream from Ottesen *et al.* (2005).

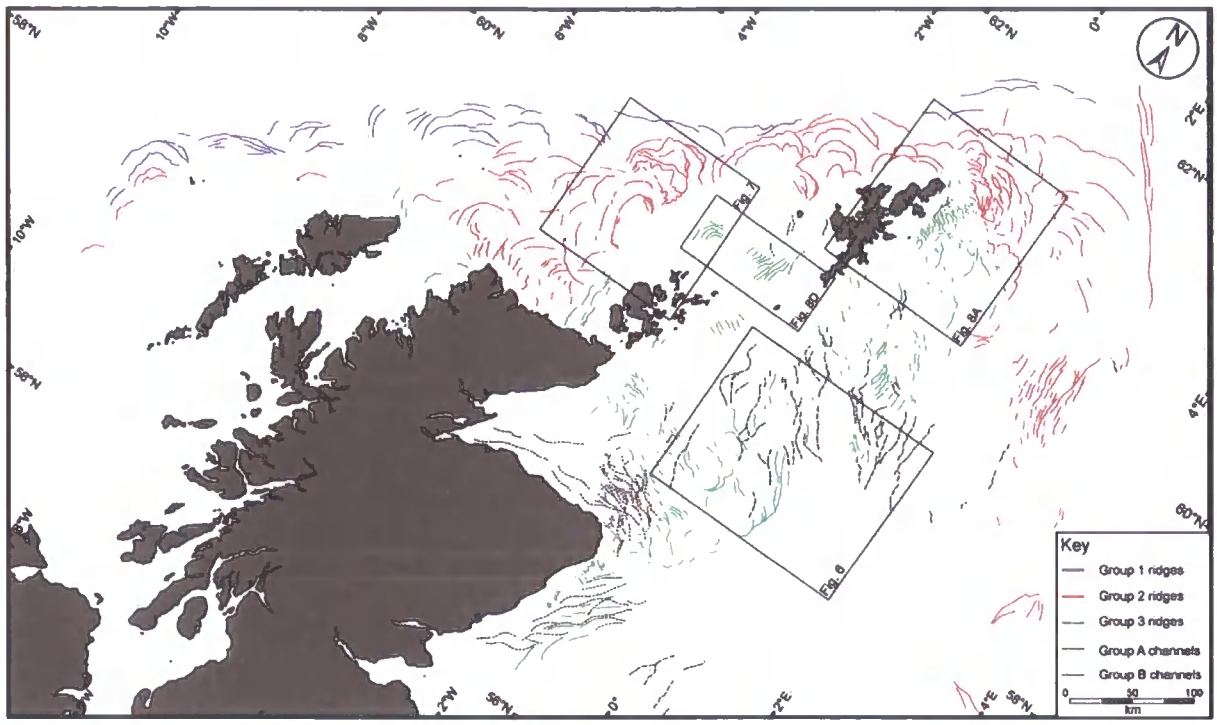

Figure 7.8: From Bradwell *et al.* (2008), mapped from the Olex dataset. Solid lines are ridges (moraines). Dashed lines are negative linear features (channels and tunnel valleys).

The crestline ridges marked on Figure 7.8 were divided into three groups. Group 1 ridges comprise the northernmost landforms, on the outermost shelf. They are large, curvilinear, arcuate ridges, trending northeast to southwest. Group 2 ridges occur on the mid-shelf to the north and west of Scotland (Bradwell *et al.*, 2008). The ridges west of Orkney and Shetland occur as nested, lobate forms, strongly concentric from west to east. Northeast of the Moray Firth is a distributed population of curvilinear ridges, aligned northwest to southeast, which are less than 10 m in height. They range in length from 1 to 35 km. The ridges in Groups 1 and 2 were interpreted by Bradwell *et al.* (2008) as end moraines formed at a grounded terrestrial ice margin. The straight, sub-parallel, sharp-crested ridges near Orkney and Shetland were interpreted as subaqueous grounding line moraines (De Geer moraines). The majority of the negative linear features were interpreted as glacial tunnel valleys (as defined by Ó Cofaigh, 1996), probably formed through erosion by subglacial meltwater flowing parallel to ice-flow (Bradwell *et al.*, 2008). The Group

1 moraines occurred in direct association with the major shelf-edge fans (Sejrup *et al.*, 2005; Bradwell *et al.*, 2008). The coupled shelf-edge fans and moraines reflected the position of a formerly extensive continental ice-sheet flowing towards the Atlantic Ocean. They were associated with the Group A tunnel valleys, whose orientation supported an ice-flow direction towards the continental shelf, and buried MSGL (Graham *et al.*, 2007; Bradwell *et al.*, 2008). The BIIS and FIS would have been confluent at this time.

The mid-shelf moraines on Figure 7.8 formed after extensive shelf-edge glaciation, probably during a retreat stage. The thinning of the ice sheet allowed topography to exert more of an influence on ice flow. The mid-shelf moraines had a lobate and convolute morphology, similar to push moraines and thrust-block complexes (Bradwell *et al.*, 2008). The number and density showed that dynamically surging lobes were common in the BIIS. The lobate margins indicated that the ice sheet was grounded and highly irregular at this stage.

The Dimlington Stadial

The Bolders Bank Fm provided Carr *et al.* (2006) with evidence for a final major advance of the Scottish and Fennoscandian ice sheets during the Late Weichselian. It is correlative with the Skipsea Member, dated to 21.7 cal. ka BP (Sejrup *et al.*, 1994; Carr *et al.*, 2006). The Bolders Bank Fm forms the south-eastward extension of the Wee Bankie Fm to the south of 56°N and east of 0°E (Figure 7.3, Figure 7.6 and Figure 7.9). It is rarely more than a metre thick, but locally it attains over 40 m. Gatliffe *et al.* (1994) described it as a reddish to greyish-brown, stiff, massive diamicton with a decreasing clast content to the east (Figure 7.9). Micromorphological analysis of the Bolders Bank Fm indicated a genesis as a subglacial till (Carr *et al.*, 2000), reflecting an ice sheet extending across the southern North Sea. The till resembles the onshore tills in eastern England (Cameron & Holmes, 1999), and Cameron *et al.* (1992) correlated the Bolders Bank Fm with the Skipsea and Withernsea Members of East Yorkshire.

Cameron *et al.* (1992) noted that the Dogger Bank Fm interfingers with and partly overlies the Bolders Bank Fm. They described it as an extensive, tabular deposit up to 42 m thick, with better-ordered internal reflectors than the Bolders Bank Fm. This indicated that it is a proglacial, water-lain body, forming an upstanding area of relief in the NSB, consisting of clay-rich diamictons with smaller, fewer clasts than the Bolders Bank Fm. They found indigenous dinoflagellate cysts indicative of severe, cold, open-water

marine conditions. Recent micromorphological analysis by Carr *et al.* (2006) of the Dogger Bank Fm provides evidence of pervasive shear, glaciotectonism and deformation. Carr *et al.* (2006) proposed that the sediments were deposited under glaciomarine conditions, and that the upper 10 m underwent subsequent glaciotectonic deformation. They suggested that the structure of the Dogger Bank itself indicates that it is a large moraine belt, comparable with the Main Stationary Line in Denmark. It is possible that the Dogger Bank was originally deposited ice-marginally or in an ice-walled, ice-contact environment, trapped between the British and Fennoscandian ice sheets.

The Wee Bankie Fm occurs in the Central North Sea (type BH 72/20). The sequence in this core extends from seabed to 33 m. Seismic data indicated that this is probably within a few metres of rockhead. The sediments are mostly stiff diamictons with thin interbeds of sand, pebbly sand and silty clay (Figure 7.9). The clasts bear striae and reflected the underlying and nearby strata. It was interpreted as a subglacial till with coarse sand and gravel deposited by subglacial streams (Stoker *et al.*, 1985). Seismostratigraphical interpretation indicated that it was correlative with the Marr Bank Fm, and it could be traced onshore in the west. Gatliffe *et al.* (1994) suggested that the Wee Bankie Fm is contiguous with the Red Series tills in the Firth of Forth and onshore Scotland. Carr *et al.* (2006) proposed that the Bolders Bank Fm and the Wee Bankie Fm are correlative subglacial tills representing ice extending eastwards from the Midland Valley of Scotland.

The third assemblage of features identified by Bradwell *et al.* (2008) on the Olex map (Group 3 ridges and Group B channels; Figure 7.8) are on the inner shelf, close to the present-day coastline of Scotland, east of groups 1 and 2. Group B channels occur in two separate areas (Figure 7.8). The first group flanked the east coast of Scotland, trending north-north-east, parallel to the coastline. They range from 2 – 30 km in length, and are evenly spaced. They are incised up to 120 m below sea level (bsl), and range from 1.5 – 3 km in width, often with branching, sinuous courses. The second set occur in the outer Moray Firth and trend west to east, ranging in length from 1.5 to 58 km (Bradwell *et al.*, 2008), and are up to 200 m deep. Both sets of channels have irregular thalwegs and undulate along the length of the channel. They begin and end abruptly, and some have branching tributaries. Some are partially infilled with sediment. Bradwell *et al.* (2008) described the Group 3 ridges as small in scale, ranging between 500 m and 25 km in length, with many occurring as concentrations of closely spaced ridges.

Bradwell *et al.* (2008) interpreted the ridges and channels as smaller near-shore moraines and meltwater channels, the Wee Bankie and Bosies Bank moraines. They form the eastern limit of the Wee Bankie Fm as a series of stacked moraine ridges 50 km offshore, interdigitating with a well-layered seismostratigraphic sediment (the Marr Bank Fm), which has been interpreted as an ice-contact glaciomarine diamicton with an ice sheet terminating in a calving margin at the limit of the Wee Bankie Fm (Stewart, 1991). The ridge is formed of subglacial till and derived glacigenic diamicton. A first-order reflector occurs at the base of the glaciomarine facies, and represents a transgression that pre-dates the deposition of the glacial tills. The expansion of the ice sheet removed the reflector. Stewart (1991) argued that the coincidence of the western edge reflector with the ridge indicated that the ridge represented the maximum regional position of the ice sheet. North of 57°N, the ridge is discontinuous and untraceable, and the sediment sequence is disturbed (Bradwell *et al.*, 2008). The highly elongate bedforms in northwest Scotland and Strathmore on land and on the seabed suggest that ice streams were still active within the BIIS at this time, and may have been prone to periods of instability. Ice streams were active in the Moray Firth, the Firth of Forth, and in the Minch (Merritt *et al.*, 2003; Stoker & Bradwell, 2005; Golledge & Stoker, 2006).

Despite poor-quality AMS dating, Carr *et al.* (2006) argued that the Bolders Bank episode (Figure 7.6) represented the advance of the BIIS after 22726 – 20166 cal. yr BP (Sejrup *et al.*, 1994), during the Dimlington Stadial in Britain (Catt & Penny, 1966; Rose, 1985; Sejrup *et al.*, 1994; Sejrup *et al.*, 2000). A final restricted glaciation of Scandinavia occurred during the 'Tampen Stadial', correlative with the Dimlington Stadial, where ice expanded beyond the Norwegian Channel to the North Sea Plateau. This is dated to between 21 and 18 cal. ka BP (Sejrup *et al.*, 2009).

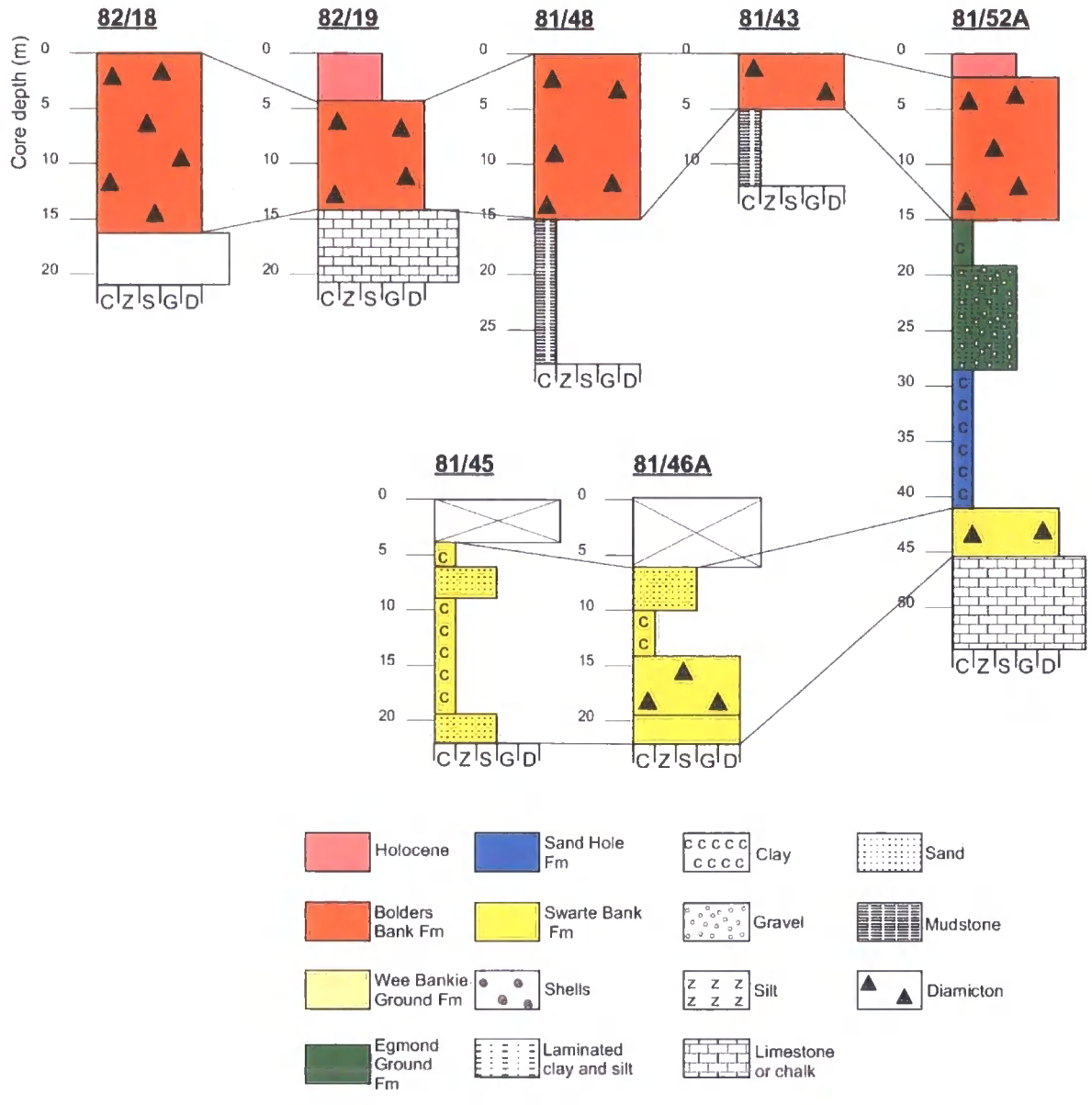

Figure 7.9: Correlation of borehole logs. From Gatliffe et al. (1994).

7.3 Sedimentology and Micromorphology

7.3.1 The Swarte Bank Fm

Sedimentology and Borehole Logs

The Swarte Bank Fm is located in the base of buried valleys in the southern North Sea Basin, south of 55°N (Figure 7.3). It is overlain by the Egmond Ground Fm, the Sand Hole Fm, the Eem Fm in the central NSB (Figure 6.9), and ultimately by Devensian glacigenic sediments. The Swarte Bank Fm was sampled from BH 81/52a at 43.07m, and BH 81/46a at 17 m and 18 m (Figure 7.10 and Figure 7.11). These boreholes are located some distance away from each other (Figure 7.1), so some difference between the samples is to be expected due to varying substrate lithologies, grain sizes and grain durabilities. Owing to the incomplete, narrow, and confined nature of the boreholes, a complete sedimentological analysis is difficult. The sediments are also disturbed during the coring process. The upper part of BH 81/52a was missing. The BGS sedimentological descriptions in the figures below provide most of the sedimentological detail.

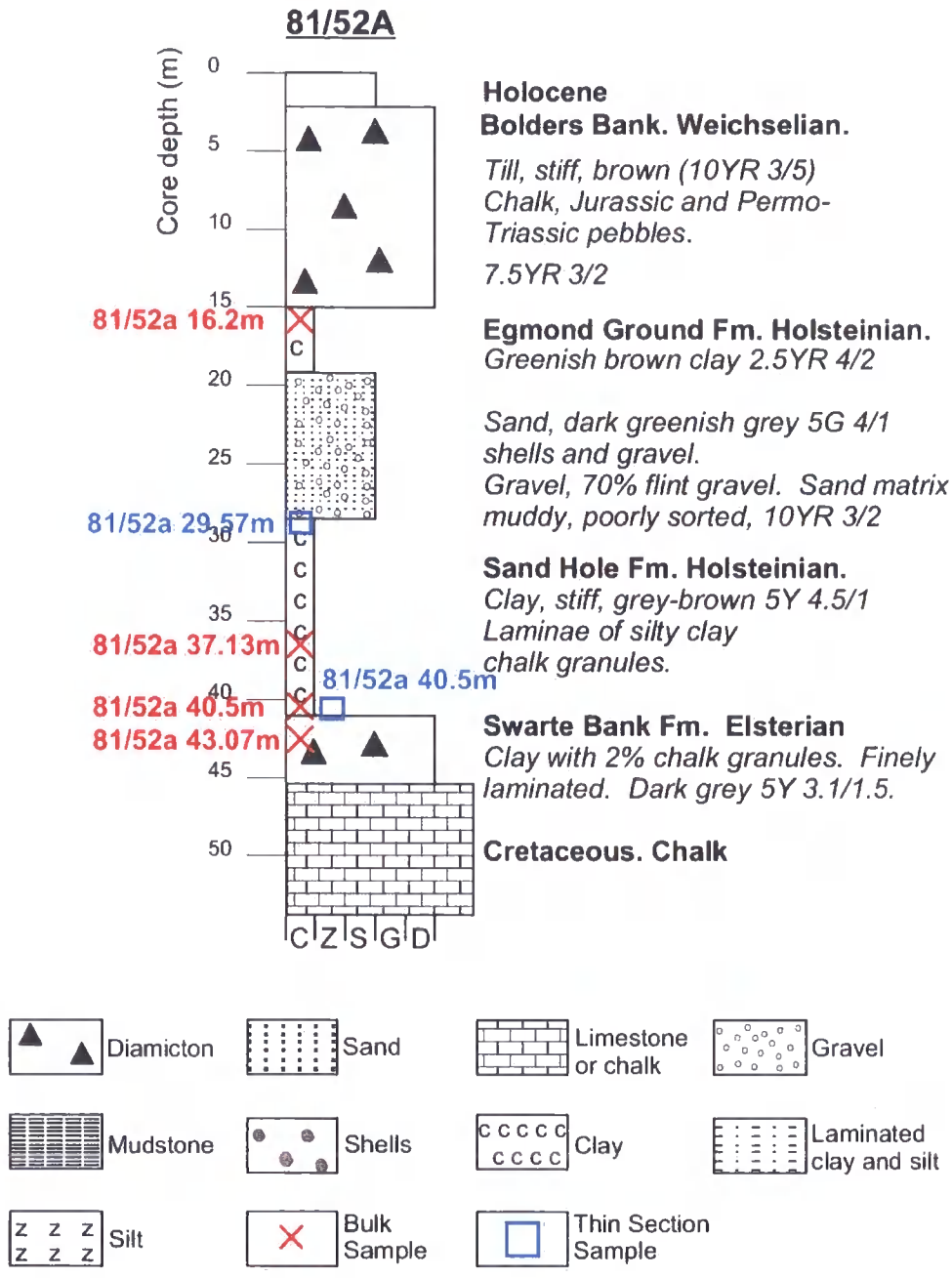

Figure 7.10: BH 81/52a from BGS Log. Formations after Cameron et al., (1992) and Scourse et al., (1998).

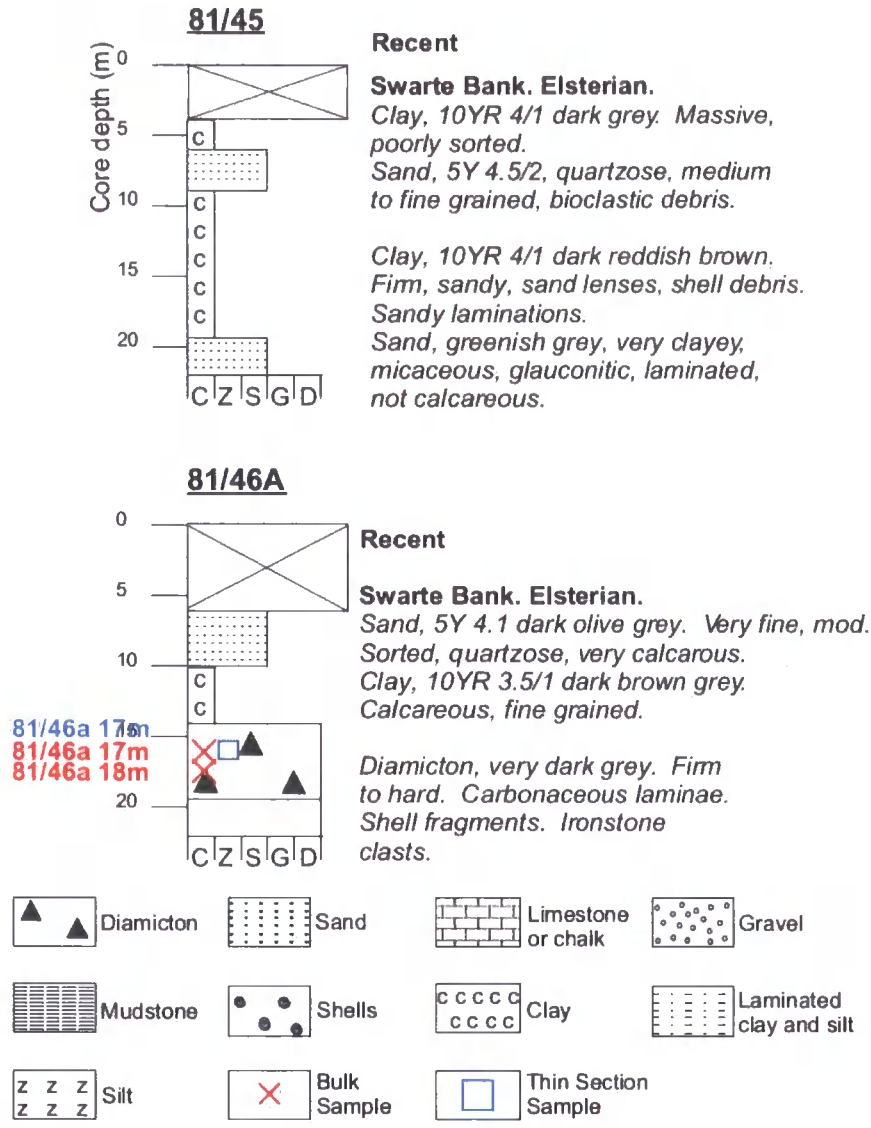

Figure 7.11: BGS BH 81/45 and BH 81/46a, using additional information from Balson and Jeffery (1991).

Thin Section Analysis

The thin section of the Swarte Bank Fm (sample 81/46a 17 m; Figure 7.12; Table 7.3) shows a brown diamicton with a variable texture. The diamicton is fine-grained, the plasma is of even density and distribution, and has few clasts larger than 150 µm (Table 7.3). There are only rare rounded red sandstone skeleton grains, which are up to 1000 µm in diameter. The diamicton incorporates abundant shell fragments, and it has small vugh and planar voids. It is dissected by a broken bed of manganese.

The thin section shows abundant turbate structures (van der Meer, 1993), both with and without core stones. They are associated with a well-developed skelsepic plasmic fabric, which is found surrounding fine skeleton grains as a thin skin. The turbates are

often associated with pressure shadows. Within the diamicton there are stretched and attenuated Type III pebbles (van der Meer, 1993), often in association with turbates and pressure shadows. There are numerous grain lineations, showing a preferred orientation of small skeleton grains. Grain stacks are also apparent.

Table 7.3: Summary of thin sections from North Sea Boreholes

Lithofacies	Skeleton			Matrix		Void Type	Sedimentary Structures				Deformation Structures													Plasmic Fabric				Other Information
	Sorting	Grain shape <500 um	Grain shape >500 um	Texture	Microfabric		Laminations	Dropstones	Microfossils	Dump Structures	Section Elements	Faulting	Folding	Rotations	Grain lineations	Pressure Shadow	Crushed Grains	Grain stacks	Pebble Type I	Pebble Type II	Pebble Type III	Water escape	Fluidised Bedding	Skelsepic	Latlisepic	Masepic	Bi-Masepic Unistrial	
Bolders Bank	D	SR	SA	F		L			•					•••	••	••	•	•			•••			••	•			Far travelled igneous / metamorphic fragments
Coal Pit Fm	D	A	SA to SR	F		P								•••	•••	••		••			•••			••				Massive diamicton; shell fragments
Fisher Fm	MS		SA to SR	M	H	L / P	•••				F	••	•••							•		•	•••			•••		Disjointed rafts of clay laminae
Sand Hole	MS	SA	SA	M	H	L / P	•••	••	•••	•	Be		••								••	•						Laminated and recumbently folded
Sand Hole	D		SA to SR	F		L / P			•••		Ba			•••	••			••		•				•••		•••		
Swarte Bank	D	R	SA to A	F		L / P					Bo / Be			•••	•••	•••		•		•	•			•••				Shell fragments

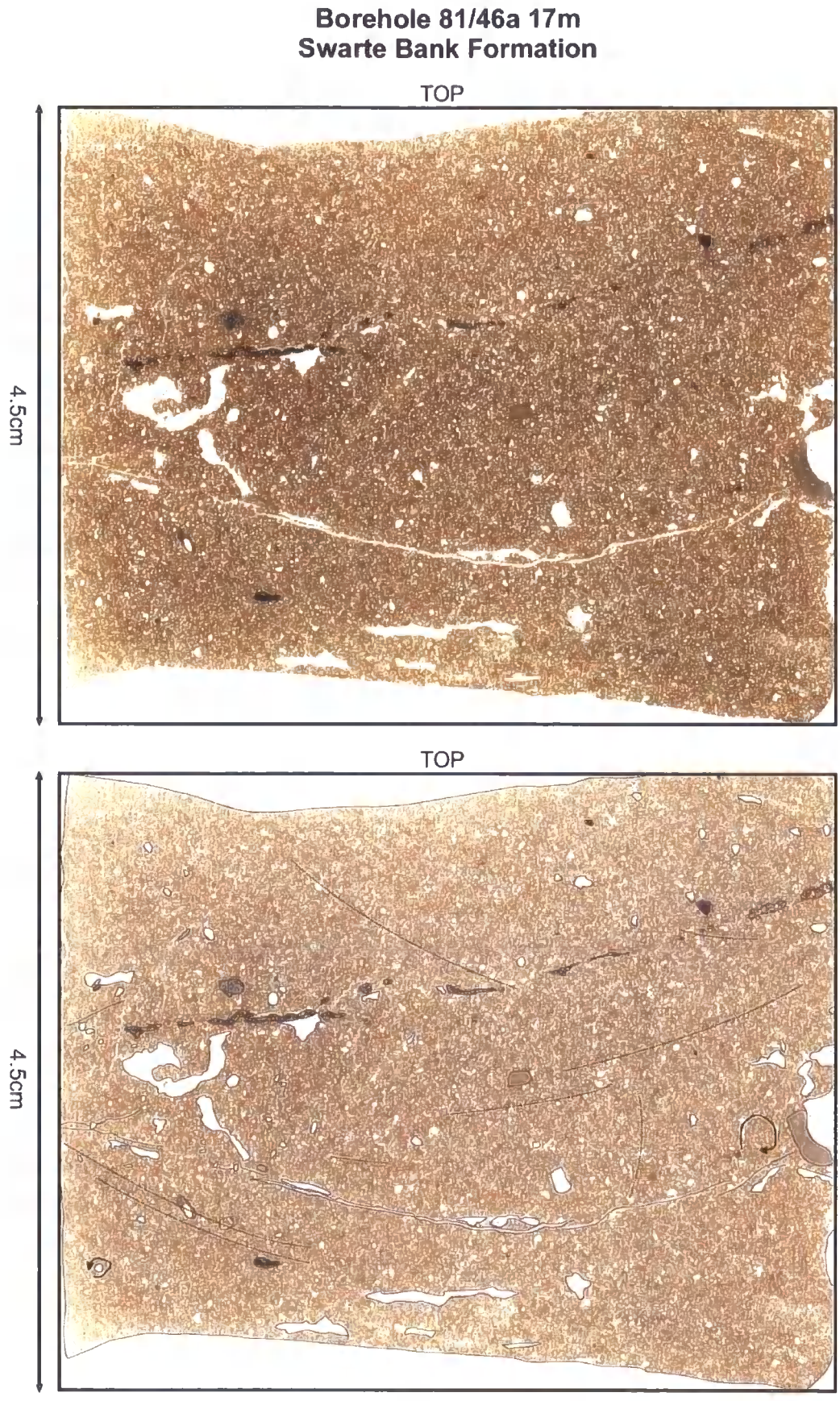

Figure 7.12: Thin section of the Swarte Bank Fm. Locations and orientations of grain lineations are highlighted.

7.3.2 The Sand Hole and Egmond Ground formations

Sedimentology and Borehole Logs

The Sand Hole Fm overlies the Swarte Bank Fm and was sampled from BH 81/52a at 37.13 m and at 40.5 m (Figure 7.13). The sediment is a well-sorted silty clay, coloured a light brownish grey (10YR 6/2) to pale brown (10YR 6/3). The reaction to HCl varies from moderate to vigorous. The clay has no gravel or shells.

The Egmond Ground Fm directly overlies the Sand Hole Fm. The single sample from the Egmond Ground Fm was taken from 16.2 m in BH 81.52a (Figure 7.13). At this depth it is a yellowish brown (10YR 5/4), poorly-sorted, coarse sand, with flint, quartz, quartzite, Magnesian Limestone and dolerite gravel. The Egmond Ground Formation has very little silt and clay, but high proportions of fine and coarse sand. There are abundant bivalve fragments, which are too small to identify. Very small foraminifera are present in extremely low numbers. The Egmond Ground Fm was too poorly consolidated for thin-section analysis.

Thin Section Analysis

The Sand Hole Fm was sampled from BH 81/52a at 40.5 m (Table 7.3). This brown diamicton is of variable texture, and exhibits macroscopic banding (Figure 7.13). Vugh and planar voids are present due to poor impregnation. The skeleton grains are matrix-supported but range widely in size. The finer silt and sand skeleton grains are subangular to subrounded, but generally exhibit edge rounding. Quartz, coal and sandstone grains are common. The silty clay has abundant marine microfossils, including foraminifera, radiolaria, diatoms and coccoliths. The slide exhibits abundant deformation structures, including the classic turbates with associated skelsepic plasmic fabrics and 'galaxy tails'. There are rare Type II Pebbles. Lineations of grains are common, and are associated with aligned clay particles and fine skeleton grains. Grain stacks are common (cf. Menzies *et al.*, 2006).

A second sample was taken from higher up the borehole, at 29.87 m below seabed (Figure 7.14). This sample is profoundly different, showing many primary sedimentary features such as graded bedding and laminations (Figure 7.15). Texturally, the sand laminations are clast-supported and are poorly sorted, with occasional larger sand grains (Figure 7.15). There are numerous Type III Pebbles (van der Meer, 1993) within them (Figure 7.15 A). The skeleton grains are mostly subangular. The intervening clay

laminations are less well sorted, and have a bedding-parallel microfabric. Microfossils such as foraminifera are very common (Figure 7.15 A and B). Macroscopically, the large recumbent fold is clearly visible, with two fine gravel rounded skeleton grains deforming the bedding beneath and above (Figure 7.15 C). There is a dump structure composed of fine sand, with the bedding draped over the top. The sand laminations in the top left corner are dragged upwards. The bedding has been disrupted by a water-escape structure. The clay laminations contain a bedding-parallel masepic plasmic fabric.

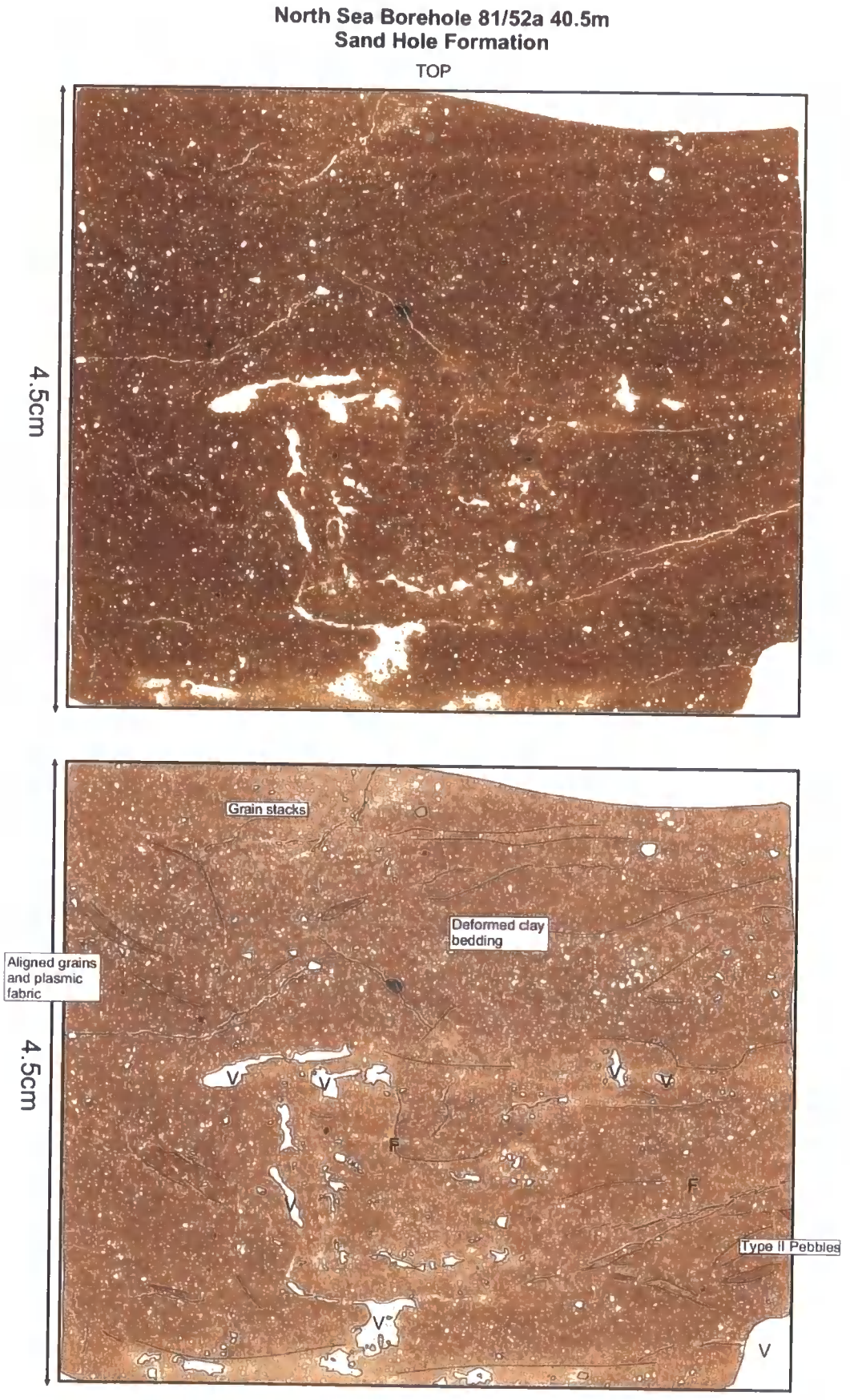

Figure 7.13: Thin Section BH 81/52a 40.5 m. Location of sub-resolution features is highlighted on the figure.

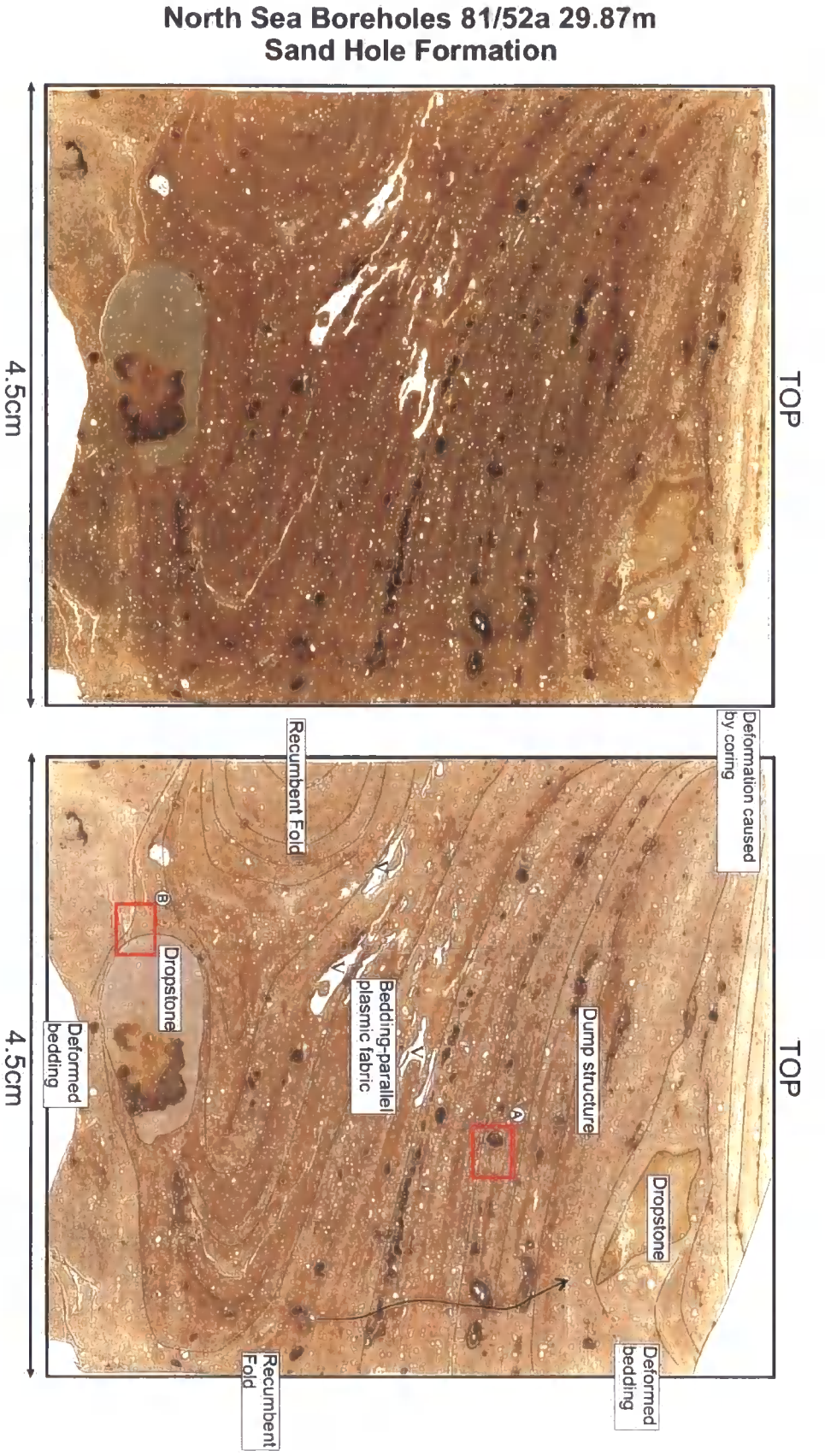

Figure 7.14: Thin Section of the Sand Hole Fm. Location of plasmic fabric development is highlighted.

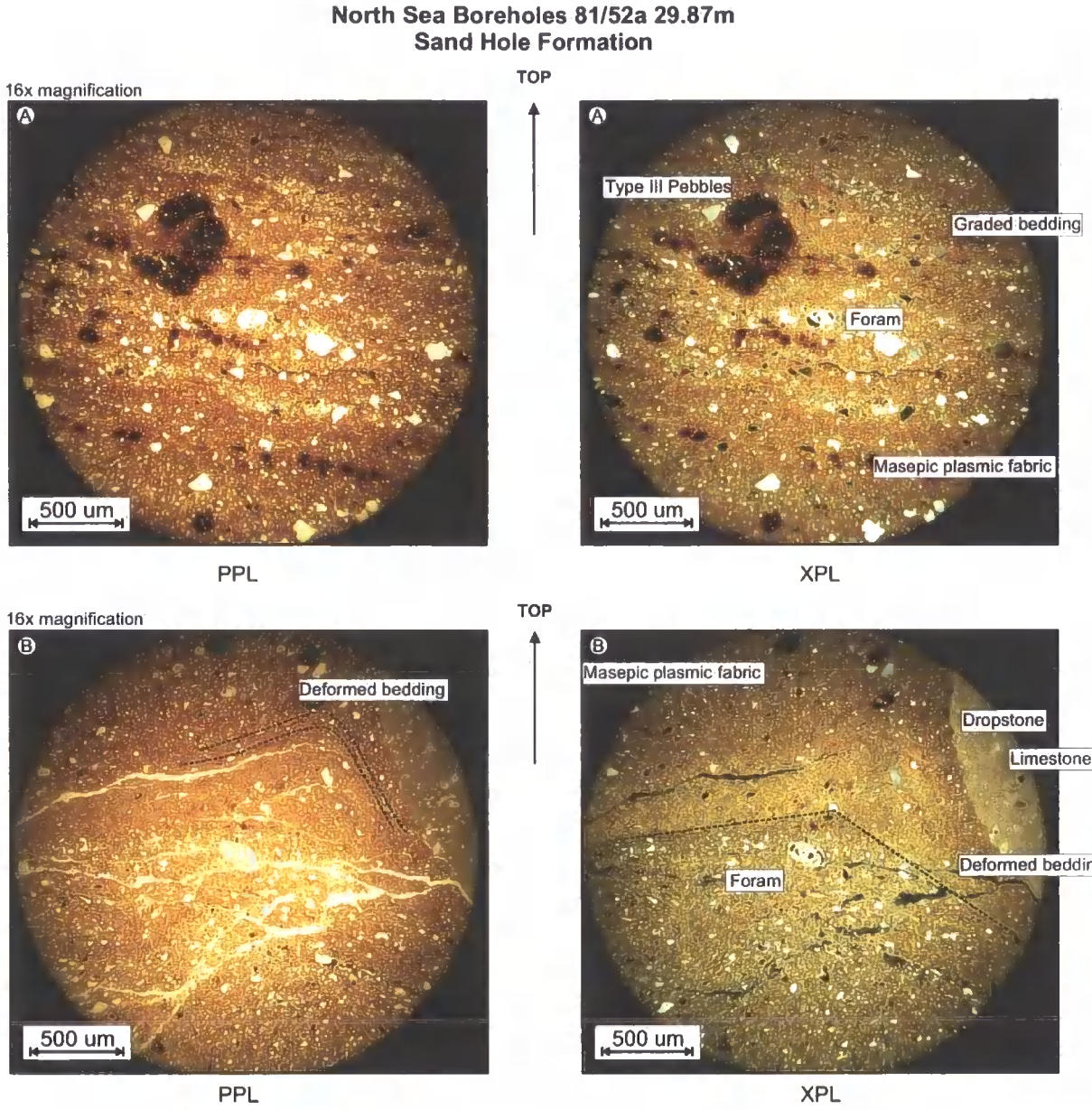

Figure 7.15: Photomicrographs of thin section sample 81/52a 29.87 m.

7.3.3 The Fisher Formation

Sedimentology and Borehole Logs

The Fisher Fm was sampled from boreholes 81/29 (Figure 7.16) and 81/34 (Figure 7.17). These boreholes are located close to each other (Figure 7.1), and the sediments in both boreholes are reasonably similar.

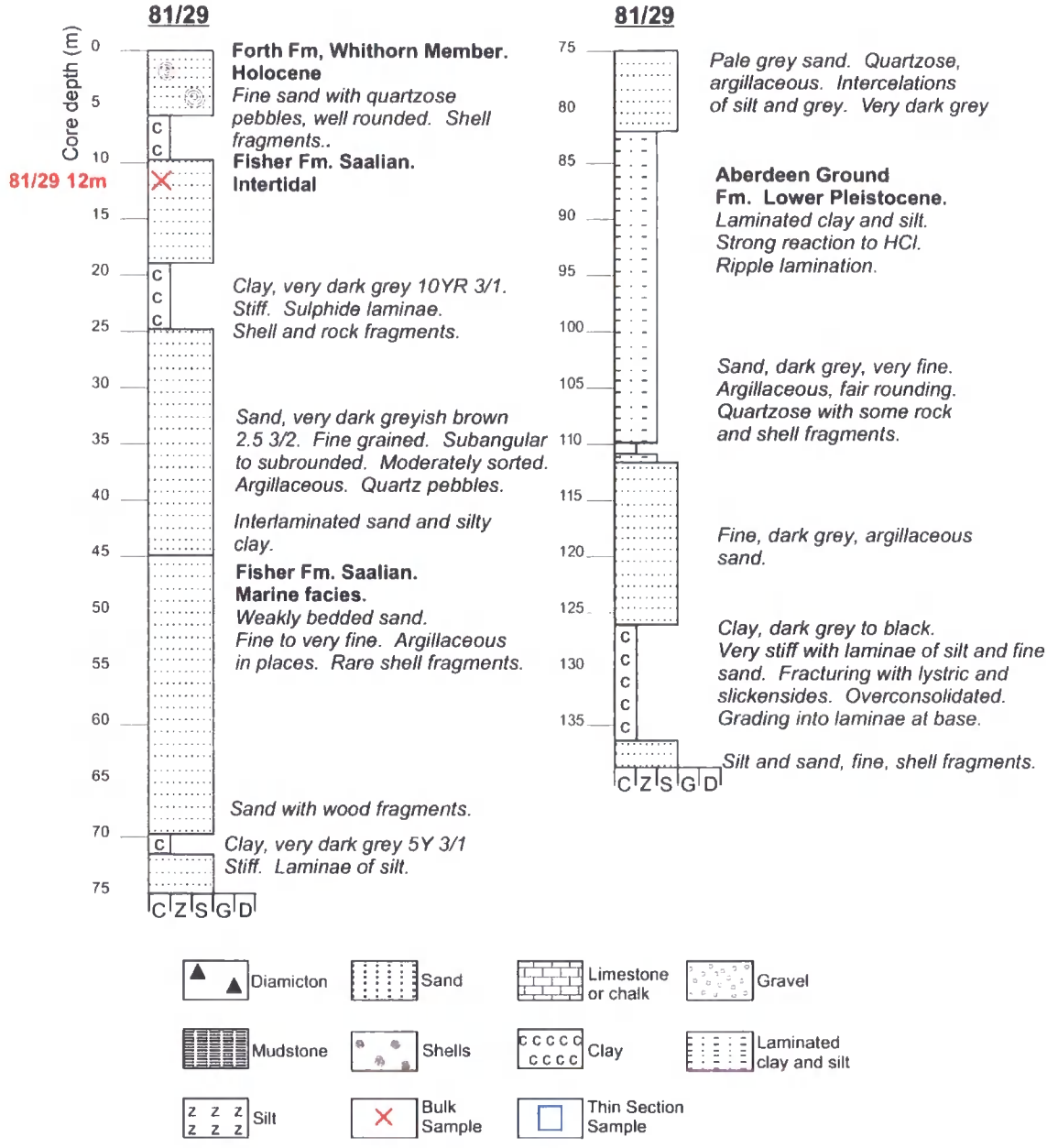

Figure 7.16: BGS Borehole 81/29 from BGS logs. Interpretations after Sejrup and Knudsen (1993).

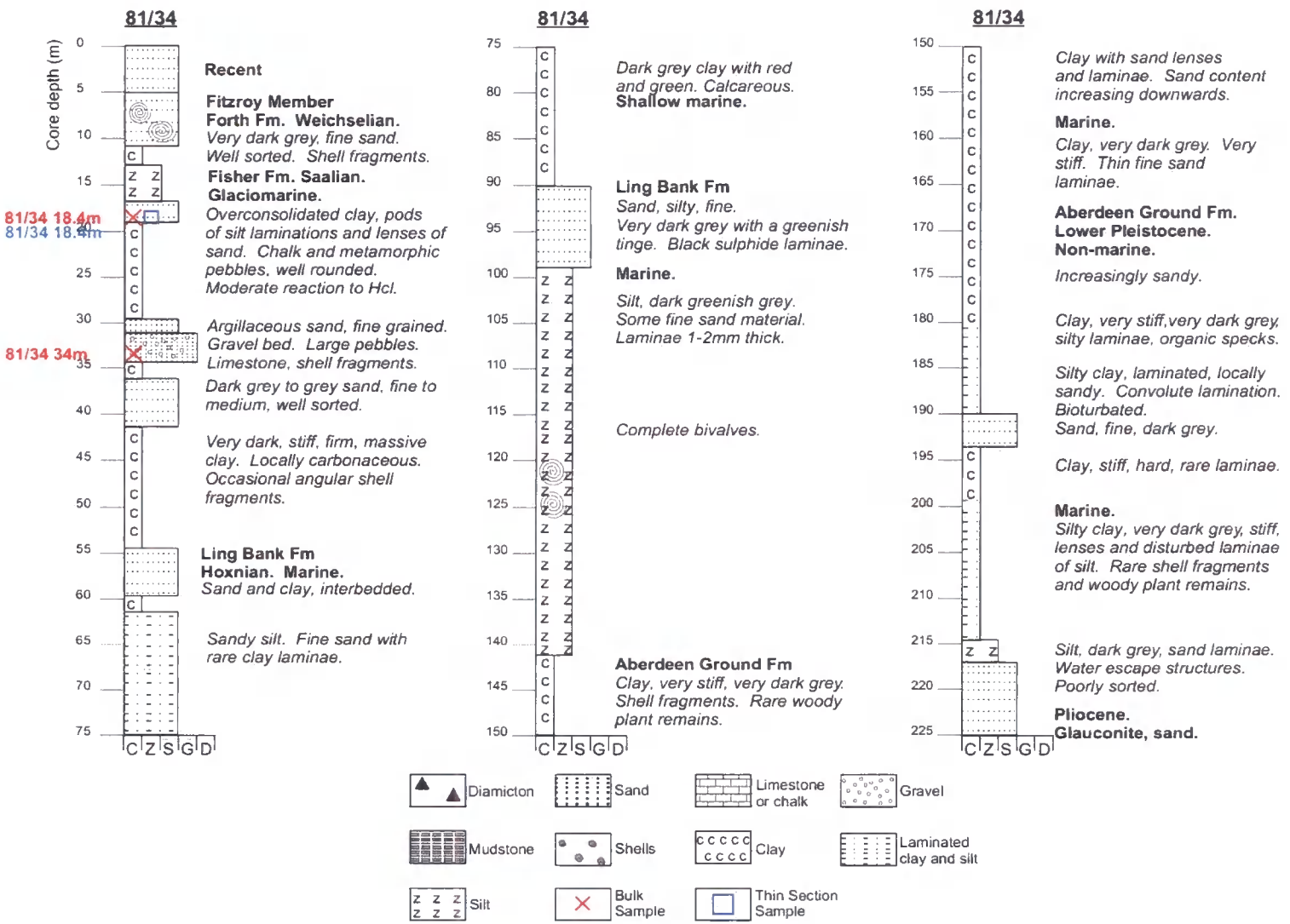

Figure 7.17: BH 81/34 from BGS core logs. Interpretations after Stoker et al. (1985) and Sejrup and Knudsen (1993).

Thin Section Analysis

The Fisher Fm was sampled from BH 81/34 at 18.4 m below seabed, and the results are summarised in Table 7.3 Macroscopically, it is a sand with strongly deformed laminations, showing extensive dewatering and fluidisation structures. There are both planar and vugh voids, induced during coring and packing, and due to poor resin impregnation in the laboratory. The slide has matrix-poor, clast-supported, well-sorted, graded sand (principally quartz) laminations. There are also some mineral and coal skeleton grains. Some laminations are composed of silty-clay laminations, and show up as a darker brown colour on Figure 7.18. These finer laminations have a horizontal microfabric and a bedding-parallel masepic plasmic fabric. Normal faults cut across the fluidised sand.

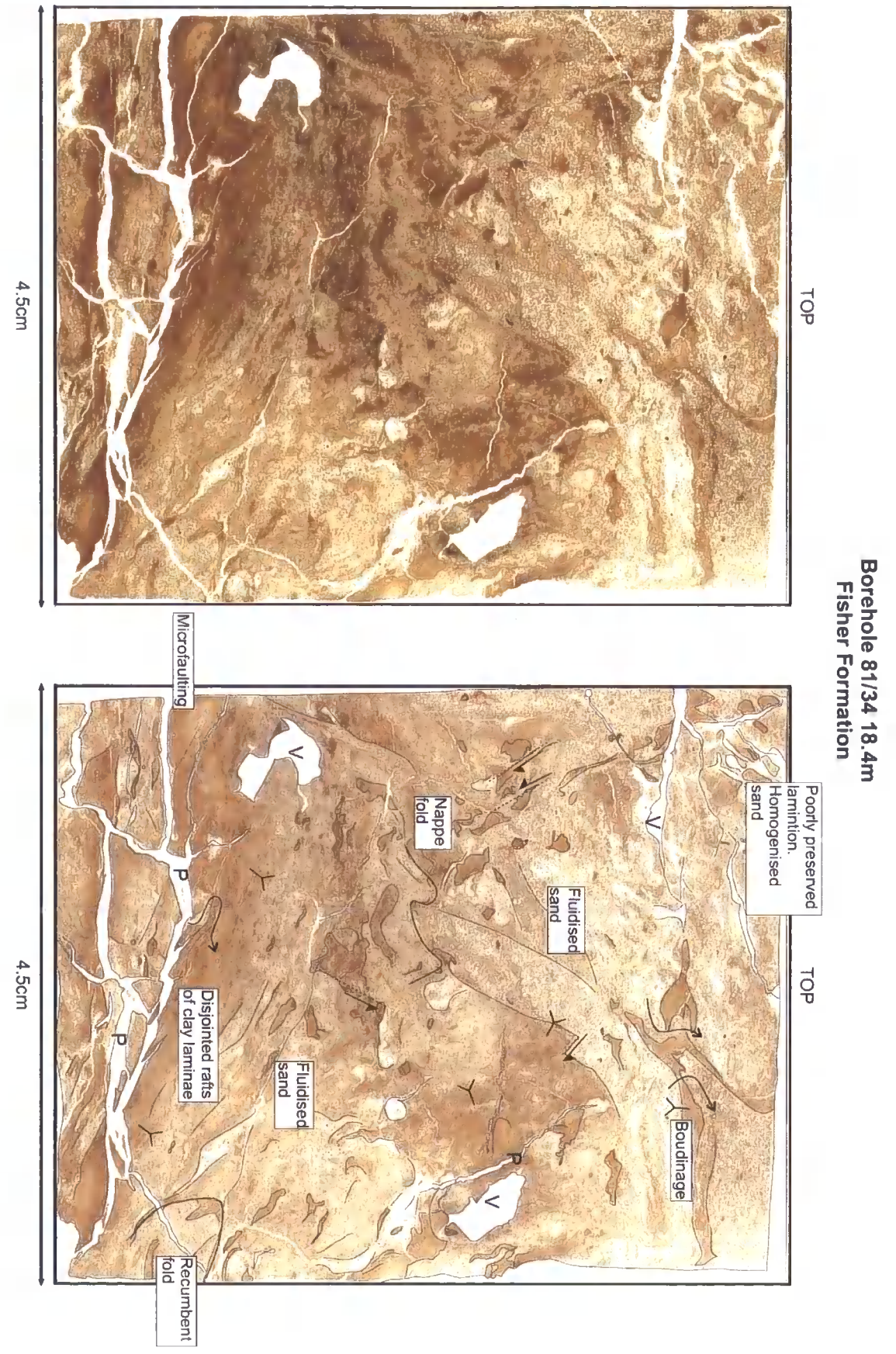

Figure 7.18: Thin Section of the Fisher Fm (BH 81/34 18.4m). Location of sub-resolution features is noted.

7.3.4 The Coal Pit Formation

Sedimentology and Borehole Logs

The Coal Pit Fm infills valleys and extends across them north of 56°N. It overlies the Fisher Fm, and is overlain by the Swatchway and Witch Ground formations (Figure 7.9). Three samples were taken from the Coal Pit Formation (Figure 7.19).

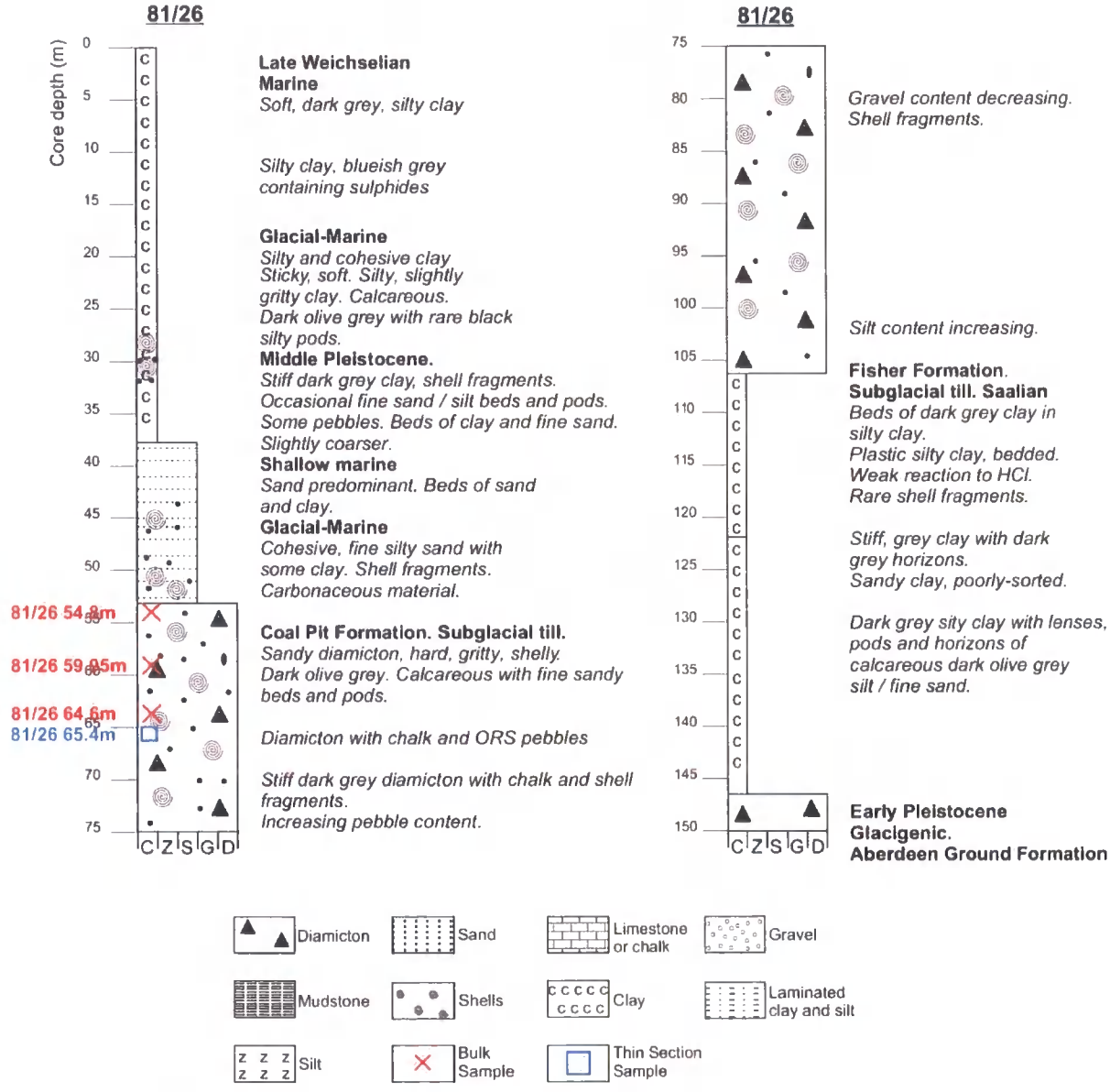

Figure 7.19: BH 81/26 from BGS core logs (interpretations after Sejrup et al., 1987; Sejrup & Knudsen, 1993; Graham et al., 2007).

Thin Section Analysis

Thin section samples were taken from the Coal Pit Fm at 65.4 m depth below seabed (Figure 7.20). The slide is a fine-grained dark-brown diamicton with numerous sand

grains, fine rounded gravel, and occasional intraclasts. It is mostly massive although the matrix is slightly variable. There are numerous shell and coal fragments. Other lithic fragments include sandstone, basalt and other igneous clasts.

There are many structures indicative of ductile deformation, including numerous turbate structures with and without core stones, with associated grain lineations, pressure shadows, necking structures, and 'tails'. The finer skeleton grains have a strong skelsepic plasmic fabric. There are abundant well-rounded silty Type III Pebbles. There are numerous grain stacks and edge-to-edge grain contacts (Table 7.3).

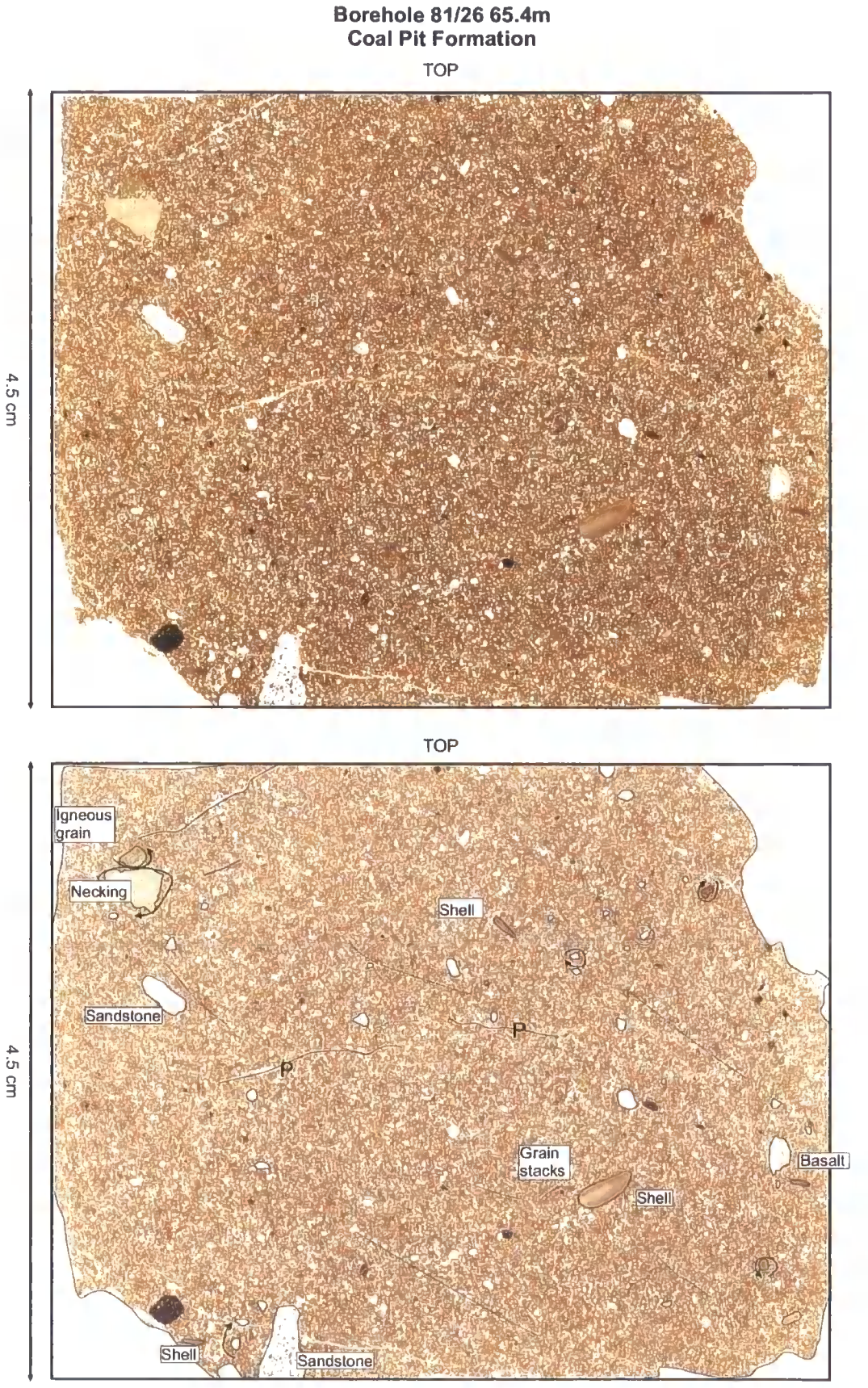

Figure 7.20: Thin Section slide BH 81/26 65.4 m. Location of sub-resolution features is highlighted.

7.3.5 The Bolders Bank Fm

Sedimentology and Borehole Logs

The Bolders Bank Fm is correlative with the Wee Bankie Fm in the NSB north of 55°N (Gatliffe *et al.*, 1994), and with the Skipsea Member of Yorkshire (Catt, 1991a; Cameron *et al.*, 1992). The stiff diamictons form the upper Pleistocene (Dimlington Stadial) sediments which widely blanket the NSB (Figure 7.3). It is overlain in the central NSB by the Dogger Bank Fm and by Holocene sediments in the northern NSB. The Bolders Bank Fm was sampled from BH 81/48, 81/43, and BH 82/19 (Figure 7.21). BH 82/18 is missing from the BGS core store.

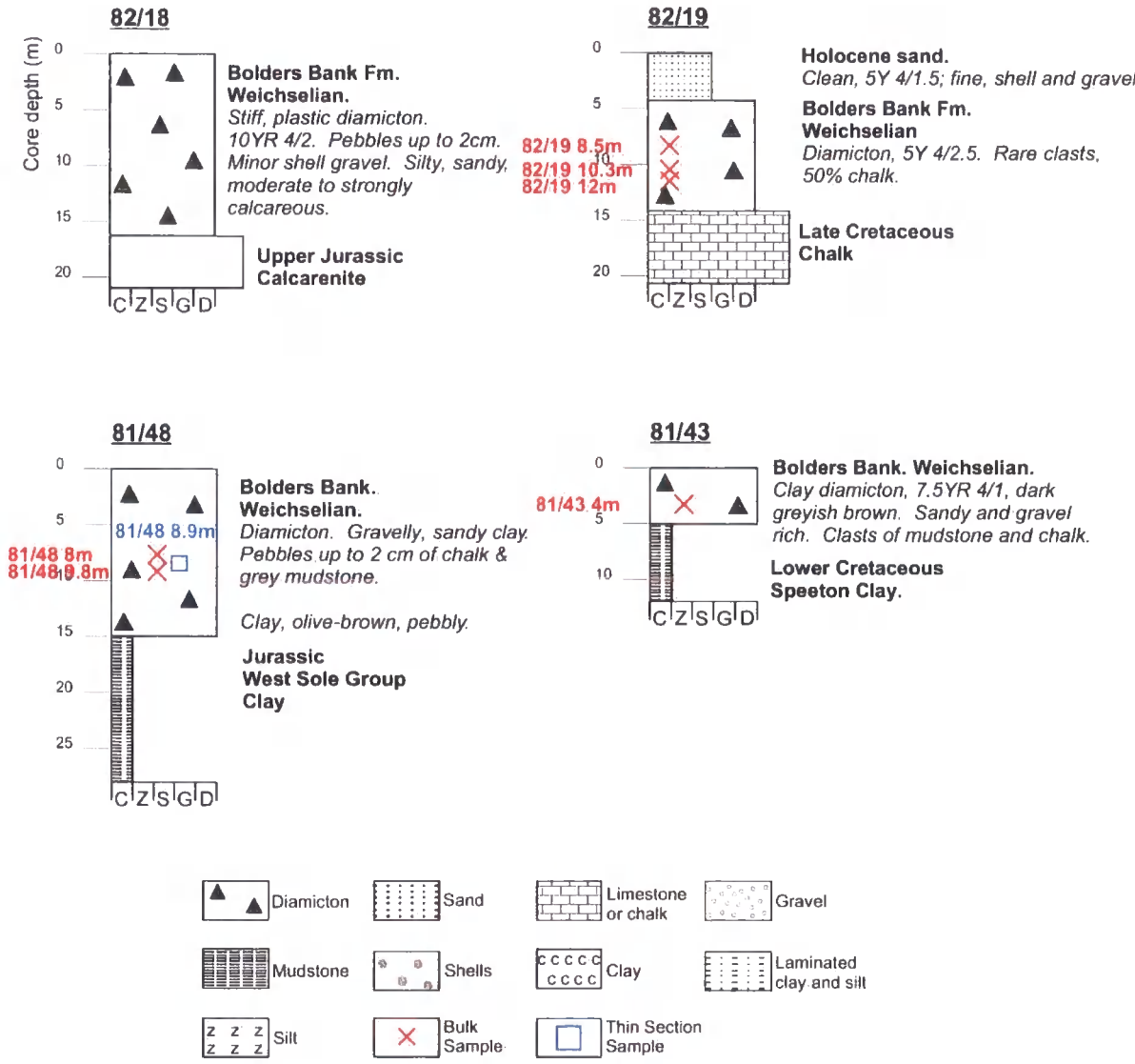

Figure 7.21: The Bolders Bank Fm. From BGS core logs, Cameron and Holmes (1999), Cameron et al. (1992), and Gatliffe et al. (1994).

Thin Section Analysis

The Bolders Bank Fm was sampled from BH 81/48 at 8.9 m below seabed (Figure 7.22). Macroscopically, the slide is a massive, reddish-brown diamicton with widely ranging grain sizes, with numerous rounded coarse sand and fine gravel grains (Figure 7.22). These range from shell fragments to lithic fragments of basalt, igneous and metamorphic rocks (Figure 7.23 A and B), limestone, sandstone, quartz, feldspar, greywacke, and numerous silty Type III rounded pebbles (Figure 7.23 F) with their own internal plasmic fabric. The smaller silt and fine sand grains are subangular. There are occasional marine microfossils (Table 7.3).

There are numerous deformation structures within the slide, including rotation structures with and without core stones (Figure 7.23). Some of these are associated with grain lineations (Figure 7.23 F), and frequently they display 'galaxy tails'. There is a loaded and broken soft-sediment intraclast. Grain stacks and edge-to-edge grain contacts are common (Figure 7.23 D & E), and there are rare fractured grains, indicative of brittle deformation. The finer skeleton grains are coated with a skelsepic plasmic fabric, and a masepic plasmic fabric is ubiquitous throughout the slide (Figure 7.23).

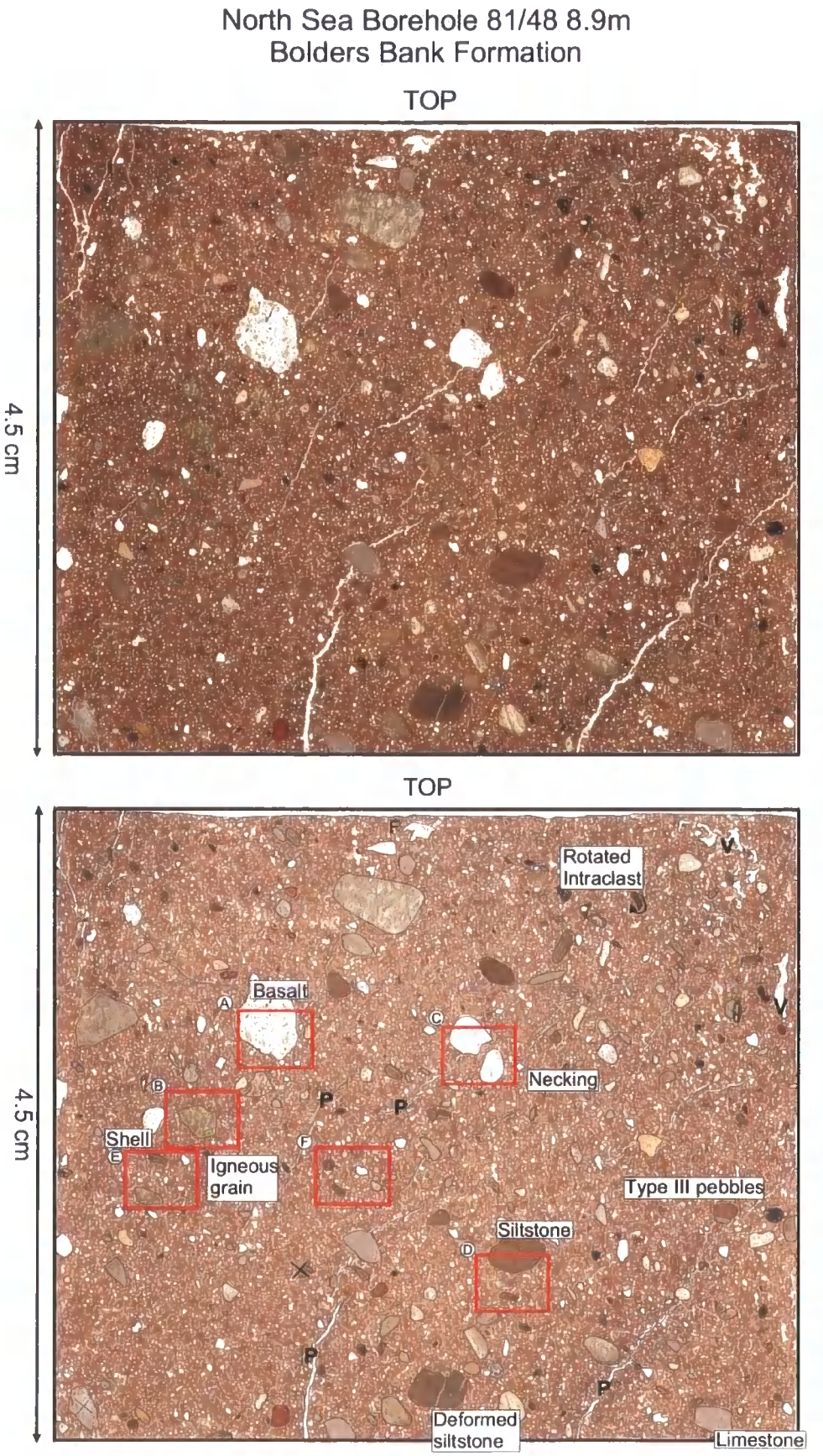

Figure 7.22: Thin Section of the Bolders Bank Fm (81/48 8.9 m). Locations of sub-resolution features are highlighted.

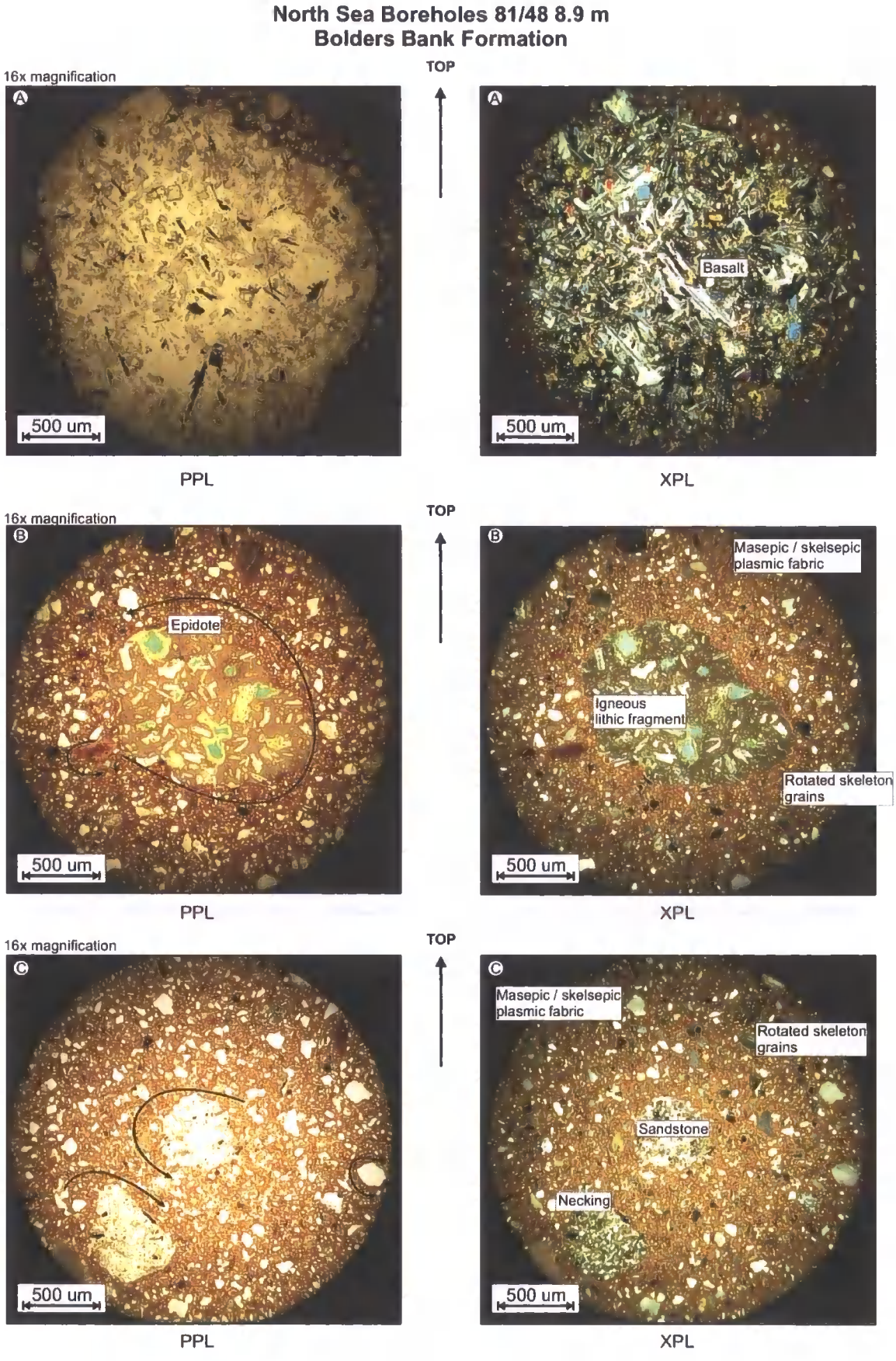
North Sea Boreholes 81/48 8.9 m
Bolders Bank Formation
16x magnification
TOP
A
500 um
Basalt
PPL
XPL
16x magnification
TOP
B
Epidote
Masepic / skelsepic plasmic fabric
Igneous lithic fragment
Rotated skeleton grains
500 um
PPL
XPL
16x magnification
TOP
C
Masepic / skelsepic plasmic fabric
Rotated skeleton grains
Sandstone
Necking
500 um
PPL
XPL

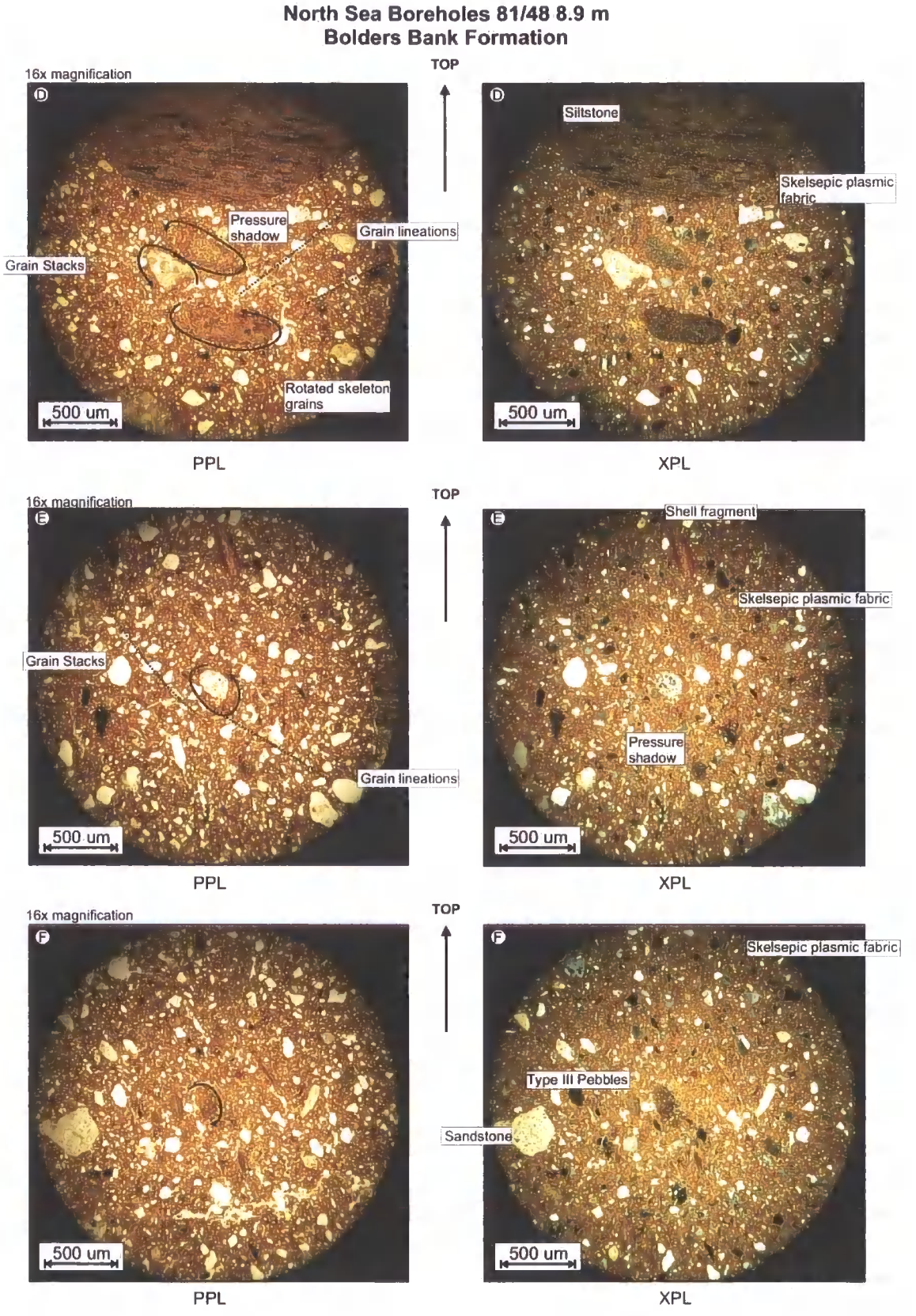

Figure 7.23: Photomicrographs of Thin Section BH 81/48 8.9 m

7.4 Lithological, Biological and Geochemical Analyses

7.4.1 Lithological Analyses

Sedimentary Description

The Swarte Bank Fm is a sandy to a silty diamicton, coloured grey in BH 81/52a (10YR 6/1), and a light brownish grey to a greyish brown in BH 81/46a (10YR 6/2 to 10YR 5/2). All samples reacted vigorously to HCl, and contained fine chalk and flint gravel. Sample 81/46a 18 m contained Magnesian Limestone and quartzite fine gravel. There were no shells found within the diamictons. The Sand Hole Fm is a light brownish-grey (10YR 6/3), with no gravel present. The Egmond Ground Fm is a poorly-sorted yellowish-brown (10YR 5/4) sand, with very little clay. It incorporates (unidentifiable) bivalve fragments, flint, quartz, quartzite, Magnesian Limestone, and dolerite gravel.

All three samples of the Fisher Fm are a grey silty clay (10YR 6/1) with a moderate reaction to HCl. They contain rare fine chalk gravel but no shell fragments. The samples of the Coal Pit Fm are fissile, sandy diamictons ranging in colour from dark grey (10YR 4/1) to greyish brown (10YR 5/2 to 4/2). The reaction to HCl is variable, from vigorous (59.95 m) to mild (64.6 m). All the samples contain rounded gravel, including Magnesian Limestone, dolerite, and quartz, a single specimen of a rounded rhomb porphyry, other porphyries, chalk, and shell fragments. The Bolders Bank Fm is highly locally variable. It is a brown silty diamicton with numerous clasts (Table 7.4). The presence of chalk in BH 82/19 is a significant difference between the three boreholes. The BH 82/19 diamicton is also lighter in colour and stiffer, with more clay present.

Table 7.4: Description of samples from Bolders Bank Formation

Sample	Texture	Colour	HCl reaction	Gravel	Shells
81/48 8 m	Silty diamicton	10YR 5/3 Brown	Moderate	Granite, Carboniferous Limestone, coal, Magnesian Limestone	
81/48 9.8 m	Silty diamicton	10YR 5/3 Brown	Moderate	Rounded gravel: Flint, chalk, dolerite, quartzite, Magnesian Limestone.	
81/43 4 m	Clay-rich diamicton	10YR 5/3 Brown	Vigorous	Magnesian Limestone, quartz, quartzite, flint, porphyry, greywacke, Old Red Sandstone, dolerite, Carboniferous Limestone, sandstone.	*Dentalium entalis; Montacuta ferruginosa; Chlamys* sp.; *Venus* sp.
82/19 8.5 m	Stiff, hard diamicton	7.5YR 6/3 Light brown	Vigorous	Chalk, quartz, flint, quartzite, dolerite, Magnesian Limestone, flint, greywacke, Carboniferous Limestone.	Bivalve fragments
82/19 10.3 m	Stiff, hard diamicton	7.5YR 6/3 Light brown	Vigorous	Chalk, flint, granite, quartz, dolerite, Magnesian Limestone, porphyry, Carboniferous Limestone, sandstone, quartzite.	
82/19 12 m	Stiff, hard diamicton; near contact with bedrock	10YR 6/3 Light brown	Vigorous	Clast poor, fine gravel. Chalk, quartz, dolerite, Magnesian Limestone, quartzite, New Red Sandstone, Carboniferous Limestone.	

Particle Size Analysis

Due to the small sample sizes in the boreholes, it was only possible to conduct particle-size analysis on the sub-2 mm fraction. Gravel analysis is descriptive only and bulk lithological analysis was not possible. The Swarte Bank Fm has a diamict matrix (Table 7.5) and the particle-size distribution plots closely to the other diamictons in the study (Figure 7.24). The Fisher Fm is dominated by large percentages of silt. The sample taken from BH 81/29 is better sorted with no sand, whilst the samples from BH 81/34 are poorly-sorted sandy-silts. The percentage of coarse sand is low in all the samples. The Sand Hole Fm, sampled from BH 81/52a at 37.13 m and at 40.50 m, is composed of around 20 % clay, 64-72 % silt, and 9-16 % sand (Table 7.5). The particle-size distribution shows that there is very little coarse material, and that high percentages of silt dominate the Sand Hole Fm.

The particle-size distribution of the Coal Pit Fm forms a tight cluster on the ternary diagram (Figure 7.24). The diamicton has high proportions of silt and sand, but only a very small percentage of coarse sand (Table 7.5). The particle-size distribution between samples

is similar, with BH 82/19 showing more variation than the other boreholes. It is also coarser-grained, with a higher percentage of coarse sand.

Table 7.5: Sub-2 mm particle-size analysis of North Sea Boreholes

	Sample	% Clay	% Silt	% Fine sand	% Coarse sand
Bolders Bank Fm	*82.19 10.3 m*	30.66	39.52	19.47	10.36
	82.19 12 m	26.37	43.47	18.61	11.55
	82.19 8.5 m	32.55	46.10	17.23	4.12
	81.48 9.8 m	25.88	48.93	19.23	5.95
	81.48 8 m	25.46	51.07	16.83	6.64
	81.43 4 m	28.95	47.56	17.37	6.12
Coal Pit Fm	*81.26 64.6 m*	24.56	39.91	24.70	10.83
	81.26 59.95 m	25.21	44.59	26.38	3.82
	81.26 54.8 m	27.99	42.35	24.47	5.19
Fisher Fm	*81.29 12 m*	56.68	43.32	0.00	0.00
	81.34 18.4 m	22.58	41.90	34.24	1.29
	81.34 34 m	37.94	45.13	15.40	1.53
Egmond Ground Fm	*81/52a 16.2 m*	5.55	10.48	45.23	38.75
Sand Hole Fm	*81.52a 37.13 m*	31.63	59.20	8.96	0.21
	81.52a 40.5 m	31.58	52.14	14.68	1.60
Swarte Bank Fm	*81.52a 43.07 m*	35.22	46.83	13.86	4.08
	81.46a 17 m	25.74	41.50	27.80	4.96
	81.46a 18 m	28.23	42.54	25.36	3.87

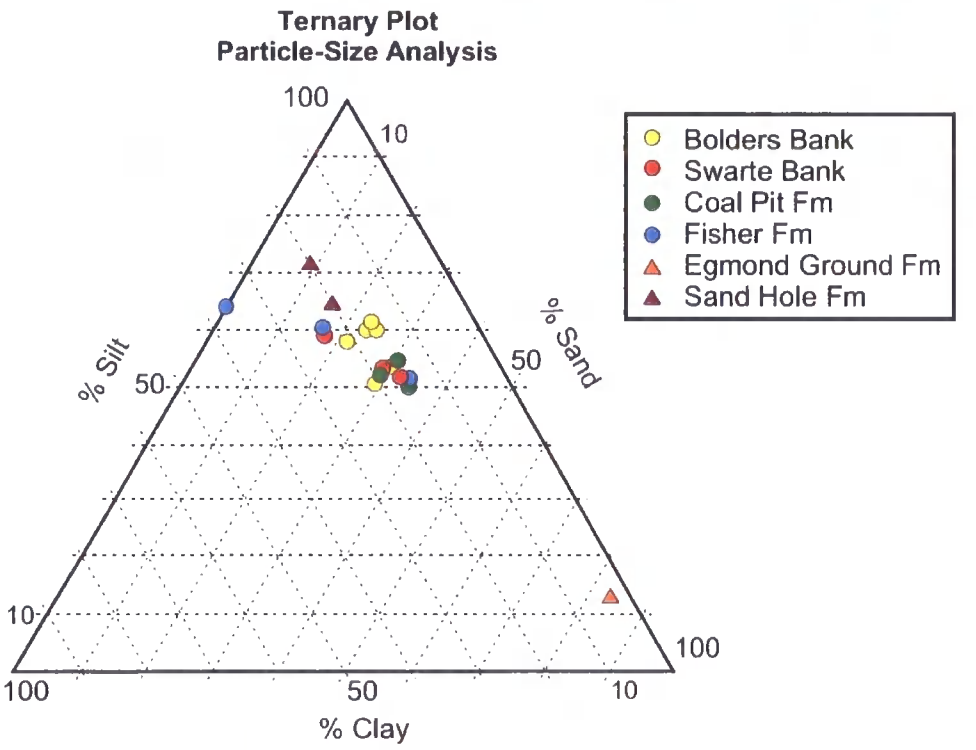

Figure 7.24: Particle-size distribution of North Sea Boreholes.

Heavy Mineral Analysis

Heavy-mineral analysis was conducted on the 63-125 μm and 125-250 μm fractions (Table 7.6). The mineralogy of the Swarte Bank Fm includes a broad suite of minerals, which vary substantially in some cases between the sediments of BH 81/52a and BH 81/46a. For example, the standard deviation of garnet is 9.2, and biotite is 8.3. The majority of the other minerals have lower standard deviations between 0 and 4. The Swarte Bank Fm is characterised by high percentages of garnet (average 17.7 %), biotite (average 10.2 %), muscovite (8.7 %), epidote (9.3 %), and carbonates (6.1 %). Minerals of secondary abundance include brookite (6 %), hornblende (5.6 %), zoisite (5.9 %), chlorite (5.2 %), andalusite (5.4 %), and kyanite (3 %).

The heavy-mineral assemblage of the Sand Hole and Egmond Ground formations reflects that of the underlying Swarte Bank Fm, with 12.8 % garnet, high percentages of micas (14.7 % muscovite, 15.7 % biotite, and 7.7 % chlorite), 5.6 % epidote, and 8 % zoisite. There are small percentages of zircon, andalusite, kyanite, phosphates, and pyroxenes. The heavy-mineral suite of the Egmond Ground Fm is richer in hornblende (8.3 %), andalusite (12.1 %) and kyanite (6.4 %) than the Swarte Bank and Sand Hole formations, though it has similar percentages of garnet (18 %), epidote (9.5 %) and zoisite (6.2 %). The formation is impoverished in micas (Table 7.6).

Heavy-mineral analysis of the Fisher Fm reveals an assemblage with an average 17 % garnet, high percentages of andalusite (8.8 %), kyanite (9 %), epidote (9.7 %), biotite (9.6 %), muscovite (7.8 %), and glaucophane (5.4 %). Closer examination shows that the heavy minerals of the Fisher Fm are widely spread, with a standard deviation of up to 9.4 in the case of glaucophane, 10 for epidote, and 11.1 for garnet (see Appendix II). The Coal Pit Fm is particularly high in garnet (26.4 %), epidote (11.4 %), and hornblende (8.5 %). Micas are abundant, followed by carbonates (5.1 %). Zoisite (5.6 %) is also common. Andalusite and kyanite are less abundant than in the other samples. The Coal Pit Fm is richer in pyroxenes than the Swarte Bank Fm, and shows similarities to the Wee Bankie Fm (Figure 7.25).

The heavy-mineral suite of the Bolders Bank Fm is widely spread, and shows little inter-formational consistency (Figure 7.25). BH 82/19 is higher in garnet, but only BH 81/48 8 m contains glaucophane. Hornblende is present in comparatively higher amounts in BH 82/19 (6.9 % cf. 2.9 %). The more southerly samples are more enriched in

carbonates, as would be expected due to the changing bedrock lithologies, and are significantly richer in detrital micas.

Table 7.6: Average Percentage Non-Opaque Heavy minerals for formations of the North Sea Basin

		Swarte Bank	Sand Hole	Egmond Ground	Fisher	Coal Pit	Bolders Bank	Bolders Bank
		81/52A and 81/46A	81/52 A	81/52A	81/29 and 81/34	81/26	81/48 and 81/43	82/19
	n	***2111***	***2208***	***878***	***1881***	***2178***	***4087***	***2766***
	% Opaques	46.01	73.27	39.75	30.02	32.09	65.62	50.68
	% Non Opaques	53.99	26.73	60.25	69.98	67.91	34.38	49.32
	% Heavy minerals	2.41	0.97	4.28	1.39	2.15	5.18	4.24
SILICATE GROUP	*Olivine GP*	2.33	0.27	1.89	1.46	2.23	1.89	1.19
	Zircon	1.63	3.76	3.02	0.70	1.34	1.05	0.99
	Sphene	1.38	1.21	1.89	2.29	2.86	2.06	2.53
	Garnet GP	17.71	12.78	17.96	17.40	26.37	15.52	34.07
	Sillimanite	0.81	0.27	1.51	0.77	1.27	0.67	0.52
	Andalusite	5.42	3.11	12.10	8.78	2.45	3.38	1.71
	Kyanite	3.04	3.78	6.43	9.01	2.41	2.99	2.58
	Staurolite	0.14	0.00	0.00	0.16	0.63	0.61	0.22
	Dumortierite	0.15	0.00	0.19	0.07	0.00	0.15	0.00
	Chloritoid	0.58	0.41	0.76	1.98	0.22	1.82	0.22
EPIDOTE GROUP	*Zoisite / Clinozoisite*	5.88	8.03	6.24	2.88	5.35	6.61	5.97
	Lawsonite	0.07	0.00	0.00	0.00	0.07	0.00	0.00
	Axinite	0.57	0.00	0.00	1.62	0.69	0.30	0.00
	Epidote	9.31	5.59	9.45	9.72	11.24	2.87	8.38
	Piemontite	0.00	0.00	0.00	0.00	0.14	0.00	0.00
	Tourmaline GP	1.67	1.72	1.13	1.22	2.31	1.42	0.78
PYROXENE GROUP	*Enstatite*	0.66	2.28	0.57	1.31	1.27	1.08	1.03
	Hypersthene	0.14	0.36	0.95	0.31	1.46	0.90	1.02
	Diopsidic Clinopyroxene	0.00	0.14	0.95	0.55	1.13	0.80	0.00
	Augitic Clinopyroxene	0.64	1.49	0.57	0.52	0.98	1.10	1.85
AMPHIBOLE GROUP	*Tremolite*	0.00	0.00	0.00	0.00	0.00	0.00	0.00
	Ferriactinolite	0.07	0.63	1.70	1.58	0.14	1.22	0.29
	Hornblende	5.56	3.98	8.32	3.73	8.50	2.85	6.94
	Diallage	0.07	0.22	0.00	0.00	0.07	0.00	0.00
	Glaucophane	0.00	0.00	0.00	5.42	0.00	3.96	0.00
MICA GROUP	*Muscovite*	8.68	14.67	8.13	7.78	5.81	5.18	4.10
	Glauconite	0.29	0.14	1.13	0.86	0.55	2.81	2.79
	Biotite	10.24	15.71	2.27	9.60	3.80	12.92	4.21
	Chlorite GP	5.17	7.69	1.70	3.36	3.14	3.81	2.56
OXIDES	*Rutile*	0.29	1.21	1.32	0.68	0.28	3.47	0.30
	Brookite	5.96	1.67	1.32	1.06	1.96	1.73	3.28
	Spinel GP	0.28	0.00	0.19	0.24	0.00	0.22	0.08
	Anatase	0.38	0.41	0.57	0.15	0.36	1.16	0.82
CARBONATES	*Calcite / Dolomite*	6.07	3.11	1.13	1.61	5.07	13.34	6.47
SULPHIDES	*Baryte*	0.00	0.00	0.00	0.00	0.00	0.00	0.00
SULPHATES	*Sphalerite*	0.07	0.00	0.00	0.40	0.07	0.38	0.00
PHOSPHATES	*Apatite*	2.98	3.86	2.65	1.80	3.64	0.55	2.02
	Monazite	1.75	1.53	3.97	0.98	2.22	1.18	3.09

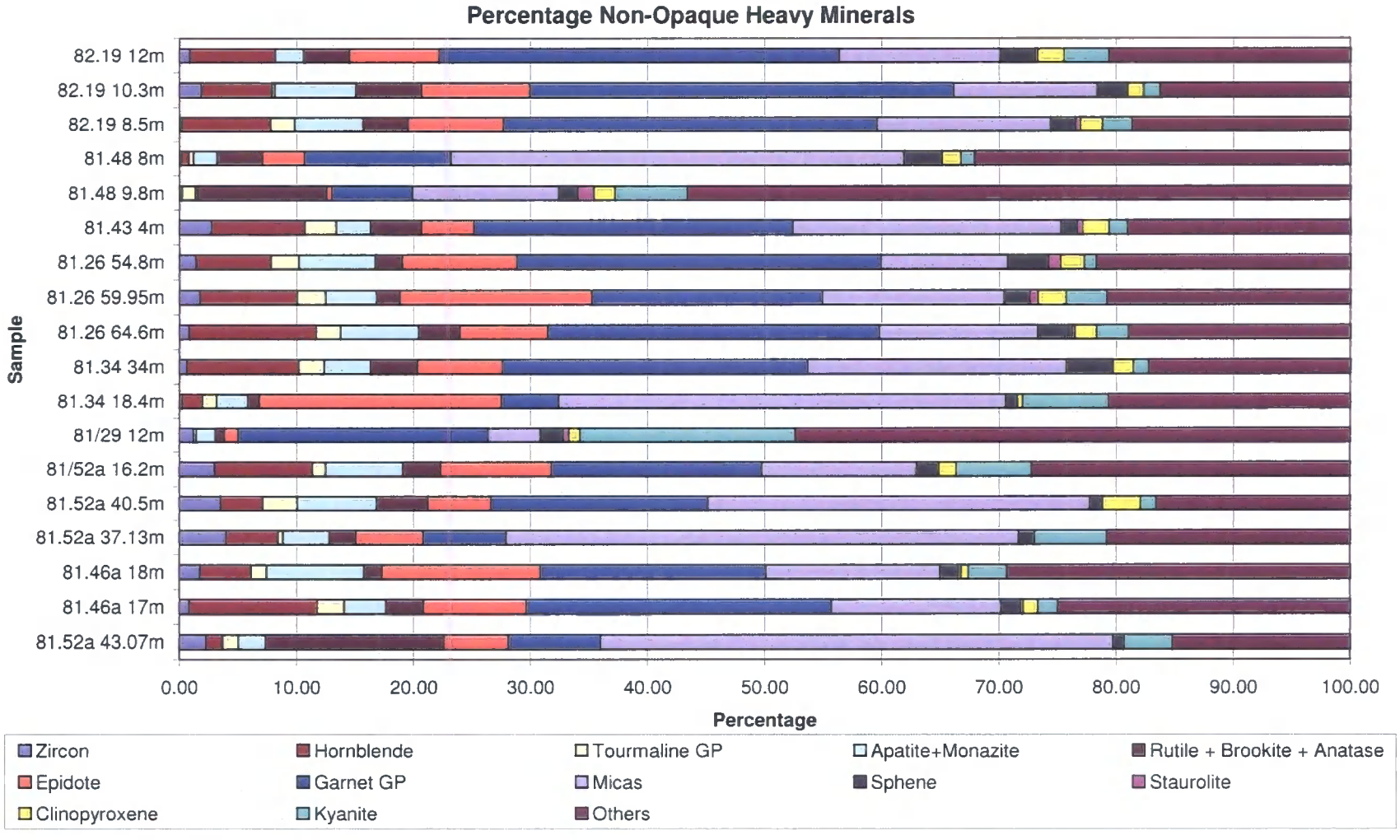

Figure 7.25: Results of heavy-mineral analysis for various North Sea Boreholes

The wide scatter of the samples is illustrated by both the ternary diagram of percentages of phosphates, pyroxenes and amphiboles (Figure 7.26), and by the heavy-mineral indices of ultra-stable heavy minerals (Figure 7.27). In some respects, all the samples are similar, as illustrated by the ternary diagram of percentages of the epidote group, amphiboles and silicates (Figure 7.26). However, the ternary diagram of pyroxene, phosphates and amphiboles does show the Swarte Bank Fm plotting towards the base of the triangle due to its low proportion of pyroxene. It is clearly distinguished from the Coal Pit, Bolders Bank and Wee Bankie formations (Figure 7.26). The Sand Hole Fm is comparatively enriched in pyroxenes compared to the Swarte Bank Fm, and it shows similarities to the Coal Pit and Fisher formations. The second ternary diagram (Figure 7.26) does little to distinguish the formations of the North Sea.

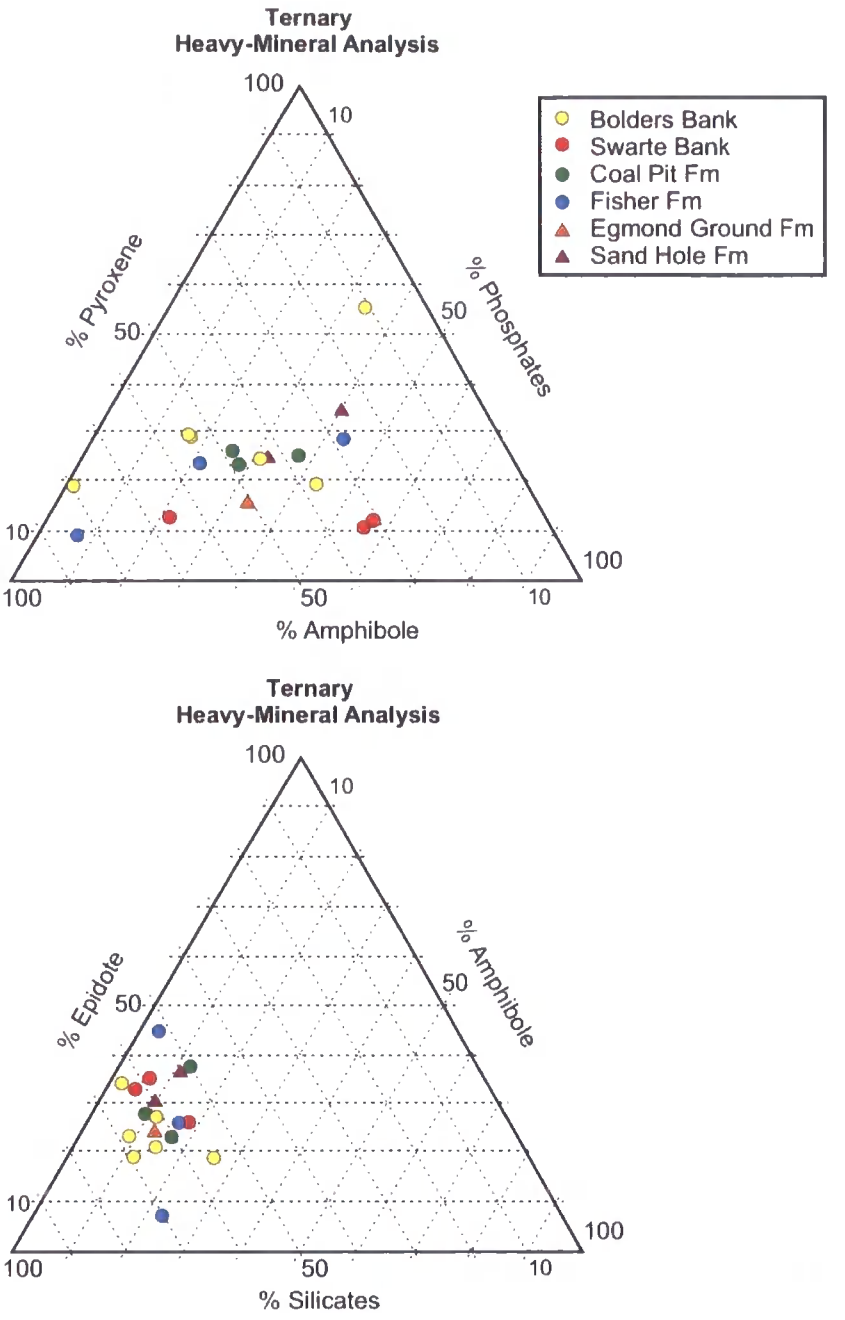

Figure 7.26: Ternary plots of percentages of pyroxenes, phosphates and amphiboles, and for epidote group, amphiboles and pyroxenes, illustrating the tight clustering of the samples.

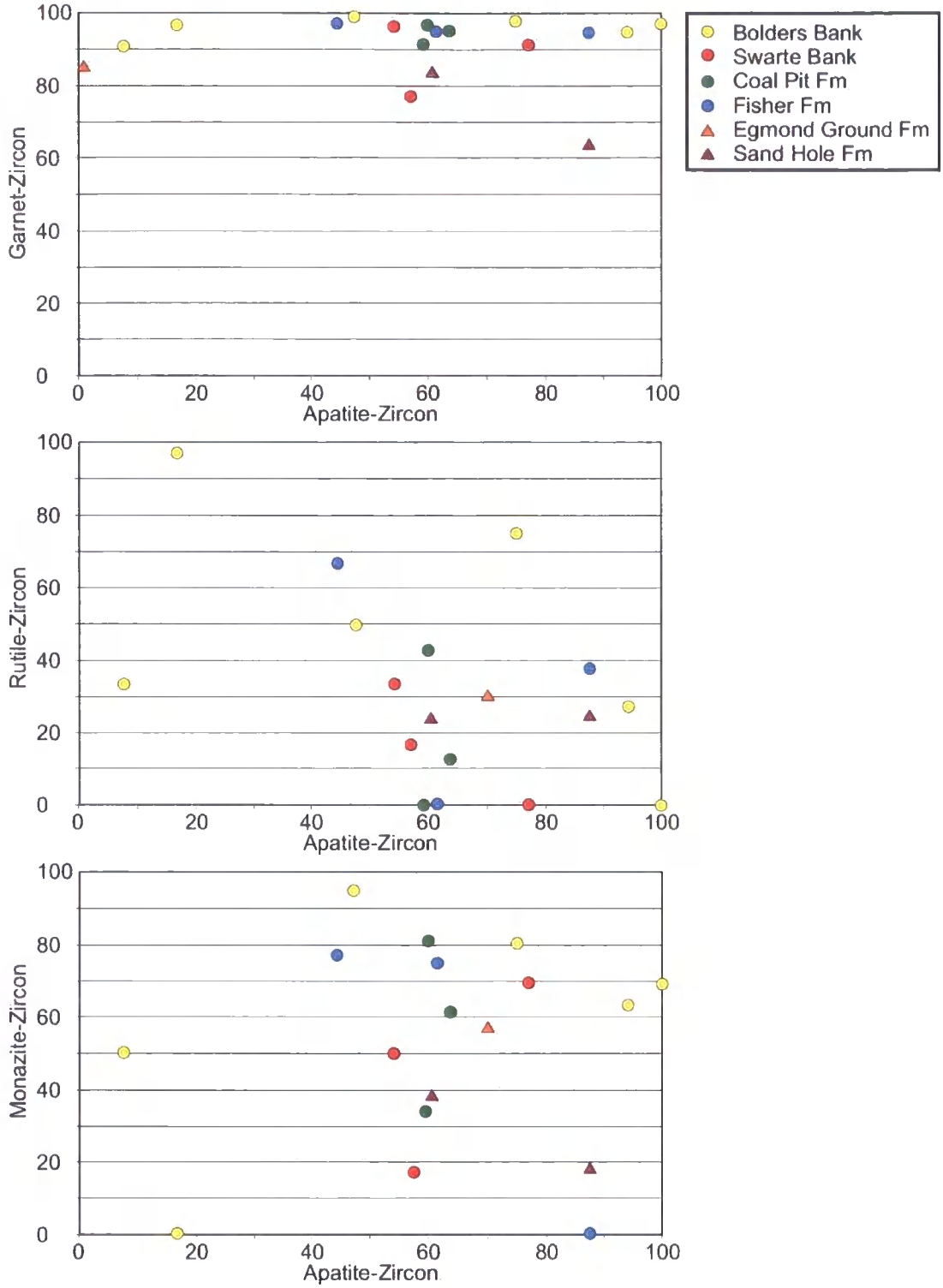

Figure 7.27: Indices of ultra-stable heavy minerals

A PCA performed on the correlation matrix is dominated by the first three components. Components 1 and 2 together explain 67 % of the variance, and the first three explain 81 %. Component 1 is composed of a number of variables, with silicates, amphiboles and micas controlling this axis most strongly. Component 2 is mostly

controlled by epidote, and secondarily by amphiboles, oxides and phosphates. This distribution is clearly illustrated by the component loadings scatter plot below (Figure 7.28). However, the scoreplot shows that the matrix mineralogy is very varied, with little inter-formational consistency. There are similarities however between the Swarte Bank, Coal Pit and Fisher formations, which tend to plot distinctly from the Bolders Bank and Wee Bankie formations. This is echoed by the scoreplot for the PCA Covariance. Samples from the same borehole tend to plot most closely together, illustrating the wide regional variations between lithofacies. This is probably related to changing bedrock lithology. Cluster analysis of the heavy-mineral suite supports this varied matrix mineralogy (Figure 7.28). In general, it is difficult to distinguish the heavy-mineral suite of the Swarte Bank Fm from those of other formations in the NSB. The cluster analysis identifies similarities between the Coal Pit Fm, the Swarte Bank Fm and the Fisher Fm. The Sand hole Fm shows little statistical similarity to either the underlying Swarte Bank Fm or the overlying Egmond Ground Fm. The mineralogy therefore varies between samples more than within formations.

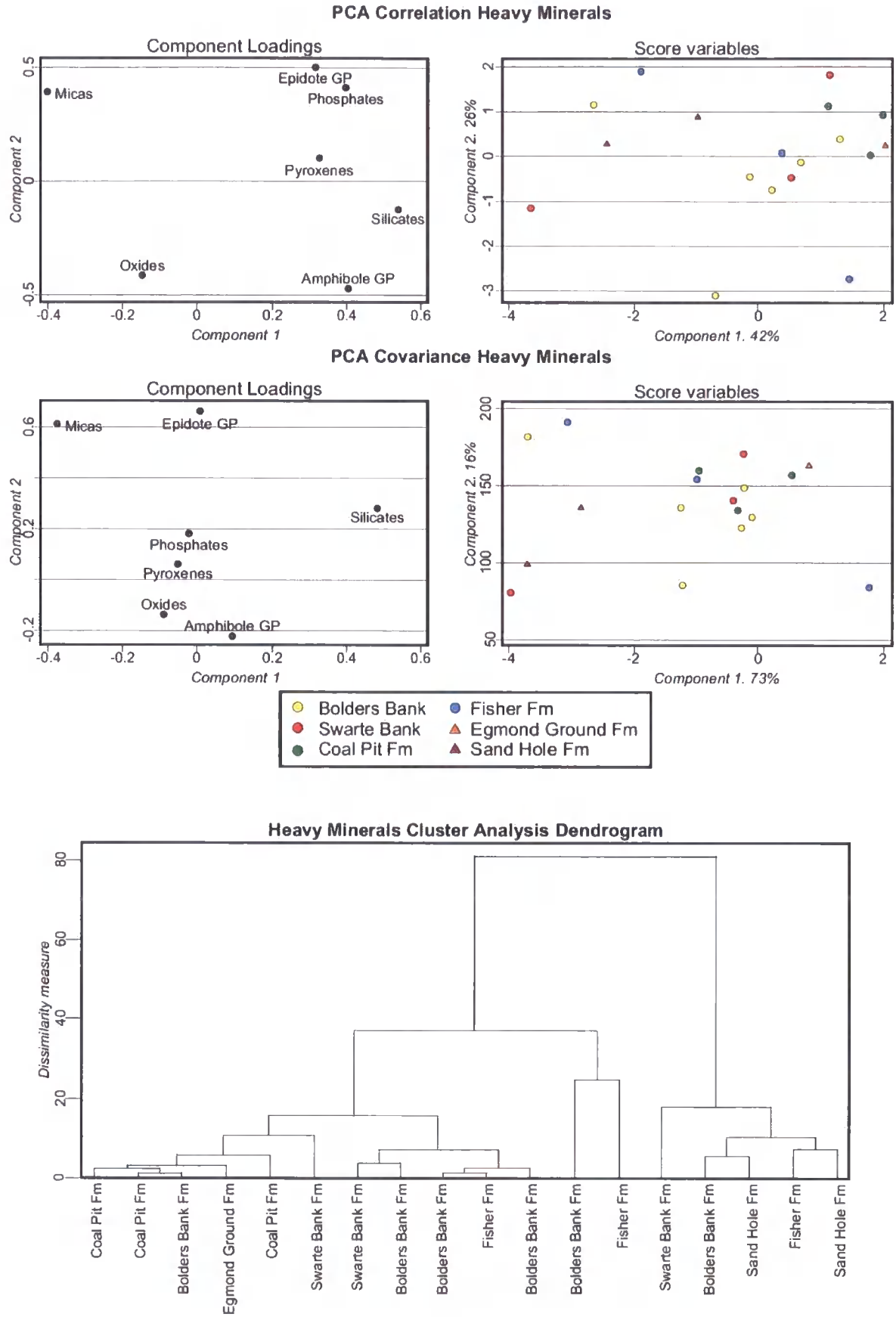

Figure 7.28: Heavy-Mineral Principle Components Analysis and Cluster Analysis

Geochemical Analysis

ICP-MS (Total Metals Extraction) was carried out on all NSB samples (Table 6.8). The matrix geochemistry is very variable between and within lithofacies associations. Analysis of the matrix geochemistry shows variations between lithofacies. A correlation matrix of the variables shows that some metals are well-correlated. A simple ternary plot of three strongly-correlated common metals (potassium, magnesium and aluminium) discriminates efficiently between the different lithofacies, although the samples cluster within boreholes. Samples, such as the Wee Bankie and Coal Pit formations, that were taken from the same borehole naturally form tight clusters, while the Swarte Bank Fm is taken from two separate boreholes (Figure 7.29).

This pattern is continued with both the correlation and covariance principle components analysis, with the same samples clustering together. The PCA (correlation) is adequately explained by the first two components (a combined 94 % of the variance), with Component 1 explaining the majority of the data. Component 1 is formed from several variables, namely potassium, magnesium, aluminium, and titanium. Component 2 is formed from silicon, potassium and iron (Figure 7.30). The matrix geochemistry of the Egmond Ground Fm also suggests a variable matrix with little clear clustering to any particular formation. Geochemically, the Fisher Fm overlaps with several of the other formations of the NSB, such as the Coal Pit Fm and the Swarte Bank Fm (Figure 7.30). In general however, the geochemical and heavy-mineral data are widely scattered, reflecting the differing locations of the samples.

Table 7.7: North Sea Boreholes matrix Geochemistry. High Abundance metals.

		High Abundance metals (mg/kg)							
	Sample ID	**Si_{14}**	**Na_{23}**	**Mg_{24}**	**Al_{27}**	**K_{39}**	**Ca_{44}**	**Ti_{48}**	**Fe_{57}**
Bolders Bank Fm	*81-43 4 m*	1025	5196	17583	38941	10601	32213	771	30252
	81-48 8 m	221152	8513	1518	14531	13762	20137	4378	37548
	81-48 9.8 m	1099	3213	11711	43349	10604	26615	673	31200
	82-19 8.5 m	800	5559	18751	34655	10067	42744	847	28189
	82-19 10.3 m	1044	4047	17141	27400	7329	71257	726	23039
	82-19 12 m	866	4000	16116	27664	8120	41762	822	24447
Coal Pit Fm	*81-26 58.8 m*	231145	8458	1590	13140	12894	21035	2792	21923
	81-26 59.95 m	217446	8570	1720	12507	14399	21560	2752	21958
	81-26 64.6 m	219137	7952	1579	13961	11834	20435	2833	22381
Fisher Fm	*81-29 12 m*	141957	10293	2268	11761	20541	22395	4112	42401
	*81-34 18.4 m **	*231517*	*8633*	*1338*	*14516*	*14955*	*19442*	*2818*	*21465*
	81-34 34 m	193918	8188	1539	15395	16341	19400	3836	35974
Egmond Ground Fm	*81-52A 16.2 m*	288514	5734	2227	17732	8308	14290	906	8353
Sand Hole Fm	*81-52A 37.13 m*	169255	10062	3017	7873	16378	32205	3760	30334
	81-52A 40.5 m	1301	4047	13147	38002	10344	49268	735	26254
Swarte Bank Fm	*81-52A 43.07 m*	1059	3585	9324	36782	8829	101228	533	28110
	81-46A 17 m	212686	7927	1761	12670	13516	21575	2776	22845
	81-46A 18 m	196184	8216	1789	12310	13375	22051	2743	23633

** Average of two runs*

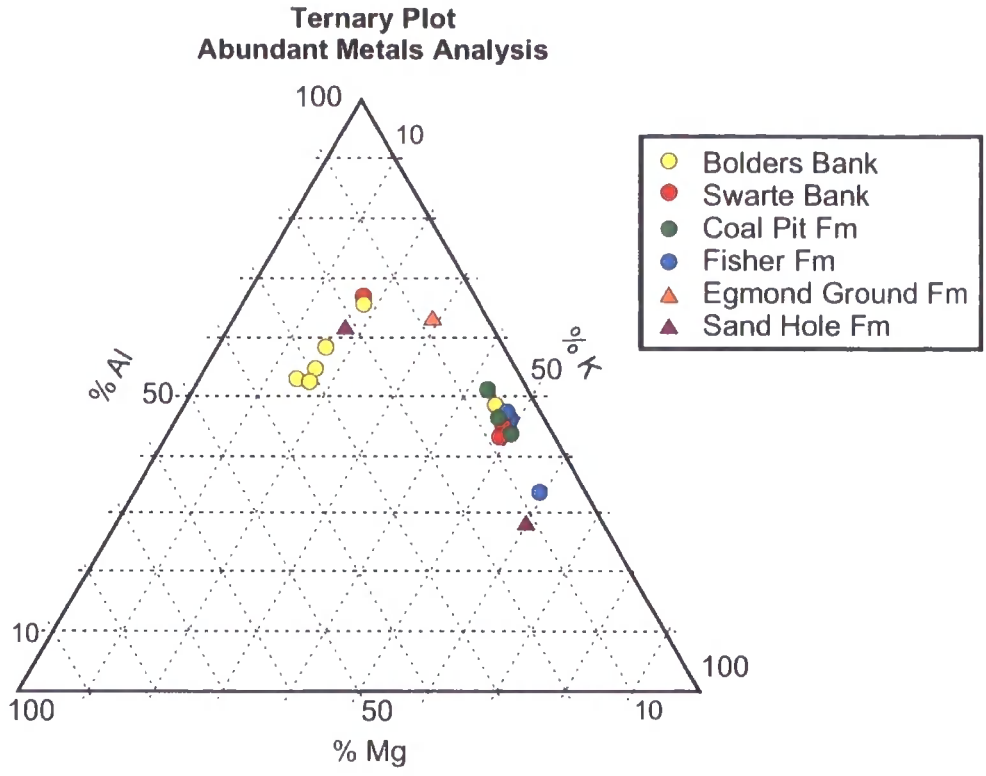

Figure 7.29: Ternary plot of three abundant metals (potassium, aluminium and magnesium) in the North Sea samples.

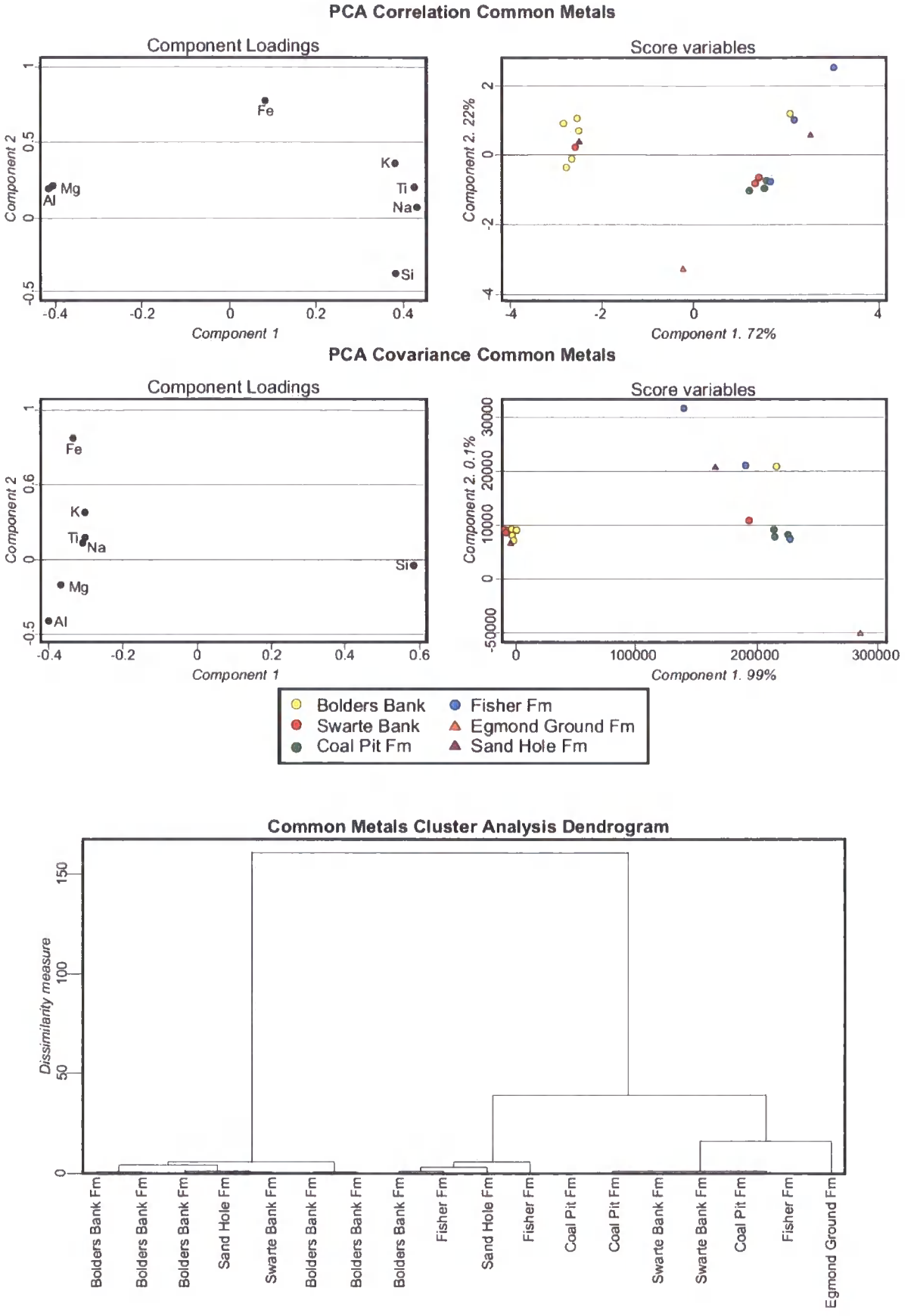

Figure 7.30: Common metals Principle Components Analysis and Cluster Analysis

Statistical analysis of the matrix geochemistry therefore reveals that although there is considerable lateral variability, the diamictons are very similar within individual boreholes. Samples from BH 82/19 consistently cluster together (Figure 7.29). The Bolders Bank Fm is clearly differentiated from the other samples, and this pattern is repeated in the PCA correlation and covariance on the abundant metals. The cluster analysis demonstrates a dichotomy between the Bolders Bank Fm and the other, mostly more northerly formations of the NSB.

7.4.2 Biological Analyses

Foraminifera

The boreholes were all examined for foraminifera. Although most contained very few, three boreholes yielded sufficient foraminifera species to make faunal counts. The Swarte Bank Fm (BH 81/52a 43.07 m) yielded rare, poorly preserved, reworked foraminifera. They are mostly benthic, calcareous species, and form a ubiquitous, mixed assemblage (Table 7.8). The Sand Hole Fm incorporates abundant, well-preserved, benthic, calcareous foraminifera (Figure 7.31). The cold-water species *Elphidium excavatum* f. *clavata* (68.8 %), with secondary percentages of *Bulimina marginata* (12.4 %) and *Cassidulina teretis* (15.5 %) dominate the faunal assemblage. Other species present in very low numbers include *Brizalina variabilis*, *Cassidulina reniforme*, and *Melonis* sp. There are two unidentified ostracods. No broken or agglutinated foraminifera were observed. Planktonic foraminifera are present in very low abundances (0.4 %). The foraminifera assemblage of the Fisher Fm entails rare, broken, calcareous benthic tests, consisting of reworked planktonics, *Elphidium* sp., and *Cassidulina reniforme* (Figure 7.31).

The Coal Pit Fm contains rare, broken, poorly preserved foraminifera, mostly *Elphidium excavatum* f. *clavata*. Although the Bolders Bank Fm (BH 81/48 9.8 m) has no shell fauna, it does contain small, battered benthic calcareous foraminifera. These are fragmented and poorly preserved. The fauna include reworked planktonics, *Brizalina variabilis*, *Cibicides lobatulus*, *Elphidium* sp., *Haynesina germanica*, and *Rosalina* sp.

Table 7.8: Foraminifera of the North Sea Boreholes

Species	Swarte Bank Fm		Sand Hole Fm		Bolders Bank	
	81/52a 43.07 m		81/52a 37.13 m		81/48 9.8 m	
	Raw	%	Raw	%	Raw	%
Planktonic	*20*	35.09	*1*	0.39	*9*	19.57
Brizalina variabilis		0.00	*2*	0.78	*6*	13.04
Bulimina marginata		0.00	*32*	12.50		0.00
Cassidulina reniforme		0.00	*3*	1.17		0.00
Cassidulina teretis		0.00	*40*	15.63		0.00
Cassidulina sp.	*9*	15.79		0.00		0.00
Cibicides lobatulus		0.00		0.00	*7*	15.22
Cibicides sp.	*17*	29.82		0.00		0.00
Elphidium excavatum f. *clavata*		0.00	*177*	69.14		0.00
Elphidium sp.		0.00		0.00	*3*	6.52
Haynesina germanica		0.00		0.00	*3*	6.52
Haynesina sp.		0.00		0.00	*1*	2.17
Melonis sp.		0.00	*1*	0.39		0.00
Rosalina sp.		0.00		0.00	*1*	2.17
Uvigerina sp.	*1*	1.75		0.00		0.00
Agglutinated		0.00		0.00	*1*	2.17
Broken	*10*	17.54		0.00	*15*	32.61
Ostracoda			*2*			
Total (n)	***57***		***256***		***46***	

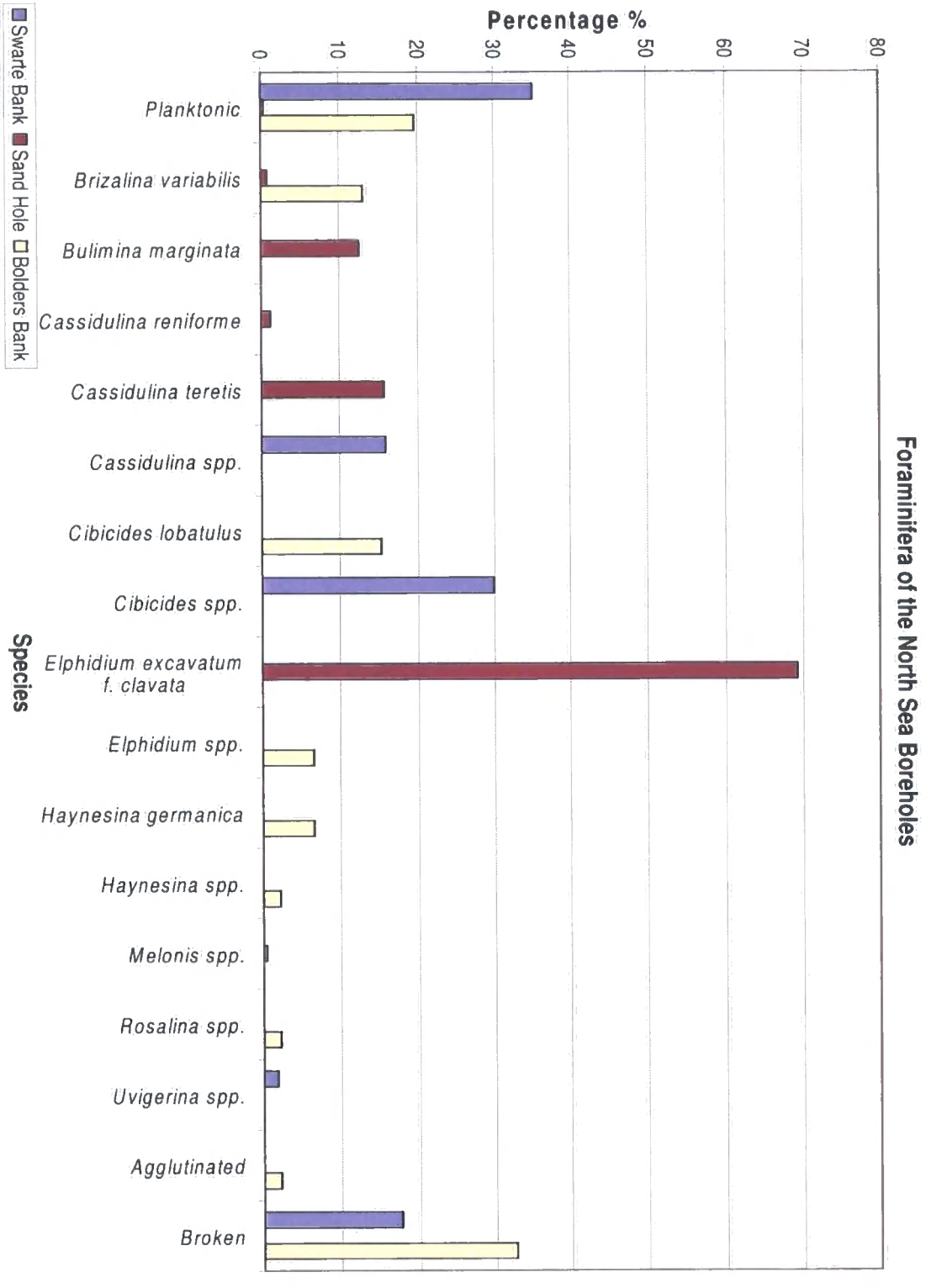

Figure 7.31: Foraminifera of the North Sea Boreholes

Palynology

A palynological investigation by Dr. Jim Riding of the BGS, Keyworth (Riding, 2008) found a wide range of palynomorphs within the Swarte Bank Fm (Table 7.9), including small percentages of age-diagnostic species from the Carboniferous, the Triassic, the Jurassic, the Cretaceous, the Palaeogene and the Quaternary. Upper Triassic miospores were recorded in very low numbers in BH 81/46 (18 m); these include *Krauselisporites reissingeri*, *Ovalipollis ovalis*, *Riccisporites turbulatus*, *Triancoraesporites ancorae* and *Zebrasporites interscriptus*. These are typical of the Rhaetian Stage (Orbell, 1973; Dunay, 1978). Marine microplankton taxa characteristic of the Lower Toarcian were observed in very low numbers in BH 81/52a (43.07 m). They include *Halosphaeropsis liassica*, *Nannoceratopsis deflandrei* subsp. *sensex*, and *Nannoceratopsis sp.* (Riding, 2008).

There are also low numbers of miospores of characteristic Middle to Upper Jurassic age within the Swarte Bank Fm (Table 7.9), including *Calamospora mesozoica*, *Callialasporites* sp., *Cerebropollenites macroverrucosus*, *Chasmatosporites* sp., *Classopollis classoides*, *Classopollis meyeriana*, *Cyathidites* sp., *Perinopollenites elatoides* and *Retitriletes* sp.(Riding, 2008). The dinoflagellate cyst species *Oligosphaeridium patulum* and *Perisseiasphaeridium pannosum* are indicative of input of the Kimmeridge Clay Formation of northern England (Riding & Thomas, 1988). Allochthonous Late Cretaceous dinoflagellate cysts were observed sporadically and occur in minor amounts in the Swarte Bank Fm, representing incorporation of the Chalk Group. Palaeogene input in BH 81/46 (18 m) is prominent and diverse, and the presence of forms such as *Deflandrea oebisfeldensis*, *Glaphyrocysta* sp., *Homotryblium* sp., *Hystrichsphaeridium turbiferum* and *Wetzeliella* sp. are indicative of the Eocene. *Deflandrea oebisfeldensis* is indicative of latest Thanetian to Ypresian (Powell, 1992).

Table 7.9: Age-Diagnostic Palynomorphs from the North Sea Basin (Riding, 2008). Non age-diagnostic palynomorphs are not shown.

Formation / Bedrock Source		Swarte Bank Fm		Coal Pit Fm	Fisher Fm		Bolders Bank Fm		
		81/46A 18 m	81/52A 43.07 m	81/26 54.8 m	81/34 34 m	81/29 12 m	82/19 10.3 m	81/43 4 m	81/48 8 m
Quaternary		ca. 2 %	?ca. 1-2 %	ca. 5 %	ca. 3-4 %	1 %	<1 %	ca. 1 %	<1 %
Palaeogene		2-3 %	ca. 1 %	0	1-2 %	0	<1 %	0	?<1 %
Cretaceous		?<1 %	<1 %	0	<1 %	0	0	0	ca. 2 %
Jurassic	*Middle & Upper*	ca. 1 %	<1 %	<1 %	1-2 %	0	? ca. 1 %	ca. 1 %	ca. 1-2 %
	L. Toarcian	0	ca. 1 %	0	0	0	<1 %	0	ca. 1 %
	Rhaetian	<1 %	<1 %	?<1 %	0	0	<1 %	0	<1 %
Carboniferous		1-2 %	<1 %	2-3 %	1-2 %	1 %	ca. 1-2 %	1-2 %	ca. 1-2 %
Silurian		0	0	0	<1 %	0	<1 %	<1 %	0

The Fisher Fm contains sparse palynomorphs in BH 81/29, but BH 81/34 is characterised by Silurian, Carboniferous, Jurassic, rare Cretaceous, Palaeogene and Quaternary palynomorphs (Table 7.9). The Silurian palynomorphs are relatively abundant, and include *Diexallophasis denticulata* and *Veryhachium* sp., characteristic of the Silurian. The Cretaceous palynomorphs are present in only minimal numbers, and include rare cavate peridinioid forms characteristic of the Late Cretaceous (Riding, 2008). *Trithyrodinium* sp. represents incorporation of the Chalk Group. Allochthonous Palaeogene dinoflagellate cysts are prominent and diverse in the Fisher Fm (BH 81/34 at 34 m). They include *Cordosphaeridium gracile*, *Deflandrea oebisfeldensis*, *Glaphyrocysta ordinata*, *Homotryblium* sp., *Hystrichosphaeridium tubiferum*, *Thalassiphora pelagica* and *Wetzeliella* sp. These species are indicative of the Eocene (Riding, 2008). The Fisher Fm also yielded significant numbers of typical Quaternary dinoflagellate cysts, including *Achomosphaera andalousiensis*, *Bitectatodinium tepikiense*, *Lingulodinium machaerophorum*, *Operculodinium centrocarpum*, *Selenopemphix quanta* and *Spiniferites* sp. (Riding, 2008). Quaternary pollen spores present include *Alnus*, *Dryopteris*, *Gramineae*, *Pinus*, *Polygonium vulgare* and *Stereisporites* (Riding, 2008).

There are significant percentages of Carboniferous dinoflagellate cysts within the Coal Pit Fm. *Densosporites* sp. and *Lycospora pusilla* are the most prominent taxa, which is typical of derived Carboniferous palynomorphs (Riding *et al.*, 2003). Also present in low numbers were *Radiizonates* sp., and *Tripartites trilinguis*, characteristic of the Westphalian

(Smith & Butterworth, 1967) and the Namurian. The Carboniferous palynomorphs therefore represent the incorporation of Namurian and Westphalian material.

The palynology of the Bolders Bank Fm is also impoverished, with BH 81/43 4 m containing only sparse palynomorphs. Both palynomorph samples contained single specimens of acritarchs of Silurian aspect, *Diexallophasis denticulata* (Riding, 2008). There are minor proportions of Carboniferous spores (Table 7.9) in all of the samples, but they are particularly prominent in BH 82/19. This sample also contained Upper Triassic (Rhaetian) miospores, including *Krauselisporites reissingeri*, *Ovalipollis ovalis*, *Riccisporites tuberculatus*, *Triancoraesporites ancorae* and *Zebrasporites interscriptus*. These forms are diagnostic of the Rhaetian Stage (Orbell, 1973; Dunay, 1978; Riding, 2008). The Early Jurassic (Lower Toarcian) marine microplankton present in both formations are *Halosphaeropsis liassica, Nannoceratopsis deflandrei* subspecies *senex*, and *Nannoceratopsis* sp. (Riding, 2008). This association is typical of the Early Toarcian oceanic anoxic event (Palliani & Riding, 2003), and this interpretation is supported by the presence of abundant levels of amorphous organic material in the Bolders Bank Fm (Riding, 2008). BH 81/48 8 m is also relatively rich in Early Cretaceous dinoflagellate cysts, and yielded *Batioladinium* sp., *Cassiculosphaeridia* sp., *Cribroperidinium gigas*, *Cyclonepherlium distinctum*, *Gochteodinia villosa*, *Goechteodina virgula, Phoberocysta neocomica*, and *Rotosphaeropsis thula* (Riding, 2008). This association is indicative of the Jurassic-Cretaceous boundary (Davey, 1982). *Phoberocysta neocomica* is indicative of earliest Cretaceous.

7.5 Interpretation

7.5.1 The Swarte Bank Fm

Processes of Deposition

Previous researchers have interpreted the Swarte Bank Fm as a subglacial till (Cameron *et al.*, 1992; Gatliffe *et al.*, 1994). This study used thin-section analysis to further investigate the processes of deposition for the Swarte Bank Fm in BH 81/46A (17 m). The diamict composition, angular small skeleton grains, and common ductile deformation structures such as turbates, skelsepic plasmic fabrics and pressure shadows indicate a derivation as a subglacial till (Carr, 2001). There are few large skeleton grains, as the diamicton is derived from reworked marine sediments. The lack of large skeleton grains and the homogeneity of grain size results in fewer turbates and other structures (Hart *et al.*, 2004). Grain lineations indicating shear are common (cf. Hiemstra & Rijsdijk, 2003). Grain stacks are present in small numbers, indicating a high-strain environment (Menzies *et al.*, 2006). Type III pebbles can indicate cannibalisation of pre-existing sediments, and is a common feature in subglacial tills (Carr, 2001; Carr *et al.*, 2006). Additionally, the sediment contains reworked marine microfauna. Based on the criteria outlined in Chapter 2 (Table 2.5), this work therefore supports previous interpretations as a subglacial till deposited by a grounded ice sheet.

Provenance

Palynological analysis of the Swarte Bank Fm provided sensitive provenance information for the sediments in the NSB (Riding, 2008). BH 81/46A contained rare Upper Triassic miospores, probably derived from northern England. BH 81/52a (43.07 m) contained rare Early Jurassic (Lower Toarcian) marine microplankton taxa, typical of the early Toarcian anoxic event. Palynomorphs of the Middle and Upper Jurassic are consistently present, which indicate the input of the Kimmeridge Clay Fm. These were probably also sourced from northern England or the Moray Firth. Both samples contained rare palynomorphs characteristic of the Late Cretaceous, representing incorporation of the Chalk Group, located to the north and east of the study site. Sparse examples of allochthonous Palaeogene dinoflagellate cysts were observed in the Swarte Bank Fm (Riding, 2008), indicative of the latest Thanetian to Ypresian interval. This Eocene

material is present in significant numbers in BH 81/46A, and represents the input of local NSB material to the east of the borehole location. The Permian bedrock for BH 81/46A left little impression, but these strata are typically poor in palynomorphs (Riding, 2007).

The heavy-mineral suite of the Swarte Bank Fm supports a derivation from northeastern Scotland. Firstly, the ferromagnesian minerals (olivine and clinopyroxenes) are from an ultramafic to a mafic source. These include gabbros, dolerites, and basalts. The most likely source for these are the Carboniferous volcanic rocks (olivine and clinopyroxenes phyric basalts) and related high-level intrusive rocks (dolerites and basalts), Upper Silurian to Lower Devonian volcanic rocks, and the Palaeogene volcanic and high-level intrusive rocks. These outcrop from the Midland Valley, southwards (Cameron & Stephenson, 1985; Trewin, 2002).

The metamorphic suite of heavy minerals (tourmaline, garnet, sillimanite, andalusite, kyanite, staurolite and chloritoid) is consistent with the source terrane including a significant amount of upper greenschist to upper amphibolite facies regionally metamorphosed pelitic metasedimentary rocks, and is very similar to the Devensian tills exposed onshore (see chapters 3 to 6). An association of garnet, staurolite and chloritoid is indicative of Stonehavian-type metamorphism. The development of this association is strongly controlled by the whole-rock chemistry of the pelitic mudstone, and is therefore only developed in very specific areas. Chloritoid in particular is a distinctive mineral only found in the Highlands of Scotland (Stephenson & Gould, 1995). Stonehavian-type metamorphism is limited to a small area to the east of Stonehaven close to the Highland Boundary Fault (Trewin, 2002). A second metamorphic suite consisting of garnet, andalusite and kyanite is a higher-grade assemblage, typical of Buchan-type metamorphism, from the Buchan coast near Aberdeen. The metamorphic minerals within the Swarte Bank Fm therefore represent an input from the Dalradian Supergroup along the coast of northeastern Scotland.

Summary of the Swarte Bank Fm

The Swarte Bank Fm has previously been interpreted as an Anglian subglacial till, and it records the first invasion of ice into the southern NSB (Cameron *et al.*, 1992). It fills an array of tunnel valleys up to 12 km wide and 450 m deep, cut into the Pleistocene deltaic and pre-Pleistocene strata (Cameron *et al.*, 1987). It has been correlated with the chalky Lowestoft till in Norfolk (Scourse *et al.*, 1998). The Swarte Bank Fm was sampled in this

study in boreholes 81/46a at 17 and 18 m depth, and in 81/52A at 43.07 m. BH 81/46a is located at 54° 59.99'N and 00° 32.275'E, almost directly due east of Co. Durham. BH 81/52a is located some distance further south at 53° 31.85'N and 00° 44.291'E, just south of the Humber estuary. The Swarte Bank Fm in these boreholes is a grey sandy diamicton with fine gravel, no shells, and a vigorous reaction to HCl. In thin section, the Swarte Bank Fm is a grey-brown, well-consolidated diamicton with turbate structures, a skelsepic plasmic fabric and reworked Type III pebbles. It is interpreted here as a subglacial till.

The Swarte Bank Fm has rare foraminifera specimen, with a significant percentage of planktonics. *Cibicides* sp. and *Cassidulina* sp. are the most common benthic species. The assemblage is poorly preserved, with the tests showing signs of reworking. The formation contains certain age-diagnostic palynomorphs, including moderately abundant Cretaceous, Palaeogene, Quaternary, and Carboniferous species. The heavy-mineral assemblage within the Swarte Bank Fm is characterised by high percentages of garnet, biotite, muscovite and epidote. Statistical analysis of the heavy-mineral suite and matrix geochemistry was not efficient enough to distinguish this formation from the Coal Pit and Fisher formations. The geochemistry, biostratigraphy and petrology all indicate a provenance from eastern Scotland near the Highland Boundary Fault, with some input from the Central North Sea Basin.

7.5.2 The Sand Hole and Egmond Ground formations

Processes of Deposition

The Sand Hole Fm has been previously interpreted as a shallow-marine sediment deposited in a restricted marine basin, immediately after the recession of the Elsterian ice sheet (Cameron *et al.*, 1992). Micromorphological analysis of the Sand Hole Fm (BH 81/52A 40.5 m) provides additional evidence and suggests that towards its base, the Sand Hole Fm was deposited under glaciomarine conditions, dominated by a combination of underflows, overflows, and turbidity currents. Evidence for a glaciomarine environment derives from the abundant pristine marine microfossils (cf. Carr, 2001; Ó Cofaigh & Dowdeswell, 2001). It shows strong evidence of subsequent reworking in the form of ductile deformation structures, including turbate structures indicating shear, skelsepic plasmic fabrics, abundant Type III pebbles, grain stacks and grain lineations (cf. Carr, 2001; van der Meer *et al.*, 2003; Hiemstra, 2007). The presence of reworked soft sediment

pebbles suggests glacial input. The large recumbent fold could have been formed during syn-depositional soft-sediment deformation. The skelsepic plasmic fabric, grain lineations, turbates and grain stacks indicate deformation in a confined environment, suggesting glaciotectonic deformation.

A second thin section at 29.87 m (Figure 7.14) is characterised by the graded, folded, silt laminations and occasional large skeleton grains. The normally graded sand and silt laminations are indicative of subaqueous sedimentation, with variable and alternating flow velocities depositing laminations of different grain sizes. The silt and clay beds relate to sedimentation in standing water, from the rapid rain-out of dense sediment-laden underflows (Lee & Phillips, 2008). The numerous marine microfossils confirm an open-marine environment. The presence of reworked soft sediment pebbles suggests an input from a glacier snout. The large skeleton grains deform the bedding beneath and are draped by bedding above, and so are interpreted as microscopic dropstones, indicative of ice-rafted debris (Hart & Roberts, 1994; Carr, 2001; Ó Cofaigh & Dowdeswell, 2001). This interpretation is supported by the lense-shaped dump structure at the top of the slide. The sediment was therefore deposited under glaciomarine conditions. It was subsequently folded and deformed, possibly by ice-push following deposition.

Provenance

The heavy-mineral suite of the Sand Hole and Egmond Ground formations reflects that of the Swarte Bank Fm, from which it is derived. The low abundances of olivine and staurolite perhaps indicate reworking and mechanical erosion of these fragile minerals.

Summary of the Sand Hole and Egmond Ground formations

The Sand Hole Fm overlies the Swarte Bank Fm and was deposited during a period of climatic amelioration following the end of the Elsterian glaciation (Gatliffe *et al.*, 1994). During the Holsteinian, the rising sea-level, combined with tectonic subsidence, led to the re-establishment of a shallow sea, landward of the present North Sea shorelines (Cameron *et al.*, 1992). The Sand Hole Fm is an early deposit in that sea. It is up to 20 m thick and is confined to the Silver Pit region. BH 81/52a has yielded laminated clays with abundant dinoflagellate cysts and a rich, diverse, interglacial, shallow-marine foraminifera assemblage. Cameron *et al.* (1992) inferred that the Sand Hole Fm was deposited during the early, warm, Holsteinian period, in a quiet, restricted, marine environment. The

overlying Egmond Ground Fm has previously been interpreted as a marine sediment deposited in warm, open-marine conditions, with typical shallow-water Holsteinian faunas (Cameron *et al.*, 1992). These faunas indicate a cool-temperate sea, similar to northern parts of the present day North Sea.

This study took two samples of the Sand Hole Fm; the first from directly above the Swarte Bank Fm in BH 81/52a (40.5 m) and the second higher up in the formation (37.13 m). The two samples are quite dissimilar. The lower sample is a poorly-sorted silty clay, with around 16 % sand. The upper sample is a silty-clay with very little sand. In thin section, the lower sample is a banded diamicton, with abundant marine microfossils. It exhibits numerous deformation features, including plasmic fabrics, rotational structures, Type II and III pebbles, and grain lineations. In contrast, the sample at 37.13 m is laminated, with a large recumbent fold. Even though these samples are relatively close together, they show little similarity and statistical analysis of the heavy-mineral suite and matrix geochemistry fails to cluster these samples closely (Figure 7.29 and Figure 7.30). The Sand Hole Fm has abundant foraminifera fossils, predominantly *Elphidium excavatum* (Figure 7.31).

The Sand Hole Fm is interpreted in this study as a reworked glaciomarine deposit, with increased sorting and laminations stratigraphically higher up in the borehole. The sediments are derived from northeastern Scotland, and reflect the provenance of the Swarte Bank Fm.

7.5.3 The Fisher Formation

Processes of Deposition

Previous workers have interpreted the Fisher Fm as a Saalian glaciomarine sand and clay (Andrews *et al.*, 1990). The present study used micromorphology to test this interpretation. The complex slide (Figure 7.18) shows a strongly deformed sand, with vestiges of primary, graded bedding. This sand is interpreted as a subaqueously deposited sediment that has suffered extensive soft-sediment deformation. The slide therefore exhibits a polyphase history of deposition and deformation. The first phase is the deposition of sand laminae. Compaction and compression by the overlying sediments, and possibly by ice-push or down-slope movement, resulted in dewatering and liquefaction of sediments (similar to that described by Phillips *et al.*, 2007). As porewater pressure

decreased after dewatering, brittle faulting crosscut the fluidised sand in the final phase of deformation. The high confining pressure of an overlying ice sheet may well have contributed to the fluidisation of the sand laminae. This sediment was therefore deposited subaqueously, possibly in a glaciomarine environment, though there is little direct evidence of this within this particular slide. No *in situ* foraminifera were found.

Provenance

The Silurian palynomorphs of BH 81/34 34 m yielded single specimens of acritarchs of Silurian aspect, including *Veryhachium* sp. The palynomorphs are light in colour, so they cannot have been derived from the cleaved Silurian slates of the Southern Uplands, as the thermal alteration of these rocks is high, and all palynomorphs are dark brown to black in colour. The only possible British source is the Midland Valley of Scotland, south of the Firth of Forth, which has not been significantly metamorphosed (Riding, 2008). A source from the NSB is not likely due to deep burial of Palaeozoic strata. The floras also seem similar to those described from the Early Silurian strata of Ringerike area, Oslo, Norway (Smelror, 1987). The Eocene input is probably local, and there are no obvious candidate sources onshore eastern England (Riding, 2008). The association of the freshwater algae Pediastrum sp. and Quaternary pollen and dinoflagellate cysts suggests reworking of Quaternary or Neogene deposits, and these palynomorphs are probably derived from Quaternary sediments covering the NSB (Riding, 2008).

The heavy-mineral suite of the Fisher Fm also supports a derivation from the Grampian Highlands, with the characteristic staurolite-garnet-chloritoid and garnet-andalusite-kyanite assemblages (Trewin, 2002) both being strongly present. Epidote is also present, suggesting the input of the epidote-amphibolite facies of the Grampian Highlands.

Summary of the Fisher Fm

Andrews *et al.* (1990) argued that the Fisher Fm is a glaciomarine mid-Saalian deposit. It is overlain by glacial and glaciomarine facies sediments attributed to a major glacial episode in the Late Saalian, with ice in the Moray Firth, and an ice-proximal environment in the outer Moray Firth area, where a large subaqueous fan was built out from a tidewater glacier, forming a series of overlapping fans. North of 58°, 30'N, subglacial sedimentation occurred. During the northward retreat of the glacier, a series of still-stands and re-advances occurred, forming large subaqueous moraines. These continue

to form significant topographic highs on the sea bed (Andrews *et al.*, 1990). The 40 m thick diamicton in BH 81/26 has previously been identified as a Saalian subglacial till (Sejrup *et al.*, 1987).

This study sampled the Fisher Fm from BH 81/34 (56° 7.68'N, 01° 35.21'E) at 18.4 and 34 m depth below seabed, and from BH 81/29 (56° 15.91'N, 0° 49.97'E) at 12 m below seabed. The samples were quite variable. The sample from BH 81/29 was a silty clay, with 36 % clay and 65 % silt. The samples from BH 81/34 contained more sand and less clay. All the samples were a light grey colour, and contained rare fine gravel but no shell fragments. In thin section (BH 81/34), the Fisher Fm was found to be a strongly deformed and distorted sand that retained some primary bedding structures. The Fisher Fm was interpreted to have been deposited sub-aqueously, possibly in a glaciomarine environment, which has undergone subsequent extensive soft-sediment deformation.
Mineralogical analysis of the sediment shows that it varies strongly between boreholes. The abundant metals, however, form a more tightly clustered group with similarities to the Coal Pit Fm and the Swarte Bank Fm (Figure 7.30). Although BH 81/34 (34 m) incorporates only rare battered and broken foraminifera, pale Silurian palynomorphs are relatively abundant, and there are low numbers of Cretaceous forms. The Silurian palynomorphs indicate derivation from the Midland Valley of Scotland. The heavy-mineral assemblage indicates a source from the Scottish Highlands, close to the Highland Boundary Fault.

7.5.4 The Coal Pit Formation

Processes of Deposition

Carr *et al.* (2006) argued that the upper facies of the Coal Pit Fm was an early Weichselian subglacial till. Micromorphological analysis of the thin section 81/26 65.4 m adds to this interpretation. Firstly, the diamict, consolidated matrix is consistent with a subglacial derivation. There are many structures indicative of ductile deformation, which again is consistent with an origin as a subglacial till. These include turbate structures with and without core stones, with trailing tails of smaller skeleton grains, a skelsepic plasmic fabric, and rounded, silty type III pebbles, indicative of cannibalisation and incorporation of pre-existing sediments (Menzies, 2000; Menzies *et al.*, 2006). The presence of marine bivalve fragments supports the reworking of marine sediments. There are also associated

grain stacks and grain lineations. This association is typical of subglacially-derived tills (Hiemstra & Rijsdijk, 2003; van der Meer *et al.*, 2003; Menzies *et al.*, 2006). The presence of far-travelled igneous lithic fragments corroborates an interpretation as a subglacial till.

Provenance

The heavy-mineral suite of the Coal Pit Fm bears some similarities to that of the Swarte Bank Fm. Principally, although there is clearly an influence of the Scottish Dalradian Supergroup (Figure 2.7), the comparatively low percentages of andalusite and kyanite may indicate a less strong influence of the Buchan metamorphism. Alternatively, the high percentage of the ultra-stable garnet and monazite phases could suggest reworking and diagenesis, with removal of less stable minerals. The high percentage of epidote could reflect an input from the epidote-amphibolite facies assemblage from the Grampian Highlands (Trewin, 2002). The Coal Pit Fm is the only suite to contain piemontite, which occurs in low-grade regionally metamorphosed schists and gneisses, such as those in the Dalradian of Scotland (Mange & Maurer, 1992). In summary, the Coal Pit Fm bears traces of both Buchan- and Stonehavian-type metamorphism, and was probably derived from the Grampian Highlands and the northeast coast of Scotland.

The Coal Pit Fm features a significant amount of characteristic Westphalian Carboniferous spores, which probably reflect a source from the Midland Valley of Scotland (Riding, 2008). It also produced a large number of Quaternary spores, probably derived from Quaternary sediments on the North Sea floor. The single rounded Scandinavian rhomb porphyry was probably reworked from the North Sea floor.

Summary of the Coal Pit Fm

Previous workers have ascribed a Late Saalian to early Weichselian age for the Coal Pit Fm (Andrews *et al.*, 1990). It includes the Eemian interglacial, and the start of the last major glaciation (Stoker *et al.*, 1985). The Coal Pit Fm fills channels in the northern North Sea, and occurs as a blanket deposit up to 40 m deep in the east of the Witch Ground Basin. It stratigraphically overlies the Fisher Fm, the Ling Bank Fm and the Aberdeen Ground Fm (Andrews *et al.*, 1990). The Coal Pit Fm has been correlated with the Ferder Fm (Carr *et al.*, 2006), and the upper facies has been interpreted as a subglacial till, implying extensive glaciation of the NSB during MIS 4.

The Coal Pit Fm was sampled in this study in BH 81/26 (58° 08.2'N, 00° 10.46'E, off the northeastern coast of northern Scotland) between 54.8 m and 64.6 m depth below seabed. These samples are fissile, dark greyish-brown, sandy diamictons with Magnesian Limestone, dolerite, quartz, rhomb porphyry, chalk and flint gravel. They contain no shell fragments. In thin section, it is a massive diamicton with numerous lithic fragments. It exhibits turbates with associated grain lineations, skelsepic and masepic plasmic fabrics, and Type III pebbles. This therefore supports previous interpretations as a subglacial till.

The heavy-mineral assemblage is tightly clustered, and the three samples are very similar to each other. They are rich in garnet, epidote and hornblende. Statistical analysis reveals similarities to the Swarte Bank Fm and the Fisher Fm, which all plot distinctly from the Devensian Bolders Bank and Wee Bankie formations. This result is echoed in the ternary plots, PCA and cluster analysis of abundant metals (Figure 7.26 and Figure 7.28). Although the formation features very few foraminifera, and the few tests are battered and poorly preserved, palynomorph analysis revealed abundant derived Quaternary and Carboniferous spores. There is clearly an input from the Southern Uplands, the Midland Valley of Scotland, and the Grampian Highlands.

7.5.5 The Bolders Bank Formation

Processes of Deposition

The presence of far-travelled igneous lithic fragments, the consolidated, diamict texture, the variable grain size, rounded soft sediment intraclasts (type III pebbles), and ductile and brittle deformation structures within thin section BH 81/48 8.9 m (Figure 7.22) supports Carr *et al.*'s (2006) interpretation of the Bolders Bank Fm as a subglacial till (refer to Table 2.5). Turbates form in response to simple shear under high pore-water pressure (Hart *et al.*, 2004). The skelsepic plasmic fabric coating fine skeleton grains forms when clay platelets are aligned in response to rotating skeleton grains (van der Meer, 1993; Menzies, 2000). The edge-to-edge contacts with individual skeleton grains are indicative of a high-strain environment (Menzies *et al.*, 2006). Grain lineations have been suggested to form under high-strain environments in response to simple shear (Menzies, 2000). The presence of soft-sediment intraclasts suggests cannibalisation of pre-existing sediments, whilst its deformation adds further support to a high-strain environment deforming with

high pore-water pressure. This slide therefore exhibits features typical of sediments deposited beneath a grounded ice sheet.

Provenance

The Silurian palynomorphs in these tills were derived from the Silurian strata of the Midland Valley of Scotland, for similar reasons as noted above with the Fisher Fm. For the Carboniferous and Upper Triassic palynomorphs, the most likely source is northern England, possibly including the Midland Valley for the Carboniferous material. The Early Jurassic palynomorphs were probably sourced from northern England (Riding, 2008). Middle and Upper Jurassic forms could be derived from northern England or the Moray Firth. The incorporation of the Kimmeridge Clay Fm is clear in BH 81/48, supported by the presence of abundant amorphous organic material. The heavy-mineral suite of the Bolders Bank Fm similarly exhibits phases and assemblages typical and diagnostic of the Grampian Highlands, Dalradian, and northeast coast of Scotland.

Summary of the Bolders Bank Fm

The Bolders Bank Fm lies directly on chalk bedrock to the east of England. It has previously been described as a diamicton with a chaotic to poorly ordered internal seismic-reflector configuration. It is characteristically a reddish to greyish brown, stiff, massive diamicton with occasional distinct, arenaceous layering and deformational structures (Cameron *et al.*, 1992). It encompasses abundant chalk clasts derived from eastern England, and the clast content decreases eastwards. In general, it is less than 5 m thick. It has been interpreted as a composite of subglacial and supraglacial deposits (Cameron *et al.*, 1992) and as a subglacial till (Carr *et al.*, 2006). Cameron *et al.* (1992) correlated the Bolders Bank Fm with the Devensian diamictons of Hunstanton and Holderness.

The Wee Bankie Fm occurs near the eastern coast of Scotland, where it has a sheet-like geometry and an uneven, ridged upper surface (Gatliffe *et al.*, 1994). It is around 40 m thick, and has a chaotic acoustic response pattern. Gatliffe *et al.* (1994) described it as a stiff, variably matrix-dominated diamicton with some interbeds of sand, pebbly sand and silty clay. It lacks *in situ* flora or fauna, but includes reworked biological material. Gatliffe *et al.* (1994) interpret the Wee Bankie Fm as a Late Weichselian subglacial lodgement till, and correlate it with the Marr Bank Fm and the Bolders Bank Fm.

The thin section taken at BH 81/48 at 9.8 m (Figure 7.22) is characterised by its diamict texture with large, far-travelled, igneous lithic fragments, the rare marine microfossils, and the numerous rounded soft sediment clasts. Microstructures include edge-to-edge grain contacts, crushed grains, numerous turbates, a well-developed skelsepic/lattisepic plasmic fabric, grain lineations and grain stacks. These indicate a genesis as a subglacial till.

The Bolders Bank Fm was sampled from the boreholes nearest to Easington, County Durham. BH 81/48 (53° 48.105'N, 01° 01.365'E), BH 81/43 (54° 48.919' N, 0° 14.509' E) and BH 82/19 (54° 47.49'N, 00° 34.132'E) all contained brown, silty to clay-rich diamictons, with granite, Carboniferous Limestone, sandstone, coal, Magnesian Limestone, flint, chalk and dolerite. They contained only tiny fragments of marine bivalve shells, but yielded abundant early Cretaceous palynomorphs, low numbers of early Jurassic marine microplankton taxa, characteristic Middle and Upper Jurassic palynomorphs, and rare Silurian acritarchs. These together suggest sediment inputs from the Grampian Highlands, the Midland Valley and Dalradian of Scotland, and northern England.

7.6 Discussion and Conclusions

7.6.1 Depositional Environments

The NSB is a sediment sink with a vast accumulation of Quaternary deposits. Some of these are deeply buried, and in every case, the only means of accessing these sediments is through coring. In general, the thin-section analysis of selected samples agrees with previously published work (Carr *et al.*, 2000; Carr *et al.*, 2006), although it has been able to add some new detail. For example, the evidence for a subglacial origin for the Swarte Bank Fm is considerably more robust. The Sand Hole Fm is more complex than previously thought, and encompasses several different facies, grading from ice-proximal, possibly ice-contact, to distal glaciomarine. It features a cold fossil microfauna, showing that the lower stages of the Sand Hole Fm are latest Elsterian, grading into the warmer Holsteinian Egmond Ground Fm. A much more detailed and rigorous study of all these samples is needed, as this will further constrain the changing processes temporally and spatially.

7.6.2 Repeat ice-flow pathways

Previous workers have provided little indication of the provenance of glacigenic sediments in the North Sea, and process interpretations have been confined to limited sedimentological interpretations from boreholes and seismostratigraphical data (Andrews *et al.*, 1990; Sejrup *et al.*, 1991; Cameron *et al.*, 1992; Merritt *et al.*, 1995; Sejrup *et al.*, 2000; Sejrup *et al.*, 2005; Graham *et al.*, 2007; Bradwell *et al.*, 2008; Golledge *et al.*, 2008), and have often at best only been vaguely attributed to 'the Scottish Mainland' (Andrews *et al.*, 1990) or Scandinavia (Gatliffe *et al.*, 1994). Interpretations of the processes of deposition of these sediments lacked detailed thin section study until the work of Carr *et al.* (2006). This study has therefore greatly contributed to the sum of knowledge regarding the Quaternary sediments of the North Sea, firstly by confining the ice accumulation areas and ice flow pathways, and secondly by clarifying the genesis of these sediments.

Statistical analysis shows that many of the sediments have similar heavy-mineral assemblages, and thus show similar ice-source areas and had similar ice-flow trajectories. This is to be expected in low-relief areas. Cluster analysis of the ICP-MS data (Figure

7.30) reveals two groups, with a clear dichotomy between them. The Bolders Bank and Wee Bankie formations plot very close to each other, with very low dissimilarity scores. The Swarte, Coal Pit and Fisher formations form a second group, with the Swarte Bank being dispersed and showing little matrix homogeneity. In both the heavy mineral and matrix geochemistry, the variations between samples is more closely related to sample location and whether they were sampled from the same borehole or not, than whether or not they are from the same formation. The PCA (correlation) on the ICP-MS data distinguishes clearly between the Devensian near-shore tills (Bolders Bank Fm), which are dominated by the abundance of magnesium and aluminium within their matrices, and the older, further afield formations. The Swarte Bank Fm shows an affinity with the Fisher and Coal Pit Fm, controlled by the high abundance of potassium, titanium, sodium and silicon within their matrices (Figure 7.30). The PCA (covariance) shows a different pattern, with the Swarte Bank Fm being more closely related with the Wee Bankie Fm. The Coal Pit and Fisher Formations remain clustered towards the right-hand side of the graph.

The NSB samples therefore contain a wide variety of minerals and have strongly variable matrix geochemistries (see Section 7.4.1, page 393). The boreholes are spread over a wide geographical area, and changing bedrock lithologies has a significant impact on the heavy-mineral suite and the abundances of various metals. However, the various glacigenic lithofacies generally share several characteristics, and show evidence of erosion from the Grampian Highlands and the northeastern coast of Scotland. The palynofloras and kerogen from the eight samples analysed for palynomorphs (Riding, 2008) proved relatively similar. Although most yielded moderately abundant and diverse palynomorph samples, BH 81/29 (12 m) and BH 81/43 (4 m) both proved to be sparse. The combination of Silurian, Carboniferous, Upper Triassic (Rhaetian), Lower Jurassic (Lower Toarcian), Middle-Upper Jurassic, Cretaceous, Palaeogene and Quaternary palynomorphs is diagnostic of a derivation from northern Britain, including the western margin of the North Sea (Riding, 2008). However, despite the similarities, some subtle differences between the samples can be discerned. For example, the Swarte Bank Fm has significantly higher percentages of Silurian palynomorphs. To entrain Silurian palynomorphs, the ice sheet would have been generated in the Scottish Highlands and then deflected eastwards along the Firth of Forth (possibly by the Southern Uplands fault scarp), before flowing southwards towards the NSB (Riding, 2008).

The provenance analysis of the NSB samples therefore imparts considerable new information. All the samples show strong evidence for derivation from northern Britain. Little previous provenance work has been conducted on the North Sea tills. Here, a Grampian and Highlands, northeast Scotland (Aberdeen) and north-west North Sea origin for the Bolders Bank, Coal Pit, Fisher and Swarte Bank formations is indicated, with inputs from northern England. The ice sheets originated in northern Britain, before entraining material from the Midland Valley of Scotland, and passing out through the Moray Firth and Firth of Forth. From here, they spread eastwards and southwards into the NSB. Geomorphological mapping indicates that at their maximum, and certainly at the LGM, these ice sheets extended northwards to the continental shelf, eastwards to meet Scandinavian ice in the NSB, and southwards towards the Wash and north Norfolk.

Previous workers have correlated the Swarte Bank Fm with the Lowestoft Fm of Norfolk, due to lithological content and stratigraphical position (Cameron *et al.*, 1992). The Scandinavian signature and presumed MIS 6 age of both the Cleaver Bank Fm and Bridlington Member could signify deposition by the same ice sheet. An MIS 4 age for the Ferder Fm could suggest possible correlation with the onshore Blackhall Member, due to the MIS 4 age gained by OSL at Warren House Gill (refer to Chapter 5.6.4). This is discussed further in Chapter 8, and is summarised briefly in Table 7.10 below.

Table 7.10: Summary of stratigraphy and formations of the North Sea

MIS	Offshore Formation	Possible Onshore Correlatives
MIS 2	Bolders Bank Fm	Skipsea Member Horden Member ? Blackhall Member
MIS 2	Cape Shore Fm	
MIS 4	Ferder Fm	? Blackhall Member
MIS 4-6	?Coal Pit Fm	
MIS 6	Fisher Fm	Welton-le-Wold Till?
MIS 6	Cleaver Bank Fm	? Bridlington Member?
MIS 12	Swarte Bank Fm	Lowestoft Fm

7.6.3 Limitations and Further Research

This study could be considered as a pilot study for investigating the genesis and provenance of various Quaternary sediments in the NSB. In this respect, the study worked well. However, the formations identified by BGS stratigraphers and mappers contain many complex facies, and these vary laterally due to changing bedrock. Identifying land-sea

correlations is difficult due to differing diagenesis and varying matrix compositions between onshore tills and offshore tills. There is substantial scope for further developing this project by conducting a more in-depth study of the boreholes, involving more intense and regular sampling, perhaps combined with the increasingly sophisticated echo-sounding datasets now available.

7.7 Conclusions

Previous seismostratigraphical and borehole analysis of Quaternary sediments in the North Sea has led to a framework for understanding Quaternary glaciations. This study operated within this paradigm, and critically tested some key ideas regarding the origin and provenance of various glacigenic sediments. While the chronostratigraphy of the NSB glacigenic sediments is generally poor, this is a very useful archive of information as the subsiding basin retains a great deal of its Quaternary sedimentation.

The principal conclusion of this research is that the glacigenic sediments in the western North Sea Basin show evidence of repeat ice-flow pathways, with ice originating from the Grampian Highlands and delivering a clear Dalradian signal to the North Sea floor. Thin-section analysis of a subsample of glacigenic sediments supports interpretations of a grounded ice sheet within the NSB at various times from the Middle Pleistocene onwards, although the complexity of the story is barely unravelled. The heterogeneity of the Quaternary sediments within the NSB require a more in-depth and fundamental reassessment to fully chronicle their provenance and process histories.

CHAPTER 8

Discussion

8.1 Regional onshore / offshore correlations

This chapter aims to bring together the observations and interpretations in all four results chapters to create a coherent model of glacial dynamics in eastern England and the North Sea during the Quaternary. It examines and compares the provenance signature of the various onshore and offshore formations, and attempts to discern ice flow pathways. Possible correlatives between the onshore and offshore succession are considered, firstly from a process point of view and, secondly, with regard to the geochemical and petrological analysis. The findings of this thesis are then discussed within a broader European ice sheet perspective.

8.1.1 Comparisons of Process, Age, and Stratigraphical Correlations

Introduction

In this section, each member is discussed in the context of its process history, age, and stratigraphical correlations. The process history of likely correlatives is examined, and together with analysis of age and provenance information, a regional lithostratigraphy is constructed, allowing a model for the interactions between British and Fennoscandian ice sheets during the Quaternary to be created.

Ash Gill Member (of the Warren House Formation)

The Ash Gill Member crops out at the base of the sequence in the bottom of a buried palaeovalley at Warren House Gill near Horden, Co. Durham. The presence of laminations, foraminifera, dropstones and the particle-size distribution show clearly that this is a distal glaciomarine deposit (see Chapter 6.5.1). This research has suggested a Middle Pleistocene age for the Ash Gill Member is most likely, due to the AAR ages on shells, suggesting a Middle Pleistocene age (Chapter 6.4), and the stratigraphical relationship with the MIS 7 age Easington Raised Beach. The Whitesides Member does not have a glacial signature, indicating climatic amelioration prior to the deposition of the overlying Blackhall Member.

An MIS 12 age for the Ash Gill Member is most probable, based on the marine oxygen isotope curve (cf. Shackleton & Opdyke, 1973).

The landscape position of the Warren House Formation, in a palaeovalley with its base near modern sea level, is difficult to reconcile with an inferred MIS 12 age, given long-term tectonic uplift during the Quaternary (cf. Westaway, in press). It should rest high in the landscape, above the Easington Raised Beach. However, the Warren House Fm was deposited in the bottom of a deep palaeovalley (possibly a tunnel valley), and is separated from the overlying Devensian sediments by a substantial unconformity. Taking into account long-term tectonic uplift, it is clear that the Warren House Formation was deposited at depth, in the base of a palaeovalley formerly well below present sea level. This effectively explains the landscape position of the Warren House Formation (refer to page 335). This palaeovalley may once have been significantly deeper, and erosion of surrounding areas has since reduced its depth. The palaeovalley at Warren House Gill declines eastwards, away from the British mainland (Figure 1.4). After ice recession, the valley was flooded, and the glaciomarine Ash Gill Member was deposited. An alternative interpretation could be that this is a prograding sequence recording an advancing ice margin, with glaciomarine sedimentation immediately preceding inundation by ice. This hypothesis is supported by the upwards-coarsening grain size and strong post-depositional deformation in the upper portions of the Ash Gill Member. It is difficult, however, to discriminate at which times deformation occurred, as this sediment is likely to have suffered multiple glaciotectonic deformation events.

Previous workers have suggested a correlation with the Bridlington Member (Lewis, 1999) of Yorkshire (Francis, 1972; Lunn, 1995; Catt, 2007). The Bridlington Member (Basement Till of Catt and Penny, 1966) is exposed in Holderness on the shore at low tide on either side of Dimlington Farm (Catt, 2001a, 2007). It was described as a massive, very dark grey diamicton with a compact matrix, which rests on the chalk bedrock at -30 to -35 m O.D. (from borehole data, Catt & Digby, 1988; Catt, 2001a). Reported erratics include chalk, black flint, Jurassic sandstones, Magnesian Limestone, Carboniferous Limestone, Scottish and metamorphic rocks, and larvikite and rhomb porphyry from Norway (Madgett & Catt, 1978; Catt & Digby, 1988; Catt, 2001a). The chalk, flint, and Jurassic erratics are locally-derived, and crop out in eastern England south of County Durham. The Bridlington Member also encompasses inclusions of the fossiliferous marine Bridlington Crag. It was interpreted as a subglacial till (Catt, 1991b). It has a minimum age of MIS 6, as it is overlain by the Sewerby Raised Beach, which bears an Ipswichian

interglacial mammalian fauna (Catt & Penny, 1966). The Bridlington Member has been correlated to the Welton Member of the Welton-le-Wold Fm in Lincolnshire on lithostratigraphical grounds (Madgett & Catt, 1978; Lewis, 1999), which overlies gravels dated to the Hoxnian by their archaeological and faunal remains (Alabaster & Straw, 1976), although this is weak evidence as hand axes are now known to occur in interglacial deposits dating from the Cromerian, which means that the till could be as old as Anglian (Bridgland *et al.*, in prep). A palaeo-argillic soil developed on the Welton Member has been interpreted to indicate that this till preceded at least one interglacial (Alabaster & Straw, 1976). The Welton-le-Wold Fm is overlain by the Late Devensian Holderness Fm (Straw, 1983; Lewis, 1999), and could therefore reasonably date from any glacial event during the Middle Pleistocene (refer to Chapter 1.2.1, page 12).

In Chapter 6, it was suggested that the Briton's Lane Fm of north Norfolk could possibly be correlative with the Ash Gill Member (see Table 6.14, page 333). These glaciofluvial outwash sediments, which form part of the Cromer Ridge push moraine (Hamblin *et al.*, 2005), were recently dated to MIS 12 (Pawley *et al.*, 2008). They are reported to contain a mixture of Scandinavian and northern British lithologies (Hamblin *et al.*, 2005; Pawley *et al.*, 2008). The differing chronostratigraphical interpretations of the Bridlington Member and the Briton's Lane Fm suggest that there have been at least two separate incursions of Scandinavian ice to the eastern British coastline during the Quaternary.

The North Sea Basin is a sediment sink that should preserve a record of Scandinavian ice movements during the Quaternary. This study investigated several Middle Pleistocene sediments to test for the presence of deposits comparable to the Ash Gill Member offshore. Several offshore glaciomarine sediments provide good analogues for the Ash Gill Member and have similar depositional interpretations. The Middle Pleistocene sediments studied were the Swarte Bank Fm, the Fisher Fm, and the Coal Pit Fm. These sediments all have a strong northeastern Scottish provenance signature (Chapter 7.5), though the Coal Pit Fm did contain a rhomb porphyry (possibly reworked). Correlating these with onshore sediments has not previously been attempted due to insufficient data. The Fisher Fm was interpreted in this study and by others (Andrews *et al.*, 1990) as a glaciomarine deposit, and Gatliffe *et al.* (1994) assigned it to the Saalian. The Coal Pit Fm is a complex sequence that probably spans a whole glacial / interglacial / glacial sequence (Carr *et al.*, 2006), and includes several different facies. The sediments studied in this sequence were subglacial

tills. Carr *et al.* (2006) have argued that the top of the Coal Pit Fm equates to an early LGM ice advance.

Whitesides Member

The Whitesides Member, of the Warren House Formation, occurs only at Warren House Gill and appears to represent a localised remnant of an ancient deposit. It was deposited subaqueously, possibly in an estuarine environment, as indicated by the presence of pristine foraminifera. It shows no sign of a glaciomarine signature (as defined in Table 2.5), and so has been suggested to indicate a period of climatic amelioration prior to the deposition of the Blackhall Member above. It has suffered extensive glaciotectonic deformation, probably during the emplacement of the Blackhall Member. There appear to be no regional correlatives, and its provenance signature reflects that of the underlying Ash Gill Member, suggesting that it was formed by littoral reworking of the latter.

Blackhall Member

The Blackhall Member is recognised from Northumberland south to Sunderland (Eyles *et al.*, 1982), where it can be observed at Whitburn Bay (see Chapter 3), to its type locality at Blackhall Rocks, and beyond (see Chapter 6). It is locally variable and missing in places, perhaps due to erosion by an overriding ice sheet. It disappears somewhere south of Durham, and does not correlate with the tills present at Dimlington (cf. Eyles *et al.*, 1994; Evans *et al.*, 1995). The Blackhall Member in Whitburn Bay is coloured yellowish-brown due to erosion of the underlying bedrock. It is massive, but has been subjected in places to squeezing upwards (as pipes) into the overlying Horden Member (see Chapter 3.3.3, page 115).

In the buried palaeo-valley exposed in Hawthorn Hive, the Peterlee Member, consisting of coarse-grained, poorly-sorted glaciofluvial outwash and ice-contact debris flows, overlies the Blackhall Member. Some sandy deformed laminations are visible in the Blackhall Member at Hawthorn Hive.

The Blackhall Member (LFA 3 at Warren House Gill) was interpreted in Chapter 6 as a subglacial traction till. It is characterised by complexly glaciotectonised sands and gravels (LF 3c), folded sand beds (LF 3d), massive diamictons (LF 3a), thickly laminated clays (LF 3e) and laminated diamictons (LF 3f). Refer to chapters 6.5.3 and 6.7.3. The Blackhall Member was therefore deposited in a submarginal environment, with abundant meltwater present. At the base of the Blackhall Member at Warren House Gill, a sand bed,

now upturned by glacioisostatic folding, was deposited sub-aerially and then overridden, suggesting an oscillating ice margin. The laminated diamictons present within the lithofacies suggests that ponded water was a characteristic feature of this ice-marginal setting. The till here is overlain by fluvial, red-coloured sands and gravels. These occur at different heights, suggesting periodic switching on and off of fluvial processes as the sediment stack accumulated, reflecting local ice-marginal processes.

Horden Member

Whitburn Bay has the best exposures of the Late Devensian tills in this study. These complex, ice-marginal sediments incorporate numerous sand and gravel-filled subglacial channels, and are dissected by both hydrofractures and pipe structures. The Horden Member extends only a short distance inland (Smith & Francis, 1967), and the margin is marked by moraines and ice-contact slopes (Smith & Francis, 1967). It forms part of an ice-marginal, terrestrial, warm-based glacial landsystem. The upper till in Co. Durham is also interpreted as the Horden Member (Thomas, 1999; see Chapter 6), which has its type site at Warren House Gill (Francis, 1972). At this site, it is a massive, gravel-rich diamicton, but the height of the cliffs makes it very difficult to observe in detail. The Horden Member is interpreted in this study as an ice-marginal subglacial traction till (Chapters 3.4.2 and 6.7.4) derived from ice in northeastern Scotland, the Grampians, and the Cheviots, which flowed down the eastern coast of England as the North Sea Lobe. It is correlative with the Skipsea Member in Yorkshire (see Chapter 3.5.3, Table 3.6, page 145).

The Skipsea Member has been correlated previously with the Bolders Bank Fm, the uppermost till in the North Sea (Balson & Jeffery, 1991; Cameron *et al.*, 1992), the limits of which have been proposed to mark the extent of the latest Dimlington glaciation (Ehlers & Wingfield, 1991; Carr, 1999; Carr *et al.*, 2000). The western edge of the Skipsea Member forms the inland ice-extent, delineating the Dimlington limit around the Yorkshire Wolds (Figure 8.1).

The Bolders Bank Fm, immediately offshore of eastern England, has recently been interpreted as a subglacial till (Carr, 1999). Micromorphological analysis conducted in this study agrees that the samples from boreholes in the North Sea have the signature characteristics of a subglacially-derived till (see Table 2.5, page 50), including a well-developed masepic / skelsepic plasmic fabric, rotational structures with associated grain lineations, and a compacted, diamict matrix. Further detailed sedimentological and petrological analysis would be required in order to distinguish if there are in fact two tills

offshore; the two onshore tills are very similar and may have both been grouped into the Bolders Bank Fm. There is currently insufficient evidence to determine whether the Blackhall Member has a correlative offshore.

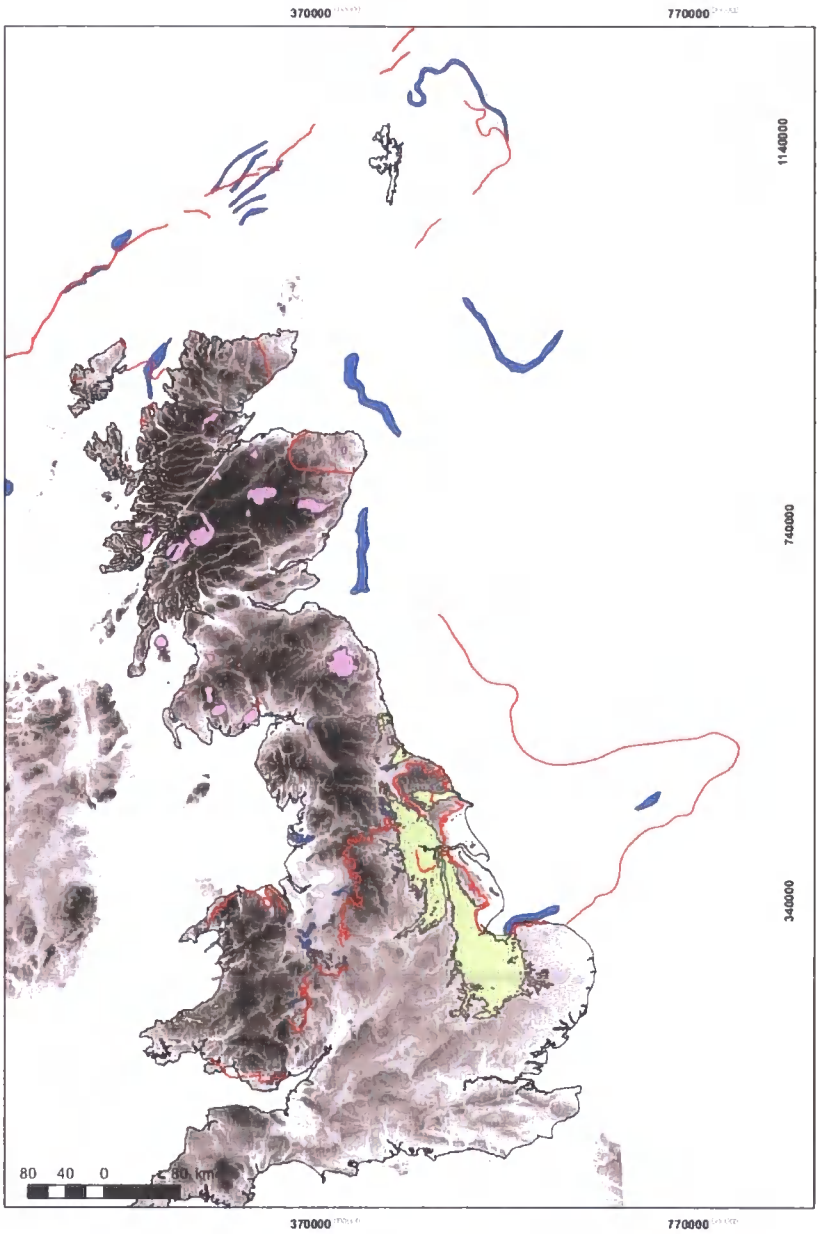

Figure 8.1: Dimlington Stadial ice limits proposed by BRITICE Map (From Clark et al., 2004a; Evans et al., 2005) and from the Olex dataset by Bradwell et al. (2008), over a topographical model. Red lines are ice margins. Blue areas are moraines; green areas are ice-dammed lakes, purple areas are erratic sources.

8.1.2 Statistical Analysis

Clast Lithological Analysis

Statistical analysis comparing the clast-lithological data from Warren House Gill, Shippersea Bay, Hawthorn Hive and Whitburn Bay reveals some interesting trends. Firstly, moving southwards from Whitburn Bay to Warren House Gill, the percentage of Magnesian Limestone in the Devensian Blackhall Member increases. The percentage of sandstone is higher in the more weathered samples at Hawthorn Hive and Shippersea Bay (as indicated by pedogenesis, oxidisation, the presence of roots, sediment dilation, and the removal of less durable lithologies and minerals (cf. Eyles & Sladen, 1981)). The Ash Gill Member and the Easington Raised Beach are typified by their comparatively high proportions of Cretaceous and igneous lithologies (Figure 8.2).

A correlation matrix of the data set showed that Cretaceous, sandstone and quartzose lithological groups were all strongly correlated. A ternary diagram of these three lithological groups highlighted the differences between the lithofacies associations (Figure 8.3). The second ternary diagram emphasises the differences in the tills in Whitburn Bay and in County Durham. The lower proportion of Permian lithologies and higher proportion of Carboniferous lithologies separates the Whitburn and the Warren House sediments, and is related to changing bedrock between the two locations (Figure 2.9, page 84). The beach gravels are differentiated by their very low percentages of sandstone or Carboniferous lithologies. Sandstone, a typical Carboniferous lithology, is also higher in the Blackhall and Horden members than in the Ash Gill Member (Figure 8.3).

In Figure 8.3B, it is clear that the Horden Member at both Hawthorn Hive and at Whitburn plots further to the left, due to its higher percentage of sandstone. The Horden Member at Warren House Gill consistently plots closer to the Blackhall Member.

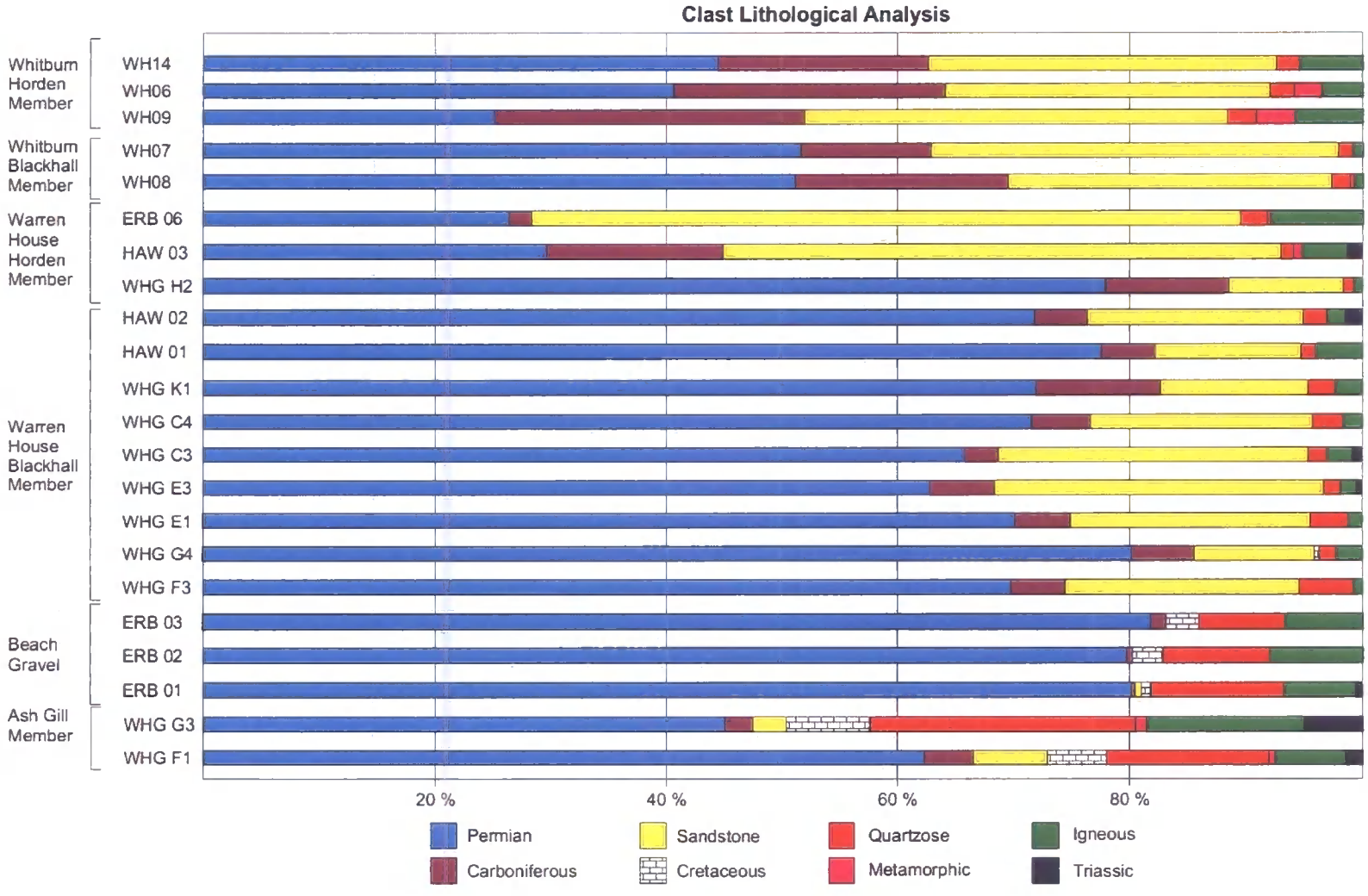

Figure 8.2: Clast-Lithological Data from this study. The Horden Member consistently has less Limestone and more Igneous material than the Blackhall Member.

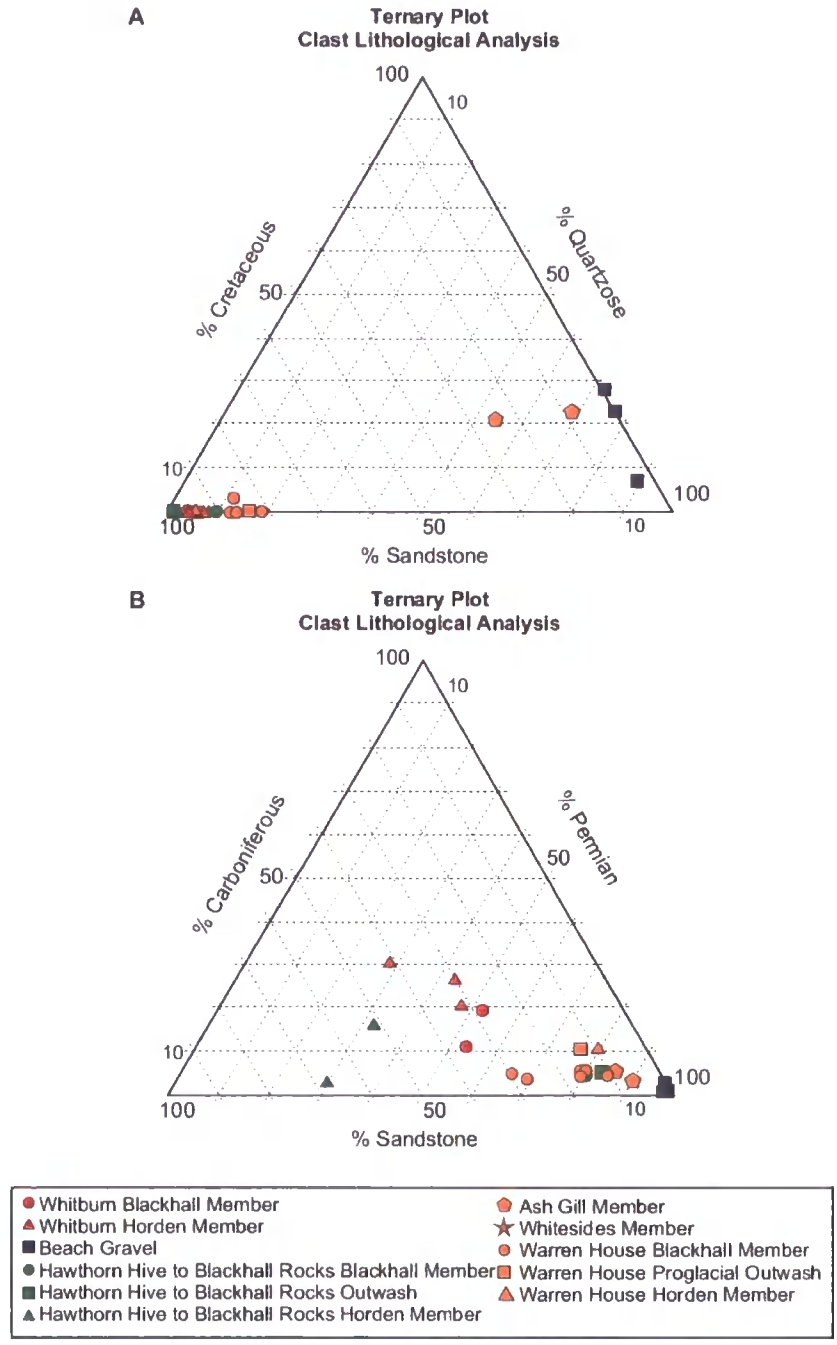

Figure 8.3: Ternary charts of clast-lithological analysis.

A PCA (covariance and correlation) was performed on the clast-lithological data. The PCA Covariance best highlighted the differences and similarities between the lithofacies associations, as the first component was more strongly loaded by fewer lithological groups. Component 1 is explained mostly by sandstone and by Cretaceous lithologies, and explains 60 % of the variance. The second component explains 17 % of the variance; therefore, the first and second components adequately represent most of the dataset. A scoreplot of both components (Figure 8.4) again clearly distinguishes between the Ash Gill Member, the

Easington Raised Beach, and the Blackhall and Horden members at Whitburn, but not between Devensian tills and the Ash Gill Member at Warren House Gill. The Devensian Tills at Whitburn are differentiated by their higher proportions of sandstone and lower proportions of Permian material. This is likely to be related to the relative positions of Warren House Gill and Whitburn Bay on the Permian bedrock; the ice lobes pass over greater distances of Permian material to the more southerly Warren House Gill (Figure 2.9).

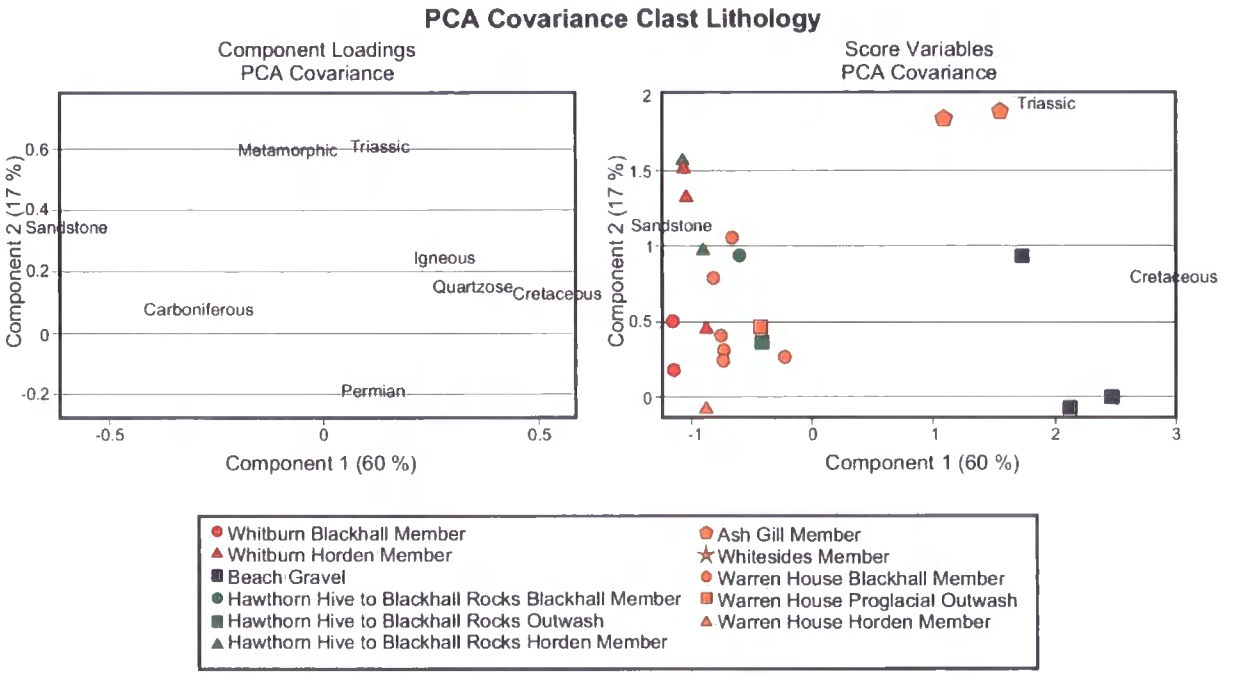

Figure 8.4: PCA Covariance on all clast lithological data.

A cluster dendrogram (Ward's Linkage) was constructed for all the clast lithological data (Figure 8.5). Two clear trends can immediately be discerned. Firstly, the Easington Raised Beach and the Ash Gill Member cluster closely together, and are clearly differentiated from the other sediments. The Whitburn tills are differentiated from the other sediments, and it is possible to discern the Blackhall Member (WH_1), and the Horden Member (WH_2), which clusters with the Horden Member from Shippersea Bay and Hawthorn Hive. Most of the middle till at Warren House Gill clusters independently (WHG_3), and the similarities with LF 4b (WHG_4) are highlighted.

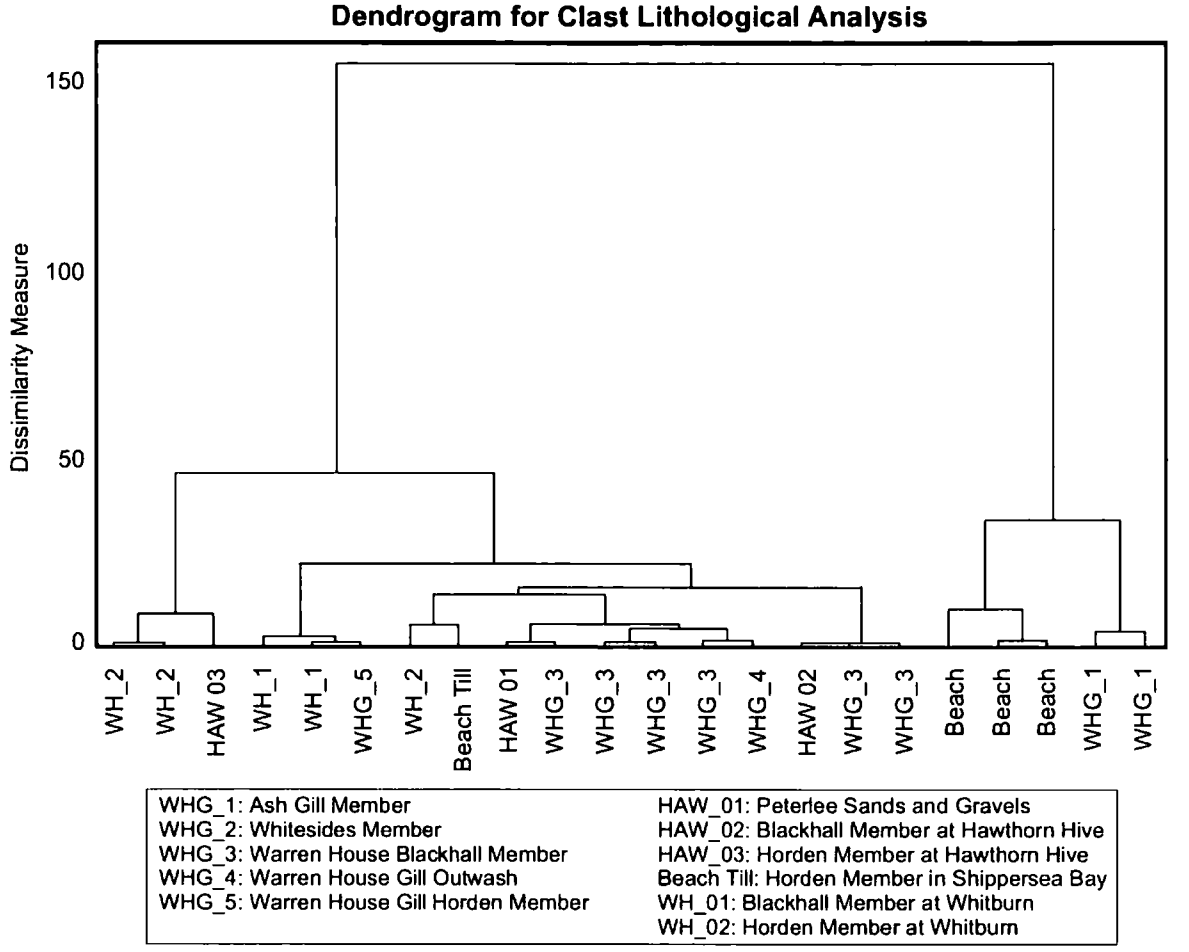

Figure 8.5: Cluster Dendrogram (Ward's Linkage) for all clast lithological data.

Heavy-Mineral Analysis

HMA allows comparison of offshore and onshore data, because sufficiently large numbers of mineral grains can be analysed from all samples. The analysis has identified some interesting trends, which will be explored in this section. Firstly, the apatite-tourmaline and monazite-zircon index identifies two overlapping groups (circled on Figure 8.6). The Whitburn sediments are not included here, as they contained no monazite. The Ash Gill Member plots with the offshore sediments, whilst the Devensian and other glacigenic sediments of Co. Durham cluster together. In all the plots, there is a certain amount of scatter in the data.

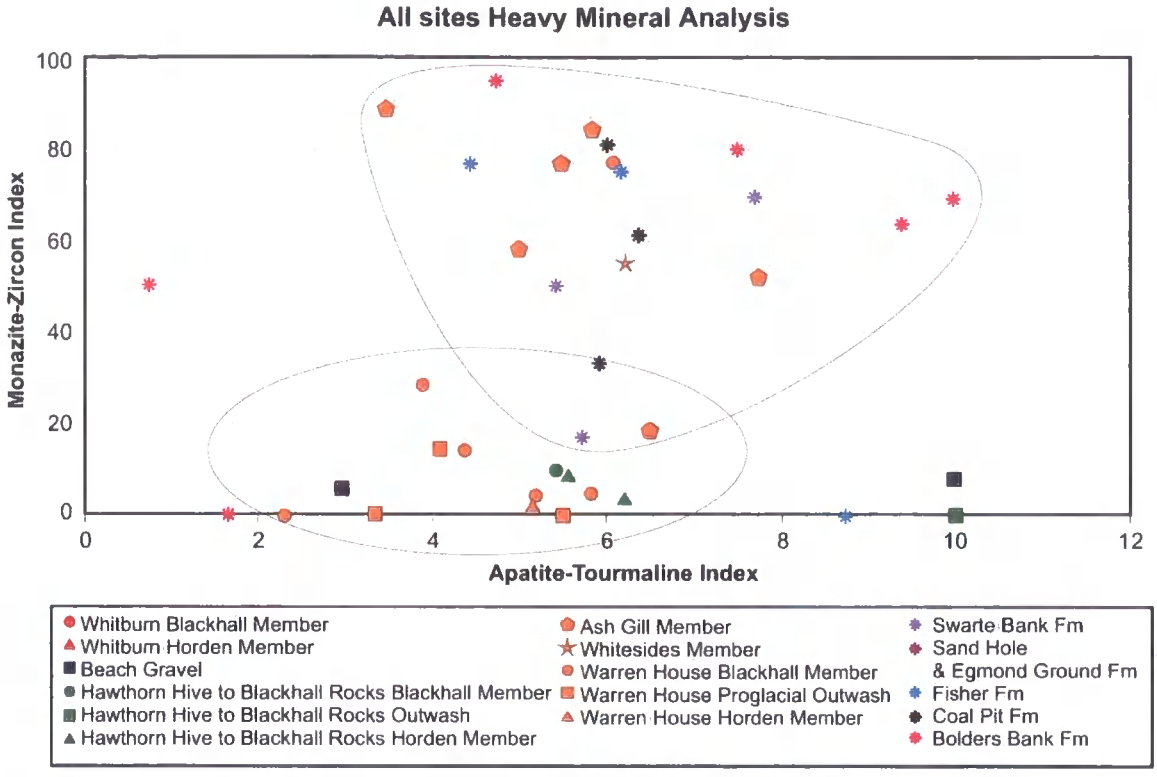

Figure 8.6: Heavy-Mineral Indices. Circles are drawn on to highlight groups.

To explore and to simplify the data further, the mineral phases were sorted into groups: silicates, epidotes, pyroxenes, amphiboles, micas, oxides, and phosphates. Carbonates were excluded from the analysis due to strong, unacceptable skew, and sulphides and sulphates were excluded due to very low numbers. A correlation matrix using all the variables showed a moderate correlation between pyroxenes, amphiboles, silicates and phosphates.

Ternary plots of these four correlated groups show a similar pattern. The samples in Ternary Plot A (pyroxenes, amphiboles and silicates) clearly fall into three distinct groups, highlighted on Figure 8.7. All the onshore glacigenic sediments plot closely together, except for the Ash Gill Member, which shows up as a distinctly separate cluster. This pattern in repeated in Ternary Plot B (Figure 8.7). In this chart, the Whitburn tills are shown to plot higher on the silicates axis. The offshore sediments and the Ash Gill Member are separated by their high amphibole content in both ternary plots A and B. This is further emphasised in Ternary Plot C, where the offshore sediments and the Ash Gill Member are separated by both the amphibole and phosphate content. These ternary plots therefore show that the proportion of amphibole and phosphate in these samples is a key

discriminating factor. The separate clusters of the offshore samples underline the importance of locally provenanced material in the North Sea.

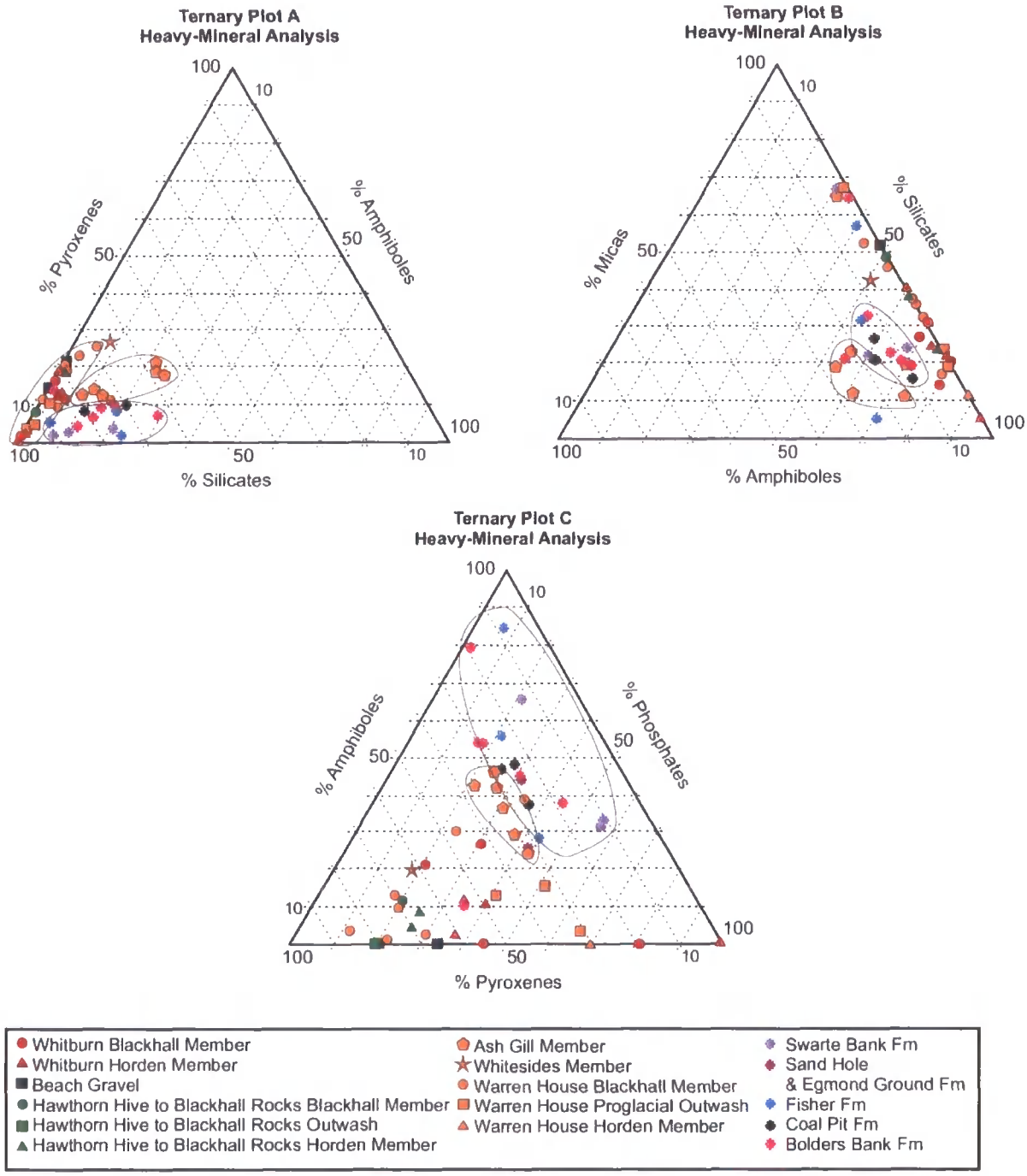

Figure 8.7: Annotated ternary charts of heavy-mineral analysis

A PCA (Correlation and Covariance) was performed on the data set. Only the correlation PCA is shown here as the correlation matrix failed to distinguish between lithofacies clearly. The first three components are shown; together they explain 75 % of the variation, and three components are adequate for representing the dataset. Component 1

comprises principally silicates, pyroxenes, amphiboles and phosphates. Component 2 is best explained by micas and oxides, whilst Component 3 is explained by epidotes, micas, and oxides. No one component is significantly loaded in any one particular variable. These loadings are illustrated in Figure 8.8.

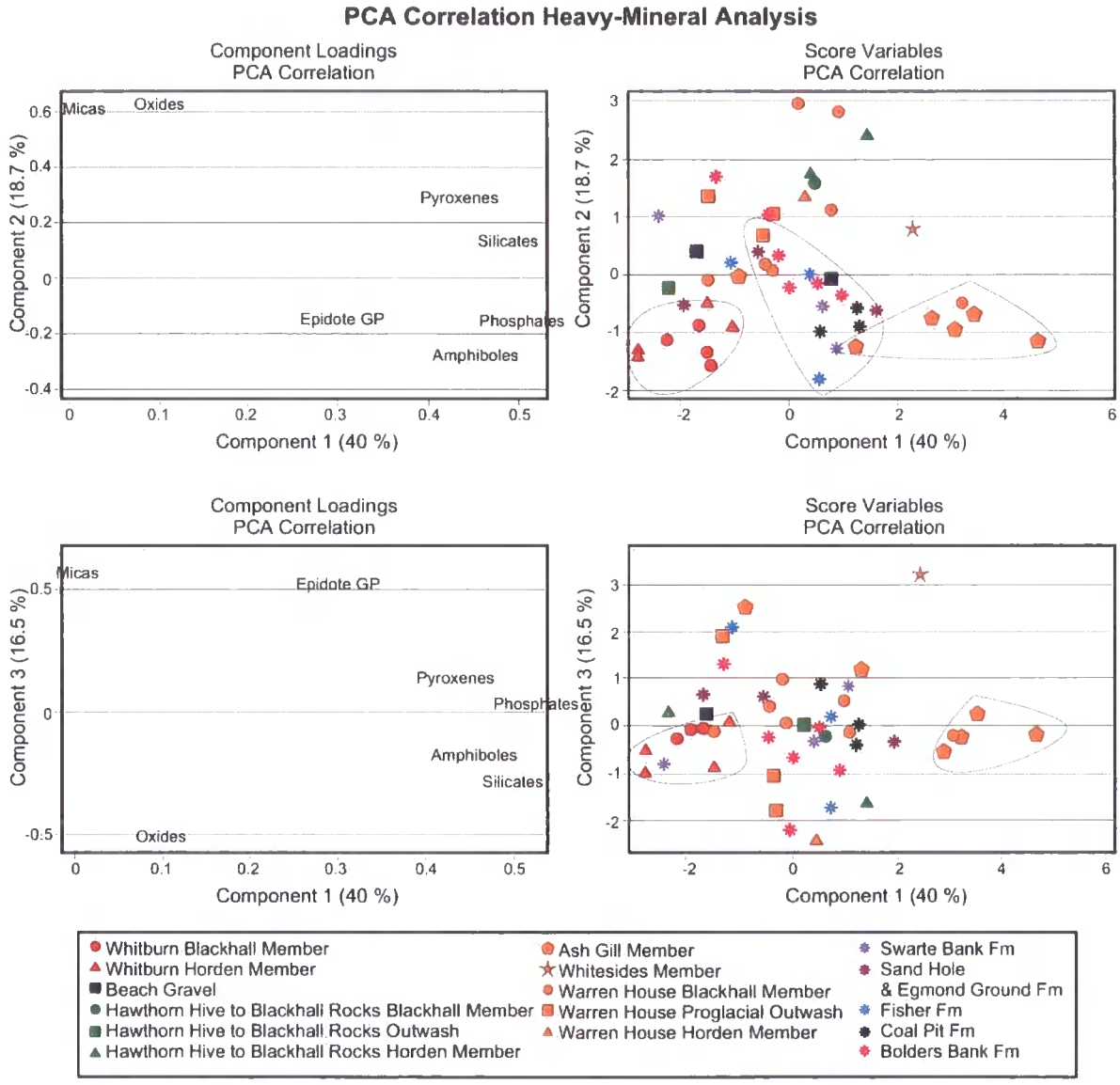

Figure 8.8: Annotated PCA Correlation on the heavy-mineral data. The first three components are shown.

In the scoreplots of components 1, 2 and 3, there is a clear pattern. The Whitburn tills group closely together, and the Ash Gill Member plots independently. The remaining samples cannot be distinguished into individual groups. This pattern is repeated in the

Component 3 / Component 1 scoreplot (Figure 8.8). The PCA clearly shows how the Scottish-derived tills plot together, and are differentiated from the Ash Gill Member, which has a Scandinavian influence. The high proportion of micas in the Whitburn tills contributes to their distinctiveness. One sample of the Ash Gill Member, WHG F1, plots as an outlier.

The cluster dendrogram (Ward's Linkage, Figure 8.9) identifies four distinct groups (annotated onto Figure 8.9). Group 1 are the Whitburn tills plus a few outliers from other groups. Group 2 are the Warren House Gill tills. Group 3 are the offshore sediments, and Group 4 is the Ash Gill Member samples. They form four tight, well-defined clusters. Again, WHG F1 plots as an outlier, and groups with the Bolders Bank / Coal Pit formations in Group 3, instead of with the Ash Gill Member in Group 4, due to the lower percentage of amphiboles in this sample. This could be due to the variable composition of the till matrix. WHG F1 was sampled much higher in the sequence than the other Ash Gill Member samples, and potentially was subjected to more mixing with the overlying Blackhall Member. A mixing hypothesis is supported, as the overlying WHG F3 sample consistently plots closely with the Ash Gill Member, and plots as an outlier in Group 4 in Figure 8.9 and in the PCA (Figure 8.8). These outliers also highlight the limitations of multivariate statistical analysis in discriminating between lithofacies.

The Whitburn and the Warren House Gill Devensian tills plot as two separate groups. This highlights the importance of changing bedrock lithologies, with Carboniferous rocks having a greater influence on the mineralogy of the Whitburn tills.

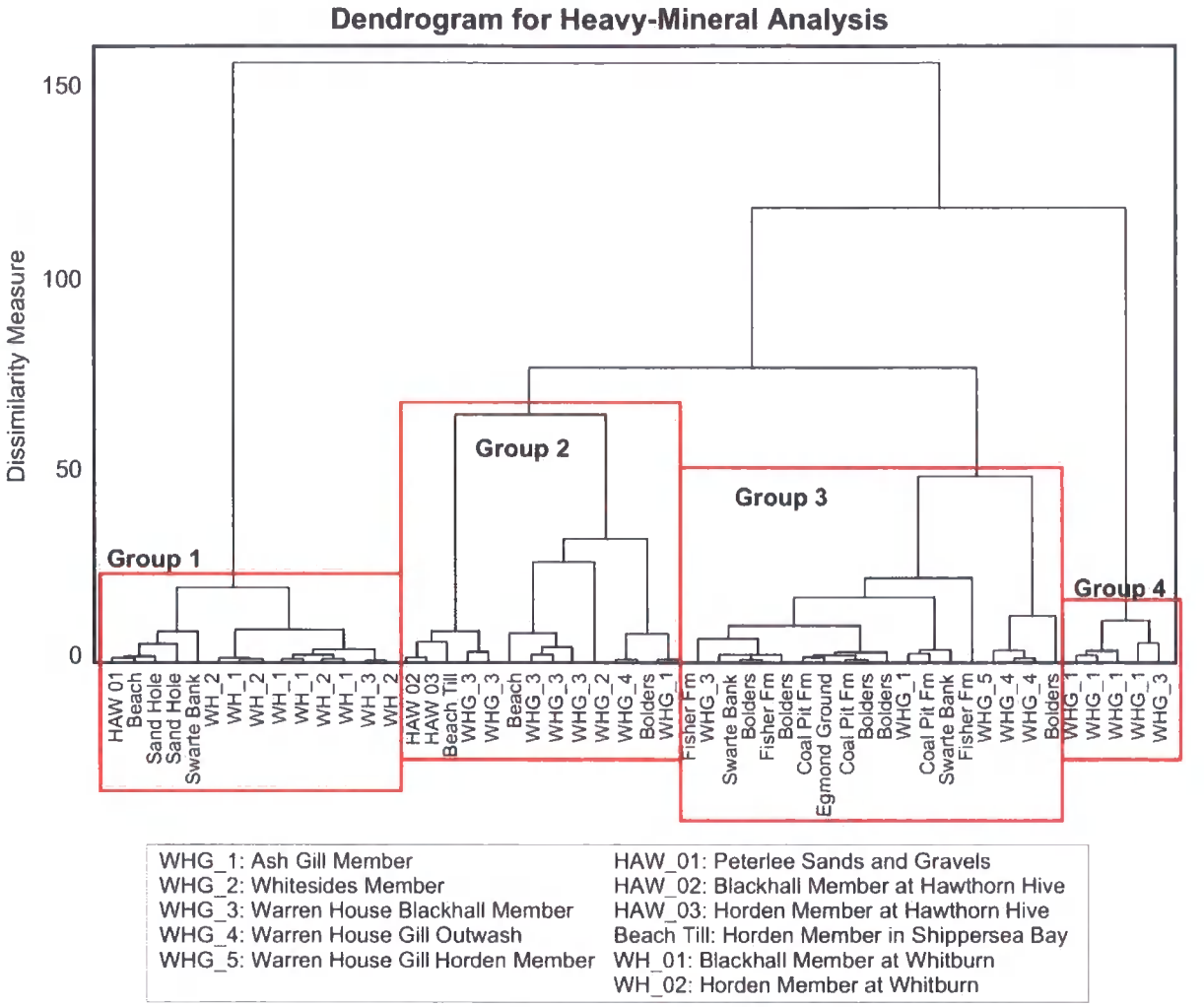

Figure 8.9: Cluster analysis (Ward's Linkage) for all heavy-mineral data.

On the basis of the various analyses of the heavy-mineral data, it is not possible to correlate any offshore sediments with any onshore sediments. The Whitburn tills are clearly differentiated from the Warren House Gill sediments. The Ash Gill Member shows its individuality in every analysis, apart from one outlier (WHG F3), which consistently plots closely to WHG F1 (see Figure 8.8 and Figure 8.9).

Geochemical Analysis

The PCA analysis of the abundant metals used the first three components, which together explain 83 % of the data. Component 1 is largely explained by titanium, whilst Component 2 is largely composed of potassium and aluminium. The variation in Component 3 is mostly explained by sodium, and secondarily by iron. The loadings of these components are shown in Figure 8.10.

The PCA and cluster analysis of the abundant elements in all the samples in this study shows considerable scatter. However, some clear patterns can still be discerned. The Bolders Bank Fm clusters to the left in scoreplot A (Figure 8.10), separated by its high Magnesium content. It clusters with the Swarte Bank Fm. This is repeated in both plot B and in the cluster dendrogram (Figure 8.11). Although the Whitburn and the Durham Devensian tills cluster together in a large group, they are not clearly differentiated from the Ash Gill Member. They also do not cluster clearly with any one offshore sediment. However, although there is scatter in the data, the Fisher Fm plots close to the Ash Gill Member.

The cluster dendrogram (Figure 8.11) identifies four groups. The first is the near-shore Bolders Bank Fm. This highlights the influence of the Scottish ice sources, with less influence of the Eocene and Cretaceous on the Bolders Bank Fm. This was deposited by the North Sea Lobe, and therefore was less influenced by more eastern bedrock lithologies. The second is a combination of the Ash Gill Member and the other offshore, older sediments. The third is composed of the tills at Whitburn Bay, and the fourth is the remaining tills at Warren House Gill.

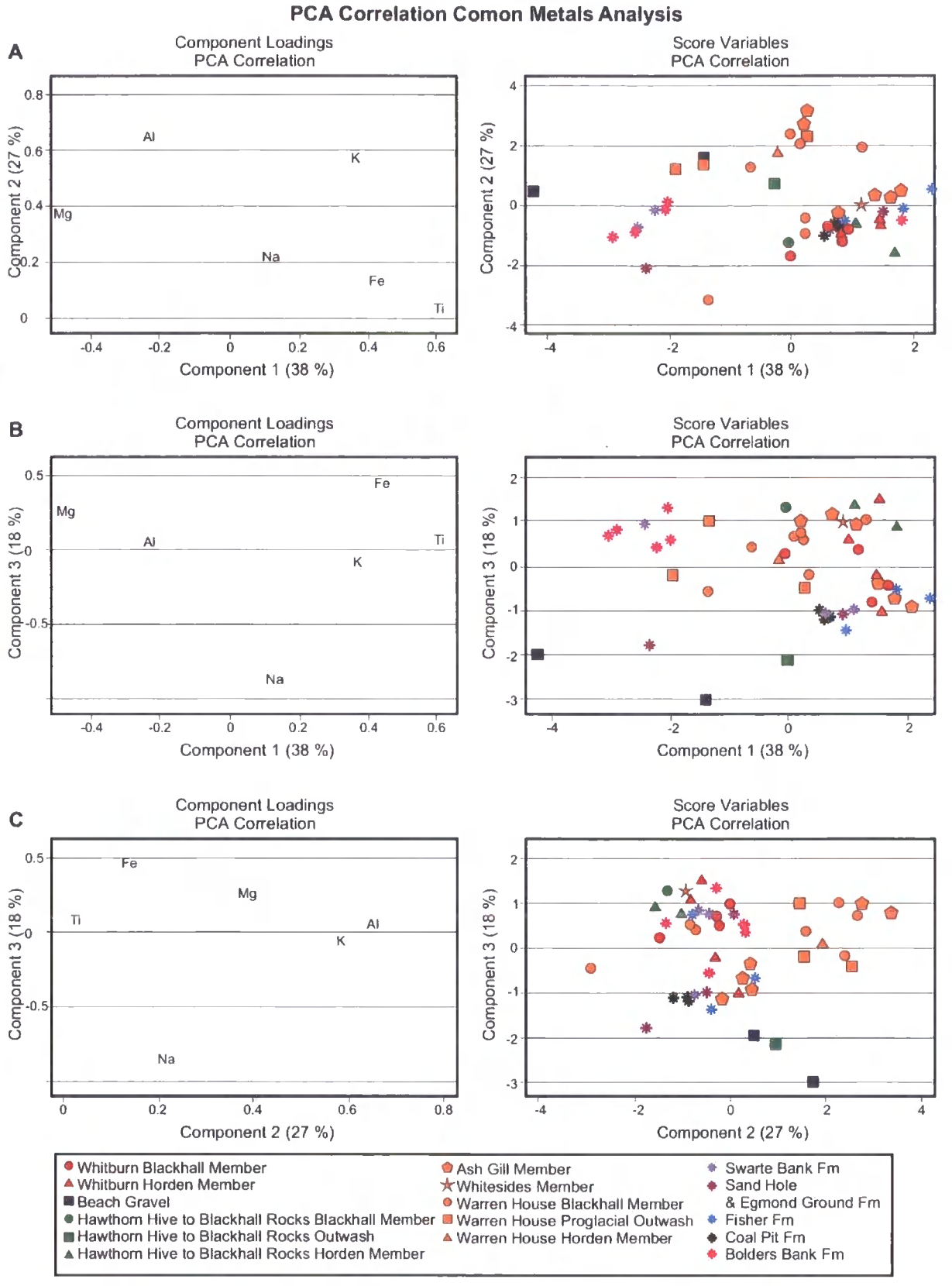

Figure 8.10: PCA Correlation, Common Metals Analysis

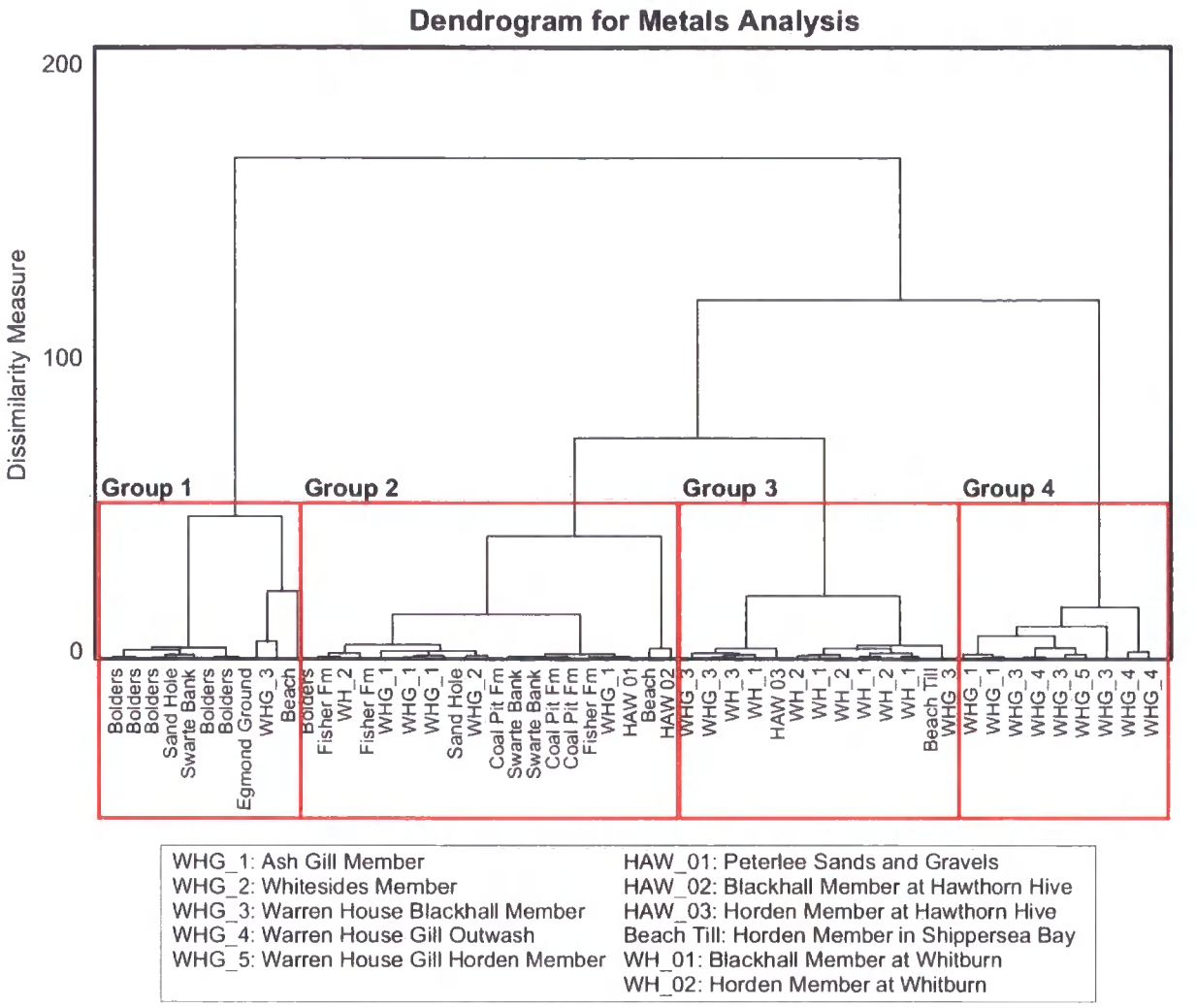

Figure 8.11: Cluster Dendrogram for abundant metals. Four groups are clearly distinguished, but they comprise a combination of lithofacies.

Summary

The statistical analysis of all the data from this project is at too low a resolution to identify onshore-offshore correlations with confidence. It was not possible to identify an offshore correlative for the Ash Gill Member, which is the only sediment with a clear Scandinavian signature. The heavy-mineral and clast-lithological analyses clearly illustrated its distinctiveness. The uniqueness of this deposit could perhaps be cited in support of the idea that it is a rare, old fragment, surviving in the bottom of a palaeovalley.

8.1.3 Onshore / offshore correlations

Difficulties with onshore / offshore correlations

It has been difficult to assign individual onshore lithofacies associations to offshore formations confidently. This had been noted previously by Cameron *et al.* (1992), as the seismostratigraphical offshore succession is difficult to compare with the onshore lithostratigraphical and biostratigraphical succession. Additionally, the onshore succession has been mapped in less detail than the offshore Quaternary sediments, and is likely to be far less comprehensive. In addition, chronostratigraphical control is poor both on- and offshore.

This study attempted to use process interpretations and lithological and petrological analyses to test accepted correlations and to identify possible new correlations. However, process interpretations from boreholes can only be very limited. The paucity of detailed sedimentological analysis compared to onshore section sites reduces the ability to identify sedimentary and glaciotectonic structures (Carr, 1999). Detailed sedimentological data is only available from thin-section analysis, as the narrow boreholes exclude much sedimentological data. Deformation and contamination may also be induced during coring.

Secondly, the varying bedrock lithologies on and offshore make precise geochemical correlations difficult. For example, Warren House Gill is located further south than Whitburn Bay, and they are separated by a considerable stretch of Magnesian Limestone bedrock. This is reflected in the clast-lithological data, in which the proportion of Magnesian Limestone is less at Whitburn Bay than in the Devensian tills between Hawthorn Hive to Blackhall Rocks; this is to be expected, as Whitburn Bay lies only just within the boundaries of the Magnesian Limestone bedrock (Figure 2.9).

The offshore sediments contain very little directly dateable material. Additionally, any glaciomarine sediments would have been deposited into deep and possibly turbid water, excluding OSL analysis (which is also excluded for the Ash Gill Member). The onshore sediments also lack dateable organic material. Some of the sorted sediments are appropriate for OSL dating, but without a reliable and robust offshore chronostratigraphy, it is difficult to apply this data to the offshore succession. The statistical analysis (PCA and cluster analysis) is not efficient enough to distinguish between the onshore Scottish tills or between the offshore successions.

Quaternary Stratigraphy in northeastern England and the North Sea

Due to the dating difficulties experienced in this study, it is not possible to assign firm ages to the sediments exposed in the coastal cliff sections in County Durham. However, a

stratigraphy can be constructed that places the Ash Gill Member earliest in the sequence as a Middle Pleistocene glaciomarine sediment (Table 8.1). The age is constrained by the Middle Pleistocene AAR ages on the shell fauna, the interglacial Whitesides Member, the overlying 80 ka BP Blackhall Member, the inferred older age than the Easington Raised Beach and correlation to the Briton's Lane Sand and Gravels. Although the shell fauna in the Ash Gill Member was difficult to date precisely by AAR, it shows an age consistently older than MIS 9-11 (refer to Chapter 6.4). The flint erratics in the Easington Raised Beach could have been derived from another, older sediment, subsequently removed by erosion, so this cannot be used to date the Ash Gill Member confidently. However, the combined evidence is highly suggestive of a Middle Pleistocene age for the Ash Gill Member.

Table 8.1: Summary of Quaternary Stratigraphy in Co. Durham.

County Durham		Process	Regional Correlatives	Chronostratigraphy
East Durham Formation	*Horden Member*	Subglacial Till	Skipsea Member Bolders Bank Fm	MIS 2 (after 21.7 cal. ka BP)
	Peterlee Member	Outwash sediments	-	Post 80 ka BP
	Blackhall Member	Subglacial Till	? Bolders Bank Fm or Cape Shore Fm?	?80 ka BP (MIS 4) to MIS 2
Easington Formation		Beach	-	MIS 7
Warren House Formation	*Whitesides Member*	Estuarine sediments	-	Post MIS 8-12
	Ash Gill Member	Glaciomarine diamicton	Briton's Lane Fm (MIS 12)	?MIS 8-12

8.1.4 Summary

The Ash Gill Member does not appear to have a correlative in the immediate offshore region, suggesting that it is simply a fragment, protected in the base of a palaeovalley, and that all other deposits of comparable age have been removed by subsequent erosion. This study accepts previous suggestions that the offshore Bolders Bank Fm is correlative with the Skipsea Member (Balson & Jeffery, 1991; Catt, 1991a), and argues that the Horden Member, not the Blackhall Member, is the County Durham correlative of the Skipsea Member (see Chapter 3). Far more research is required at a high resolution to comprehend the offshore stratigraphy better.

8.2 Implications for British and Fennoscandian Ice Sheet Interactions during the Quaternary

The onshore and offshore sediments analysed in this study have provided a means to analyse the dynamic and sensitive nature of the northwest Atlantic margin, and their rapid responses to climatic change during the Quaternary. This section attempts to create a coherent model of British and Fennoscandian interactions throughout the Quaternary, by taking a holistic approach and incorporating new findings from this study with published research in Britain, the North Sea and in Europe.

8.2.1 Middle Pleistocene

MIS 12

The complex glacigenic sediments in north Norfolk provide strong evidence of an MIS 12 glaciation (Hamblin *et al.*, 2005). The Lowestoft and Swarte Bank formations both indicate an extensive British, Scottish-sourced ice sheet (Fish & Whiteman, 2001). Provenance work in this project indicates that the Swarte Bank Fm was deposited by an ice-sheet with accumulation areas in the northeastern Scottish Highlands, showing input from the Dalradian and the Midland Valley of Scotland. These sediments infill tunnel valleys in the NSB, and represent a sediment deposited at the ice-bed interface. The Lowestoft Fm is overlain by the mixed Scottish-Norwegian Briton's Lane Fm (Hamblin *et al.* 2005), which Pawley *et al.* (2008) recently dated to MIS 12 using OSL, and which is tentatively (lithologically) correlated with the Ash Gill Member (see Chapter 6). This suggests that after the recession of the main BIIS, the Fennoscandian Ice Sheet offshore was still large and active. The Scottish-Norwegian provenance of both the Ash Gill Member and the Briton's Lane Fm indicates that large ice sheets sourced in Britain and Fennoscandia were active in the British sector of the NSB during MIS 12. After initial recession, large proglacial rivers were active, carrying material derived from both ice sheets. After continued recession, both Scottish and Fennoscandian icebergs calved into a glaciomarine embayment in the modern North Sea Basin.

The MIS 12 glaciation was a significant event in continental Europe, with glaciers sourced in Norway extending into the European lowlands and into the North Sea Basin. The Elsterian (MIS 12) is considered to have been the most significant and extensive

glaciation in Germany (Figure 8.12), where there is evidence to at least two substages, each resulting in a large-scale readvance (Eissmann, 2002). The Elsterian age of the tills is constrained by river terrace chronology (Bridgland *et al.*, 2004). The sediments are overlain by Holsteinian lake sediments in a few localities, and then ubiquitously by Saalian (MIS 6) glacial sediments (Eissmann, 2002). In the northern Bohemian Massif, Elsterian ice sheets advanced into the Czech Republic. Here, there is evidence of two advances, with no intervening interglacial deposits (Šibrava, 1982).

The Elsterian in the North Sea Basin is recorded by the Swarte Bank Fm, which lies in the base of numerous tunnel valleys (Praeg, 2003). These vast swathes of tunnel valleys (Figure 8.12) provide evidence for extensive glaciation (Kristensen *et al.*, 2007). A two-stage Elsterian glaciation in Norway has significant ramifications for the interpretation of Middle Pleistocene glacial sediments in Norfolk. Chronostratigraphy here remains poor, and tills controversially dated to MIS 16 could in fact be related to a two-stage MIS 12 glaciation.

In Finnmarksvidda, northern Norway, there is a rolling plain with Quaternary deposits, including till beds and interglacial deposits and soils, representing glaciations in MIS 8 and 10. In Jæren, the lowlands in southern Norway, there are glacial and interglacial deposits from MIS 10 upwards (Mangerud, 2004).

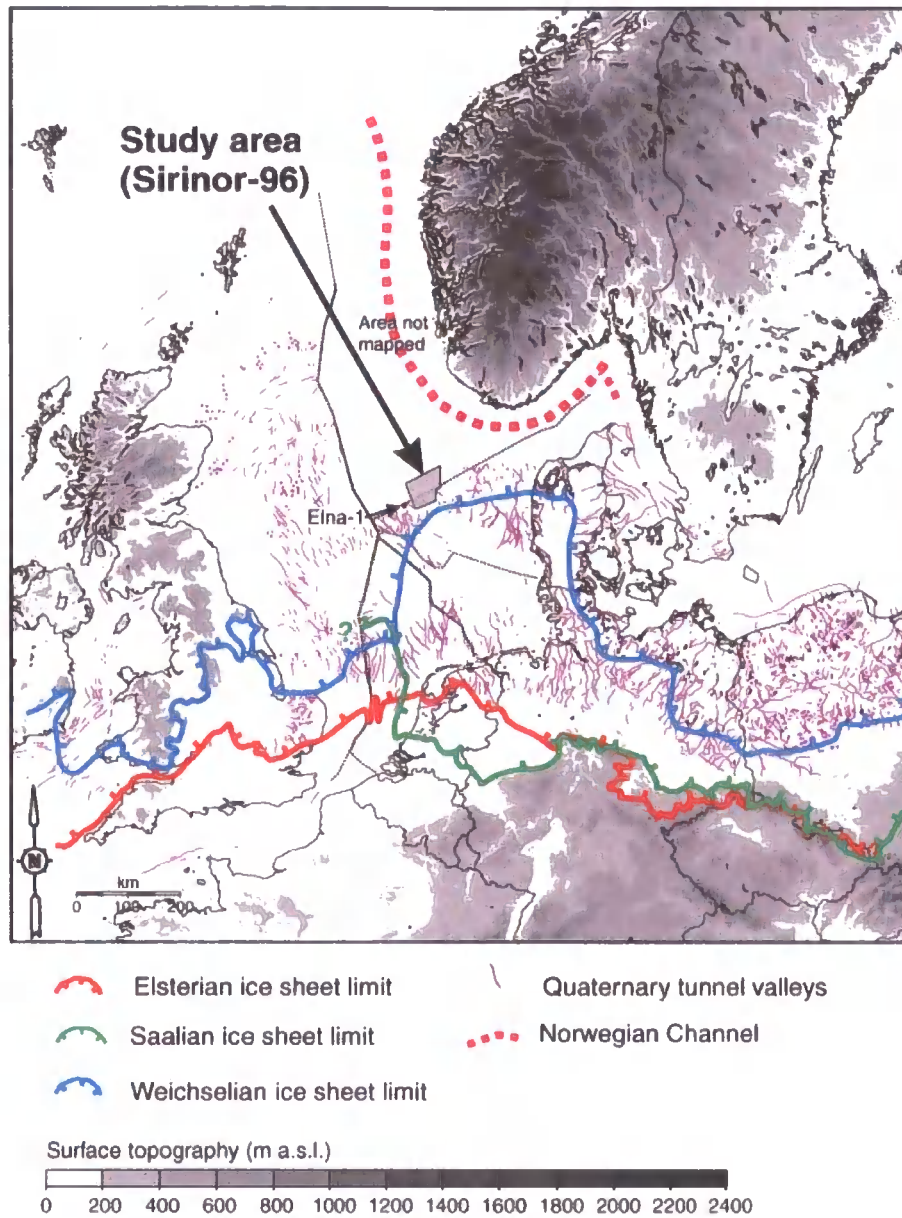

Figure 8.12: Pleistocene ice limits in northwest Europe and tunnel valleys in the North Sea Basin. From Kristensen et al., (2007).

MIS 6

There is strong evidence that the Fennoscandian Ice Sheet reached the coast of eastern England at this time, in the Bridlington Member of east Yorkshire (Catt & Penny, 1966; Catt, 1991b) and the Welton Till from east Lincolnshire (Alabaster & Straw, 1976; Straw, 2005), as these sediments both contain Scandinavian erratics. The Bridlington Member has been attributed to MIS 6 because it is overlain by the Sewerby Raised Beach, which has been dated to MIS 5e based on faunal remains (Bateman & Catt, 1996; Catt, 2001b). The age however remains poorly constrained, and the Bridlington Member could be as old as

MIS 12. There is additional evidence for Scandinavian ice in the central North Sea in MIS 6 in the form of the Cleaver Bank Fm (Gatliffe *et al.*, 1994), which, unfortunately, it was not possible to sample in this study. This formation occurs beneath the Dogger Bank as an 8 m thick tabular body of stiff, laminated dark grey clays with scattered angular granules of chalk and chert, with intercalations of micaceous sands. It is a partly marine, partly proglacial diamicton of eastern provenance. It laterally transforms into the subglacial, Saalian, Borkumriff Formation, east of 4°E (Gatliffe *et al.*, 1994; Rijsdijk *et al.*, 2005). This formation provides additional evidence for coalescence of the BIIS and FIS during the Saalian. The MIS 6 limit is poorly constructed in the North Sea, but was drawn by Svendsen *et al.*, (2004) as below (Figure 8.13).

Evidence for a Scottish-sourced MIS 6 glaciation is limited. The glaciomarine Fisher Fm provides evidence of a Scottish ice sheet calving into the NSB during the Middle Pleistocene; however, the chronostratigraphy remains poor (see Chapter 6). Again, the northeastern Scottish Highlands are shown to be an important ice-accumulation area. The Cromer Ridge in Norfolk has been attributed by some to MIS 6 (Hamblin *et al.*, 2005), but recent OSL dating has suggested that these sediments are in fact of MIS 12 age (Pawley *et al.*, 2008). Straw (1979) argued that a Wolstonian glaciation covered much of Lincolnshire, and extended southwards to Norfolk and Suffolk, but age limits remain poorly constrained. None the less, the sequence at Welton-le-Wold has often been regarded as likely to include deposits of post-Anglian, pre-Devensian glacial sediments (Straw, 1979; Straw, 1983; Lewis, 1999; Straw, 2005).

The MIS 6 glaciation in the Netherlands and Germany is widely acknowledged to have been particularly extensive, with ice sheets extending southwards and eastwards from Norway (Ehlers *et al.*, 1984; Baumann *et al.*, 1995; Eissmann, 2002; Houmark-Nielsen & Gibbard, 2004). This Saalian glaciation was presumably coalescent with the BIIS (Figure 8.13). This is supported by the presence of tunnel valleys offshore (Huuse & Lykke-Andersen, 2000; Praeg, 2003). An extensive MIS 6 continental glaciation would imply that the MIS 6 glaciation was also prominent in Britain (as suggested in Figure 8.13), and that the evidence has largely been eradicated by subsequent glaciation during the Devensian.

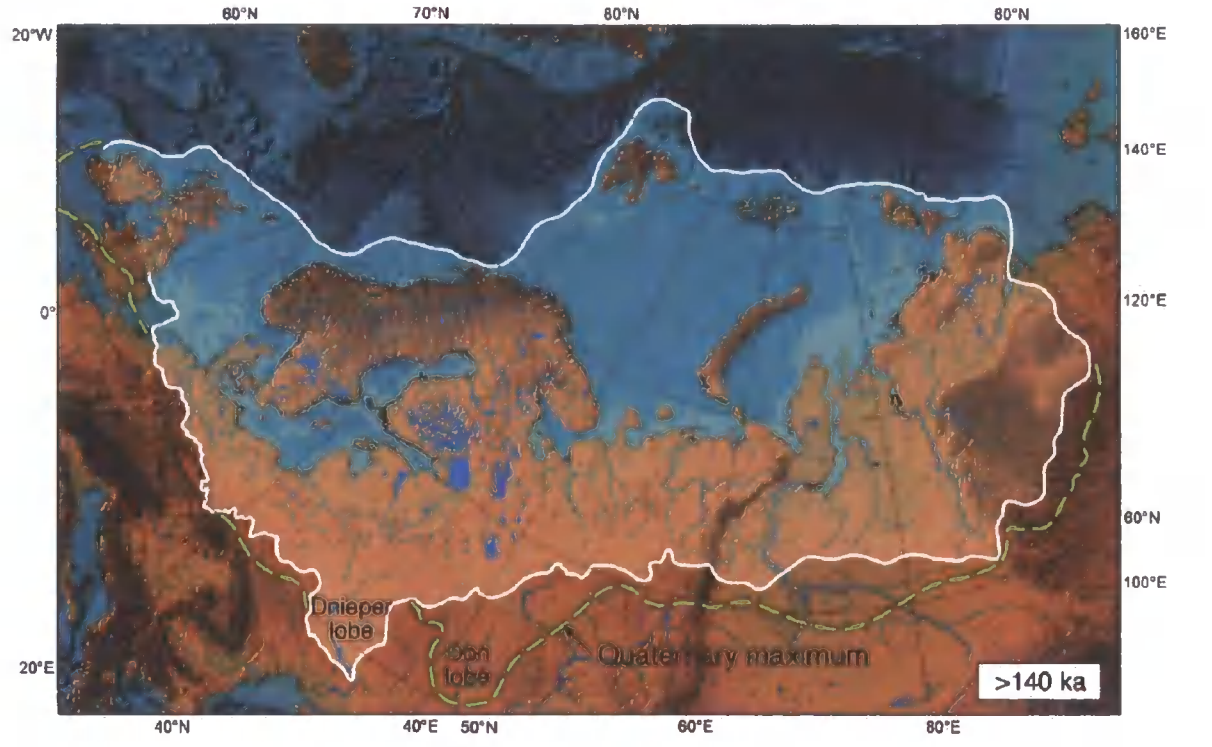

Figure 8.13: Saalian ice sheet limits in Europe. From Svendsen et al., (2004).

Eissmann (2002) noted that the Main Terrace Complex of the Rhine in Germany preserves evidence of two Saalian advances, separated by at least one pronounced warming event. These are the Warthe, a younger advance correlated to MIS 6, and the Drenthe, an older advance correlated to MIS 8. In Scandinavia, the first Drenthe advance was from the north, and this ice sheet covered the whole of Denmark. The second Warthe glacial advance was from the Baltic area (Lundqvist, 1987). Significant features of the Late Saalian were extremely low winter temperatures, and a two-step deglaciation (similar to the Younger Dryas in the British Late Glacial) marking the transition into the Eemian (Biñka & Nitychoruk, 2001). The complexity of Middle Pleistocene glacial sediments on the continent suggests that the British sequence is far from complete.

8.2.2 The Early to Late Devensian

The Blackhall Member was deposited by an ice sheet flowing out from eastern England. This was sourced in the Grampian Highlands, and flowed southwards through the Midland Valley of Scotland and the Tyne Gap (Harmer, 1928; Beaumont, 1967; Francis, 1972). It overwhelmed and deflected flow from the Lake District ice cap, as a result of

which, there is no evidence of Lake District or Cheviot erratics within the Blackhall Member. The North Sea Boreholes have only distinguished one till within the Bolders Bank Fm, but it is possible that careful and detailed heavy-mineral and geochemical work would separate two superimposed tills within this formation, such as is recognised on land. The North Sea Lobe may also have removed much of the Blackhall Member offshore, and incorporated it into the Horden Member.

The age of the Blackhall Member remains contentious, and it is subject to further OSL analysis. However, it is possible that it was deposited during an early to middle phase of the Devensian BIIS, possibly during the Ferder Episode in MIS 4 or the Cape Shore Fm at the LGM (Figure 7.6), as defined by Carr *et al.*, (2006). Deposition of the Blackhall Member may have continued for a considerable time, before a period of retreat and quiescence, during which time the glaciofluvial Peterlee Member and the proglacial Durham Member lake sediments were deposited (Thomas, 1999). At Whitburn Bay, there is no evidence for deglaciation between the deposition of the Blackhall and Horden members. This suggests an MIS 2 age for both of these, and presents problems for stratigraphic correlation with Warren House Gill. The error terms on the OSL date for the Blackhall Member are very large, and an MIS 4 age for the entire Blackhall sequence is chronologically insecure. It is possible that the Blackhall Member at Warren House Gill encompasses sediments deposited over a long period of time, extending from MIS 4 to 2, with ice occupying the Tyne Gap for the duration of the Devensian glaciation. Repeat ice-flow pathways would result in a very similar sedimentological signal for the sediments at the top of the member and those preserved in the palaeovalley at Warren House Gill. It is therefore possible that the MIS 4 age on the sand fold represents a fragment of older sediment, preserved in the palaeovalley, in a manner similar to the Warren House Formation.

The Blackhall Member was subsequently overridden by the North Sea Lobe, which deposited the Horden Member. The lower percentages of Permian lithologies in the Horden Member indicate that it was protected from the bedrock by a mantle of till. There is no southern equivalent of the Blackhall Member, indicating that the ice lobe that deposited it flowed eastwards into the North Sea Basin, and did not extend southwards.

Early and Middle Weichselian (MIS 5d to 4) glaciations are poorly known in the UK, in mainland Europe and in the North Sea Basin. There is possible evidence of an MIS 4 glaciation in east Lincolnshire and east Yorkshire (Clark *et al.*, 2004b), with glacial

deposits and glacial meltwater landforms associated with tills that are younger than the Ipswichian (MIS 5e). They are associated with lacustrine and fluviatile sediments that have been dated to earlier than the Middle Devensian. There is also evidence of an extensive MIS 4 glaciation in Scotland, with more extensive MIS 4 deposits separated from less extensive MIS 2 deposits (Bowen, 1999a).

Lundqvist (2004) argued that the first Weichselian glaciation in Sweden occurred in MIS 5d. It was warm-based, and highly erosive. The ice sheet was centred in the Kjolen mountain region and was controlled by a maritime climate, the result of a warm ocean in the Eemian. Mangerud *et al.* (1996) noted that at the Fjøsanger site, a glaciomarine silt shows that the glacier reached within 1-3 km of the coast during MIS 5d. Above this silt are deposits of the milder Fana interstadial, which are correlated with the Brørup Interstadial, and the thick Bønes Till, which is correlated with MIS 5b (Šibrava, 1987).

From MIS 4 to 2, all of Sweden was glaciated. The ice front may have reached southern Sweden by MIS 4. The Baltic ice stream reached the European continent in MIS 4, and southeastern Denmark by late MIS 3 (Lundqvist, 2004). The Karmøy Diamicton at Bø in Norway was placed in MIS 4 by Baumann *et al.* (1995), based on the underlying Torvastad and the overlying Bø Interstadial deposits.

Returning to more general issues, recent research within the central sector of the BIIS has highlighted complex flow phasing and changing ice divides during the Devensian (Livingstone *et al.*, in press). Eight phases of flow were recognised by Livingstone *et al.* (in press) in the central BIIS during the Devensian. The first refers to when the ice was sufficiently thick to cross the Pennines, and to flow eastwards through the Tyne Gap, with a significant influence of Southern Uplands ice, and less influence of Lake District ice. This flow phase, with minimal Lake District influence, and strong Scottish and Pennine influence (*ibid.*), resulted in ice reaching the Durham coast, and the deposition of the Blackhall Member (Figure 3.14). A key point is the lack of Lake District erratics in the Blackhall Member in County Durham, indicating that ice in Durham from the Tyne Gap was mainly sourced from Scottish ice sources. Later drawdown into the Irish Sea Basin resulted in a major flow switch, cutting off the Tyne Gap (Livingstone *et al.*, in press). This would have encouraged downwasting and recession in eastern England, allowing the east-coast ice to become dominant, with proglacial lakes forming between the two ice lobes.

The Blackhall Member at Warren House Gill and at Whitburn Bay contains detrital material sourced from the Grampian Highlands, Buchan, and from the eastern Highland

Boundary Fault. Chloritoid in particular is derived only from the Highlands of Scotland. It is a non-durable mineral (Morton & Hallsworth, 2007), so reworking is unlikely. Current published flowlines (see Figure 8.15) do not allow ice to flow southwards from Buchan and Stonehaven. There are two possibilities; either the published flowlines are inaccurate, and ice from Scotland did reach eastern England, as shown with the queried orange arrow on Figure 8.15 (MIS 4), or the detrital material in the eastern England till is reworked and contains recycled sedimentary minerals. Flowlines are very poorly developed for MIS 4, and there is poor chronological control for this glacial event. Many of the ice streams that operated during MIS 2 (including the Strathmore Ice Stream) may not have been active at this time. This work therefore provides key new evidence in constraining the flow dynamics of the BIIS during MIS 4 to MIS 2.

8.2.3 The North Sea Lobe

Research in Russia and Europe has indicated that the Late Weichselian Fennoscandian Ice Sheet was the largest since the Late Saalian (Svendsen *et al.*, 2004), where the limit is defined by fresh moraines and a hummocky landscape (Figure 8.14). Some researchers have argued that the limit was more restricted in the Russian Plain than in other glaciations (Krasnov, 1971; Svendsen *et al.*, 2004). The Devensian maximum limit was reached at around 29 cal. ka (Sejrup *et al.*, 2009). At 26890 – 277690 cal. yr BP, the British and Fennoscandian ice sheets were still conjoined in the NSB (Svendsen *et al.*, 2004; Sejrup *et al.*, 2005; Sejrup *et al.*, 2009), with separation at around 25 cal. ka, possibly as a result of sea level rise. At the LGM, the FIS reached the Norwegian shelf edge along its entire length, from the mouth of the Norwegian Channel to North Cape (Mangerud, 2004).

The onset of Late Weichselian glaciation in Estonia dates after 20-22 cal. ka BP. Mammoth bone remains indicate that the SIS did not reach eastern Finland prior to 22.5 cal. ka BP, whereas the LGM in Poland occurred after 21 cal. ka BP and in Denmark at around 22 cal. ka BP (Kalm, 2005). A large ice sheet formed over the north-western Barents Sea Shelf at the LGM, but the southern and eastern extension of this ice sheet has been difficult to determine accurately (Svendsen *et al.*, 2004). This highlights the spatial and temporal variability of the Eurasian ice sheet, and signifies the difficulties in correlation between different places.

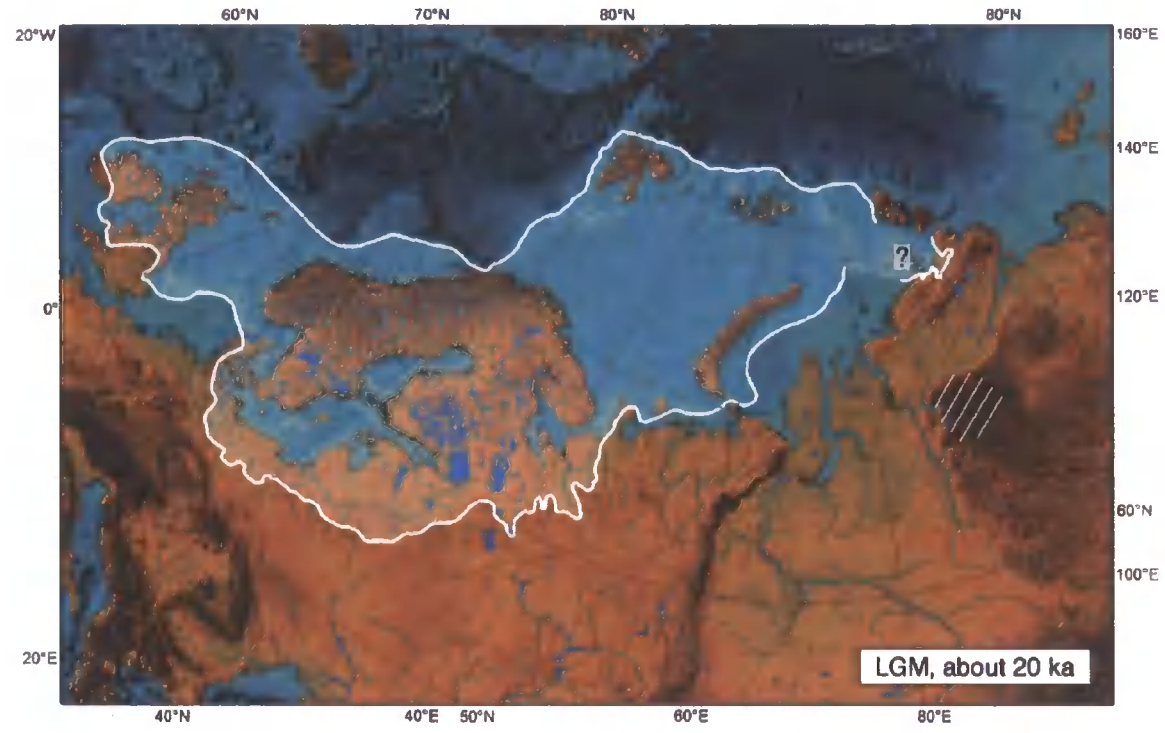

Figure 8.14: Extent of the European ice sheet at 20 cal. ka BP. From Svendsen et al., (2004).

The North Sea Lobe was an important and major artery of ice flow during the Late Devensian BIIS, and was plainly influenced by the FIS in the North Sea Basin. The North Sea Lobe was sourced in the Scottish Highlands, and combined ice from the Southern Uplands and ice flowing eastwards out of the Midland Valley of Scotland (Figure 8.15). Further south, it coalesced with the Tweed ice stream (Everest *et al.*, 2005; Mitchell, 2008), where drumlins and glacial lineations clearly show a sharp change in direction (Raistrick, 1931). The North Sea Lobe deposited a subglacial till that stretches from Northumberland southwards, and consistently shows a trend to flow onshore (Beaumont, 1967; Eyles *et al.*, 1982; Teasdale & Hughes, 1999). The offshore lateral margins are taken as the limits of the Bolders Bank Fm (Catt, 1991a; Ehlers & Wingfield, 1991).

The shape the North Sea Lobe (see Figure 8.1) is normally taken as the boundary of the Bolders Bank Fm in the North Sea Basin (Balson & Jeffery, 1991; Catt, 1991a; Gatliffe *et al.*, 1994; Carr *et al.*, 2006). The Bolders Bank Fm is overlain by the Dogger Bank (Carr, 1999), which creates a region of upstanding relief. It comprises clay-rich, stratified and laminated diamictons. It has a fauna indicative of glaciomarine conditions. It is incised by channels infilled with diamictons, which are orientated normal to the margins of the deposit. Gatliffe *et al.* (1994) therefore suggest that the Dogger Bank is a waterlain deposit, formed close to the margin of a grounded ice sheet. It largely underlies the Bolders Bank

Fm The hypothetical configuration of the FIS, as demonstrated in Figure 8.15, suggests that it is likely to be a recessional, thrusted, glaciomarine complex, possibly representing waters trapped between the two ice sheets in the North Sea Basin during the Late Devensian. It lies underneath the likely position of the two ice sheets in Figure 8.15.

It is difficult to explain the shape of the North Sea Lobe and its tendency to flow in a south-easterly, onshore direction (see Figure 8.15), without constraint from Fennoscandian ice immediately to the east. It flows onshore in County Durham, Yorkshire and in The Wash, whilst flowing out to the east to form a piedmont lobe shape in the southern NSB. Svendsen *et al.* (2004) have argued for coalescence of the British and Fennoscandian ice sheets in the North Sea Basin until 20 cal. ka BP (Figure 8.14), but Carr *et al* (2006) and Sejrup *et al.* (1994) have argued for separate ice sheets and the deposition of the Skipsea Member by the North Sea Lobe during a later, post-LGM phase of restricted glaciation (after 22476 – 21456 cal. yr BP). This date corresponds to the restricted Tampen Stadial reached by the FIS in the North Sea Basin (Sejrup *et al.*, 1987; Sejrup *et al.*, 1994; Sejrup *et al.*, 2005), where it reached the edge of the Norwegian Channel, which supports ice-free conditions in the central North Sea Basin during the existence of the North Sea Lobe. The Marr Bank Fm also provides evidence of glaciomarine conditions at 21.7 cal. yr BP (Holmes, 1977; Stoker *et al.*, 1985). However, early coalescence during the main LGM phase, around 26 cal. ka BP (cf. Sejrup *et al.*, 2005), provides a mechanism for the southward trajectory of the Late Devensian North Sea Lobe operating down the eastern coast of Britain. This trajectory would have continued after recession of the FIS, despite eastward relaxation of the North Sea Lobe, due to ice inertia. The existence of the North Sea Lobe during Heinrich Event 1 is indicated by the existence of Glacial Lake Humber at 16.6 kyr BP (Bateman *et al.*, 2008). This mechanism explains the continued shape of the North Sea Lobe during Heinrich Event 1.

There is no other obvious reason for the lobe turning so sharply southwards from Scotland to The Wash, though Teasdale and Hughes (1999) suggested several alternative reasons, including: the presence of an offshore ice centre, deflecting ice to the west; the presence of a glacio-isostatic fore-bulge to the east, forming a topographic high; glacio-isostatic down-warping of the eastern margin of the BIIS, producing a relatively low region running parallel to the present coast; and slippy Jurassic and Cretaceous sediments offshore. It is possible that some of these factors provided additional impetus to the southward-flowing North Sea Lobe. However, glacio-isostatic downwarping to the east of

the UK is glaciologically difficult to model. A glacio-isostatic forebulge has been modelled in the North Sea Basin (Busschers *et al.*, 2007), but this is far too small to either deflect an ice stream or to exist as an independent centre of ice accumulation. It is glaciologically implausible that glacio-isostatic downwarping would result in a low region to the east of the BIIS, as the load is displaced concentrically beyond the ice sheet.

Alternatively, it is plausible that the confluence of the BIIS and FIS at the LGM may have resulted in a stagnant dome of ice, flowing outwards under the weight of its own gravity. This may have existed throughout the Late Devensian, continuing to deflect the North Sea Lobe southwards during the Dimlington Stadial, whilst allowing ice-free conditions in the northern North Sea Basin. Detailed modelling work is required to test this possibility. In addition, a well-constrained chronostratigraphy could have the potential to test the existence of an independent ice dome, whilst allowing for ice-free conditions to the north. These points are, however, speculative, and there is as yet no hard data to suggest which theory is superior.

Some researchers have suggested that the North Sea Lobe was surging down the eastern coast of Britain (Eyles *et al.*, 1982; Eyles *et al.*, 1994; Evans *et al.*, 1995), with the incorporation of muddy marine sediments indicating stacking, and undulating, hummocky topography, and discontinuous cross-cutting ridges. More geomorphological research in County Durham and Yorkshire is needed to determine the precise landsystem imprint. This may have been a late surge during Heinrich Event 1 (Bateman *et al.*, 2008), where the North Sea Lobe retained its shape even after the opening of a marine embayment between it and the FIS. OSL dates on the formation of Glacial Lake Humber (Bateman *et al.*, 2008) suggest that the lake formed around 16.6 ka BP. This lake required the presence of the North Sea Lobe to block the Humber Gap, and so dates for the lake provide a constraint on the minimum age of the lobe. This dating indicates that the North Sea Lobe may have surged during Heinrich Event 1 (see Chapter 3.5.2). The North Sea Lobe therefore surged at the same time as several other ice streams within the last BIIS and FIS (McCabe *et al.*, 1998; Lekens *et al.*, 2005; Knies *et al.*, 2007; McCabe *et al.*, 2007; Bateman *et al.*, 2008; Bradwell *et al.*, 2008); refer to Chapter 1, Figure 1.3.

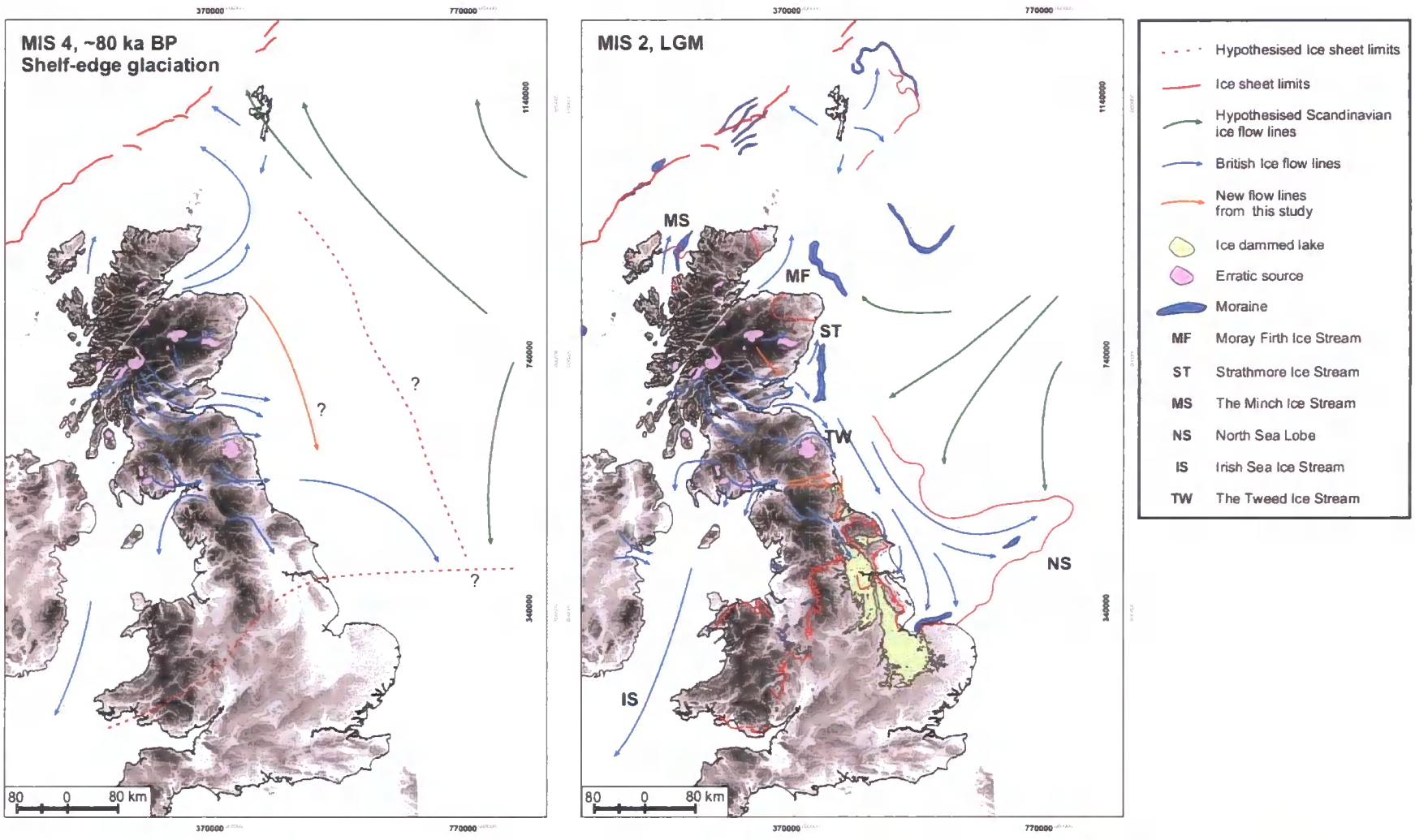

Figure 8.15: Weichselian glaciations of the Britain and the North Sea. Flow lines adapted from Carr *et al.* (2006), Roberts *et al.* (2007), Graham *et al.* (2007), Golledge and Stoker (2006), and Livingstone *et al.* (in press); moraines and ice limits from Bradwell *et al.* (2008), Evans *et al.* (2005), Clark *et al.* (2004a). The Blackhall Member was deposited during the earlier MIS 4, and the Horden Member during the later readvance of the North Sea Lobe at the LGM (~22 ka BP). Original flowlines are highlighted in orange.

The North Sea Lobe was a significant part of the glaciation of central England. South of Durham, the North Sea Lobe interacted with ice flowing through the Stainmore Gap (Bridgland *et al.*, in press). Pennine ice to the west was several hundred metres thick during the Dimlington Stadial, and the Pennine ice contributed significantly to this ice lobe. Ice in the Vale of York formed a composite lobe, with elements of Pennine ice, ice from Stainmore and the Lake District, and a branch of the east coast ice lobe (Chapter 3 and Bridgland *et al.*, in press). The Vale of York ice lobe has previously been interpreted as an ice stream, exhibiting classic highly convergent flow (Mitchell, 1994; Mitchell & Clark, 1994).

The Horden Member was probably deposited during the Dimlington Stadial, at around 21 cal. ka BP. This is suggested by correlation with the Skipsea Member, which overlies the Dimlington Silts (Penny *et al.*, 1969). This is the Bolders Bank Episode (see Figure 7.6, page 361), as defined by Carr *et al.* (2006). The North Sea Lobe was sourced in the Grampian Highlands and northeastern Scotland, near the Highland Boundary Fault. It flowed southwards down the eastern coast of Britain, joined the Tweed Ice Stream north of the Cheviots, and deflected the Cheviot ice stream sharply southwards (see Figure 3.14, page 143, and Figure 8.15).

Analysis of the sediments of the Horden Member and the landforms associated with its eastern margin (Figure 1.6) indicates that it was deposited in a marginal to submarginal environment. Detailed sedimentological work at Whitburn Bay indicated that subglacial canals, hydrofractures and boulder pavements were a key feature of the subglacial environment at this location. The sediments at Warren House Gill showed that an ice-marginal sandur preceded deposition of the Horden Member.

These different ice lobes therefore dominated the region at different times. The first advance into Holderness, by east coast ice, deposited the Horden Member in County Durham and the Skipsea Member in Holderness, possibly during Heinrich Event 1. South of Durham, it coalesced with ice flowing eastwards from the Stainmore Gap, overwhelmed the Stainmore ice, and diverted it southwards (Bridgland *et al.*, in press). The southwards flowing trajectory was also sufficiently strong to turn the Tweed ice stream southwards. Part of this branch also subsequently flowed down the Vale of York, being joined there by local Pennine (Yorkshire Dales) ice (refer to Figure 1.1 and Figure 3.14). Eskers within the Vale of York define the lateral margins and medial suture lines of the various ice lobes (Bridgland *et al.*, in press). The east coast ice reached Yorkshire first and deposited the

Skipsea Member, with Cheviot erratics. Later, the coastal ice became less strong, and the Stainmore and Vale of York ice was able to flow eastwards, overwhelming Holderness, flowing out beyond the present coastline, and depositing the Withernsea Member, with Lake District and southwest Scotland erratics (Catt, 1991b; Bridgland *et al.*, in press).

An alternative interpretation has, however, been suggested for the glacigenic deposits of eastern Yorkshire (Boston *et al.*, in prep). Geochemical analysis of tills at Dimlington found repeated elemental packages upwards throughout the exposure. Boston *et al.* (in prep) proposed that the tills at Dimlington were deposited through thrusting, folding, attenuation and stacking of layers of material during glaciotectonic transportation. This interpretation fits well with the presence of fossiliferous rafts of marine sediments within the Holderness Fm. Boston *et al.* (in prep) were unable to identify clear differences between the Withernsea and Skipsea members, and argued that Stainmore and Vale of York ice never reached Dimlington. The discontinuous ridges at Dimlington that Eyles *et al.* (1994) interpreted as evidence for surging, Boston *et al.* (in prep) interpret as a glaciotectonically folded and thrust push moraine, reflecting dynamic oscillation of the North Sea Lobe. However, this interpretation is not supported by the erratic content of the Skipsea and Withernsea tills.

Within the above context, it can be seen that this research has therefore provided new and significant information regarding a British Devensian glaciation that is recognised as being increasingly more complex. Dynamic and surging ice lobes advanced and receded, and in some cases, trapped large proglacial lakes between them.

8.3 Key findings of this research

This study has attempted to answer several key questions regarding the timing, frequency, and dynamics of Middle Pleistocene to Devensian glaciations in eastern England and the adjoining offshore region. These questions mainly concerned the provenance, stratigraphy, and interactions of the various lobes of the last BIIS, and how they were influenced by the Fennoscandian ice sheet. While there is clear evidence for Fennoscandian ice onshore eastern England on multiple occasions during the Quaternary, the interaction with the British Ice Sheet offshore is harder to reconstruct.

8.3.1 New research into the British Quaternary

A systematic thin-section study integrated with multi-proxy provenance data of various North Sea Quaternary sediments was conducted for the first time in this project. This provided substantial new evidence supporting a subglacial genesis for the Swarte Bank, Coal Pit and Bolders Bank formations. The Sand Hole Fm, previously attributed to the Holsteinian (Gatliffe *et al.*, 1994), was shown in this study to stretch from latest Elsterian to earliest Holsteinian, adding important detail to this formation. The Fisher Fm in BH 81/34 was deposited in a glaciomarine environment. This indicates that ice was calving from the coast of Scotland into a marine embayment in MIS 6.

The provenance of Middle and Upper Pleistocene sediments in the NSB has been much more tightly confined in this study. This project applied the first systematic, fully quantified, multi-proxy provenance analysis of Quaternary sediments in the North Sea. The North Sea Basin is a sediment sink where glacigenic deposits from numerous Pleistocene glaciations are preserved, and which provides direct evidence of repeated ice-flow pathways during the Quaternary. The northeastern coast of the Scottish Highlands has been shown in this study to have been an important ice-accumulation area throughout the Quaternary, with ice repeatedly flowing through the Midland Valley of Scotland and the Southern Uplands.

The detailed process and provenance analysis of the onshore sediments has revealed new information regarding the timing and dynamics of the BIIS and FIS during the Quaternary. While the chronostratigraphy remains problematic and subject to further work, this research showed that the Warren House Formation is a glaciomarine diamicton, with

material derived from both Scottish and Norwegian sources. This evidence shows that, at the time of deposition, there was a large marine embayment in the NSB, with tidewater glaciers sourced in the Grampian Highlands and in Southern Norway calving directly into the North Sea. The Ash Gill Member was subsequently overridden and subglacially deformed. The Briton's Lane Fm, which also shows a mixed provenance, is similarly composed of lithologies derived from both Norway and Scotland. This glaciofluvial deposit indicates that at the time of deposition, although the ice sheets had 'unzipped', allowing the sands and gravels to be deposited subaerially, the ice fronts remained close, with Fennoscandian ice grounded in the NSB.

This research has shown that the eastern-central part of the last British-Irish Ice Sheet received ice from multiple sources during the Devensian, and that changing ice divides and ice-accumulation areas led to the dominance of different ice lobes and ice streams at different times. An Early Devensian ice lobe first overwhelmed the area. It was sourced in the Highlands of Scotland. It flowed eastwards through the Midland Valley, and southwards around the Southern Uplands. Here it coalesced with or overwhelmed Lake District and Southern Uplands ice. Build up of ice in the Irish Sea Basin blocked south-westward flowing ice from the Lake District (Livingstone *et al.*, in prep), and resulted in the ice flowing eastwards, through the Tyne Gap (Livingstone *et al.*, in press) towards the coast of eastern England. Eastern County Durham received ice mostly from western Scotland, and ice from the Lake District did not factor here. The glacial sediments at Warren House Gill were therefore deposited in an ice-marginal setting under an ice-lobe flowing eastwards into the North Sea Basin.

After recession of the Tyne Gap ice, an ice lobe advanced down the eastern coast of Britain, ultimately reaching Norfolk, possibly as late as Heinrich Event 1. It trapped vast quantities of meltwater between its flanks and the higher ground onshore, resulting in numerous proglacial lakes. Abundant fluvioglacial meltwater deposited sands and gravels, which were overridden by later glaciation of east coast ice. This North Sea Lobe was sourced in the Scottish Highlands, and its sediments bear Scottish and Cheviot erratics. It coalesced with the Tweed ice stream, which it deflected southwards, most likely due to the presence of a Scandinavian ice sheet in the North Sea Basin. It deposited the Horden and Skipsea members on the coast of eastern England.

Complex glacigenic sediments at Whitburn Bay suggest that this ice lobe was flowing rapidly, possibly surging, with an onshore flow direction. A distributed subglacial drainage

network at the ice-bed interface indicates an excess of meltwater, with high-energy gravel channels and hydrofractures reflecting periodic changes in the subglacial hydraulic system. These channels may have drained directly into Glacial Lake Wear.

This PhD thesis has highlighted the complexity and dynamism of the BIIS throughout the Quaternary. It was a sensitive and mobile ice sheet, strongly and rapidly influenced by ocean forcing. Its position on the northwest Atlantic Margin placed the BIIS at the frontline of changing ocean dynamics, and this sensitivity is recorded in the multiple flow phases and flow pathways that are recorded in eastern England.

8.3.2 Further Research and Limitations

Limitations of the study

The chronostratigraphy proved to be a consistent difficulty in this research project. Despite repeated attempts using different methods, it was difficult to date the Ash Gill Member and the Blackhall Member accurately. Ongoing research is attempting to address this problem. Other limitations of the study include the minimal number of bulk and thin-section samples obtained from boreholes in the North Sea. With a finite amount of material and limited resources to obtain further boreholes, this was difficult.

Methodological errors and limitations include clast and mineral misidentification by the author, although these were minimised because the heavy-mineral identifications were independently tested. Any errors will be consistent throughout the thesis as the same person counted all the samples.

Further Research and Further Research Methodologies

The lithostratigraphy, stratigraphical correlations and process interpretations of the formations of the North Sea remain weak. It remains difficult to quantify onshore-offshore correlations, and though lithostratigraphical correlations between the Bolders Bank Fm and the Horden Member were attempted in this study, they were inconclusive. Without a robust chronological framework, this situation is unlikely to improve. However, the boreholes of the NSB contain a wealth of information, which, when combined with new DEMs of the North Sea floor, should help to further test the theory of contact between the BIIS and the FIIS during the Late Devensian. Further sampling of tills both south and west (inland) of the study location would broaden this research, allow firmer correlations, and strengthen depositional interpretations. This could be supported by analysis of boreholes and quarries

through Quaternary sediments, allowing a 3D model of the Quaternary sediments of northeastern England to be constructed. A key part of this would be strengthening the chronostratigraphical framework, an ongoing task. Additionally, detailed geomorphological mapping would allow the creation of a detailed landsystem model for the Late Quaternary.

Another area of potential further research is the Vale of York (Figure 1.1), which was a zone of confluence of ice sourced in the Lake District and the Cheviots (Raistrick, 1932; Gaunt, 1981). The Grampian Highlands, Cheviot Hills and the Lake District uplands are regions of distinctive igneous geology, with several key indicator erratics allowing discrimination between ice sources. Detailed lithostratigraphy and analysis of erratic trains and heavy mineral trains in the small area would allow the identification of the boundaries of the Vale of York ice lobe and North Sea Lobe. The different ice lobes would principally be defined by the presence of Shap Granite, Cheviot Andesite, Scottish schists, ferromagnesian heavy minerals from a mafic to ultramafic source, and key associations of heavy minerals from the north-eastern coast of Scotland (with Buchan and Stonehavian-type metamorphism). Recent work in the Vale of York has identified an esker system, and interpreted this as complex interlobate system. This composite ice lobe (Bridgland *et al.*, in press) should exhibit different lithological suites on either side of the 'interlobate glaciofluvial complexes', which define the boundaries of the Lake District, Pennine, and Durham ice. If the ice lobes flowed down the Vale of York simultaneously, there will be a strong east-west divide in the lithological character of the sediments in the Vale of York. If they flowed down at different times, then two glacigenic sediments of different character will be visible in superposition in the Vale of York. The Vale of York system ends in the distinct York Moraine (Edwards *et al.*, 1950; Catt, 1991b; Evans *et al.*, 2005), so erratics here can be easily traced to an end-moraine system.

8.4 Conclusions

This thesis used extensive process interpretations, quantitative methods, and a comprehensive analysis of ice-sheet dynamics to create a coherent stratigraphy of the glacigenic sediments of northeastern England. It provided the first detailed, quantitative, sedimentological, geochemical, and petrological analysis of the glacigenic sediments of northeastern England, and the first quantitative petrological analysis of the tills of the North Sea. This research argues for a complex, multi-lobate, dynamic ice sheet on the eastern coast of Britain during the Late Devensian, with periods of quiescence and retreat, indicated by subaerial fluvial sediments, and periods of surging and fast ice flow.

This research deductively tested previously proposed onshore-offshore and north-south correlations, and in some cases has found these to be inaccurate. The Horden Member and not the Blackhall Member was found to be correlative with the Skipsea Member of Yorkshire. However, the Bolders Bank Fm was found to be correlated with the Skipsea Member and the Horden Member.

The Quaternary sediments at Warren House Gill were found to contain significantly more complex glacigenic sediments than had been previously described by Trechmann (1915; 1931b; 1952). Amino acid racemisation, using a new technique developed by Kirsty Penkman, indicates that the shell fauna within the Ash Gill Member is MIS 9 to Cromerian in age (Chapter 5.6.2), though this dating requires further work to definitively constrain the ages. Though a precise chronostratigraphical framework for these sediments is still under development, the interpretation of the Warren House Formation 'Ash Gill Member' as a glaciomarine deposit, derived from both Scottish and Fennoscandian sources, is a significant new development. No correlatives were identified in the immediate offshore region. The overlying silts, the Whitesides Gill Member, are marine or estuarine (possibly including reworked loess), and reflect an ameliorating climate. A substantial unconformity separates the Warren House Formation from the overlying Early Devensian sediments at Warren House Gill. Although MIS 10, 8 and 6 glaciations have been reported elsewhere in Britain (Straw, 1983; Catt, 1991b; Gibbard *et al.*, 1992; Beets *et al.*, 2005), they are unrepresented at Warren House Gill. The Warren House Formation is therefore a peculiarly fortuitous survival in the bottom of a deep palaeovalley.

The Easington Raised Beach, dated to MIS 7 by OSL, was cemented during the Holocene. The Devensian age of some of the samples may indicate that cementation occurred in multiple stages, with cementation during the Eemian and the Holocene. The Easington Raised Beach contains far-travelled erratics of an easterly provenance, which are found in no other presently extant deposits other than the Ash Gill Member. This may indicate that the erratic lithologies within the Easington Raised Beach gravels could have been derived from reworking of the Ash Gill Member, although this is difficult to prove.

The Ash Gill Member of the Warren House Formation is overlain by the Blackhall Member, which was deposited from the Early to Middle Devensian, ~80 ka BP. This is the first evidence of an Early Devensian glacigenic deposit in northeastern England. The ice was sourced from the northeastern Grampian Highlands, and subsequently flowed eastwards through the Tyne Gap. It is overlain by the Horden Member, which flowed down the eastern coast of Britain as a North Sea Lobe, constrained by Fennoscandian ice in the North Sea. A proglacial sandur formed in front and between these ice lobes, depositing the Peterlee Sands and Gravels. Large amounts of meltwater were trapped between the two ice lobes and the higher ground to the south and east, forming large proglacial lakes. OSL dating of Glacial Lake Humber suggests that this ice lobe may have continued to surge forwards during Heinrich Event 1 (Bateman *et al.*, 2008). This North Sea Lobe deposited the Horden Member in County Durham, the Bolders Bank Fm offshore, and the Skipsea Member in east Yorkshire.

The Horden Member was deposited as part of an ice-marginal landsystem, and in Whitburn Bay is characterised by subglacial canals, hydrofractures, and boulder pavements. The landsystem includes end moraines and ice-contact slopes (Figure 1.6). It overlies subaerially deposited sands and gravels in County Durham, and the lowlands of Durham and Sunderland are characterised by proglacial lake sediments. The surging of the North Sea Lobe has been linked to Heinrich Event 1 forcing.

This study has led to a greater understanding of the dynamics of the BIIS and its interaction with the FIS during the Quaternary. The BIIS was a complex, dynamically changing ice sheet, with numerous lobes and ice streams operating at different times during its history. The Grampian Highlands were important as an ice-accumulation region, and erratics and minerals derived from here consistently exist in the tills of northeast England. This study found that ice from the Lake District was a not significant contributor to glaciation in County Durham.

The FIS was a significant influence on the British ice sheet, with Fennoscandian ice encroaching on the British coastline at least twice during the Quaternary, during MIS 6 and MIS 12. It was a significant presence in the North Sea Basin at other times, and may have been confluent with a large BIIS during the Early and Middle Devensian, as well as confining the BIIS during the Dimlington Stadial in the Late Devensian.

References

Adamiec, G. & Aitken, M.J., 1998. Dose-rate conversion factors: update. *Ancient TL*, **16**, 37-50.

Agar, R., 1954. Glacial and post-glacial geology of Middlesbrough and the Tees estuary. *Proceedings of the Yorkshire Geological Society*, **29**, 237-253.

Aitken, M.J., 1985. *Thermoluminescence Dating*. Academic Press, London, 359 pp.

Alabaster, C. & Straw, A., 1976. The Pleistocene context of faunal remains and artefacts discovered at Welton-le-Wold, Lincolnshire. *Proceedings of the Yorkshire Geological Society*, **41**, 75-94.

Alexanderson, H., Adrielsson, L., Hjort, C., Möller, P., Antonov, O., Eriksson, S. & Pavlov, M., 2002. Depositional history of the North Taymyr ice-marginal zone, Siberia - a landsystem approach. *Journal of Quaternary Science*, **17**, 361-382.

Allen, J.R.L., 1963. The classification of cross-stratified units, with notes on their origin. *Sedimentology*, **2**, 93-114.

Allen, J.R.L., 1982. *Developments in Sedimentology: Their character and physical basis. Volume I.* Elsevier, Oxford, 663 pp.

Alley, R.B., Blankenship, D.D., Bentley, C.R. & Rooney, S.T., 1986. Deformation of till beneath Ice Stream B, West Antarctica. *Nature*, **322**, 57-59.

Andersen, B.G., Wangen, O.P. & Østmo, S.R., 1987. *Quaternary geology of Jæren and adjacent areas, south-western Norway*, **411**. Norges Geologiske Undersøkelse Bulletin, 55 pp.

Andrews, I.J., Long, D., Richards, P.C., Thomson, A.R., Brown, S., Cheshive, J.A. & McCormac, M., 1990. *The Geology of the Moray Firth. United Kingdom Offshore Regional Report.* Memoir of the British Geological Survey. HMSO, London, 99 pp.

Armitage, S.J. & Bailey, R.M., 2005. The measured dependence of laboratory beta dose rates on sample grain size. *Radiocarbon Measurements*, **39**, 123-127.

Ashley, G.M., 1975. Rhythmic sedimentation in Glacial Lake Hitchcock, Massachusetts-Connecticut. In: A.V. Jopling and B.C. McDonald (Editors), *Glaciofluvial and Glaciolacustrine Sedimentation.* Special Publications of the Society of Economic Palaeontologists and Mineralogists. Tulsa 23, 304-320.

Ashley, G.M., 1995. Glaciolacustrine Environments. In: J. Menzies (Editor), *Modern Glacial Environments. Processes, dynamics and sediments.* Butterworth-Heinemann. Oxford, 417-444.

Ashley, G.M., Shaw, J. & Smith, N.D., 1985. Proglacial Lacustrine Environment. In: G.M. Ashley, J. Shaw and N.D. Smith (Editors), *Glacial Sedimentary Environments.* Society of Economic Palaeontologists and Mineralogists. Short Course No. 16, 135-175.

Ashley, G.M. & Warren, W.P., 1997. The ice-contact environment. *Quaternary Science Reviews*, **16**, 629-634.

Ashley, M.D., Southard, J.B. & Boothroyd, J.C., 1982. Deposition of climbing-ripple beds: a flume simulation. *Sedimentology*, **29**, 67-79.

Ballantyne, C.K., 1999. Maximum altitude of Late Devensian glaciation on the Isle of Mull and Isle of Jura. *Scottish Journal of Geology*, **35**, 97-106.

Ballantyne, C.K., McCarroll, D., Nesje, A., Dahl, S.O. & Stone, J.O., 1998. The last ice sheet in north-west Scotland: Reconstruction and implications. *Quaternary Science Reviews*, **17**, 1149-1184.

Balson, P. & Cameron, T.D.J., 1985. Quaternary mapping offshore East Anglia. *Modern Geology*, **9**, 231-239.

Balson, P.S. & Jeffery, D.H., 1991. The Glacial Sequence of the southern North Sea. In: J. Ehlers, P. Gibbard and J. Rose (Editors), *Glacial Deposits in Great Britain and Ireland.* A.A. Balkema. Rotterdam, 245-253.

Banham, P.H., 1968. A preliminary note on the Pleistocene stratigraphy of north-east Norfolk. *Proceedings of the Geologists Association*, **79**, 469-474.

Banham, P.H., 1977. Glaciotectonites in till stratigraphy. *Boreas*, **6**, 101-105.

Barclay, W., Brown, M., McMillan, A.A., Pickett, E., Stone, P. & Wilby, P., 2005. *The Old Red Sandstone of Great Britain. Geological Conservation Review Series No. 31.* Joint Nature Conservation Committee, Peterborough, 393 pp.

Bateman, M.D., Buckland, P.C., Chase, B., Frederick, C.D. & Gaunt, G.D., 2008. The Late-Devensian proglacial Lake Humber: new evidence from littoral deposits at Ferrybridge, Yorkshire, England. *Boreas*, **37**, 195-210.

Bateman, M.D. & Catt, J.A., 1996. An absolute chronology for the raised beach and associated deposits at Sewerby, East Yorkshire, England. *Journal of Quaternary Science*, **11**, 389-395.

Bateman, R.M. & Catt, J.A., 2007. Provenance and palaeoenvironmental interpretation of superficial deposits, with particular reference to post-depositional modification of heavy mineral assemblages. In: M.A. Mange and D.T. Wright (Editors), *Heavy Minerals in Use*. Developments in Sedimentology 58. Elsevier, 151-188.

Baumann, K.-H., Lackschewitz, K.S., Mangerud, J., Spielhagen, R.F., Wolf-welling, T.C.W., Henrich, R. & Kassens, H., 1995. Reflection of Scandinavian Ice Sheet Fluctuations in Norwegian Sea Sediments during the Past 150,000 Years. *Quaternary Research*, **43**, 185-197.

Bé, A.W.H. & Tolderhund, D.S., 1971. Distribution and ecology of living planktonic foraminifera in surface waters of the Atlantic and Indian Oceans. In: B.M. Funnel and W.R. Riedel (Editors), *The Micropaleontology of Oceans*. Cambridge University Press. Cambridge, 105-149.

Beaumont, P., 1967. *The glacial deposits of eastern Durham*. Unpublished PhD Thesis, Department of Geography, Durham University, 568 pp.

Beaumont, P., 1971. Stone orientation and stone count data from the lower till sheet, eastern Durham. *Proceedings of the Yorkshire Geological Society*, **38**, 343-360.

Beets, D., Meijer, T., Beets, C., Cleveringa, P., Laban, C. & van der Spek, A., 2005. Evidence for a Middle Pleistocene glaciation of MIS 8 age in the southern North Sea. *Quaternary International*, **133-134**, 7-19.

Bell, T., Rogerson, R.J. & Mengel, F., 1989. Reconstructed ice-flow patterns and ice limits using drift pebble lithology, outer Nuchvak Fiord, northern Labrador. *Canadian Journal of Earth Sciences*, **26**, 577-590.

Bell, T., Rogerson, R.J. & Mengel, F., 1990. Reconstructed ice-flow patterns and ice limits using drift pebble lithology, outer Nachvak Fiord, northern Labrador: Reply. *Canadian Journal of Earth Sciences*, **27**, 1007-1011.

Benediktsson, Í.Ö., Möller, P., Ingólfsson, Ó., van der Meer, J.J.M., Kjær, K.H. & Krüger, J., 2008. Instantaneous end moraine and sediment wedge formation during the 1890 glacier surge of Brúarjökull, Iceland. *Quaternary Science Reviews*, **27**, 209-234.

Benn, D.I., 1994. Fabric strength and the interpretation of sedimentary fabric data. *Journal of Sedimentary Research*, **A64**, 910-915.

Benn, D.I., 2004. Macrofabric. In: D.J.A. Evans and D.I. Benn (Editors), *A practical guide to the study of glacial sediments*. Arnold. London, 93-114.

Benn, D.I., 2007a. Clast Form Analysis. In: S.A. Elias (Editor), *Encyclopedia of Quaternary Science*. Elsevier. Oxford, 904-909.

Benn, D.I., 2007b. Till Fabric Analysis. In: S.A. Elias (Editor), *Encyclopedia of Quaternary Science*. Amsterdam, Elsevier, 954-959.

Benn, D.I. & Evans, D.J.A., 1996. The interpretation and classification of subglacially-deformed materials. *Quaternary Science Reviews*, **15**, 23-52.

Benn, D.I. & Evans, D.J.A., 1998. *Glaciers and Glaciation*. Arnold, London, 734 pp.

Benn, D.I. & Evans, D.J.A., 2004. Introduction and rationale. In: D.J.A. Evans and D.I. Benn (Editors), *A practical guide to the study of glacial sediments*. Arnold. London, 1-10.

Benn, D.I. & Gemmell, A.M.D., 2002. Fractal dimensions of diamictic particle-size distributions: simulations and evaluation. *Geological Society of America Bulletin*, **114**, 528-532.

Bennett, M., Waller, R., Glasser, N., Hambrey, M. & Huddart, D., 1999. Glacigenic clast fabrics: genetic fingerprints or wishful thinking? *Journal of Quaternary Science*, **14**, 125-135.

Bennett, M.R., Huddart, D. & McCormick, T., 2000. An integrated approach to the study of

glaciolacustrine landforms and sediments: a case study from Hagavatn, Iceland. *Quaternary Science Reviews*, **19**, 633-665.

Bennett, M.R., Huddart, D. & Thomas, G.S.P., 2002. Facies architecture within a regional glaciolacustrine basin: Copper River, Alaska. *Quaternary Science Reviews*, **21**, 2237-2279.

Berthelsen, A., 1979. Recumbent folds and boudinage structures formed by subglacial shear: an example of gravity tectonics. *Geologie en Mijnbouw*, **58**, 253-260.

Bevington, P.R. & Robinson, D.K., 1992. *Data reduction and error analysis for the physical sciences. 2nd Edition.* McGraw-Hill, New York, London., 328 pp.

Biñka, K. & Nitychoruk, J., 2001. Late Saalian climate changes in Europe in the light of pollen analysis and the problem of two-step deglaciation at the Oxygen Isotope Stage 6/5e transition. *Boreas*, **30**, 307-316.

Björnsson, H., 1998. Hydrological characteristics of the drainage system beneath a surging glacier. *Nature*, **395**, 771-774.

Bluck, B.J., 2002. The Midland Valley Terrane. In: N.H. Trewin (Editor), *The Geology of Scotland. 4th Edition.* The Geological Society. Bath, 149-166.

Boston, C.M., Evans, D.J.A. & Ó Cofaigh, C., in prep. An examination of the geochemical properties of Late Devensian glacigenic sediments in eastern England.

Boswell, P.G.H., 1916. The Petrology of the North Sea Drift and the Upper Glacial Brickearths in East Anglia. *Proceedings of the Geologists' Association*, **27**, 78-98.

Boulton, G.S., 1970. On the deposition of subglacial and melt-out tills at the margins of certain Svalbard glaciers. *Journal of Glaciology*, **9**, 231-245.

Boulton, G.S., 1996. Theory of glacial erosion, transport and deposition as a consequence of subglacial sediment deformation. *Journal of Glaciology*, **42**, 43-62.

Boulton, G.S. & Deynoux, M., 1981. Sedimentation in glacial environments and the identification of tills and tillites in ancient sedimentary sequences. *Precambrian Research*, **15**, 397-422.

Boulton, G.S., Dobbie, K.E. & Zatsepin, S., 2001. Sediment deformation beneath glaciers and its coupling to the subglacial hydraulic system. *Quaternary International*, **86**, 3-28.

Boulton, G.S. & Hagdorn, M., 2006. Glaciology of the British Isles Ice Sheet during the last glacial cycle: form, flow, streams and lobes. *Quaternary Science Reviews*, **25**, 3359-3390.

Boulton, G.S. & Hindmarsh, R.C.A., 1987. Sediment deformation beneath glaciers: rheology and geological consequences. *Journal of Geophysical Research*, **92**, 9059-9082.

Boulton, G.S., Jones, A.S., Clayton, K.M. & Kenning, M.J., 1977. A British Ice-Sheet Model and patterns of glacial erosion and deposition in Britain. In: F.W. Shotton (Editor), *British Quaternary Studies, Recent Advances.* Clarenden Press. Oxford, 231-146.

Boulton, G.S. & Paul, M.A., 1976. The influence of genetic processes on some geotechnical properties of glacial tills. *Quarterly Journal of Geological Engineering*, **9**, 159-194.

Boulton, G.S., Peacock, J.D. & Sutherland, D.G., 1991. Quaternary. In: G.Y. Craig (Editor), *Geology of Scotland, 3rd Edition.* The Geological Society. London, 503-537.

Bowen, D.Q., 1999a. On the correlation and classification of Quaternary deposits and land-sea correlations, *A revised correlation of Quaternary deposits in the British Isles. Geological Society Special Report.* Geological Society of London. London, 1-10.

Bowen, D.Q., 1999b. Only four major 100-ka glaciations during the Brunhes Chron? *International Journal of Earth Sciences*, **88**, 276-284.

Bowen, D.Q. (Editor), 1999c. *A revised correlation of Quaternary deposits in the British Isles. Geological Society Special Report 23.* The Geological Society, London, 174 pp.

Bowen, D.Q., Phillips, F.M., McCabe, A.M., Knutz, P.C. & Sykes, G.A., 2002. New data for the Last Glacial Maximum in Great Britain and Ireland. *Quaternary Science Reviews*, **21**, 89-101.

Bowen, D.Q., Rose, J., McCabe, A. & Sutherland, D.G., 1987. Correlation of Quaternary Glaciations in England, Ireland, Scotland and Wales. In: V. Šibrava, D.Q. Bowen and D. Richmond (Editors), *Quaternary Glaciations in the Northern*

Hemisphere, Report of the International Geological Correlation Programme, Project 24. Pergamon Press. Oxford, 148-170.

Bowen, D.Q., Smith, D.B. & Sykes, G.A., 1991. The age of the Easington Raised Beach, County Durham. *Proceedings of the Yorkshire Geological Society*, **48**, 415-420.

Boylan, P.J., 1967. The Pleistocene mammalia of the Sewerby-Hessle buried cliff. *Proceedings of the Yorkshire Geological Society*, **36**, 115-125.

Bradwell, T., Stoker, M. & Larter, R., 2007. Geomorphological signature and flow dynamics of The Minch palaeo-ice stream, northwest Scotland. *Journal of Quaternary Science*, **22**, 609-617.

Bradwell, T., Stoker, M.S., Golledge, N.R., Wilson, C.K., Merritt, J.W., Long, D., Everest, J.D., Hestvik, O.B., Stevenson, A.G., Hubbard, A.L., Finlayson, A.G. & Mathers, H.E., 2008. The northern sector of the last British Ice Sheet: Maximum extent and demise. *Earth-Science Reviews*, **88**, 207-226.

Bridgland, D.R., 1986. *Clast Lithological Analysis. Technical Guide No. 3.* Quaternary Research Association, Cambridge, 207 pp.

Bridgland, D.R., 1999. The Pleistocene of north-east England. In: D.R. Bridgland, B.P. Horton and J.B. Innes (Editors), *The Quaternary of north-east England. Field Guide.* Quaternary Research Association. London, 1-9.

Bridgland, D.R. & Austin, W.E.N., 1999. Shippersea Bay to Hawthorn Hive. In: D.R. Bridgland, B.P. Horton and J.B. Innes (Editors), *The Quaternary of North-East England. Field Guide.* Quaternary Research Association. London, 51-56.

Bridgland, D.R., Howard, A.J., White, M.J. & White, T.S., in prep. *The Quaternary of the Trent.* Oxbow Books, Oxford.

Bridgland, D.R., Innes, J.B., Long, A.J. & Mitchell, W.A., in press. *Late Quaternary landscape evolution of the Swale-Ure Washlands, North Yorkshire.* Oxbow Books, Oxford.

Bridgland, D.R., Schreve, D.C., Keen, D.H., Meyrick, R. & Westaway, R., 2004. Biostratigraphical correlation between the late Quaternary sequence of the Thames and key fluvial localities in central Germany. *Proceedings of the Geologists' Association*, **115**, 125-140.

Bridgland, D.R. & Westaway, R., 2007. Preservation patterns of Late Cenozoic fluvial deposits and their implications: results from IGCP 440. *Quaternary International*, **198**, 5-38.

Briggs, L.I., McCulloch, D.S. & Moser, F., 1962. The hydraulic shape of sand particles. *Journal of Sedimentary Research*, **32**, 645-656.

Brown, N.E., Hallet, B. & Booth, D.B., 1987. Rapid soft bed sliding of the Puget glacial lobe. *Journal of Geophysical Research*, **92**, 8985-8997.

Bryhni, I. & Andréasson, P.-G., 1985. Metamorphism in the Scandinavian Caledonides. In: D.G. Gee and B.A. Sturt (Editors), *The Caledonide Orogen - Scandinavia and Related Areas.* John Wiley & Sons Ltd. Chichester, 763-781.

Bullock, P., Federoff, N., Jongerius, A., Stoops, G., Tursina, T. & Babel, U., 1985. *Handbook for soil thin section description.* Waine Research Publications, Wolverhampton, 152 pp.

Busschers, F.S., Kasse, C., van Balen, R.T., Vandenberghe, J., Cohen, K.M., Weerts, H.J.T., Wallinga, J., Johns, C., Cleveringa, P. & Bunnik, F.P.M., 2007. Late Pleistocene evolution of the Rhine-Meuse system in the Southern North Sea basin: imprints of climate change, sea-level oscillation and glacio-isostacy. *Quaternary Science Reviews*, **26**, 3216-3248.

Cameron, I.B. & Stephenson, D., 1985. *British Regional Geology No. 5: the Midland Valley of Scotland.* Memoir of the British Geological Survey. HMSO, London, 172 pp.

Cameron, T. & Holmes, R., 1999. The Continental Shelf. In: D.Q. Bowen (Editor), *A Revised Correlation of Quaternary Deposits in the British Isles. Geological Society Special Report. Vol. 23.* Geological Society. London, 125-139.

Cameron, T.D.J., Crosby, A., Balson, P.S., Jeffery, D.H., Lott, G.K., Bulat, J. & Harrison, D.J., 1992. *United Kingdom Offshore Regional Report: The Geology of the Southern North Sea.* HMSO, London, 149 pp.

Cameron, T.D.J., Stoker, M.S. & Long, D., 1987. The history of Quaternary sedimentation in the UK sector of the North Sea Basin. *Journal of the Geological Society, London*, **144**, 43-58.

Campbell, A.C. & Nicholls, J., 1986. *The Hamlyn Guide to seashores and shallow seas of Britain and Europe.* Hamlyn, London, 302 pp.

Candy, I., 2002. Formation of a rhizogenic calcrete during a glacial stage (Oxygen Isotope Stage 12): its palaeoenvironmental stratigraphic significance. *Proceedings of the Geologists' Association*, **113**, 259-270.

Candy, I., 2008. *Petrography, Stable isotope chemistry and U-Series chronology of the Easington Raised Beach, N.E. England.* Royal Holloway, University of London, Egham, Personal Communication, 1-8.

Candy, I., Black, S. & Sellwood, B.W., 2004. Quantifying timescales of pedogenic calcrete formation using U-Series disequilibria. *Sedimentary Geology*, **170**, 177-187.

Candy, I., Black, S. & Sellwood, B.W., 2005. U-Series isochron dating of immature and mature calcretes as a basis for constructing Quaternary landform chronologies; Examples from the Sorbas Basin, southeast Spain. *Quaternary Research*, **64**, 100-111.

Candy, I., Rose, J. & Lee, J.R., 2006. A seasonally 'dry' interglacial climate in eastern England during the early Middle Pleistocene: palaeopedological and stable isotopic evidence from Pakefield, UK. *Boreas*, **35**, 2255-2265.

Candy, I. & Schreve, D., 2007. Land-sea correlation of Middle Pleistocene temperate sub-stages using high-precision uranium-series dating of tufa deposits from southern England. *Quaternary Science Reviews*, **26**, 1223-1235.

Carr, S., 1999. The micromorphology of Last Glacial Maximum sediments in the Southern North Sea. *Catena*, **35**, 123-145.

Carr, S.J., 2001. Micromorphological criteria for distinguishing subglacial and glacimarine sediments: evidence from a contemporary tidewater glacier, Spitsbergen. *Quaternary International*, **86**, 71-79.

Carr, S.J., 2004a. Micro-scale features and structures. In: D.J.A. Evans and D.I. Benn (Editors), *A practical guide to the study of glacial sediments.* Arnold. London, 115-144.

Carr, S.J., 2004b. The North Sea Basin. In: J. Ehlers and P. Gibbard (Editors), *Quaternary Glaciations - extent and chronology. Part I: Europe.* Elsevier. Amsterdam, 261-270.

Carr, S.J., Haflidason, H. & Sejrup, H.P., 2000. Micromorphological evidence supporting Late Weichselian glaciation of the northern North Sea. *Boreas*, **29**, 315-328.

Carr, S.J., Holmes, R., van der Meer, J.J.M. & Rose, J., 2006. The Last Glacial Maximum in the North Sea: Micromorphological evidence of extensive glaciation. *Journal of Quaternary Science*, **21**, 131-153.

Carr, S.J. & Rose, J., 2003. Till fabric patterns and significance: particle response to subglacial stress. *Quaternary Science Reviews*, **22**, 1415-1426.

Carver, R.E., 1971. Heavy Mineral Separation. In: R.E. Carver (Editor), *Procedures in Sedimentary Petrology.* Wiley-Interscience. New York 427-452.

Catt, J.A., 1991a. Late Devensian glacial deposits and glaciations in eastern England and the adjoining offshore region. In: J. Ehlers, P.L. Gibbard and J. Rose (Editors), *Glacial deposits in Great Britain and Ireland.* A.A. Balkema. Rotterdam, 61-68.

Catt, J.A., 1991b. The Quaternary history and glacial deposits of East Yorkshire. In: J. Ehlers, P. Gibbard and J. Rose (Editors), *Glacial Deposits in Great Britain and Ireland.* Balkema. Rotterdam, 185-191.

Catt, J.A., 2001a. Dimlington Cliff. In: M.D. Bateman, P.C. Buckland, C.D. Frederick and N.J. Whitehouse (Editors), *The Quaternary of east Yorkshire and North Lincolnshire. Field Guide.* Quaternary Research Association. London, 53-68.

Catt, J.A., 2001b. Sewerby. In: M.D. Bateman, P.C. Buckland, C.D. Frederick and N.J. Whitehouse (Editors), *The Quaternary of east Yorkshire and north Lincolnshire. Field Guide.* Quaternary Research Association. London, 83-88.

Catt, J.A., 2007. The Pleistocene glaciations of eastern Yorkshire: a review. *Proceedings of the Yorkshire Geological Society*, **56**, 177-208.

Catt, J.A. & Digby, P.G.N., 1988. Boreholes in the Wolstonian Basement Till at Easington, Holderness, July 1985. *Proceedings of the Yorkshire Geological Society*, **47**, 21-27.

Catt, J.A. & Penny, L.F., 1966. The Pleistocene deposits of Holderness, East Yorkshire. *Proceedings of the Yorkshire Geological Society*, **35**, 375-420.

Chadwick, R.A. & Pharaoh, T.C., 1998. The seismic reflection Moho beneath the United Kingdom and adjacent areas. *Tectonophysics*, **299**, 255-279.

Chamberlin, T.C., 1895. Recent glacial studies in Greenland. *Bulletin of the Geological Society of America*, **6**, 199-220.

Church, M.A., McLean, D.G. & Wolcott, J.F., 1987. River bed gravels: sampling and analysis. In: C.R. Thorne, J.C. Bathurst and R.D. Hey (Editors), *Sediment Transport in gravel-bed rivers*. Wiley. New York, 43-79.

Clark, C.D., Evans, D.J.A., Khatwa, A., Bradwell, T., Jordan, C.J., Marsh, S.H., Mitchell, W.A. & Bateman, M.D., 2004a. Map and GIS database of glacial landforms and features related to the last British Ice Sheet. *Boreas*, **33**, 359-375.

Clark, C.D., Gibbard, P.L. & Rose, J., 2004b. Pleistocene glacial limits in England, Scotland and Wales. In: J. Ehlers and P.L. Gibbard (Editors), *Quaternary Glaciations - Extent and Chronology. Part I - Europe*. Elsevier. Amsterdam, 47-82.

Clark, C.D. & Meehan, R.T., 2001. Subglacial bedform geomorphology of the Irish Ice Sheet reveals major configuration changes during growth and decay. *Journal of Quaternary Science*, **16**, 483-496.

Clark, P.U., 1991. Striated clast pavements: Products of deforming subglacial sediment? *Geology*, **19**, 530-533.

Clark, P.U. & Hansel, A.K., 1989. Clast ploughing, lodgement and glacier sliding over a soft glacier bed. *Boreas*, **18**, 201-207.

Clayton, L., Mickelson, D.M. & Attig, J.W., 1989. Evidence against pervasively deformed bed material beneath rapidly moving lobes of the southern Laurentide Ice Sheet. *Sedimentary Geology*, **62**, 203-208.

Collinson, J., 1986. Alluvial Sediments. In: H. Reading (Editor), *Sedimentary Environments: Processes, facies and stratigraphy. Third Edition.* Blackwell Science. Oxford, UK, 37-82.

Davey, R.J., 1982. The stratigraphic distribution of dinocysts in the Portlandian (latest Jurassic) to Barremian (Early Cretaceous) of northwest Europe. *American Association of Stratigraphic Palynologists Contributions Series*, **5B**, 49-81.

Davies, B.J., Roberts, D.H., Bridgland, D.R., Ó Cofaigh, C., Riding, J.B., Phillips, E.R. & Teasdale, D.A., in press. Interlobate ice sheet dynamics during the Last Glacial Maximum at Whitburn Bay, County Durham, England. *Boreas*.

Davis, J.C., 1986. *Statistics and data analysis in Geology. Second Edition.* John Wiley and Sons, New York, 646 pp.

de Vernal, A., Rochon, A. & Radi, T., 2007. Dinoflagellates. In: S. Elias (Editor), *Encyclopaedia of Quaternary Science*. Elsevier, 1652-1667.

Deer, W.A., Howie, R.A. & Zussman, J., 1992. *An introduction to the rock-forming minerals (2nd Edition).* Longman Scientific & Technical, Harlow, 696 pp.

Domack, E.W., 1984. Rhythmically bedded glaciomarine sediments on Whidbey Island, Washington. *Journal of Sedimentary Petrology*, **54**, 589-602.

Domack, E.W. & Lawson, D.E., 1985. Pebble fabric in an ice-rafted diamicton. *Journal of Geology*, **93**, 577-591.

Dreimanis, A., 1989. Tills, their genetic terminolog and classification. In: R.P. Goldthwait and C.L. Matsch (Editors), *Genetic Classification of Glacigenic Deposits*. Balkema. Rotterdam, 17-84.

Dreimanis, A., Hamilton, J.P. & Kelly, P.E., 1986. Complex subglacial sedimentation of Catfish Creek Till at Bradtville, Ontario, Canada. In: J.J. van der Meer (Editor), *Tills and Glaciotectonics*. Proceedings of an INQUA symposium on genesis and lithology of glacial deposits. Amsterdam, 73-87.

Drewey, D.J., 1986. *Glacial geologic processes.* Arnold, London, 276 pp.

Dunay, R.E., 1978. Late Triassic and Early Jurassic subsurface palynostratigraphy in northwestern Europe. *Palinological número extraordinario*, **1**, 355-365.

Dwerryhouse, 1902. The glaciation of Teesdale, Weardale and the Tyne Valley. *Quarterly Journal of the Geological Society of London*, **58**, 572.

Eastwood, T., 1946. *British Regional Geology: Northern England.* HMSO, London, 68 pp.

Ebbing, J., Weerts, H. & Westerhoff, W., 2003. Towards an integrated land-sea stratigraphy of the Netherlands. *Quaternary Science Reviews*, **22**, 1579-1587.

Edwards, W., Mitchell, G.H. & Whitehead, T.H., 1950. *Geology of the district north and east of Leeds. Memoir of the Geological Survey of Great Britain, Sheet 70.* HMSO, London, 93 pp.

Ehlers, J., Meyer, K.-D. & Stephan, H.-J., 1984. The Pre-Weichselian glaciations of North-West Europe. *Quaternary Science Reviews*, **3**, 1-40.

Ehlers, J. & Wingfield, R., 1991. The extension of the Late Weichselian / Late Devensian ice sheets in the North Sea Basin. *Journal of Quaternary Science*, **6**, 313-326.

Eissmann, L., 2002. Quaternary Geology of eastern Germany (Saxony, Saxon-Anhalt, South Brandenburg, Thüringia), type area of the Elsterian and Saalian stages in Europe. *Quaternary Science Reviews*, **21**, 1275-1346.

Elias, S.A., 2007. Societal Relevance of Quaternary Research. In: S.A. Elias (Editor), *Encyclopedia of Quaternary Science*. Elsevier. Oxford, 1-10.

Elson, J.A., 1961. The geology of tills. In: E. Penner and J. Butler (Editors), *Proceedings of the 14th Canadian soil mechanics conference*. Commission for Soil and Snow Mechanics, Technical Memoir, vol. 69, **69**, 5-36.

Emiliani, C., 1955. Pleistocene temperatures. *Journal of Geology*, **63**, 538-578.

England, P. & Molnar, P., 1990. Surface uplift, uplift of rocks, and exhumation of rocks. *Geology*, **18**, 1173-1177.

Evans, D., Owen, L. & Roberts, D.H., 1995. Stratigraphy and sedimentology of Devensian (Dimlington Stadial) glacial deposits, east Yorkshire, England. *Journal of Quaternary Science*, **10**, 241-265.

Evans, D.J.A., 2003a. Ice-marginal terrestrial landsystems: active temperate glacier margins. In: D.J.A. Evans (Editor), *Glacial Landsystems*. Arnold. London, 12-43.

Evans, D.J.A., 2003b. Introduction to glacial landsystems. In: D.J.A. Evans (Editor), *Glacial Landsystems*. Arnold. New York, 1-11.

Evans, D.J.A., 2007a. Glacial Erratics and Till Dispersal Indicators. In: S.A. Elias (Editor), *Encyclopedia of Quaternary Science*. Elsevier. Oxford, 975-978.

Evans, D.J.A., 2007b. Glacial Land Systems. In: S.A. Elias (Editor), *Encyclopedia of Quaternary Science*. Elsevier. Oxford, 808-818.

Evans, D.J.A. & Benn, D.I., 2004. Facies description and the logging of sedimentary exposures. In: D.J.A. Evans and D.I. Benn (Editors), *A practical guide to the study of glacial sediments*. Arnold. London, 11-50.

Evans, D.J.A. & Benn, D.I., 2007. Glacial Landforms. Introduction. In: S.A. Elias (Editor), *Encyclopedia of Quaternary Science*. Elsevier. Oxford, 757-772.

Evans, D.J.A., Clark, C.D. & Mitchell, W.A., 2005. The last British Ice Sheet: A review of the evidence utilised in the compilation of the Glacial Map of Britain. *Earth-Science Reviews*, **70**, 253-312.

Evans, D.J.A., Phillips, E.R., Hiemstra, J.F. & Auton, C.A., 2006. Subglacial till: Formation, sedimentary characteristics and classification. *Earth-Science Reviews*, **78**, 115-176.

Evans, D.J.A. & Twigg, D.R., 2002. The active temperate glacial landsystem: a model based on Breiethamerkurjokull and Fjallsjokull, Iceland. *Quaternary Science Reviews*, **21**, 2143-2177.

Evans, I.S., 1999. Castle Eden Dene and Blunts Dene. In: D.R. Bridgland, B.P. Horton and J.B. Innes (Editors), *The Quaternary of north-east England. Field Guide*. Quaternary Research Association. London, 57-64.

Everest, J., Bradwell, T. & Golledge, N., 2005. Subglacial landforms of the Tweed palaeo-ice stream. *Scottish Geographical Journal*, **121**, 163-173.

Eyles, C.H. & Eyles, N., 1983. Sedimentation in a large lake: a reinterpretation of the late Pleistocene stratigraphy at Scarborough Bluffs, Ontario, Canada. *Geology*, **11**, 146-152.

Eyles, C.H., Eyles, N. & Miall, A.D., 1985. Models of glaciomarine sediments and their application to the interpretation of ancient glacial sequences. *Palaeogeography, Palaeoclimatology, Palaeoecology*, **15**, 15-84.

Eyles, N., 1987. Late Pleistocene debris-flow deposits in large glacial lakes in British Columbia and Alaska. *Sedimentary Geology*, **53**, 33-71.

Eyles, N., Eyles, C.H. & McCabe, A.M., 1989. Sedimentation in an ice-contact subaqueous setting: The mid-Pleistocene `North Sea Drifts' of Norfolk, U.K. *Quaternary Science Reviews*, **8**, 57-74.

Eyles, N. & Lazorek, M., 2007. Glacial Landforms, Sediments. Glacigenic Lithofacies. In: S.A. Elias (Editor), *Encyclopedia of Quaternary Science*. Elsevier. Oxford, 920-932.

Eyles, N., McCabe, A.M. & Bowen, D.Q., 1994. The stratigraphic and sedimentological significance of Late Devensian Ice Sheet surging in Holderness, Yorkshire, U.K. *Quaternary Science Reviews*, **13**, 727-759.

Eyles, N. & Miall, A.D., 1984. Glacial Facies. In: R.G. Walker (Editor), *Facies Models*. Geological Association of Canada. Toronto, 15-38.

Eyles, N. & Sladen, J.A., 1981. Stratigraphy and geotechnical properties of weathered lodgement till in Northumberland, England. *Quarterly Journal of Geological Engineering*, **14**, 129-141.

Eyles, N., Sladen, J.A. & Gilroy, S., 1982. A depositional model for stratigraphic complexes and facies superposition in lodgement tills. *Boreas*, **11**, 317-333.

Firman, R.J., 1978. Intrusions. In: F. Moseley (Editor), *The Geology of the Lake District*. Yorkshire Geological Society. Occasional Publication No. 3. Leeds, 146-163.

Fischer, U. & Clarke, G.K.C., 1997. Stick-slip sliding behaviour at the base of a glacier. *Annals of Glaciology*, **24**, 390-396.

Fischer, U.H. & Hubbard, B., 1999. Subglacial sediment textures: character and evolution at Haut Glacier d'Arolla, Switzerland. *Annals of Glaciology*, **28**, 241-246.

Fish, P.R. & Whiteman, C.A., 2001. Chalk micropalaeontology and the provenancing of Middle Pleistocene Lowestoft Formation till in eastern England. *Earth Surface Processes and Landforms*, **26**, 953-970.

Fitzpatrick, E.A., 1984. *Micromorphology of soils*. Chapman and Hall, London and New York, 433 pp.

Floyd, J.D., 1999. *Geology of the Carrick - Loch Doon district: Memoir for the 1:50,000 Geological Sheets 8W and 8E (Scotland)*. HMSO, London, 122 pp.

Fountain, A.G. & Walder, J.S., 1998. Water flow through temperate glaciers. *Review of Geophysics*, **36**, 299-328.

Francis, E.A., 1972. Quaternary. In: G.A.L. Johnson and G. Hickling (Editors), *Geology of Durham County*. Transactions of the Natural History Society of Northumberland, Durham and Newcastle upon Tyne, **41**, 134-153.

Gale, S.J. & Hoare, P.G., 1991. *Quaternary Sediments: Petrographic methods for the study of unlithified rocks*. John Wiley & Sons, New York, 323 pp.

Gale, S.J. & Hoare, P.G., 1992. Bulk sampling of coarse clastic sediments for particle-size analysis. *Earth Surface Processes and Landforms*, **17**, 729-733.

Gatliffe, R.W., Richards, P.C., Smith, K., Graham, C.C., McCormac, M., Smith, N.J.P., Long, D., Cameron, T.D.J., Evans, D., Stevenson, A.G., Bulat, J. & Ritchie, J.D., 1994. *The Geology of the Central North Sea. United Kingdom Offshore Regional Report*. British Geological Survey. HMSO, London, 118 pp.

Gaunt, G.D., 1981. Quaternary History of the Southern Part of the Vale of York. In: J. Neale and J. Flenley (Editors), *The Quaternary in Britain*. Pergamon Press. Oxford, 82-97.

Gaunt, G.D., Fletcher, T.P. & Wood, C.J., 1992. *Geology of the country around Kingston upon Hull and Brigg*. HMSO, London, 172 pp.

Gibbard, P., 2003. Definition of the Middle-Upper Pleistocene boundary. *Global and Planetary Change*, **36**, 201-208.

Gibbard, P.L., Moscariello, A., Bailey, H.W., Boreham, S., Koch, C., Lord, A.R., Whittaker, J.E. & Whiteman, C.A., 2008. Comment: Middle Pleistocene sedimentation at Pakefield, Suffolk, England. *Journal of Quaternary Science*, **23**, 85-92.

Gibbard, P.L., West, R.G., Andrew, R. & Pettit, M., 1992. The margin of a middle Pleistocene ice advance at Tottenhill, Norfolk, England. *Geological Magazine*, **129**, 59-76.

Glasser, N.F., Hambrey, M.J., Huddart, D., Gonzales, S., Crawford, K.R. & Maltman, A.J., 2001. Terrestrial glacial sedimentation on the eastern margin of the Irish Sea Basin: Thursaston, The Wirral. *Proceedings of the Geologists' Association*, **112**, 131-146.

Golledge, N.R., Finlayson, A., Bradwell, T. & Everest, J.D., 2008. The last glaciation of Shetland, North Atlantic. *Geografiska Annaler Series A - Physical Geography*, **90A**, 37-53.

Golledge, N.R. & Stoker, M.S., 2006. A palaeo-ice stream of the British ice sheet in eastern Scotland. *Boreas*, **35**, 231-243.

Goudie, A., Anderson, M., Burt, T., Lewin, J., Richards, K., Whalley, B. & Worsley, P., 1994. *Geomorphological Techniques, 2nd Edition.* British Geomorphological Research Group. Allen and Unwin, London, 570 pp.

Graham, A.G.C., Lonergan, L. & Stoker, M.S., 2007. Evidence for Late Pleistocene ice stream activity in the Witch Ground Basin, central North Sea, from 3D seismic reflection data. *Quaternary Science Reviews*, **26**, 627-643.

Greig, D.C., 1971. *British Regional Geology: The South of Scotland (third edition).* Memoir of the British Geological Survey. HMSO, Edinburgh, 126 pp.

Gribble, C.D. & Hall, A.J., 1992. *A Practical Introduction to Optical Mineralogy.* Chapman and Hall, London, 250 pp.

Haavisto-Hyvärinen, M., 1997. Pre-crag ridges in southwestern Finland. *Sedimentary Geology*, **111**, 147-159.

Hald, M. & Korsun, S., 1997. Distribution of modern benthic foraminifera from fjords of Svalbard, European Arctic. *Journal of Foraminiferal Research*, **27**, 101-122.

Haldorsen, S., 1981. Grain-size distribution of subglacial till and its relation to subglacial crushing and abrasion. *Boreas*, **10**, 91-105.

Hamblin, R.J.O., Moorlock, B.S.P., Rose, J., Lee, J.R., Riding, J.B., Booth, S.J. & Pawley, S.M., 2005. Revised Pre-Devensian glacial stratigraphy in Norfolk, England, based on mapping and till provenance. *Netherlands Journal of Geosciences-Geologie En Mijnbouw*, **84**, 77-85.

Hansen, H.J. & Lykke-Andersen, A., 1976. Wall Structure and classification of fossil and recend elphidiid and nonionid Foraminifera. In: A. Martinsson (Editor), *Fossils and Strata.* Universitetsforlaget, **10**. Oslo.

Harmer, F.W., 1928. The distribution of erratics and drift. *Proceedings of the Yorkshire Geologists' and Polytechnic Society*, **21**, 79-150.

Harris, A., 1991. The Growth and Structure of Scotland. In: G.Y. Craig (Editor), *Geology of Scotland, 3rd Edition.* The Geological Society. London, 1-24.

Hart, J. & Rose, J., 2001. Approaches to the study of glacier bed deformation. *Quaternary International*, **86**, 45-58.

Hart, J.K., 1997. The relationship between drumlins and other forms of subglacial glaciotectonic deformation. *Quaternary Science Reviews*, **16**, 93-107.

Hart, J.K., 2007. An investigation of subglacial shear zone processes from Weybourne, Norfolk, UK. *Quaternary Science Reviews*, **26**, 2354-2374.

Hart, J.K. & Boulton, G.S., 1991. The interrelation of glaciotectonic and glaciodepositional processes within the glacial environment. *Quaternary Science Reviews*, **10**, 335-350.

Hart, J.K., Hindmarsh, R.C.A. & Boulton, G.S., 1990. Styles of Subglacial Glaciotectonic Deformation within the Context of the Anglian Ice-Sheet. *Earth Surface Processes and Landforms*, **15**, 227-241.

Hart, J.K., Khatwa, A. & Sammonds, P., 2004. The effect of grain texture on the occurrence of microstructural properties in subglacial till. *Quaternary Science Reviews*, **23**, 2501-2512.

Hart, J.K. & Pelgar, S., 1990. Further evidence for the timing of the Middle Pleistocene Glaciation in Britain. *Proceedings of the Geologists Association*, **101**, 187-196.

Hart, J.K. & Roberts, D.H., 1994. Criteria to distinguish between subglacial glaciotectonic and glaciomarine sedimentation: I - Deformation styles and sedimentology. *Sedimentary Geology*, **91**, 191-214.

Hicock, S.R., 1991. On subglacial stone pavements in till. *Journal of Geology*, **99**, 607-619.

Hicock, S.R. & Fuller, E.A., 1995. Lobal interactions, rheologic superposition, and implications for a Pleistocene ice stream on the continental shelf of British Columbia. *Geomorphology*, **14**, 167-184.

Hicock, S.R., Goff, J.R., Lian, O.B. & Little, E.C., 1996. On the interpretation of subglacial till fabric. *Journal of Sedimentary Research*, **66**, 928-945.

Hiemstra, J.F., 2001. Microscopic analyses of Quaternary glacigenic sediments of Marguerite Bay, Antarctic Peninsula. *Arctic Antarctic and Alpine Research*, **33**, 258-265.

Hiemstra, J.F., 2007. Micromorphology of Glacial Sediments. In: S.A. Elias (Editor), *Encyclopedia of Quaternary Science*. Elsevier. Amsterdam, London, 945-954.

Hiemstra, J.F., Evans, D.J.A. & Ó Cofaigh, C., 2007. The role of glacitectonic rafting and comminution in the production of subglacial tills: examples from southwest Ireland and Antarctica. *Boreas*, **36**, 386-399.

Hiemstra, J.F., Evans, D.J.A., Scourse, J.D., McCarroll, D., Furze, M.F.A. & Rhodes, E., 2006. New evidence for a grounded Irish Sea glaciation of the Isles of Scilly, UK. *Quaternary Science Reviews*, **25**, 299-309.

Hiemstra, J.F. & Rijsdijk, K.F., 2003. Observing artificially induced strain: implications for subglacial deformation. *Journal of Quaternary Science*, **18**, 373-383.

Hindmarsh, R., 1997. Deforming beds: Viscous and plastic scales of deformation. *Quaternary Science Reviews*, **16**, 1039-1056.

Hjelstuen, B.O., Sejrup, H.P., Haflidason, H., Nygard, A., Berstad, I.M. & Knorr, G., 2004. Late Quaternary seismic stratigraphy and geological development of the south Voring margin, Norwegian Sea. *Quaternary Science Reviews*, **23**, 1847-1865.

Hoare, P.G. & Connell, E.R., 2005. The first appearance of Scandinavian indicators in East Anglia's glacial record. *Bulletin of the Geological Society of Norfolk*, **54**, 3-14.

Hoey, T.B., 2004. The size of sedimentary particles. In: D.J.A. Evans and D.I. Benn (Editors), *A practical guide to the study of glacial sediments*. Arnold. London, 51-76.

Holmes, R., 1977. *Quaternary deposits of the central North Sea, 5. The Quaternary geology of the UK sector of the North Sea between 56° and 58°N*, Institute of Geological Sciences.

Hooke, R.L. & Iverson, N.R., 1995. Grain-size distribution in deforming subglacial tills: role of grain fracture. *Geology*, **23**, 57-60.

Hooke, R.L. & Jennings, C.E., 2006. On the formation of the tunnel valleys of the southern Laurentide ice sheet. *Quaternary Science Reviews*, **25**, 1364-1372.

Hooyer, T.S. & Iverson, N.R., 2000. Clast fabric development in a shearing granular material: implications for subglacial till and fault gauge. *Geological Society of America Bulletin*, **112**, 683-692.

Horton, B.P. & Edwards, R.J., 2006. Quantifying Holocene sea-level change using intertidal foraminifera: lessons from the British Isles. *Cushman Foundation for Foraminiferal research.*, **Special Publication No. 40**, 97 p.

Houmark-Nielsen, M. & Gibbard, J.E.a.P.L., 2004. The Pleistocene of Denmark: A review of stratigraphy and glaciation history, *Developments in Quaternary Science*. Elsevier, **Volume 2, Part 1**, 35-46.

Howarth, J.H., 1908. The ice-bourne boulders of Yorkshire. *The Naturalist*, 97-255.

Hubbard, B. & Glasser, N.F., 2005. *Field Techniques in Glaciology and Geomorphology*. Wiley, 412 pp.

Hubert, J.F., 1971. Analysis of Heavy-Mineral Assemblages. In: R.E. Carver (Editor), *Procedures in Sedimentary Petrology*. Wiley-Interscience. New York, 453-478.

Hudson, J.D. & Trewin, N.H., 2002. Jurassic. In: N.H. Trewin (Editor), *Geology of Scotland. 4th Edition*. The Geological Society. Bath, 323-350.

Humphrey, N., Kamb, B., Fahnestock, M. & Englehardt, H., 1993. Characteristics of the bed of the Lower Columbia Glacier, Alaska. *Journal of Geophysical Research*, **98**, 837-846.

Huuse, M. & Lykke-Andersen, H., 2000. Overdeepened Quaternary valleys in the eastern Danish North Sea: morphology and origin. *Quaternary Science Reviews*, **19**, 1233-1253.

Ildefonse, B., Launeau, P., Bouchez, J.L. & Ferdandez, A., 1992. Effects on mechanical interactions on the development of preferred orientations: a two-dimensional experimental approach. *Structural Geology*, **14**, 73-83.

Iverson, N.R., Jansson, P. & Hooke, R.L., 1995. In-situ measurement of the strength of deforming subglacial till. *Journal of Glaciology*, **40**, 497-503.

Jansonius, J. & McGregor, D.C., 1996. Chapter 1: Introduction. In: J. Jansonius and D.C. McGregor (Editors), *Palynology: principles and applications*. American Association of Stratigraphic Palynologists Foundation, **1**. Dallas, 1-10.

Jansson, K.N. & Glasser, N.F., 2005. Palaeoglaciology of the Welsh sector of the British-Irish Ice Sheet. *Journal of the Geological Society, London*, **162**, 25-37.

Jennings, A.E., Weiner, N.J., Helgadottir, G. & Andrews, J.T., 2004. Modern foraminiferal faunas of the southwestern to northern Iceland shelf: Oceanographic and environmental controls. *Journal of Foraminiferal Research*, **34**, 180-207.

Jennings, C.E., 2006. Terrestrial ice streams - a view from the lobe. *Geomorphology*, **75**, 100-124.

Johnson, G.A.L., 1995. *Robson's Geology of North East England*. Transaction of the Natural History Society of Northumbria. Volume 56 Part 5, Newcastle, 165 pp.

Johnson, M.R.W., 1991. Dalradian. In: G.Y. Craig (Editor), *Geology of Scotland. 3rd Edition*. The Geological Society. London, 125-151.

Jones, A.P., Tucker, M.E. & Hart, J.K., 1999. *The description and analysis of Quaternary stratigraphic field sections. Technical Guide No. 7*. Quaternary Research Association, Cambridge, 293 pp.

Jones, J.M., Magraw, D. & O'Mara, P.T.O., 1995. Carboniferous Westphalian Coal Measures. In: G.A.L. Johnson (Editor), *Robson's Geology of North East England*. Transactions of the Natural History Society of Northumbria. Volume 56 Part 5. Newcastle, 267-276.

Jónsdóttir, H.E., Sejrup, H.P., Larsen, E. & Stalsberg, K., 1999. Late Weichselian ice-flow direction in Jæren, SW Norway; clast fabric and clast lithology evidence in the uppermost till. *Norweigian Journal of Geography*, **53**, 177-189.

Jørgensen, F. & Piotrowski, J.A., 2003. Signature of the Baltic Ice Stream on Funen Islands, Denmark, during the Weichselian glaciation. *Boreas*, **32**, 242-255.

Jørgensen, F. & Sandersen, P.B.E., 2006. Buried and open tunnel valleys in Denmark - erosion beneath multiple ice sheets. *Quaternary Science Reviews*, **25**, 1339-1363.

Kalm, V., 2005. Pleistocene chronostratigraphy for Estonia, south-eastern sector of the Scandinavian glaciation. *Quaternary Science Reviews*, **25**, 960-975.

Kaufman, D.S. & Manley, W.F., 1998. A new procedure for determining DL amino acid ratios in fossils using reverse phase liquid chromotography. *Quaternary Science Reviews*, **17**, 987-1000.

Keen, D.H., Coope, G.R., Jones, R.L., Field, M.H., Griffiths, H.I., Lewis, S.G. & Bowen, D.Q., 1997. Middle Pleistocene deposits at Frog Hall Pit, Stretton-on-Dunsmore, Warwickshire, English Midlands, and their implications for the age of the type Wolstonian. *Journal of Quaternary Science*, **12**, 183-208.

Kendall, P.F. & Howarth, J.H., 1902. The Yorkshire Boulder Committee and its fifteenth year's work, 1900-1901. *The Naturalist*, 211-222.

Khatawa, A. & Tulaczyk, S., 2001. Microstructural interpretations of modern and Pleistocene subglacially deformed sediments: the relative role of parent material and subglacial process. *Journal of Quaternary Science*, **16**, 507-517.

Klassen, R.A., 1999. The application of glacial dispersal models to the interpretation of till geochemistry in Labrador, Canada. *Journal of Geochemical Exploration*, **67**, 245-269.

Kleman, J. & Stroeven, A.P., 1997. Preglacial surface remnants and Quaternary glacial regimes in northwestern Sweden. *Geomorphology*, **19**, 35-54.

Knies, J., Vogt, C., Matthiessen, J., Nam, S.-I., Ottesen, D., Rise, L., Bargel, T. & Eilertsen, R.S., 2007. Re-advance of the Fennoscandian Ice Sheet during Heinrich Event 1. *Marine Geology*, **240**, 1-18.

Knight, J. & McCabe, A.M., 1997. Drumlin evolution and ice sheet oscillations along the NE

Atlantic margin, Donegal Bay, western Ireland. *Sedimentary Geology*, **111**, 57-72.

Knight, J., McCarron, S.G. & McCabe, A.M., 1999. Landform modification by palaeo-ice streams in east-central Ireland. *Annals of Glaciology*, **28**, 161-167.

Knudsen, K.L. & Austin, W.E.N., 1996. Late Glacial Foraminifera. In: J.T. Andrews, W.E.N. Austin, H. Bergsten and A.E. Jennings (Editors), *Late Quaternary Palaeoecology of the North Atlantic Margins*. Geological Society of London Special Publication 111. London, 7-10.

Knutz, P.C., Austin, W.E.N. & Jones, E.J.W., 2001. Millennial-scale depositional cycles related to British Ice Sheet variability and North Atlantic paleocirculation since 45 kyr BP, Barra Fan, UK margin. *Paleoceanography*, **16**, 53-64.

Knutz, P.C., Jones, E.J.W., Austin, W. & van Weering, T.C.E., 2002. Glaciomarine slope sedimentation, contourite drifts and bottom current pathways on the Barra Fan, UK North Atlantic margin. *Marine Geology*, **188**, 129-146.

Korsun, S., Polyak, L., Febo, L. & Lubinski, D., 2001. *Foraminiferal research*. Byrd Polar Research Centre, http://bprc.osu.edu/foram/home.htm.

Kovach, W.L., 1995. Multivariate data analysis. In: D. Maddy and J.S. Brew (Editors), *Statistical modelling of Quaternary Science Data. Technical Guide No. 5*. Quaternary Research Association. Cambridge, 1-38.

Krasnov, I.I., 1971. *Map of Quaternary deposits of the European USSR and adjacent regions, scale 1:1 500 000*. VSEGEI, Leningrad, 16 sheets.

Kristensen, T.B., Huuse, M., Piotrowski, J.A. & O.L., C., 2007. A morphometric analysis of tunnel valleys in the eastern North Sea based on 3D seismic data. *Journal of Quaternary Science*, **22**, 801-815.

Kristensen, T.B., Piotrowski, J.A., Huuse, M., Clausen, O.R. & Hamberg, L., 2008. Time-transgressive tunnel valley formation indicated by infill sediment structure, North Sea - the role of glaciohydraulic supercooling. *Earth Surface Processes and Landforms*, **33**, 546-559.

Krüger, J. & Kjaer, K.H., 1999. A data chart for field description and genetic interpretation of glacial diamicts and associated sediments - with examples from Greenland, Iceland, and Denmark. *Boreas*, **28**, 386-402.

Lachniet, M.S., Larson, G.J., Lawson, D.E., Evenson, E.B. & Alley, R.B., 2001. Microstuctures of sediment flow deposits and subglacial sediments: a comparison. *Boreas*, **30**, 254-262.

Lajoie, K.R., Wehmiller, J.F. & Kennedy, G.L., 1980. Inter- and intra-generic trends in apparent racemisation kinetics of amino acids in Quaternary molluscs. In: P.E. Hare, T.C. Hoering and J.K. King (Editors), *Biogeochemistry of Amino Acids*. Wiley. New York, 305-340.

Larsen, N.K. & Piotrowski, J.A., 2003. Fabric pattern in a basal till succession and its significance for reconstructing subglacial processes. *Journal of Sedimentary Research*, **73**, 725-734.

Larsen, N.K., Piotrowski, J.A. & Kronborg, C., 2004. A multiproxy study of a basal till: a time-transgressive accretion and deformation hypothesis. *Journal of Quaternary Science*, **19**, 9-21.

Lawson, D.E., 1979. A comparison of the pebble orientations in ice and deposits of the Matamuska Glacier, Alaska. *Journal of Geology*, **87**, 629-645.

Lee, J. & Kemp, R.A., 1994. *Thin sections of unconsolidated sediments and soils: a recipe*. Royal Holloway, University of London, Egham, 45 pp.

Lee, J.R., 2003. *Early and Middle Pleistocene lithostratigraphy and palaeoenvironments in northern East Anglia, UK.*, Unpublished PhD Thesis, Royal Holloway University of London, 421 pp.

Lee, J.R. & Phillips, E.R., 2008. Progressive soft sediment deformation within a subglacial shear zone - a hybrid mosaic-pervasive deformation model for Middle Pleistocene glaciotectonised sediments from eastern England. *Quaternary Science Reviews*, **27**, 1350-1362.

Lee, J.R., Rose, J., Candy, I. & Barendregt, R.W., 2006. Sea-level changes, river activity, soil development and glaciation around the western margins of the southern North Sea Basin during the Early and early Middle Pleistocene: evidence from Pakefield, Suffolk, UK. *Journal of Quaternary Science*, **21**, 155-179.

Lee, J.R., Rose, J., Candy, I., Barendregt, R.W., Moorlock, B.S.P., Riding, J.B. & Hamblin, R.J.O., 2008. Reply: Middle Pleistocene sedimentation at Pakefield, Suffolk, England. *Journal of Quaternary Science*, **23**, 93-98.

Lee, J.R., Rose, J., Hamblin, R.J.O. & Moorlock, B.S.P., 2004. Dating the earliest lowland glaciation of eastern England: a pre-MIS 12 early Middle Pleistocene Happisburgh glaciation. *Quaternary Science Reviews*, **23**, 1551-1566.

Lee, J.R., Rose, J., Riding, J.B., Moorlock, B.S.P. & Hamblin, R.J.O., 2002. Testing the case for a Middle Pleistocene Scandinavian glaciation in Eastern England: evidence for a Scottish ice source for tills within the Corton Formation of East Anglia, UK. *Boreas*, **31**, 345-355.

Lee, M.K., Brown, G.C., Webb, P.C., Wheildon, J. & Rollin, K.E., 1987. Heat flow, heat production and thermo-tectonic setting in mainland UK. *Journal of the Geological Society*, **144**, 35-42.

Lekens, W.A.H., Sejrup, H.P., Haflidason, H., Petersen, G.O., Hjelstuen, B. & Knorr, G., 2005. Laminated sediments preceding Heinrich event 1 in the Northern North Sea and Southern Norwegian Sea: Origin, processes and regional linkage. *Marine Geology*, **216**, 27-50.

Lewis, S.G., 1999. Eastern England. In: D.Q. Bowen (Editor), *A revised correlation of Quaternary deposits in the British Isles*. Geological Society Special Report no. 23. London, 10-27.

Lian, O.B., 2007. Optically-Stimulated Luminescence. In: S.A. Elias (Editor), *Encyclopedia of Quaternary Science*. Amsterdam, Elsevier, 1491-1505.

Lian, O.B. & Hicock, S.R., 2000. Thermal conditions beneath parts of the last Cordilleran Ice Sheet near its centre as inferred from subglacial till, associated sediments, and bedrock. *Quaternary International*, **68-71**, 147-162.

Lian, O.B. & Roberts, R.G., 2006. Dating the Quaternary: progress in luminescence dating of sediments. *Quaternary Science Reviews*, **25**, 2449-2468.

Licht, K.J., Dumbar, N.W., Andrews, J.T. & Jennings, A.E., 1999. Distinguishing subglacial till and glacial marine diamictons in the western Ross Sea, Antarctica: Implications for a last glacial maximum grounding line. *Bulletin of the Geological Society of America*, **111**, 91-103.

Livingstone, S.J., Ó Cofaigh, C. & Evans, D.J.A., in prep. A Major ice drainage outlet of the last British-Irish ice sheet: the Tyne Gap, northern England.

Livingstone, S.J., Ó Cofaigh, C. & Evans, D.J.A., in press. Glacial geomorphology of the central sector of the last British-Irish Ice Sheet. *Journal of Maps*.

Long, D., Laban, C., Streif, H., Cameron, T.D.J. & Schüttenhelm, R.T.E., 1988. The sedimentary record of climatic variation in the southern North Sea. *Philosophical Transactions of the Royal Society of London B*, **318**, 523-537.

Loubere, P. & Austin, W., 2007. Benthic Foraminifera. In: S. Elias (Editor), *Encyclopaedia of Quaternary Science*. Elsevier, 1618-1627.

Ludwig, K.R. & Paces, J.B., 2002. Uranium-series dating of pedogenic silica and carbonate, Crater Flat, Nevada. *Geochemica et Cosmochimica Acta*, **66**, 487-506.

Lukas, S., 2006. Morphostratigraphic principles in glacier reconstruction - a perspective from the British Younger Dryas. *Progress in Physical Geography*, **30**, 719-736.

Lundqvist, J., 1987. Stratigraphy of the central area of the Scandinavian glaciation. In: V. Sibrava, D.Q. Bowen and D. Richmond (Editors), *Correlation of Quaternary Depostits in the Northern Hemisphere*. Report of the International Geological Correlation Programme, Project 24. Pergamon Press. Oxford, 251-268.

Lunkka, J.P., 1994. Sedimentation and lithostratigraphy of the North Sea Drift and Lowestoft Till formations in the coastal cliffs of northeast Norfolk, England. *Journal of Quaternary Science*, **9**, 209-233.

Lunn, A.G., 1995. Quaternary. In: G.A.L. Johnson (Editor), *Robson's Geology of north-east England*. Transactions of the Natural History Society of Northumbria. Volume 56 Part 5. Newcastle, 297-312.

Luo, X., Rehkämper, M., Lee, D.-C. & Halliday, A.N., 1997. High precision (230) Th/(232)Th and (234)U/(238)U measurements using energy-filtered ICP magnetic sector multiple collector mass spectrometry. *International Journal of Mass Spectrometry Ion Processes*, **171**, 105-117.

MacKenzie, W.S. & Adams, A.E., 2001. *A colour atlas of rocks and minerals in thin section.* Manson Publishing, London, 192 pp.

Madgett, P.A. & Catt, J.A., 1978. Petrography, stratigraphy, and weathering of the Late Pleistocene tills in East Yorkshire, Lincolnshire and North Norfolk. *Proceedings of the Yorkshire Geological Society*, **42**, 55-108.

Maizels, J., 1995. Sediments and Landforms of Modern Proglacial Terrestrial Environments. In: J. Menzies (Editor), *Modern Glacial Environments: Processes, dynamics and sediments*. Butterworth-Heinemann. Oxford, 365-416.

Mange, M.A., Dewey, J.F. & Floyd, J.D., 2005. The origin, evolution, and provenance of the Northern Belt (Ordovician) of the Southern Uplands Terrane, Scotland: a heavy mineral perspective. *Proceedings of the Geologists' Association*, **116**, 251-280.

Mange, M.A. & Maurer, H.F.W., 1992. *Heavy Minerals in Colour*. Chapman and Hall, London, 147 pp.

Mange, M.A. & Otvos, E.G., 2005. Gulf coastal plain evolution in West Louisiana: Heavy mineral provenance and Pleistocene alluvial chronology. *Sedimentary Geology*, **182**, 29-57.

Mangerud, J., 2004. Ice sheet limits in Norway and on the Norwegian continental shelf. In: J. Ehlers and P. Gibbard (Editors), *Quaternary Glaciations - extent and chronology*. Elsevier, 271-294.

Mangerud, J., Jansen, E. & Landvik, J., 1996. Late Cenozoic history of the Scandinavian and Barents Sea ice sheets. *Global and Planetary Change*, **12**, 11-26.

Mauz, B., Packman, S. & Lang, A., 2006. The alpha effectiveness of silt-sized quartz: new data obtained by single aliquot regeneration in dose protocols. *Ancient TL*, **24**, 47-52.

May, R.W., Dreimanis, A. & Stankowski, W., 1980. Quantitative evaluation of clast fabrics within the Catfish Creek Till, Bradtville, Ontario. *Canadian Journal of Earth Sciences*, **17**, 1064-1074.

McCabe, A.M., Bowen, D.Q. & Penney, D.N., 1993. Glaciomarine facies from the western sector of the last British ice sheet, Malin Beg, County Donegal, Ireland. *Quaternary Science Reviews*, **12**, 35-45.

McCabe, A.M. & Clark, P.U., 1998. Ice-sheet variability around the North Atlantic ocean during the last deglaciation. *Nature*, **392**, 373-377.

McCabe, A.M., Clark, P.U. & Clark, J., 2005. AMS 14C dating of deglacial events in the Irish Sea Basin and other sectors of the British-Irish ice sheet. *Quaternary Science Reviews*, **24**, 1673-1690.

McCabe, A.M., Clark, P.U., Clark, J. & Dunlop, P., 2007. Radiocarbon constraints on readvances of the British-Irish Ice Sheet in the northern Irish Sea Basin during the last deglaciation. *Quaternary Science Reviews*, **26**, 1204-1211.

McCabe, M., Knight, J. & McCarron, S., 1998. Evidence for Heinrich event 1 in the British Isles. *Journal of Quaternary Science*, **13**, 549-568.

McCarroll, D. & Harris, C., 1992. The glacigenic deposits of western Lleyn, North Wales: terrestrial or marine? *Journal of Quaternary Science*, **7**, 19-29.

McCarroll, D. & Rijsdijk, K.F., 2003. Deformation styles as a key for interpreting glacial depositional environments. *Journal of Quaternary Science*, **18**, 473-489.

McClenaghan, M.B., 1992. Surface till geochemistry and implications for exploration, Black River - Matheson area, northeastern Ontario. *Exploration and Mining Geology*, 1, 327-337.

McMillan, A., 2005. A provisional Quaternary and Neogene lithostratigraphical framework for Great Britain. *Netherlands Journal of Geosciences - Geologie en Mijnbouw*, **84**, 87-107.

Mejdahl, V., 1979. Thermoluminescence dating: beta attenuation in quartz grains. *Archaometry*, **21**, 61-73.

Menzies, J., 2000. Micromorphological analyses of microfabrics and microstructures indicative of deformation processes in glacial sediments. In: A.J. Maltman, A.J. Hubbard and M.J. Hambrey (Editors), *Deformation of Glacial Materials. Geological Society Special Publication 176.* Geological Society of London, **176**. London, 245-257.

Menzies, J. & Maltman, A.J., 1992. Microstructures in diamictons - evidence of

subglacial bed conditions. *Geomorphology*, **6**, 27-40.

Menzies, J., van der Meer, J.J.M. & Rose, J., 2006. Till-as a glacial "tectomict", its internal architecture, and the development of a "typing" method for till differentiation. *Geomorphology*, **75**, 172-200.

Menzies, J. & Zaniewski, K., 2003. Microstructures within a modern debris flow deposit derived from Quaternary glacial diamicton - a comparative micromorphological study. *Sedimentary Geology*, **157**, 31-48.

Merritt, J.W., Auton, C.A., Connell, E.R., Hall, A.M. & Peacock, J.D., 2003. *Cainozoic geology and landscape evolution of north-east Scotland: Memoir for the drift editions of 1:50 000 geological sheets 66E, 67, 76E, 77, 86E, 87W, 87E, 95, 96W, 96E, and 97 (Scotland).* HMSO, British Geological Survey, Edinburgh, 178 pp.

Merritt, J.W., Auton, C.A. & Firth, C.R., 1995. Ice-proximal glaciomarine sedimentation and sea-level change in the Inverness area, Scotland: A review of the deglaciation of a major ice stream of the British Late Devensian ice sheet. *Quaternary Science Reviews*, **14**, 289-329.

Miller, G.H. & Clarke, S.J., 2007. Amino-Acid Dating. In: S.A. Elias (Editor), *Encyclopedia of Quaternary Science*. Amsterdam, Elsevier, 41-52.

Mills, P.C., 1983. Genesis and diagnostic value of soft-sediment deformation structures - A review. *Sedimentary Geology*, **35**, 83-104.

Millward, D., Moseley, F. & Soper, N.J., 1978. The Eycott and Borrowdale Volcanic Rocks. In: F. Moseley (Editor), *The Geology of the Lake District*. Yorkshire Geological Society. Special Publication No. 3. Bath, 99-120.

Mitchell, W.A., 1994. Drumlins in ice sheet reconstructions with special reference to the western Pennines. *Sedimentary Geology*, **91**, 313-332.

Mitchell, W.A., 2007. Reconstructions of the Late Devensian (Dimlington Stadial) British-Irish Ice Sheet: the role of the upper Tees drumlin field, north Pennines, England. *Proceedings of the Yorkshire Geological Society*, **56**, 221-234.

Mitchell, W.A., 2008. Quaternary geology of part of the Kale Water catchment, Western Cheviot Hills, southern Scotland. *Scottish Journal of Geology*, **44**, 51-63.

Mitchell, W.A. & Clark, C.D., 1994. The last ice sheet in Cumbria. In: J. Boardman and J.S. Walden (Editors), *Cumbria Field Guide*. Quaternary Research Association. Cambridge, 4-14.

Morton, A.C. & Hallsworth, A.C., 1994. Identifying provenance-specific features of detrital heavy mineral assemblages in sandstones. *Sedimentary Geology*, **90**, 241-256.

Morton, A.C. & Hallsworth, A.C., 2007. Stability of detrital heavy minerals during burial diagenesis. In: M.A. Mange and D.T. Wright (Editors), *Heavy Minerals in Use*. Developments in Sedimentology 58. Elsevier, 215-245.

Morton, A.C., Whitham, A.G. & Fanning, C.M., 2005. Provenance of Late Cretaceous to Paleocene submarine fan sandstones in the Norwegian Sea: Integration of heavy mineral, mineral chemical and zircon age data. *Sedimentary Geology*, **182**, 3-28.

Murphy, C.P., 1986. *Thin section preparation of soils and sediments*. A B Academic Publishers, Berkhampstead, 149 pp.

Murray, A.S. & Funder, S., 2003. Optically stimulated luminescence dating of a Danish Eemian coastal marine deposit: a test of accuracy. *Quaternary Science Reviews*, **22**, 1177-1183.

Murray, A.S. & Olley, J.M., 2002. Precision and accuracy in the optically stimulated luminescence dating of quartz: a status review. *Geochronometriea*, **41**, 1-16.

Murray, A.S. & Roberts, R.G., 1997. Determining the burial time of single grains of quartz using optically stimulated luminescence. *Earth and Planetary Science Letters*, **32**, 57-73.

Murray, A.S. & Wintle, A.G., 2000. Luminescence dating of quartz using an improved single-aliquot regenerative-dose protocol. *Radiation Measurements*, **32**, 57-73.

Murray, J.W., 1979. British nearshore foraminiferids. In: D.M. Kermack and R.S.K. Barnes (Editors), *Synopses of the British Fauna, New Series. No. 16*. Academic Press. London, New York, and San Francisco, 68 pp.

Nelson, A.E., Willis, I.C. & Ò Cofaigh, C., 2005. Till genesis and glacier motion inferred from sedimentological evidence associated with the surge-type glacier, Brùarjökill, Iceland. *Annals of Glaciology*, **42**, 14-22.

Ng, F.S.L., 2000. Canals under sediment-based ice sheets. *Annals of Glaciology*, **30**, 146-152.

Norton, P.E.P., 1967. Marine molluscan assemblages in the Early Pleistocene of Sidestrand, Bramerton and the Royal Society Borehole at Ludham, Norfolk. *Philosophical Transactions of the Royal Society of London B*, **252**, 161-200.

Ó Cofaigh, C., 1996. Tunnel Valley Genesis. *Progress in Physical Geography*, **20**, 1-19.

Ó Cofaigh, C. & Dowdeswell, J.A., 2001. Laminated sediments in glacimarine environments: diagnostic criteria for their interpretation. *Quaternary Science Reviews*, **20**, 1411-1436.

Ó Cofaigh, C., Dowdeswell, J.A., Allen, C.S., Hiemstra, J.F., Pudsey, C.J., Evans, J. & Evans, D.J.A., 2005. Flow dynamics and till genesis associated with a marine-based Antarctic palaeo-ice stream. *Quaternary Science Reviews*, **24**, 709-740.

Ó Cofaigh, C. & Evans, D.J.A., 2001. Deforming bed conditions associated with a major stream of the last British ice sheet. *Geology*, **29**, 795-798.

Ó Cofaigh, C., Evans, D.J.A. & Hiemstra, J., 2008. Till sedimentology and stratigraphy on the Dingle Peninsula, SW Ireland: implications for Late Quaternary regional ice flow patterns. *Proceedings of the Geologists' Association*, **119**, 137-152.

Oftedahl, C., 1960. *Permian Igneous Rocks of the Oslo Graben, Norway. Guide to excursions A.11 and C.7.* International Geological Congress XXI Session. Norden 1960.

Oliver, G.J.H., Stone, P. & Bluck, B.J., 2002. The Ballantrae Complex and Southern Uplands terrane. In: N.H. Trewin (Editor), *Geology of Scotland. Fourth Edition.* Geological Society of London. Bath, 167-200.

Orbell, G., 1973. Palynology of the British Rhaeto-Liassic. *Bulletin of the Geological Survey*, **44**, 1-44.

Ottesen, D., Dowdeswell, J. & Rise, L., 2005. Submarine landforms and the reconstruction of fast-flowing ice streams within a large Quaternary ice sheet: the 2500-km-long Norwegian-Svalbard margin (57°-80°N). *Geological Society of America Bulletin*, **117**, 1033-1050.

Ottesen, D., Dowdeswell, J.A., Benn, D.I., Kristensen, L., Christiansen, H.H., Christensen, O., Hansen, L., Lebesbye, E., Forwick, M. & Vorren, T.O., 2008. Submarine landforms characteristic of glacier surges in two Spitsbergen fjords. *Quaternary Science Reviews*, **27**, 1583-1599.

Palliani, B.R. & Riding, J.B., 2003. Biostratigraphy, provincialism and evolution of European Early Jurassic (Pliensbachian to early Toarcian) dinoflagellate cysts. *Palynology*, **27**, 179-214.

Pankhurst, R.J. & Sutherland, D.S., 1982. Caledonian granites and diorites of Scotland and Ireland. In: D.S. Sutherland (Editor), *Igneous Rocks of the British Isles.* John Wiley & Sons. Chichester, 149-190.

Parent, M., Paradis, S.J. & Doiron, A., 1996. Palimpsest glacial dispersal trains and their significance for drift prospecting. *Journal of Geochemical Exploration*, **56**, 123-140.

Parfitt, S.A., Barendregt, R.W., Breda, M., Candy, I., Collins, M.J., Coope, G.R., Durbridge, P., Field, M.H., Lee, J.R., Lister, A.M., Mutch, R., Penkman, K.E.H., Preece, R.C., Rose, J., Stringer, C.B., Symmons, R., Whittaker, J.E., Wymer, J.J. & Stuart, A.J., 2005. The earliest record of human activity in northern Europe. *Nature*, **438**, 1008-1012.

Passchier, S., 2007. The use of heavy minerals in the reconstruction of ice-sheet drainage patterns: an example from the edge of the east Antarctic ice sheet. In: M.A. Mange and D.T. Wright (Editors), *Heavy Minerals in Use.* Developments in Sedimentology 58. Elsevier, **58**, 677-699.

Pawley, S.M., Bailey, R.M., Rose, J., Moorlock, B.S.P., Hamblin, R.J.O., Booth, S.J. & Lee, J.R., 2008. Age limits on Middle Pleistocene glacial sediments from OSL dating, north Norfolk, UK. *Quaternary Science Reviews*, **27**, 1363-1377.

Pawley, S.M., Rose, J., Lee, J.R., Moorlock, B.S.P. & Hamblin, R.J., 2004. Middle Pleistocene sedimentology and lithostratigraphy of Weybourne, northeast Norfolk, England. *Proceedings of the Geologists Association*, **115**, 25-42.

Pedersen, S.A.S., 1988. Glaciotectonite: brecciated sediments and cataclastic sedimentary rocks formed subglacially. In: R.P. Goldthwait and C.L. Matsch (Editors), *Genetic Classification of Glacigenic Deposits.* Balkema. Rotterdam, 89-91.

Peel, R.F., 1956. The profiles of glacial drainage channels. *The Geographical Journal*, **122**, 483-487.

Peltier, W.R. & Fairbanks, R.G., 2006. Global glacial ice volume and Last Glacial Maximum duration from an extended Barbados sea level record. *Quaternary Science Reviews*, **25**, 3322-3337.

Penkman, K.E.H., Kaufman, D.S., Maddy, D. & Collins, M.J., 2008. Closed-system behaviour of the intra-crystalline fraction of amino acids in mollusc shells. *Quaternary Geochronology*, **3**, 2-25.

Penkman, K.E.H., Preece, R.C., Keen, D.H., Maddy, D., Schreve, D.C. & Collins, M.J., 2007. Testing the aminostratigraphy of fluvial archives: the evidence from intra-crystalline proteins within freshwater shells. *Quaternary Science Reviews*, **26**, 2958-2969.

Penny, L.F. & Catt, J.A., 1967. Stone orientation and other structural features of tills in East Yorkshire. *Geological Magazine*, **104**, 344-360.

Penny, L.F., Coope, G.R. & Catt, J.A., 1969. Age and Insect fauna of the Dimlington Silts, East Yorkshire. *Nature*, **224**, 65-67.

Perkins, D., 1998. *Mineralogy*. Prentice Hall, New Jersey, 484 pp.

Perrin, R.M.S., Rose, J. & Davies, H., 1979. The distribution, variation and origins of pre-Devensian tills in Eastern England. *Philosophical Transactions of the Royal Society of London*, **B 275**, 535-570.

Phillips, E., 2006. Micromorphology of a debris flow deposit: evidence of basal shearing, hydrofracturing, liquefaction and rotational deformation during emplacement. *Quaternary Science Reviews*, **25**, 720-738.

Phillips, E., Lee, J.R. & Burke, H., 2008. Progressive proglacial to subglacial deformation and syntectonic sedimentation at the margins of the Mid-Pleistocene British Ice Sheet: evidence from north Norfolk, UK. *Quaternary Science Reviews*, **27**, 1848-1871.

Phillips, E., Merritt, J., Auton, C. & Golledge, N., 2007. Microstructures in subglacial and proglacial sediments: understanding faults, folds and fabrics, and the influence of water on the style of deformation. *Quaternary Science Reviews*, **26**, 1499-1528.

Phillips, E.R., Evans, D.J.A. & Auton, C.A., 2002. Polyphase deformation at an oscillating ice margin following the Loch Lomond Readvance, central Scotland, UK. *Sedimentary Geology*, **149**, 157-182.

Pin, C. & Joannon, S., 2001. Isotope dilution-chemical separation: a powerful combination for high precision analysis at the ultra-trace level using ICP Mass Spectrometry; example of U and Th determination in silicate rocks. *Journal of Analytical Atomic Spectrometry*, **16**, 739-743.

Piotrowski, J.A. & Kraus, A.M., 1997. Response of sediment to ice sheet loading in northwestern Germany: effective stresses and glacier-bed stability. *Journal of Glaciology*, **43**, 495-502.

Piotrowski, J.A., Larsen, N.K. & Junge, F.W.F.W., 2004. Reflections on soft subglacial beds as a mosaic of deforming and stable spots. *Quaternary Science Reviews*, **23**, 993-1000.

Piotrowski, J.A., Larsen, N.K., Menzies, J. & Wysota, W., 2006. Formation of subglacial till under transient bed conditions: deposition, deformation, and basal decoupling under a Weichselian ice sheet lobe, central Poland. *Sedimentology*, **53**, 83-106.

Piotrowski, J.A., Mickelson, D.M., Tulaczyk, S., Krzyszkowski, D. & Junge, F.W., 2001. Were deforming subglacial beds beneath past ice sheets really widespread? *Quaternary International*, **86**, 139-150.

Powell, A.J., 1992. Dinoflagellate cysts of the Tertiary System. In: A.J. Powell (Editor), *A Stratigraphic Index of Dinoflagellate Cysts*. Chapman and Hall. London, 155-251.

Powell, R.D., 1984. Glacimarine processes and inductive lithofacies modelling of ice shelf and tidewater glacier sediments based on Quaternary examples. *Marine Geology*, **57**, 1-52.

Powell, R.D. & Molnia, B.F., 1989. Glacimarine sedimentary processes, facies and morphology of the south-southeast Alaska shelf and fjords. *Marine Geology*, **85**, 359-390.

Praeg, D., 2003. Seismic imaging of Mid-Pleistocene tunnel-valleys in the North Sea Basin-high resolution from low frequencies. *Journal of Applied Geophysics*, **53**, 273-298.

Preece, R.C., Parfitt, S.A., Bridgland, D.R., Lewis, S.G., Rowe, P.J., Atkinson, T.C., Candy, I., Debenham, N.C., Penkman, K.E.H., Rhodes,

E.J., Schwenninger, J.L., Griffiths, H.I., Whittaker, J.E. & Gleed-Owen, C., 2007. Terrestrial environments during MIS 11: evidence from the Palaeolithic site at West Stow, Suffolk, UK. *Quaternary Science Reviews*, **26**, 1236-1300.

Prescott, J.R. & Hutton, J.T., 1994. Cosmic ray contributions to dose rates for luminescence and ESR dating: large depths and long-term variations. *Radiation Measurements*, **23**, 497-500.

Raistrick, A., 1931. Glaciation. *Proceedings of the Geologists' Association*, **42**, 281-291.

Raistrick, A., 1932. The correlation of glacial retreat stages across the Pennines. *Proceedings of the Yorkshire Geological Society*, **22**, 199-214.

Randall, B.A.O., 1995. The Great Whin Sill and its associated Dyke suite. In: G.A.L. Johnson (Editor), *Robson's Geology of North East England*. Transactions of the Natural History Society of Northumbria. Volume 56 Part 5. Newcastle, 319-326.

Rawson, P., Allen, P., Brenchley, P., Cope, J., Gale, A., Evans, J., Gibbard, P., Gregory, F., Hailwood, E., Hesselbo, S., Knox, R., Marshall, J., Oates, M., Riley, N., Smith, A., Trewin, N. & Zalasiewicz, J., 2002. *Stratigraphical Procedure*. The Geological Society, London, 57 pp.

Reid, E.M., 1920. On two preglacial floras from Castle Eden (County Durham). *Quaterly Journal of the Geological Society of London*, **76**, 104-144.

Richards, A.E., 1998. Re-evaluation of the Middle Pleistocene stratigraphy of Herefordshire, England. *Journal of Quaternary Science*, **13**, 115-136.

Richards, K., 1996. Samples and cases: generalisation and explanation in geomorphology. In: B. Rhoads and C. Thorn (Editors), *The Scientific Basis of Geomorphology*. Elsevier. Binghampton Symposium in Geomorphology, 171-190.

Riches, P.F., Norton, P.E.P., Schreve, D.C. & Rose, J., 2008. Bramerton Pits SSSI. In: I. Candy, J.R. Lee and A.M. Harrison (Editors), *The Quaternary of Northern East Anglia. Field Guide*. Quaternary Research Association. London, 84-96.

Riding, J.B., 2007. *A Palynological investigation of diamictons and tills from northeast England. Internal Report IR/07/021R*. British Geological Survey, Nottingham, 9 pp.

Riding, J.B., 2008. *A Palynological investigation of tills from the North Sea Basin. Internal Report IR/08/025*. British Geological Survey, Nottingham, 12 pp.

Riding, J.B. & Kyffin-Hughes, J.E., 2004. A review of the laboratory preparation of palynomorphs with a description of an effective non-acid technique. *Revista Brasileira de Paleontologia*, **7**, 13-44.

Riding, J.B. & Kyffin-Hughes, J.E., 2006. Further testing of a non-acid palynological preparation procedure. *Palynology*, **30**, 69-87.

Riding, J.B., Rose, J. & Booth, S.J., 2003. Allochthonous and indigenous palynomorphs from the Devensian of the Warham Borehole, Stiffkey, north Norfolk, England: evidence for sediment provenance. *Proceedings of the Yorkshire Geological Society*, **54**, 223-235.

Riding, J.B. & Thomas, J.E., 1988. Dinoflagellate cyst stratigraphy of the Kimmeridge Clay (Upper Jurassic) from the Dorset coast, southern England. *Palynology*, **12**, 65-88.

Rijsdijk, K.F., Owen, G., Warren, W.P., McCarroll, D. & van der Meer, J.J.M., 1999. Clastic dykes in over-consolidated tills: evidence for subglacial hydrofracturing at Killiney Bay, eastern Ireland. *Sedimentary Geology*, **129**, 111-126.

Rijsdijk, K.F., Passchier, S., Weerts, H.J.T., Laban, C., van Leeuwen, R.J.W. & Ebbing, J.H.J., 2005. Revised Upper Cenozoic stratigraphy of the Dutch sector of the North Sea Basin: towards an integrated lithostratigraphic, seismostratigraphic and allostratigraphic approach. *Netherlands Journal of Geosciences-Geologie En Mijnbouw*, **84**, 129-146.

Roberts, D.H., Chiverrell, R.C., Innes, J.B., Horton, B.P., Brooks, A.J., Thomas, G.S.P., Turner, S. & Gonzalez, S., 2006. Holocene sea levels, Last Glacial Maximum glaciomarine environments and geophysical models in the northern Irish Sea Basin, UK. *Marine Geology*, **231**, 113-128.

Roberts, D.H., Dackombe, R.V. & Thomas, G.S.P., 2007. Palaeo-ice streaming in the central sector of the British-Irish Ice Sheet during the Last Glacial Maximum: evidence from the northern Irish Sea Basin. *Boreas*, **36**, 115-129.

Roberts, D.H. & Hart, J.K., 2005. The deforming bed characteristics of a stratified till assemblage in north East Anglia, UK: investigating controls

on sediment rheology and strain signatures. *Quaternary Science Reviews*, **24**, 123-140.

Robson, D.A., 1976. *A Guide to the Geology of the Cheviot Hills*. Transactions of the Natural History Society of Northumbria. Volume 43 No. 1. Natural History Society of Northumbria, Newcastle-upon-Tyne, 23 pp.

Robson, D.A., 1995. Igneous Rocks. The Lower Old Red Sandstone (Cheviot) igneous complex. In: G.A.L. Johnson (Editor), *Robson's Geology of North-eastern England*. Transactions of the Natural History Society of Northumbria. Volume 56 Part 5. Newcastle, 314-316.

Robson, D.A. & Johnson, G.A.L., 1995. Devonian or Old Red Sandstone. In: G.A.L. Johnson (Editor), *Robson's Geology of North East England*. Transactions of the Natural History Society of Northumbria. Volume 56 Part 5. Newcastle, 247-248.

Rose, J., 1985. The Dimlington Stadial / Dimlington Chronozone: a proposal for naming the main glacial episode of the Late Devensian in Britain. *Boreas*, **14**, 225-230.

Rose, J., Candy, I., Moorlock, B.S.P., Wilkins, H., Lee, J.A., Hamblin, R.J.O., Lee, J.R., Riding, J.B. & Morigi, A.N., 2002. Early and early Middle Pleistocene river, coastal and neotectonic processes, southeast Norfolk, England. *Proceedings of the Geologists' Association*, **113**, 47-67.

Rose, J. & Menzies, J., 1996. Glacial Stratigraphy. In: J. Menzies (Editor), *Past Glacial Environments: Sediments, Forms and Techniques*. Butterworth-Heinemann Ltd. Oxford, 253-284.

Rose, J., Moorlock, B.S.P. & Hamblin, R.J.O., 2001. Pre-Anglian fluvial and coastal deposits in Eastern England: lithostratigraphy and palaeoenvironments. *Quaternary International*, **79**, 5-22.

Rust, B.R. & Koster, E.H., 1984. Coarse alluvial deposits. In: R.G. Walker (Editor), *Facies Models, 2nd Edition*. Geoscience Canaca Reprint Service, 53-70.

Ryan, P.D., Mange, M.A. & Dewey, J.F., 2007. Statistical analysis of high-resolution heavy mineral stratigraphic data from the Ordovician of Western Ireland and its tectonic consequences. In: M.A. Mange and D.T. Wright (Editors), *Heavy Minerals in Use*. Developments in Sedimentology 58. Elsevier, **58**, 465-489.

Salt, K.E. & Evans, D.J.A., 2004. Superimposed subglacially streamlined landforms of southwest Scotland. *Scottish Geographical Journal*, **120**, 133-147.

Salvador, A., 1994. *The International Stratigraphic Guide: a guide to stratigraphic classification, terminology, and procedure*. International Subcommission on Stratigraphic Classification. International Union of Geological Sciences, Boulder, 214 pp.

Scourse, J.D., Ansari, M.H., Wingfield, R.T.R., Harland, R. & Balson, P.S., 1998. A middle Pleistocene shallow marine interglacial sequence, Inner Silver Pit, southern North Sea: Pollen and dinoflagellate cyst stratigraphy and sea-level history. *Quaternary Science Reviews*, **17**, 871-900.

Sejrup, H.P., Aarseth, I., Ellingsen, K.L., Reither, E. & Jansen, E., 1987. Quaternary stratigraphy of the Fladen area, central North Sea: a multidisciplinary study. *Journal of Quaternary Science*, **2**, 35-58.

Sejrup, H.P., Aarseth, I. & Haflidason, H., 1991. The Quaternary succession in the northern North Sea. *Marine Geology*, **101**, 103-111.

Sejrup, H.P., Haflidason, H., Hjelstuen, B.O., Nygard, A., Bryn, P. & Lien, R., 2004. Pleistocene development of the SE Nordic Seas margin. *Marine Geology*, **213**, 169-200.

Sejrup, H.P., Haflidason, N., Aarseth, I., King, E., Forsberg, C.F., Long, D. & Rokoengen, K., 1994. Late Weichselian glaciation of the northern North Sea. *Boreas*, **23**, 1-13.

Sejrup, H.P., Hjelstuen, B.O., Torbjorn Dahlgren, K.I., Haflidason, H., Kuijpers, A., Nygard, A., Praeg, D., Stoker, M.S. & Vorren, T.O., 2005. Pleistocene glacial history of the NW European continental margin. *Marine and Petroleum Geology*, **22**, 1111-1129.

Sejrup, H.P., Larsen, E., Landvik, J., King, E.L., Haflidason, H. & Nesje, A., 2000. Quaternary glaciations in southern Fennoscandia: evidence from southwestern Norway and the northern North Sea region. *Quaternary Science Reviews*, **19**, 667-685.

Sejrup, H.P., Nygård, A., Hall, A.M. & Haflidason, H., 2009. Middle and Late Weichselian (Devensian) glaciation history of south-western Norway, North Sea and eastern UK. *Quaternary Science Reviews*, **28**, 370-380.

Seth, B., Thirlwall, M.F., Houghton, S.L. & Craig, C.A., 2003. Accurate measurements of Th-U isotope ratios for carbonate geochronology using MC-ICP-MS,. *Journal of Analytical Atomic Spectrometry*, **18**, 1323-1330.

Shackleton, N.J., 1967. Oxygen isotope analyses and Pleistocene temperatures re-assessed. *Nature*, **215**, 15-17.

Shackleton, N.J., Berger, A. & Peltier, W.R., 1990. An alternative astronomical calibration based on ODP Site 677. *Royal Society of Edinburgh Transactions: Earth Sciences*, **81**, 251-261.

Shackleton, N.J. & Opdyke, N.D., 1973. Oxygen isotope and palaeomagnetic stratigraphy of equatorial Pacific core V28-238: oxygen isotope temperatures and ice volumes on a 10^5 and 10^6 year scale. *Quaternary Research*, **3**, 39-55.

Sharp, M.J., 1984. Annual moraine ridges at Skalafellsjokull, south-east Iceland. *Journal of Glaciology*, **30**, 82-93.

Sharp, M.J., Jouzel, J., Hubbard, B. & Lawson, W., 1994. The character, structure and origin of the basal ice layer of a surge-type glacier. *Journal of Glaciology*, **40**, 327-340.

Sharp, W.D., Ludwig, K.R., Chadwick, R.A., Amundson, R. & Glaser, L.L., 2003. Dating fluvial terraces by 230Th/U on pedogenic carbonate, Wind River Basin, Wyoming. *Quaternary Research*, **59**, 139-150.

Shaw, J., 1987. Glacial sedimentary processes and environmental reconstruction based on lithofacies. *Sedimentology*, **34**, 103-116.

Šibrava, V., 1982. Scandinavian glaciations in the Bohemiam Massif and Carpathian Foredeep, and their relationship to the extraglacial areas. Correlation of Quaternary deposits in the Northern Hemisphere, Report of the International Geological Correlation Programme, Project 24. *Quaternary Science Reviews*, **5**, 381-386.

Sissons, J.B., 1967. *The evolution of Scotland's Scenery*. Oliver and Boyd, Edinburgh, 259 pp.

Smed, P. & Ehlers, J., 1994. *Steine aus dem Norden*. Borntraeder, G., Berlin, 194 pp.

Smelror, M., 1987. Early Silurian acritarchs and prasinophycean algae from the Rinerike District, Olso region (Norway). *Review of Palaeobotany and Palynology*, **52**, 137-159.

Smith, A.H.V. & Butterworth, M.A., 1967. Miospores in the coal seams of the Carboniferous of Great Britain. *Special Papers in Palaeontology*, **1**, 324.

Smith, D.B., 1979. Rapid marine transgressions and regressions of the Upper Permian Zechstein Sea. *Journal of the Geological Society of London*, **136**, 155-156.

Smith, D.B., 1994. *Geology of the Country around Sunderland. Memoir of the British Geological Survey*. Her Majesty's Stationery Office, London, 162 pp.

Smith, D.B., 1995a. *The Marine Permian of England*. Geological Conservation Review Series 8, Kluwer, UK., 205 pp.

Smith, D.B., 1995b. Permian and Triassic. In: G.A.L. Johnson (Editor), *Robson's Geology of North East England*. Transactions of the Natural History Society of Northumbria. Volume 56 Part 5. Newcastle, 283-296.

Smith, D.B. & Francis, E.A., 1967. *Geology of the Country between Durham and West Hartlepool (Explanation of one-inch Geological Sheet 27, New Series)*. Memoirs of the Geological Survey of Great Britain. Her Majesty's Stationary Office, London, 354 pp.

Solomon, J.D., 1932. The glacial succession of the north Norfolk coast. *Proceedings of the Geologists' Association*, **32**, 241-271.

Stephenson, D. & Gould, D., 1995. *British Regional Geology: The Grampian Highlands. Fourth Edition. Memoir of the British Geological Survey*. Her Majesty's Stationery Office, London, 262 pp.

Stewart, F.S., 1991. *A reconstruction of the eastern margin of the Late Weichselian Ice Sheet in Northern Britain*. Unpublished PhD Thesis. University of Edinburgh.

Stoker, M. & Bradwell, T., 2005. The Minch palaeo-ice stream, NW sector of the British-Irish Ice Sheet. *Journal of the Geological Society*, **162**, 425-428.

Stoker, M.S., Long, D. & Fyfe, J.A., 1985. *A revised Quaternary stratigraphy for the central North Sea. British Geological Survey Report 17 (2)*. HMSO, London, 35 pp.

Strachan, R.A., Stewart, A.D. & Wright, D.T., 2002. The Northern Highland and Grampian

Terranes. In: N.H. Trewin (Editor), *Geology of Scotland. Fourth Edition.* Geological Society of London. Bath, 81-148.

Straw, A., 1979. The Geomorphological Significance of the Wolstonian Glaciation of Eastern England. *Transactions of the Institute of British Geographers*, **4**, 540-549.

Straw, A., 1983. Pre-Devensian glaciation of Lincolnshire (eastern England) and adjacent areas. *Quaternary Science Reviews*, **2**, 239-260.

Straw, A., 2005. *Glacial and pre-glacial deposits at Welton-le-Wold, Lincolnshire.* The Studio Publishing Services Ltd, 39 pp.

Stuiver, M. & Reimer, P.J., 1993. Extended 14C data base and revised CALIB 3.0 14C age calibration program. *Radiocarbon*, **35**, 215-230.

Stuiver, M., Reimer, P.J. & Reimer, R.W., 2009. *CALIB 5.0.1. Program and Documentation.* http://www.calib.qub.ac.uk/.

Sutherland, D.G., 1984. The Quaternary Deposits and Landforms of Scotland and the Neighbouring Shelves - a Review. *Quaternary Science Reviews*, **3**, 157-254.

Sutherland, D.G., 1991. Late Devensian glacial deposits and glaciation in Scotland and the adjacent offshore region. In: J. Ehlers, P.L. Gibbard and J. Rose (Editors), *Glacial Deposits in Great Britain and Ireland.* A.A. Balkema. Rotterdam, 53-60.

Svendsen, J.I., Alesanderson, H., Astakhov, V.I., Demidov, I., Dowdeswell, J.A., Funder, S., Gataullin, V., Henricksen, M., Hjort, C., Houmark-Nielsen, M., Hubberten, H.W., Ingólfsson, O., Jakobsson, M., Kjær, K., Larsen, E., Lokrantz, H., Lunkka, J.P., Lysså, A., Mangerud, J., Matiouchkov, A., Murray, A., Moller, P., Niessen, F., Nikolskaya, O., Polyak, L., Saarnisto, M., Siegert, C., Siegert, M.J., Spielhagen, R. & Stein, R., 2004. Late Quaternary ice sheet history of northern Eurasia. *Quaternary Science Reviews*, **23**, 1229-1271.

Swift, D.A., Nienow, P.W., Spedding, N. & Hoey, T.B., 2002. Geomorphic implications of subglacial drainage configuration: rates of basal sediment evacuation controlled by seasonal drainage system evolution. *Sedimentary Geology*, **149**, 5-19.

Teasdale, D.A. & Hughes, D.B., 1999. The glacial history of north-east England. In: D.R. Bridgland, B.P. Horton and J.B. Innes (Editors), *The Quaternary of north-east England. Field Guide.* Quaternary Research Association. London, 10-17.

Thamó-Bozsó, E. & Kovács, L.Ó., 2007. Evolution of Quaternary to Modern Fluvial network in the Mid-Hungarian plain, indicated by heavy mineral distributions and statistical analysis of heavy mineral data. In: M.A. Mange and D.T. Wright (Editors), *Heavy Minerals in Use.* Developments in Sedimentology 58. Elsevier, **58**, 491-513.

Thomas, G.S.P., 1999. Northern England. In: D.Q. Bowen (Editor), *A Revised Correlation of Quaternary Deposits in the British Isles.* Geological Society, Special Report 23. London, 91-98.

Thomas, G.S.P., Chiverrell, R.C. & Huddart, D., 2004. Ice marginal depositional responses to readvance episodes in Late Devensian deglaciation of the Isle of Man. *Quaternary Science Reviews*, **23**, 85-106.

Thomas, R.D. & Gleeson, C.F., 2000. Use of till geochemistry and mineralogy to outline areas underlain by diamondiferous spessartite dikes near Wawa, Ontario. *Exploration and Mining Geology*, **9**, 215-231.

Thompson, W.G., 2007. U-Series Dating. In: S.A. Elias (Editor), *Encyclopedia of Quaternary Science.* Elsevier. Amsterdam, 3099-3104.

Toghill, P., 2000. *The Geology of Britain. An Introduction.* Swanhill Press, Wiltshire, UK, 192 pp.

Trechmann, C.T., 1915. The Scandinavian Drift of the Durham Coast and the general glaciology of south-east Durham. *Quarterly journal of Geological Society of London*, **71**, 53-83.

Trechmann, C.T., 1920. On a deposit of Interglacial loess, and some transported preglacial freshwater clays on the Durham coast. *Quarterly Journal of the Geological Society of London*, **75**, 173-303.

Trechmann, C.T., 1931a. The 60-foot raised beach at Easington, Co. Durham. *Proceedings of the Geologists' Association*, **42**, 295-297.

Trechmann, C.T., 1931b. The Scandinavian Drift or Basement Clay on the Durham Coast. *Proceedings of the Geologists' Association*, **42**, 292-294.

Trechmann, C.T., 1952. On the Pleistocene of East Durham. *Proceedings of the Yorkshire Geological Society*, **28**, 164-179.

Trewin, N.H., 2002. *The Geology of Scotland. Fourth Edition.* The Geological Society of London, London, 576 pp.

Trotter, F.M., 1929. The glaciation of East Edenside, the Alston Block and the Carlisle Plain. *Quarterly Journal of the Geological Society of London*, **85**, 549-612.

Tucker, M.E. & Wright, V.P., 1990. *Carbonate Sedimentology.* Blackwell Scientific Publications, Oxford, 494 pp.

van der Meer, J.J.M., 1993. Microscopic Evidence of Subglacial Deformation. *Quaternary Science Reviews*, **16**, 827-831.

van der Meer, J.J.M., 1997. Particle and aggregate mobility in till: Microscopic evidence of subglacial processes. *Quaternary Science Reviews*, **16**, 827-831.

van der Meer, J.J.M., Menzies, J. & Rose, J., 2003. Subglacial till: the deforming glacier bed. *Quaternary Science Reviews*, **22**, 1659-1685.

van der Wateren, F.M., 1995. Processes of Glaciotectonism. In: J. Menzies (Editor), *Modern Glacial Environments: Processes, Dynamics and Sediments.* Butterman-Heinemann. Oxford, 309-335.

van der Wateren, F.M., 1999. Structural geology and sedimentology of the Heiligenhafen till section, Northern Germany. *Quaternary Science Reviews*, **18**, 1625-1639.

van der Wateren, F.M., Kluiving, S.J. & Bartek, L.R., 2000. Kinematic indicators of subglacial shearing. In: A.J. Maltman, B. Hubbard and M.J. Hambrey (Editors), *Deformation of glacial materials.* Geological Society of London, Special Publication, vol. 176. London, 259-278.

Vincent, E. & Berger, W.H., 1981. Planktonic foraminifera and their use in paleoceanography. In: C. Emiliani (Editor), *The Sea: the Oceanic Lithosphere.* Wiley. New York, 1025-1119.

Walden, J.S., 2004. Particle Lithology (or mineral and geochemical analysis). In: D.J.A. Evans and D.I. Benn (Editors), *A practical guide to the study of glacial sediments.* Arnold. London, 145-180.

Walden, J.S. & Fowler, A., 1994. Channelised subglacial drainage over a deformable bed. *Journal of Glaciology*, **40**, 3-15.

Weerts, H.J.T. & Westerhoff, W.E., 2007. Quaternary Stratigraphy. Lithostratigraphy. In: S.A. Elias (Editor), *Encyclopedia of Quaternary Science.* Elsevier. Amsterdam, 2826-2840.

Westaway, R., in press. Quaternary vertical crustal motion and drainage evolution in East Anglia and adjoining parts of southern England: chronology of the Ingham River terrace deposits. *Boreas.*

Westaway, R., Bridgland, D.R. & White, M.J., 2006. The Quaternary uplift history of central southern England: evidence from the terraces of the Solent River system and nearby raised beaches. *Quaternary Science Reviews*, **25**, 2212-2250.

Westaway, R., Maddy, D. & Bridgland, D.R., 2002. Flow in the lower continental crust as a mechanism for the Quaternary uplift of south-east England: constraints from the Thames terrace record. *Quaternary Science Reviews*, **21**, 559-603.

Wingfield, R., 1990. The origin of major incisions within the Pleistocene deposits of the North Sea. *Marine Geology*, **91**, 31-52.

Woodcock, N. & Strachan, R., 2000. *Geological History of Britain and Ireland.* Blackwell Science, Oxford, 423 pp.

Woolacott, D., 1900. On the Boulder Clay, Raised Beaches, and Associated Phenomena in the East of Durham. *Proceedings of the University of Durham Philosophical Society*, **1**, 247-258.

Woolacott, D., 1910. Boulder's Committee. *Proceedings of the University of Durham Philosophical Society*, **3**, 61-62, 175-176, 331-333.

Yorke, L., Fuller, I.C., Howard, A.J. & Passmore, D.G., 2007. Preliminary investigations of outwash environments in the Tyne Valley: implications for Late Devensian (Dimlington Stadial) deglaciation. *Proceedings of the Geologists Association*, **118**, 201-211.

Appendix I: Methodologies

Micromorphology

Table 1: Impregnation of unlithified sediments by David Sales (Murphy, 1986).

1. The samples are left to dry at room temperature for at least 5 days.
2. The samples are cut on a rock saw with a 10" diamond blade. The cutting was done dry (without coolant / lubricant) and with dust extraction. Two cuts were made to give a slice 5-7 mm thick. Edges were trimmed down to final thin section size (55x45cm).
3. The slab was dried on a hotplate at 120°C for two hours.
4. The sample was impregnated with epoxy resin (SpeciFix-40). Most samples are poorly impregnated, so impregnation was improved by:
    a. The sample was placed in a polythene mould (treated with a release agent) and left on a hotplate at around 70°C.
    b. A mix of resin and hardener (10:4) was prepared and diluted with acetone (approximately 4 parts resin/hardener to 1 part acetone).
    c. The sample and mould were removed from the hotplate and the resin mix was poured over the sample. The mould lid was clipped in place and the sample was left undisturbed at room temperature for about 1 hour.
    d. The lid was removed from the mould and the sample was kept under vacuum (at room temperature) until bubbling of the resin subsided. (Initially, air is removed, then at lower pressure the acetone boils off.)
    e. The mould and sample were put back on the 70°C hotplate and left to allow the resin to cure (at least 24 hours).
5. Once the resin has fully cured, the sample is removed from the mould and surplus resin was trimmed off using the rock saw, with coolant.

Table 2: Methodology for preparation of thin sections by David Sales. After Murphy, 1986.

1. Subsequent preparation followed standard thin section preparation:
   A 5 mm slice (slab) of the sample is cut using a rock saw fitted with a diamond-impregnated blade. From this slab a representative rectangular block or chip, around 30 x 20 mm, is cut.
2. A rotary grinder with a grinding disc impregnated with diamond abrasive is then used to grind the faces of the chip flat.
3. To prepare a scratch-free surface, the chip is lapped for 5 minutes on a precision lapping machine.
4. Before attaching the chip to a slide, it is cleaned with a little detergent, rinsed thoroughly in tap water and dried on a hotplate.
5. An epoxy resin (Type 301) is used to bond the chip to a pre-ground microscope slide. A drop of resin/hardener is placed on the prepared face of the chip and the slide carefully lowered onto it. Air bubbles are removed by gently pressing the slide against the chip. The slide is then turned over and secured in a clamping jig until the resin has hardened (1 hour at 30-40°C, overnight at room temperature).
6. A cut-off saw is used to remove the bulk of the chip from the slide prior to grinding.

7. At this stage, the section thickness is around 0.5mm. There are two ways of getting closer to the required 30μm (0.03mm),
   i. The cut-off saw incorporates a diamond-impregnated cup wheel which can be used to thin the section to around 50μm.
   ii. The section can be lapped on the precision lapping machine to around 35μm.

8. The final grinding is done by hand on a glass plate using a fine silicon carbide abrasive powder (1000 grit) dispersed in water. The section thickness is checked either with a micrometer or, if the sample includes quartz, by the appearance of the quartz crystals under the microscope in crossed polars (should be grey to white/pale yellow at 30 μm).

9. A coverslip or coverglass is fixed to the section using a mounting medium or mountant. A coverglass protects the section and the mountant improves the appearance of it under the microscope (mounting media have a refractive index close to that of glass – around 1.54). The medium used in this workshop is Canada balsam which is a resin dissolved in a solvent.
   i. The slide is placed on a hotplate (70°C) and a drop of balsam is applied to one end of the section.
   ii. A cleaned coverglass is picked up with forceps, warmed in a Bunsen flame and drawn through the balsam to spread it over the section.

10. The coverglass is then gently lowered onto the section and pressed down with the tips of the forceps to remove air bubbles. The section is left for an hour or so for the balsam to thicken.

11. A toothbrush and methylated spirit are used to remove surplus mountant from around the coverglass before the section is cleaned in soapy water, dried and labelled.

12. The sample is analysed under a petrological microscope.

Lithological and Geochemical Analysis

Particle Size Analysis

Table 3: Methodology for Particle Size analysis.

A.	**Less than 2mm fraction**
1.	A small sample (10g) is air dried.
2.	A sub-sample (0.5g) is passed through a 2mm sieve, and then weighed into a 50ml centrifuge tube.
3.	20 ml of 20% Hydrogen Peroxide is added in excess to break down organic matter.
4.	Sample is lowered into a boiling water bath to aid the oxidisation of organic matter, and are left for 2 hours. Aluminium foil is placed over the top.
5.	If all the organic matter has been dissolved after 2 hours, leaving the liquid a transparent colour, the sample is centrifuged at 4000 rpm for 4 minutes. The supernatant liquid is decanted off.
6.	The sample is topped up with distilled water, and then centrifuged again at 4000 rpm for 4 minutes.
7.	20 ml of distilled water and 2 ml of Sodium Hexametaphosphate solution is added to the solution.
8.	The sample is then analysed on the Coulter Laser Granulometer.
B.	**Greater than 2mm fraction.**
1.	Bulk sample (> than 10kg) is air dried and then weighed.
2.	The sample is decanted into a bucket and filled with Sodium Hexametaphosphate solution. The sample is left overnight.
3.	The bulk sample is wet sieved through a 2mm sieve. The residue on the sieve is retained and air dried.
4.	The remaining sample is dry sieved through a set of steel sieves at one phi intervals. The sample remaining on each residue is retained and weighed.

Heavy-mineral analysis

Table 4: Methodology for separation of heavy minerals.

1. A sub sample (10g) of the air dried matrix is gently disaggregated using a rubber bung in a mortar, and is then placed in distilled water in an ultrasonic bath for 20 minutes to complete the disaggregation procedure. Sodium Hexametaphosphate may be added to aid disaggregation in clay-rich samples.

2. The sample is then wet sieved to obtain the 63-125 μm size fraction, and is then air dried.

3. 1 g of sample is weighed and then placed in a 100 ml centrifuge tube. 50 ml of deionised Sodium Polytungstate solution with a specific gravity of 2.85 is added. The tube is shaken and is then centrifuged for 15 minutes at 3000 rpm.

4. The heavy minerals sink to the bottom of the centrifuge tube, leaving the lights floating on the top. The centrifuge tube is placed in a beaker of liquid nitrogen until all of the deionised Sodium Polytungstate solution is frozen. The light minerals are melted with deionised water and are poured through a filter paper in a 'lights' funnel (Figure 1). The Sodium Polytungstate solution is collected below for recycling.

5. When all of the light minerals have been washed into the 'lights' funnel, the heavy minerals are washed into a different, labelled funnel.

6. The heavy minerals remaining on the filter paper are labelled, air dried, placed in a 2 ml vial and weighed to 4 d.p. The percentage of heavy minerals in the sample can then be determined.

7. For observation the heavy minerals are mounted in clove oil on a slide and are identified under a petrological microscope.

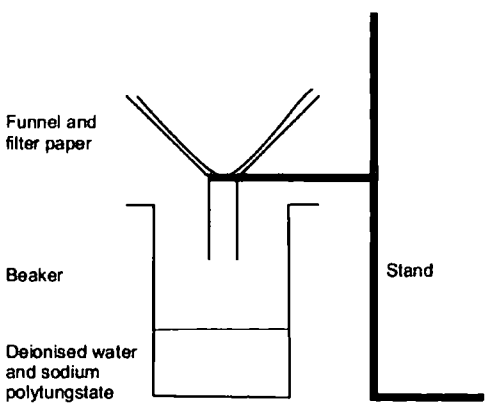

Figure 1: Diagram illustrating set-up required for density separation of heavy minerals.

ICP-Mass Spectrometry

Table 5: Methodology by Atomic Absorption by Amanda Hayton.

1. A 10g sub-sample was air dried and then disaggregated using a pestle and mortar. Dissaggregation was then aided by placing the sample in deionised water in a sonic water bath for 20 minutes.

2. The sample was air dried and then passed through a 2mm sieve.

3. The sample was then freeze dried and then homogenised in a ball mill. Samples are stored in a desiccator at 20°C.

4. A known mass (~250 mg) of the sample is weighed into an HF-resistant microwave extraction vessel. The internal wall of the vessel is rinsed with 5 ml of deionised water followed by the addition of 2 ml of concentrated hydrogen peroxide (100 volumes = >30% w/v).

5. A vented cap is placed on the vessel and it is left overnight to react.

6. 9 ml of HNO_3 is carefully added to the sample taking care that no sample is lost if efflorescence occurs.

7. 3 ml of Hydrochloric acid (HCl) and 2 ml of Hydroflouric acid (HF) are then added.

8. Vessels are capped and are placed in a MARS pressurised microwave extraction system. An extraction program based on EPA method 3052 is used (reaching 180 ± 5°C in less than 5 minutes and remaining at 180 ± 5°C for 9.5 minutes). The samples are cooled to 40°C before removing from the microwave.

9. The samples are then filtered into Class A 100 ml Plastic volumetric flasks through a pre-washed Whatman 542 filter paper and made up to the mark with deionised water.

Table 6: Methodology for ICP-MS Total Metals Extraction by Martin West.

1. In order to bring the elements within a reasonable dilution range, the analysis is split into two runs; one for high abundance metals and one for low abundance metals.

2. The ICP-MS settings and internal standards are based on EPA method 200.8 r5.4. A suite of internal standards are used. The internal standards are chosen to cover a range of masses and first ionisation potentials. The internal standards used give a final concentration of 500 ppb in both standards and samples. The choice of standards depends on sample composition and the metals requested, but typically includes four or more of the following: Sc_{35}, Ge_{72}, Rh_{103}, In_{115}, Tb_{159}, or Re_{185}.

3. **For the low abundance metals:**
   a) An appropriate aliquot (usually 5 ml) of digested sample solution is taken and made up to approximately 90 ml with 2 % v/v nitric acid in a 100 ml plastic volumetric flask.
   b) 1 ml of internal standard solution is added to the flask and then the solution is made up to the mark with 2 % v/v nitric acid.
   c) Typical internal standards: Rh, In, Tb, Re.

   For the high abundance metals:
   a) An appropriate aliquot (usually 1 ml) of the low abundance sample solution is taken and made up to approximately 90 ml with 2 % v/v nitric acid in a 100 ml plastic volumetric flask.
   b) 1 ml of internal standard solution is added to the flask and then the solution is made up to the mark with 2 % v/v nitric acid.
   c) Typical internal standard: Sc.

Microfossil Techniques

Foraminifera

Table 7: Separation of Foraminifera.

1. 10 g of sediment (less if sand-rich, more if clay-rich) is soaked in a beaker of tap water overnight. If the sample is clay-rich, a small amount of Sodium Hexametaphosphate is added as a dispersant.
2. The sediment is gently stirred.
3. The sediment is gently wet-sieved with distilled water between 500 µm and 63 µm sieves. The fraction coarser than 500 µm and the fraction finer than 63 µm are discarded.
4. The sediment is stored in a 50 ml vial in distilled water prior to analysis.
5. a) Forams are observed in water on a black picking tray under reflected white light under a binocular microscope (*'Motic SMZ-168'*).
   b) Forams are picked up using a very fine paintbrush and are transferred to a counting slide divided into 40 numbered boxes.
   c) Forams of the same species are placed in the same box and are counted.
   d) At least 250 forams are counted unless the sample is very poor in fauna; in which case as many as possible are counted.

Palynomorph Analysis

Table 8: Principle steps in the palynological preparation procedure (Riding and Kyffin-Hughes, 2004).

1. Clean the raw sample and crush to c. pea –sized fragments.
2. Treat the sample with clean, warm/hot water and detergent, stir, and leave overnight.
3. Stir the mixture, add Sodium Hexametaphosphate flakes and stir again for c. 20 minutes.
4. Wet-sieve to separate > 500 µm fraction; retain both fractions.
5. **Less than 500 µm fraction:**
   a) Sieve to separate the fine (< 10 µm) clay-rich fraction; retain both fractions.
   b) Archive the fines.
6. **Greater than 500 µm fraction:**
   a) Treat any large (> 500 µm) fragments with hydrogen peroxide, repeatedly if necessary, to break down the sediment/rock.
   b) Sieve to separate fine (< 10 µm) fraction from the < 500 µm fraction.
   c) Retain both fractions and archive the fines.
7. Mix the two resultant < 500 µm and > 10 µm fractions
8. Remove any resistant mineral grains by density separation
9. Concentrate the final organic residue as desired and mount on coverslips and microscope slides.

Dating Techniques

Amino Acid Racemisation

Table 9: Methodology for preparation and analysis of intra-crystalline amino acids (Penkman *et al.*, 2008). Amino Acid Racemisation analysis was conducted by Beatrice Demarchi.

Pre-treatment Procedure

1. Individual shells were sonicated and rinsed in HPLC-grade water. The shells were air-dried overnight, crushed with a mortar and pestle, and sieved to separate particles between 0.425 and 0.090 mm, then split into two sub-samples, unbleached and bleached.

2. The bleached subsample:
    a) 10mg of powder was transferred to an eppendorf tube and 50 µL of 12% NaOCl (BHD) was added per mg of carbonate.
    b) The tubes were shaken, left for 24 hours, re-shaken to ensure complete exposure to bleach, and soaked for a further 24 hours.
    c) The NaOCl was pipetted off, the power rinsed with water, centrifuged, and rinsed again. This was repeated 5 times.
    d) HPLC-grade Methanol (BDH) was then added to ensure complete removal of the bleach, left for a few minutes, centrifuged, and pipetted off. The bleached powder was air dried overnight.

3. Dry powders (bleached and unbleached) were further split into two subsamples and weighed accurately into sterile glass vials: one for the analysis of the unbound amino acids (free amino acid fraction; FAA), and one for all the amino acids present (total hydolysable amino acids; THAA).

4. The FAA subsamples were demineralised with 10 µL 2M HCl (Aristar) per mg of $CaCO_3$ and dried overnight in a centrifuged evaporator.

5. The THAA subsamples were demineralised in 20 µL of 7M HCl (Aristar) per Mg of $CaCO_3$.

6. The vials were flushed with N_2 to minimise oxidisation reactions, and hydrolysed to release peptide-bound amino acids by heating in a 110°C oven for 24 hours.

7. Following hydrolysis, vials were placed in a centrifugal evaporator overnight to dry.

Analytical Procedure

1. Samples were rehydrated with 0.01 mM HCl containing an internal standard of L-*homo*-arginine, and analysed by reverse-phase high performance liquid chromatography (RP-HPLC) using fluorescence detection (Kaufman & Manley, 1998).

2. A solution volume of 2 µL was mixed online with 2.2 µL of derivatising agent (260mM *N*-isobutyryl-L-cysteine (IBC), 170 mM *o*-phthaldiahyde (OPA) in 1 M potassium borate buffer, adjustedto pH 10.4 with KOH) immediately prior to injection.

3. The derivitised amino acids were separated on a C_{18} HyperSil BDS column (5 mm x 250 mm) at 25°C using a gradient elution of three solvents (sodium acetate buffer [23 mM sodium acetate trihydrate, 1.5 mM sodium azide, 1.3 µM EDTA, adjusted to pH 6.00 ± 0.01 with 10% acetic acid and sodium hydroxide], methanol and acetonitrile).

4. The L and D isomers of 10 amino acids were routinely detected, but the amino acids studied in detail were those whose both L and D enantiomers were well resolved:
   - Asx
   - Glx
   - Ser
   - Ala
   - Val
   - Phe
5. Amino acid concentrations were calculated as the mean of the duplicate analyses using peak areas normalised to the internal standard, and expressed as picomols (pmol) per mg of shell.

Optically Stimulated Luminescence Dating

Table 10: Methodology for Optically Stimulated Luminescence Dating by Dr. Steve Pawley of RHUL.

1. Samples were collected by hammering opaque plastic tubes into sand beds. Cemented sediments were sampled as intact blocks, with the light-exposed edges removed by dissolution by 10% HCl.
2. All samples were processed under subdued orange light by Dr. Steve Pawley in the luminescence laboratories at the Department of Geography, RHUL.
3. Quartz was extracted in the 150-250 or 180-250 μm grain size fractions following HCl and H_2O_2 treatment.
4. Heavy minerals were removed by density separation and the remaining grains were etched in 40% HF solution for 50 minutes. See section 3.4.2.
5. All samples were subsequently placed in Flurosilicic acid for 5 days to dissolve any remaining feldspar grains, followed by an HCl wash for 1 hour and re-sieving.
6. External dose rates were calculated from the concentration of radioactive isotopes (U, Th, K) determined by ICP-MS and AES (Department of Geology at RHUL) and/or *in situ* dose rate measurements using an Ortec MicroNomad γ-spectrometer.
7. The dose rate conversion factors of Adamiec and Aitken (1998) were used throughout and the internal quartz dose rate of 0.06 Gy/ka was assumed based on previous measurements in eastern England and using an alpha efficiency factor of 0.10 ± 0.02 in the dose rate conversion (Mauz *et al.*, 2006). The beta dose attenuation/absorption was accounted for using the factors of Mejdahl (1979).
8. Cosmic ray contributions were calculated from the altitude, latitude and longitude of the section as well as the thickness and density of the overburden (Prescott & Hutton, 1994).
9. *In situ* water contents were measured after drying the samples at 110°C for 24hrs and saturated water contents were assessed from the volume/density of material within the OSL sampling tubes or undisturbed blocks. Water contents were placed at 0.5 ± 0.3 of the saturated value and dose rates were corrected for water attenuation (Aitken, 1985).
10. Luminescence measurements were performed on a Risø OSL/TL-DA-15 system using blue light LED stimulation (470 nm, ~40 mW/cm^3) and a U-340 detection filter. Laboratory irradiation used a ^{90}Sr / ^{90}Y beta source which was calibrated against quartz which had been γ-irradiated quartz at the National Physical Laboratory (Teddington, UK).
11. Prepared quartz grains were mounted onto 10 mm sized steel discs with the inner 5 mm part

of the disc covered with a monolayer of grains using viscous silicone oil.

12. The single aliquot regeneration (SAR) protocol was used to estimate sample D_e values and all luminescence measurements were performed for 50s whilst the sample was held at 130°C to prevent re-trapping in 110°C TL trap (Murray & Roberts, 1997; Murray & Wintle, 2000; Murray & Funder, 2003).

13. Five regenerative doses up to 400 Gy were used to bracket the D_e of each sample and a 15 Gy test dose was used. The luminescence signal was integrated from the initial 0.8s of the decay curve and a background was subtracted from the last 5 s of the stimulation.

14. The test dose background was taken from the previous natural or regenerative measurement (Murray & Wintle, 2000). A residual IR signal presumed to originate from feldspar formed <2% of the blue light (BL) stimulated signal and any small feldspar contribution was effectively eliminated using a post-IR blue SAR procedure with a 50s room temperature IR-shine used prior to each blue OSL measurement.

15. Equivalent doses were calculated using a saturating exponential plus linear function in custom written software in C++ employing the Levenberg-Marquardt algorithm implementation (Bevington & Robinson, 1992). Errors on the equivalent dose were calculated using the Monte Carlo method with 1000 iterations.

16. In order to ensure sufficient quality and precision during each measurement, aliquots were rejected from the analysis if their recycling ratios (difference between a repeated data point and the first regenerative measurement) exceeded 10% from unity, and IR/BL ratio on the natural test dose OSL measurement was >10%.

17. Individual D_e estimates were combined using the central age model of Galbraith *et al.* (1999) and errors in the final age calculations include systematic errors from beta source calibration of 3% (Armitage & Bailey, 2005), dose rate conversion of 3%, (Murray & Olley, 2002), and gamma-ray spectrometry calibration (3%) (Murray & Funder, 2003), and cosmic ray contribution (calculated from Prescott and Hutton, 1994).

18. Random uncertainties include ICP-MS dosimetry measurement (estimated at 5%), moisture content, and the standard error of the D_e estimates.